The background is a full-page abstract painting. It features a dramatic sky with a bright sun or moon in the center, surrounded by swirling orange, yellow, and blue brushstrokes. Below the sky, the landscape is composed of wavy, horizontal bands of color in shades of purple, pink, blue, and yellow, creating a rainbow-like effect. In the foreground, a winding white path leads through a valley. A small, dark silhouette of a cyclist is visible on the path in the lower right corner. The overall style is expressive and painterly, with visible brushstrokes throughout.

# **Advanced diagnostics and novel therapeutic strategies in ischemic heart disease**

**Bas van Klarenbosch**



# **Advanced diagnostics and novel therapeutic strategies in ischemic heart disease**

Bas Rémond van Klarenbosch



***Advanced diagnostics and novel therapeutic strategies in ischemic heart disease***

© B.R. van Klarenbosch, 2024

PhD thesis, Utrecht University, The Netherlands

ISBN/EAN: 978-94-6510-072-2

DOI:10.33540/2471

Financial support by the Dutch Heart Foundation for the publication of this thesis is gratefully acknowledged.

Design and print: [www.proefschriftmaken.nl](http://www.proefschriftmaken.nl)

Cover: Image was created with assistance of DALL·E 3 and modified by Stephan van Reisen

All rights reserved. No parts of this publication may be reproduced, stored in a retrieval system or transmitted in any form by any means without prior permission of the author.



# **Advanced diagnostics and novel therapeutic strategies in ischemic heart disease**

**Geavanceerde diagnostiek en nieuwe therapieën  
in ischemische hartziekten**  
(met een samenvatting in het Nederlands)

## **Proefschrift**

ter verkrijging van de graad van doctor aan de  
Universiteit Utrecht  
op gezag van de  
rector magnificus, prof. dr. H.R.B.M. Kummeling,  
ingevolge het besluit van het College voor Promoties  
in het openbaar te verdedigen op  
dinsdag 10 september 2024 des middags te 4.15 uur

door

**Bas Rémond van Klarenbosch**  
geboren op 4 november 1990 te Utrecht

**Promotor:**

Prof. dr. S.A.J. Chamuleau

**Copromotor:**

Dr. A.J. Teske

**Beoordelingscommissie:**

Prof. dr. J.J. Bax

Prof. dr. P.A.F.M. Doevendans

Prof. dr. M.H. Emmelot-Vonk (voorzitter)

Prof. dr.J. Kluin

Prof. dr. J.P.G. Sluijter

# TABLE OF CONTENTS

Chapter 1	General introduction and thesis outline	7
<b>Part I</b>	<b>Advanced diagnostics in ischemic cardiac damage</b>	23
Chapter 2	Global, segmental, and layer-specific two-dimensional speckle tracking echocardiography immediately after acute myocardial infarction as a predictive tool to assess myocardial viability and scar size <i>Submitted – Journal of Echocardiography</i>	25
Chapter 3	Conventional echocardiography versus two-dimensional speckle tracking derived global and segmental longitudinal strain and myocardial work in the detection of myocardial scar and assessment of myocardial viability <i>Submitted – International Journal of Cardiovascular Imaging</i>	51
Chapter 4	Correlation between circulating biomarkers of collagen homeostasis and scar size using magnetic resonance imaging in patients after acute myocardial infarction <i>In preparation</i>	73
<b>Part II</b>	<b>Application of advanced imaging in cell-based therapeutic strategies</b>	97
Chapter 5	Deformation imaging to assess global and regional effects of cardiac regenerative therapy in ischemic heart disease - a systematic review <i>Journal of Tissue Engineering and Regenerative Medicine 2019;30:1978-85</i>	99
Chapter 6	Rationale and design of the European multicentre study on Stem Cell therapy in IschEmic Non-treatable Cardiac disease (SCIENCE) <i>European Journal of Heart Failure 2019;21:1032-41</i>	121
Chapter 7	Effect of allogeneic adipose tissue derived mesenchymal stromal cells treatment in chronic ischemic heart failure with reduced ejection fraction – The SCIENCE Trial <i>European Journal of Heart Failure 2023;25:576-87</i>	139
Chapter 8	General discussion	165
Appendix	Nederlandse samenvatting	188
	List of publications	192
	Acknowledgements / dankwoord	194
	Curriculum vitae	199



## CHAPTER

# 1

# General introduction & thesis outline

Worldwide, cardiovascular disease is the leading cause of morbidity and premature mortality. A considerable portion of patients with cardiovascular disease present with acute myocardial infarction (AMI), with the European Society of Cardiology (ESC) reporting an estimated incidence of 5.8 million per year and a prevalence of 47.6 million people in its associated countries [1,2]. Over the past decades, incidence rates of AMI have been slightly on the decline [3]. Despite advances in cardiovascular risk management [4], the prevalence of cardiovascular risk factors is nevertheless on the rise, which results in an expected increasing incidence of myocardial infarction [5,6] towards 2060. Similarly, the prevalence of ischemic heart disease has remained stable over the past two decades [2], but in the United States of America, the prevalence of cardiovascular disease is expected to increase by 31.1% towards 2060 [5]. Figure 1 demonstrates the expected increasing incidence of AMI towards 2060 in the United States of America.

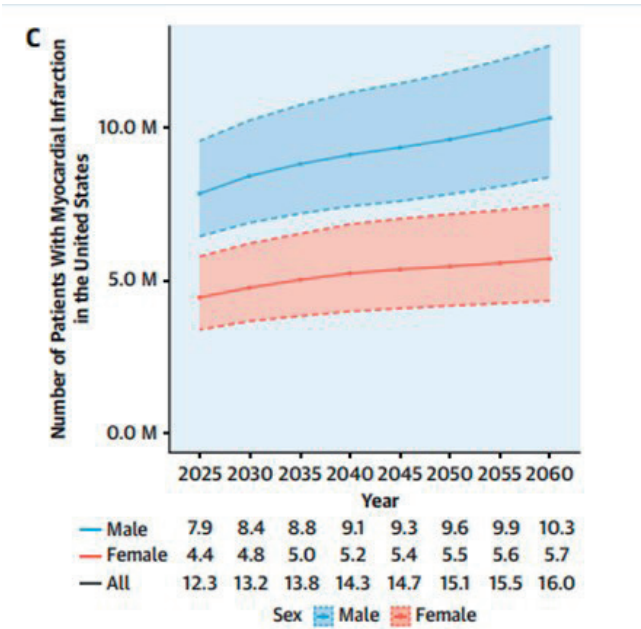


**Figure 1** – Projected incidence of myocardial infarction in the US. Mohebi et al. J Am Coll Cardiol 2022;80(6):565-78.

Despite the stable prevalence of ischemic heart disease, mortality attributable to AMI has decreased spectacularly by 60% over the past three decades [7]. This is attributable to enhanced therapeutic strategies. For example, thrombolysis, a mainstay in the treatment of AMI since the mid-1980s, has mostly been replaced by percutaneous coronary intervention (PCI) at the end of the twentieth century [2]. Furthermore, improvements



in primary PCI strategies and concomitant medical therapies such as dual antiplatelet therapy were made [1].

Nevertheless, the growing population of patients surviving AMI with mild to severe myocardial scarring after AMI will lead to patients with some form of left ventricular (LV) dysfunction. This suggests a potential role for enhanced diagnostics in order to diagnose those who will benefit from intensified therapy. Part I of this thesis will focus on this diagnostic challenge and explores the value of novel imaging techniques as well as biomarkers of collagen homeostasis in patients after myocardial infarction. For patients in whom significant scar size is to be expected, aggressive antifibrotic medical therapy consisting of at least angiotensin-converting enzyme (ACE) inhibitors and mineralocorticoid-receptor antagonists (MRA) is prudent [8,9]. Furthermore, in patients with non-transmural myocardial scar and non-culprit lesions that are potential targets for PCI, an aggressive reperfusion strategy should be considered [10].

Despite the aforementioned advances in the management of patients with AMI, ischemic heart disease is still, and will remain for the foreseeable future, an important cause of heart failure. As of yet, there is no clinically applicable cure for ischemic heart failure. In the last two decades, many efforts have been made in the field of cardiac regenerative therapy. Part II of this thesis will focus on a novel allogeneic adipose tissue-derived mesenchymal stromal cell-based therapeutic agent, as well as advanced imaging techniques and their potential application in the evaluation of the efficacy of cell-based therapeutic strategies.

## PART I – ADVANCED DIAGNOSTICS IN ISCHEMIC MYOCARDIAL DAMAGE

### *Advanced imaging and scar assessment*

Advanced imaging techniques hold potential in the timely assessment of, or prediction for, scar size and scar transmural. Currently, the 2023 ESC guideline for the management of acute coronary syndromes [1] advises the use of antifibrotic therapy based on LVEF, a parameter of global myocardial function. Current clinical practice is to measure LVEF through echocardiography, where the LV volume is traced in both the end-diastolic and end-systolic phases in two two-dimensional planes [1]. However, this technique is hampered by significant inter- and intra-operator variability [11–13]. Moreover, in the days following acute myocardial infarction, LVEF might underestimate the actual extent of scar because of the compensation of healthy segments which become hyperdynamic to maintain adequate cardiac output. On the other hand, post-acute LVEF assessment could be prone to overestimation of the myocardial infarction size due to stunning in the post-acute setting. To summarize, in the quest for scar assessment shortly after AMI, LVEF assessment might not be the preferred technique.

The gold standard to assess myocardial scar is late gadolinium enhancement (LGE) cardiac magnetic resonance imaging (CMR) [14–16], where intravenously administered gadolinium quickly washes out of healthy myocardium, but slowly washes out of scarred myocardium.

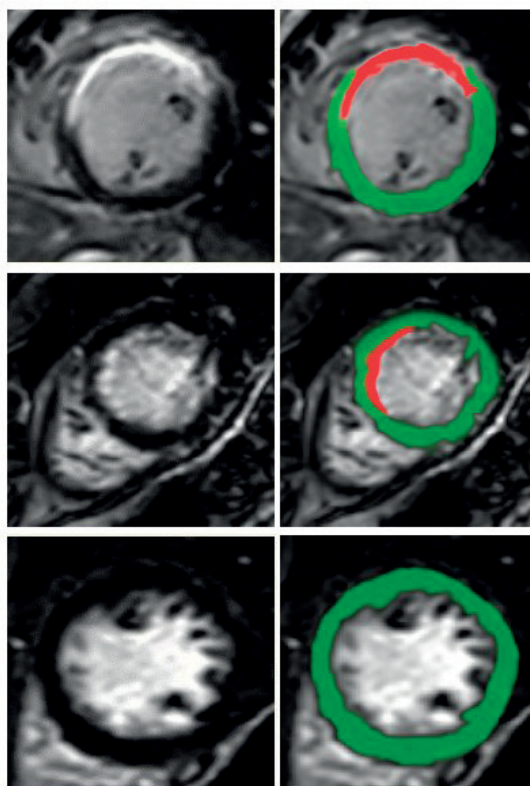


**Figure 2** – Three cases of LGE CMR. Red = delayed enhancement reflecting scar; green = healthy myocardium. Top: A transmural scar in the anterior wall; mid: a subendocardial scar in the anterior wall. Bottom: no scar.

When scans are performed 10-15 minutes after gadolinium infusion, this translates into images that reveal not only the location but also the extent of myocardial scar. Figure 2 shows examples of scar assessment using LGE CMR. However, availability, costs, and the requirement of a contrast agent are drawbacks of this technique, resulting in sparse use in the post-AMI setting. Moreover, LGE CMR in the post-acute setting will reflect fibrosis as well as myocardial inflammation [17]. An alternative method for assessment of myocardial fibrosis might therefore aid clinical decision making.

Quantitative assessment of regional myocardial function emerges as a possible alternative for scar assessment. Wall motion scoring (WMS), where each of the 16 segments of the myocardium is qualitatively assessed on wall motion, is not hampered by the compensation of remote segments as is the case with LVEF [18]. It is a

subjective interpretation and therefore requires training and experience, but it seems to be a reproducible technique following AMI [19]. However, due to stunning of reperfused segments, the WMS and wall motion scoring index (WMSI) might overestimate the infarct size at follow-up. Two-dimensional speckle-tracking echocardiography (2D-STE) derived myocardial deformation analysis is a technique by which acoustic backscatter is tracked frame-by-frame to measure deformation in a longitudinal, circumferential, and radial direction (figure 3). This result is strain, a one-dimensional parameter expressed as a percentage that is defined as the magnitude of deformation over one cardiac cycle relative to the original length at the onset of the cardiac cycle [20,21].

When plotting strain over time, the resultant strain curves give detailed insight into cardiac mechanics and its many aspects, allowing for discrimination of active and passive motion and therefore potentially discriminating between stunned and scarred myocardium [21]. Most importantly, objective quantification of systolic function can

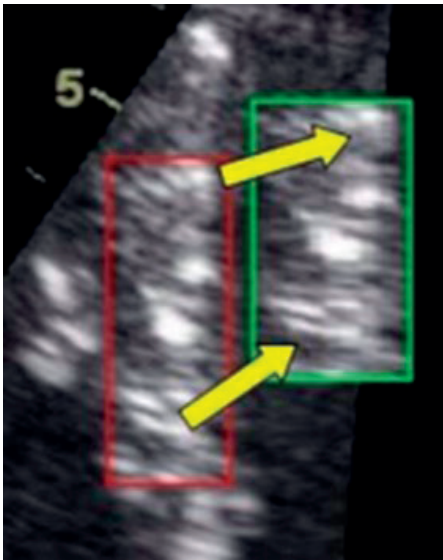


**Figure 3** – Example of the unique speckled pattern of the myocardium. In red, speckles at end-diastole are depicted whereas in green, the speckles at end-systole are depicted. The distance of speckles relative to each other has decreased, allowing for the determination of deformation. *Adapted from Teske et al, Cardiovasc Ultrasound 2007;5:27*

be performed. Strain values are generated for each of the 17 segments [22] of the heart providing information on segmental deformation characteristics. In addition, a mean value for the whole LV myocardium is provided, thereby generating a global strain value. Segmental strain could hold value in the assessment of scar transmuralty in a specific segment of interest, whereas global strain would be a parameter of interest in the evaluation of scar size. An example of strain assessment is displayed in Figure 4.

In the past years, novel applications of 2D-STE were developed which provide additional information on myocardial deformation. First, current software allows for the discrimination between endocardial, mid-myocardial, and epicardial myocardial layers [23,24]. This holds specific potential in transmuralty assessment since scar typically first affects the subendocardial layers. In addition, a strain gradient across the myocardial (transmural strain gradient) can be generated which

might provide additional insight into the complex mechanics of deformation in scarred hearts [25]. A noteworthy downside of 2D-STE is that it does not take loading conditions into account. This is of particular importance in the period after myocardial infarction, where changes in myocardial function and initiation of medication that alters loading conditions take place. Myocardial work analysis incorporates cuffed brachial blood pressure measurements into myocardial strain analysis, to generate a pressure-strain loop. The area of this loop reflects the work that is performed by the myocardium [26–29]. Figure 5 is an illustrative representation of the myocardial work analysis method. By reducing the influence of loading conditions on the measurement of myocardial function, work analysis could provide a more reliable assessment of myocardial scar in the post-AMI period.

### *Circulating biomarkers*

Patients surviving AMI are at risk of undergoing adverse myocardial remodeling, ultimately culminating in heart failure. A hallmark of adverse remodeling, both in ischemic and in non-ischemic myocardial damage, is the disturbed equilibrium between collagen synthesis and collagen breakdown, leading to increased interstitial myocardial



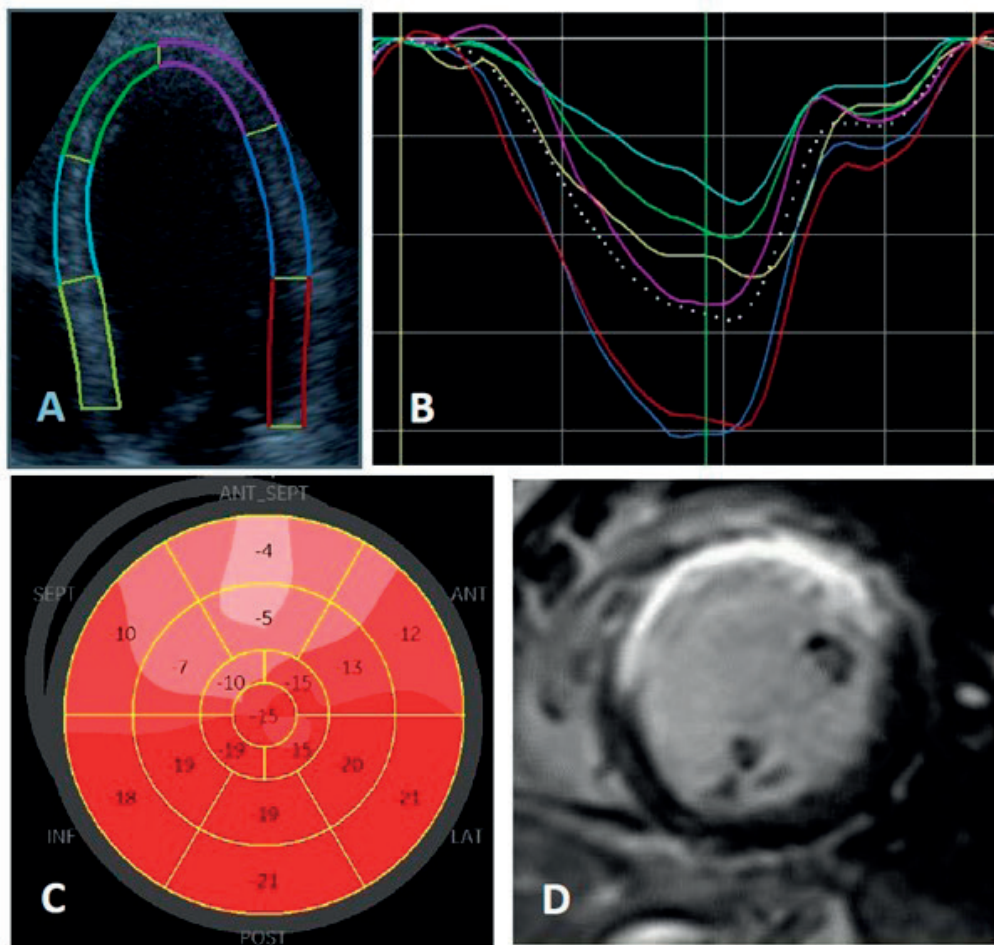


**Figure 4 – strain analysis in patient after anterior myocardial infarction.** (A) Tracing and segmentation in apical four chamber view; (B) The resultant strain curves; (C): Bull's eye graph of strain output according to 17-segment AHA model; (D) LGE CMR in the same patient, showing delayed washout of gadolinium (depicted as light colored myocardium) in the anterior wall.

fibrosis which is associated with heart failure [30]. Timely recognition of AMI survivors who are at risk of significant myocardial fibrosis, and therefore heart failure, could prompt the intensification of medical and reperfusion therapy in these patients. Currently, creatine kinase (CK), its myocardial fraction (CK-MB), and troponin are the biomarkers that clinicians use to predict scar size after AMI [31]. However, these biomarkers reflect the breakdown and apoptosis of myocardial cells and are therefore not necessarily reflective of myocardial fibrosis nor do they predict the resulting amount of myocardial dysfunction. Circulating biomarkers of collagen homeostasis hold the potential for improving myocardial fibrosis assessment post-AMI. Multiple biomarkers of collagen homeostasis have been identified. Examples of these include peptides that derive from the synthesis of collagen type I, such as propeptides of procollagen at the carboxy (C)-terminus (PICP), and products of cleavage

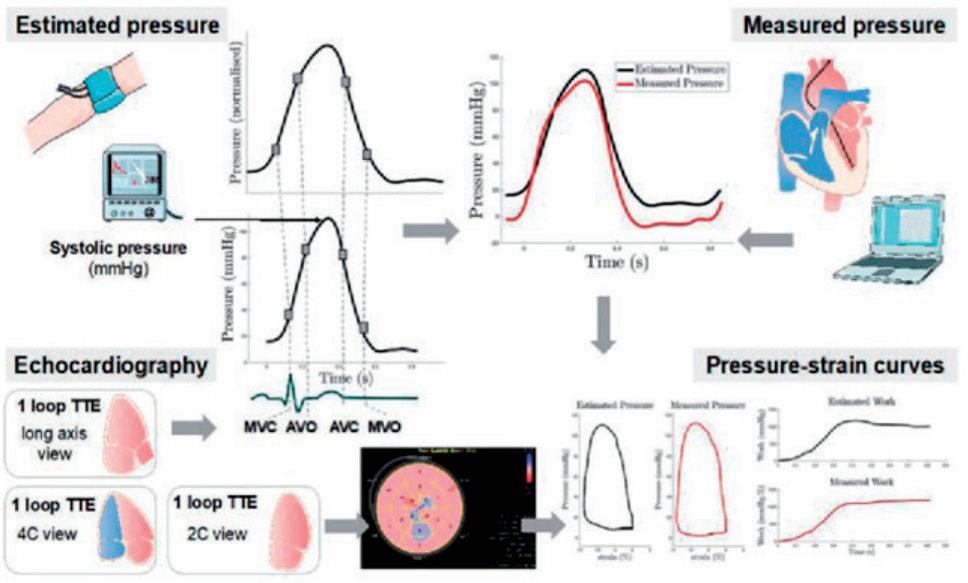


**Figure 5** – Adapted from Hubert et al. (Eur Heart J Cardiovasc Imaging 2018;19:1372–9). Schematic overview of myocardial work analysis. Using the method described by Russell et al. (Eur Heart J 2012;33:724–33), LV pressures are estimated from cuffed brachial blood pressure measurements. Using 2D-speckle tracking echocardiography derived strain measurements, a pressure-strain loop can be generated from which the surface area reflects myocardial work performed. TTE = transthoracic echocardiography; MVC = mitral valve closure; AVO = aortic valve opening; AVC = aortic valve closure; MVO = mitral valve opening.

of fibrillar collagen, such as C-terminal telopeptide of type I collagen (ICTP) [32]. However, there are many processes both within and outside of the heart that are involved in collagen homeostasis. Therefore, these parameters need to be studied in patients in whom minimal bias due to both intra- and extracardiac collagen homeostasis is to be expected.

## PART II – ADVANCED IMAGING IN CELL-BASED THERAPEUTIC STRATEGIES

### *The quest for cardiac regeneration*

Currently, heart failure is managed with four classes of medication, reperfusion therapy, or with mechanical circulatory support or heart transplantation in selected cases [33]. However, no guideline-endorsed therapeutic strategy involves regeneration of the infarcted myocardium. Contrary to zebrafish, unfortunately, the human heart has no functionally relevant intrinsic mechanism of regeneration, and the infarcted myocardium is generally considered to have definitively lost its contractile function [34,35]. When AMI gives rise to significant LVEF impairment, the resultant ischemic cardiomyopathy consequently represents a chronic condition. Exploration of mechanisms of myocardial regeneration opened the door for human cardiac regenerative research, and unraveling

the mystery of human myocardial regeneration is considered to be one of the holy grails in the field of cardiology. A substantial part of the research involved the administration of cell-based therapeutic agents into the heart. Initially, studies focused on the actual regeneration of infarcted myocardium into healthy myocardium. After promising preclinical research [36], in 2002, the first clinical trial on the effect of a cell-based therapeutic agent, an intracoronary-infused bone marrow-derived mononuclear cell, was published [37]. LV ventriculography revealed a significantly smaller infarct size in the therapy group compared to the placebo group. The new field of clinical cardiac regenerative research emerged rapidly and early evidence seemed to confirm the ability of cardiac stem cells to regenerate the heart.

Unfortunately, inspiring results of early hallmark trials were never replicated in the years thereafter, and the field was startled by several cases of scientific misconduct [38]. However, extensive systematic reviewing and meta-analyses revealed that in vivo cell-based regenerative therapy did show a very modest improvement of LVEF of approximately 2.9% [39–41]. The focus of research shifted from the autocrine hypothesis, aiming for cell-based therapeutic agents to differentiate into cardiomyocytes, to the paracrine hypothesis where paracrine and endocrine mechanisms by which secreted mediators sort beneficial effects. These include angiogenesis, activation of endogenous progenitor cells, immunomodulatory effects, and inhibition of inflammation, apoptosis, and fibrosis [42]. As a result, efforts were made to elucidate what the best application of cell-based therapy would be. In this quest, various patient groups, cell types, delivery strategies, methods of cell retention, timing of administration, and cell dosages were investigated [39,40]. In Figure 6, an overview of the proposed mechanisms of action of cardiac cell-based therapy is shown.

#### *Allogeneic adipose tissue-derived mesenchymal stromal cell in search of the optimal cell-based therapeutic agent*

Various cell populations have been studied since the emergence of cell-based cardiac regenerative therapy, with conflicting results regarding efficacy [43,44]. As the field progressed, many research groups focused on mesenchymal stromal cells as the cell of choice for regeneration. This was mainly due to its attributed immunomodulatory traits and the possibility for extracting these cells from various sources and culture-expanding them into large quantities. However, clinical efficacy data remained conflicting [45]. One of the hypotheses for this variation is that the administered cell product is not uniform. Compared to autologous cell products, allogeneic cell products have the advantage of being a much more controllable and therefore homogeneous cell product. It has not been exposed to the risk factors that cell products from patients themselves have been exposed to, they can be stored as a standard dosage off-the-shelf product and no complex cell harvesting procedures are required in the patient. With this in mind, the research group of Jens Kastrup developed a production line of clinical-grade allogeneic adipose



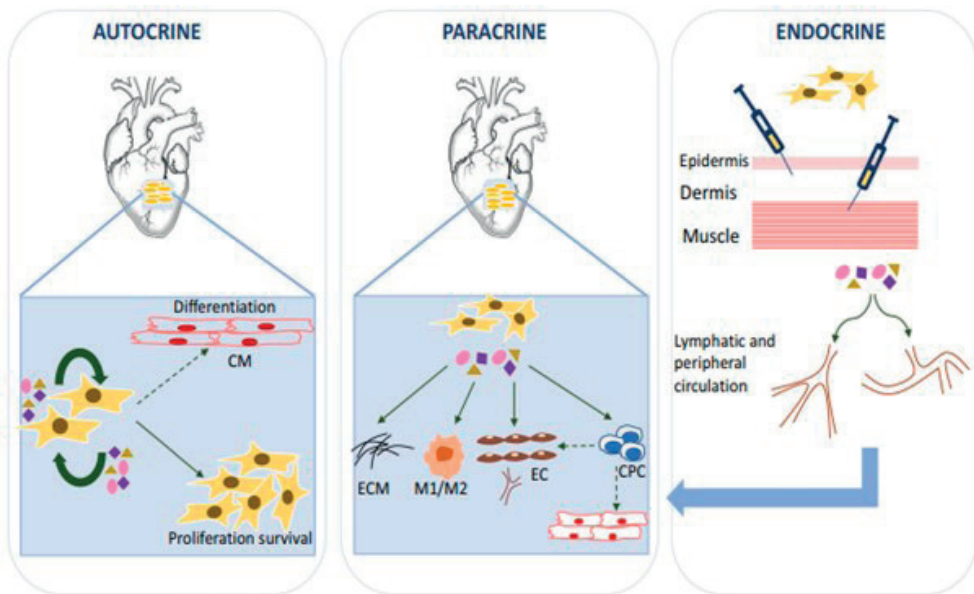


**Figure 6** – Proposed mechanisms of action of cardiac cell based therapy. Sid-Otmane e.a.; J Transl Med 2020;18:336

tissue-derived mesenchymal stem cells (CSCC\_ASCs) from healthy donors. A phase I trial of this product was successful [46]. CSCC\_ASC holds the potential for improved efficacy compared to previously investigated cell products, all while overcoming some important logistical challenges that hamper the clinical applicability of cardiac cell-based therapies [47,48].

#### *Imaging end-points in cardiac regenerative research*

LVEF is a commonly used end-point in cardiac regenerative research and is known to correlate well to clinical end-points such as mortality and rehospitalization [49–51]. However, the global nature of LVEF measurement is potentially not suitable for detecting the subtle regional attenuations in myocardial function that cardiac cell therapy is expected to sort. This is highlighted by the aforementioned beneficial effect of cell-based therapeutics on LVEF of only 2.9%, which is notably smaller than the intra-operator variability of LVEF assessment which is in the range of 6–10% [11,41]. Earlier in this section, the potential of 2D-STE derived myocardial strain analysis was elaborated upon in the light of ischemic heart disease. This technique is also promising for end-point assessment in cardiac regenerative therapy, because of its capability to assess and quantify myocardial function on the regional level at which the cell-based therapies are expected to sort their effect [52]. It seems to outperform LVEF measurement regarding its accuracy and inter-operator variability [53,54]. Importantly for the sake of end-point measurement in cardiac

regenerative therapy, and similar to LVEF, global longitudinal strain (GLS) has proven to be an excellent prognosticator [55,56]. Indeed, several clinical trials on the efficacy of cell-based therapeutic agents have incorporated myocardial deformation parameters [57,58].

## THESIS OUTLINE

### *Part I – Advanced diagnostics in ischemic myocardial damage*

Part I of this thesis explores novel imaging techniques and biomarkers in the assessment of myocardial scar after AMI, aiming to identify patients who stand to benefit from more aggressive antifibrotic medical therapy and revascularization strategies. In **chapter 2**, we study the value of 2D-STE, including layer-specific strain, in the days after AMI as an alternative for CMR in the prediction of scar size and scar transmural. We compare the results to conventional echocardiographic parameters of myocardial function and provide cut-off values of segmental strain for predicting for non-scarred, endocardially scarred, and transmurally scarred segments. In **chapter 3**, we analyze the behavior of novel myocardial work parameters after myocardial infarction and explore their value in myocardial scar assessment. In **chapter 4**, the behavior of biomarkers of collagen homeostasis PICP and ICTP after myocardial infarction is displayed, and correlated to LGE CMR results.

### *Part II – Application of advanced imaging in cell-based therapeutic strategies*

Part II of this thesis is aimed at cell-based regenerative therapy in ischemic heart disease. In **chapter 5**, the current application of strain analysis in cell-based regenerative therapy is reviewed, both in the preclinical setting and the clinical setting, as well as both in patients after AMI as patients with chronic ischemic heart failure. From the available data, we hypothesize on the added value of 2D-STE in this field of research. **Chapter 6** clarifies the study protocol of the SCIENCE trial, a double-blind placebo-controlled randomized trial into the clinical benefit of allogeneic adipose tissue-derived mesenchymal stromal cells. **Chapter 7** elaborates on the results of the SCIENCE trial regarding the effect of allogeneic adipose tissue-derived mesenchymal stromal cells on the primary end-point measure, echocardiography-derived biplane measured LV end-systolic volume.

To summarize, this thesis studies novel diagnostic opportunities for scar assessment in patients after AMI, and it explores the application of advanced imaging and a novel cell type in the field of cardiac regenerative therapy. **Chapter 8** concludes this thesis, providing a general summary of the results together with their implications and future perspectives.

## REFERENCES

- [1] Byrne RA, Rossello X, Coughlan JJ, et al. 2023 ESC Guidelines for the management of acute coronary syndromes. *Eur Heart J* 2023;44:3720–826. Doi:10.1093/eurheartj/ehad191.
- [2] Timmis A, Vardas P, Townsend N, et al. European Society of Cardiology: cardiovascular disease statistics 2021. *Eur Heart J* 2022;43:716–99. Doi:10.1093/eurheartj/ehab892.
- [3] Ibanez B, James S, Agewall S, et al. 2017 ESC Guidelines for the management of acute myocardial infarction in patients presenting with ST-segment elevation. The Task Force for the management of acute myocardial infarction. *Eur Heart J* 2018;39:119–77. Doi:10.1093/eurheartj/ehx393.
- [4] Visseren F, Mach F, Smulders YM, et al. 2021 ESC Guidelines on cardiovascular disease prevention in clinical practice. *Eur Heart J* 2021;42:3227–337. Doi:10.1093/eurheartj/ehab484.
- [5] Mohebi R, Chen C, Ibrahim NE, et al. Cardiovascular Disease Projections in the United States Based on the 2020 Census Estimates. *J Am Coll Cardiol* 2022;80:565–78. Doi:10.1016/j.jacc.2022.05.033.
- [6] Roth GA, Mensah GA, Johnson CO, et al. Global Burden of Cardiovascular Diseases and Risk Factors, 1990-2019: Update From the GBD 2019 Study. *J Am Coll Cardiol* 2020;76:2982–3021. Doi:10.1016/j.jacc.2020.11.010.
- [7] Hartley A, Marshall DC, Saliccioli JD, et al. Trends in Mortality From Ischemic Heart Disease and Cerebrovascular Disease in Europe: 1980 to 2009. *Circulation* 2016;133:1916–26. Doi:10.1161/CIRCULATIONAHA.115.018931.
- [8] ACE Inhibitor Myocardial Infarction Collaborative Group. Indications for ACE Inhibitors in the Early Treatment of Acute Myocardial Infarction Systematic Overview of Individual Data From 100 000 Patients in Randomized Trials. *Circulation* 1998;97:2022–12. Doi:10.1161/01.cir.97.22.2202
- [9] Montalescot G, Pitt B, Lopez de Sa E, et al. Early eplerenone treatment in patients with acute ST-elevation myocardial infarction without heart failure: The Randomized Double-Blind Reminder Study. *Eur Heart J* 2014;35:2295–302. Doi:10.1093/eurheartj/ehu164.
- [10] van Loon RB, Veen G, Baur LHB, et al. Improved clinical outcome after invasive management of patients with recent myocardial infarction and proven myocardial viability: Primary results of a randomized controlled trial (VIAMI-trial). *Trials* 2012;13. Doi:10.1186/1745-6215-13-1.
- [11] Wood PW, Choy JB, Nanda NC, Becher H. Left ventricular ejection fraction and volumes: It depends on the imaging method. *Echocardiography* 2014;31:87–100. Doi:10.1111/echo.12331.
- [12] O'Dell WG. Accuracy of Left Ventricular Cavity Volume and Ejection Fraction for Conventional Estimation Methods and 3D Surface Fitting. *J Am Heart Assoc* 2019;8:e009124. Doi:10.1161/JAHA.118.009124.
- [13] Dorosz JL, Lezotte DC, Weitzenkamp DA, et al. Performance of 3-dimensional echocardiography in measuring left ventricular volumes and ejection fraction: A systematic review and meta-analysis. *J Am Coll Cardiol* 2012;59:1799–808. Doi:10.1016/j.jacc.2012.01.037.
- [14] Flett AS, Hasleton J, Cook C, et al. Evaluation of techniques for the quantification of myocardial scar of differing etiology using cardiac magnetic resonance. *JACC Cardiovasc Imaging* 2011;4:150–6. Doi:10.1016/j.jcmg.2010.11.015.

- [15] Wu E, Judd RM, Vargas JD, et al. Visualisation of presence, location, and transmural extent of healed Q-wave and non-Q-wave myocardial infarction. *Lancet* 2001;357:21–8. Doi:10.1016/S0140-6736(00)03567-4.
- [16] Hendel RC, Patel MR, Kramer CM, et al. ACCF/ACR/SCCT/SCMR/ASNC/NASCI/SCAI/SIR 2006 Appropriateness Criteria for Cardiac Computed Tomography and Cardiac Magnetic Resonance Imaging: A Report of the American College of Cardiology Foundation Quality Strategic Directions Committee Appropriateness Criteria Working Group, American College of Radiology, Society of Cardiovascular Computed Tomography, Society for Cardiovascular Magnetic Resonance, American Society of nuclear Cardiology, North American Society for Cardiac Imaging, Society for Cardiovascular Angiography and Interventions, and Society of Interventional Radiology. *J Am Coll Cardiol* 2006;48:1475–97. Doi:10.1016/j.jacc.2006.07.003.
- [17] Doltra A, Amundsen BH, Gebker R, et al. Emerging Concepts for Myocardial Late Gadolinium Enhancement MRI. *Curr Cardiol Rev* 2013;9:185–90. Doi:10.2174/1573403x113099990030
- [18] Van Mourik MJW, Zaar DVJ, Smulders MW, et al. Adding Speckle-Tracking Echocardiography to Visual Assessment of Systolic Wall Motion Abnormalities Improves the Detection of Myocardial Infarction. *J Am Soc Echocardiogr* 2019;32:65–73. Doi:10.1016/j.echo.2018.09.007.
- [19] Poller A, Jha S, Espinosa AS, et al. Inter- and intra-observer variability in the echocardiographic evaluation of wall motion abnormality in patients with ST-elevation myocardial infarction or takotsubo syndrome – A novel approach. *Echocardiography* 2023;40:711–9. Doi:10.1111/echo.15638.
- [20] Becker M, Bilke E, Kühl H, et al. Analysis of myocardial deformation based on pixel tracking in two dimensional echocardiographic images enables quantitative assessment of regional left ventricular function. *Heart* 2006;92:1102–8. Doi:10.1136/hrt.2005.077107.
- [21] Teske AJ, De Boeck BWL, Melman PG, et al. Echocardiographic quantification of myocardial function using tissue deformation imaging, a guide to image acquisition and analysis using tissue Doppler and speckle tracking. *Cardiovasc Ultrasound* 2007;5. Doi:10.1186/1476-7120-5-27.
- [22] Cerqueira MD, Weissman NJ, Dilsizian V, et al. Standardized Myocardial Segmentation and Nomenclature for Tomographic Imaging of the Heart: A Statement for Healthcare Professionals From the Cardiac Imaging Committee of the Council on Clinical Cardiology of the American Heart Association. *Circulation* 2002;105:539–42. Doi:10.1161/hc0402.102975
- [23] Altiok E, Neizel M, Tiemann S, et al. Layer-specific analysis of myocardial deformation for assessment of infarct transmural: Comparison of strain-encoded cardiovascular magnetic resonance with 2D speckle tracking echocardiography. *Eur Heart J Cardiovasc Imaging* 2013;14:570–8. Doi:10.1093/ehjci/jes229.
- [24] Nagata Y, Wu VCC, Otsuji Y, Takeuchi M. Normal range of myocardial layer-specific strain using two-dimensional speckle tracking echocardiography. *PLoS One* 2017;12:e0180584. Doi:10.1371/journal.pone.0180584.

- [25] Alcidi GM, Esposito R, Evola V, et al. Normal reference values of multilayer longitudinal strain according to age decades in a healthy population : A single-centre experience. *Eur Heart J Cardiovasc Imaging* 2018;19:1390–6. Doi:10.1093/ehjci/jex306.
- [26] Russell K, Eriksen M, Aaberge L, et al. Assessment of wasted myocardial work: A novel method to quantify energy loss due to uncoordinated left ventricular contractions. *Am J Physiol Heart Circ Physiol* 2013;305:996–1003. Doi:10.1152/ajpheart.00191.2013.
- [27] Russell K, Eriksen M, Aaberge L, et al. A novel clinical method for quantification of regional left ventricular pressurestrain loop area: A non-invasive index of myocardial work. *Eur Heart J* 2012;33:724–33. Doi:10.1093/eurheartj/ehs016.
- [28] Hubert A, Le Rolle V, Leclercq C, et al. Estimation of myocardial work from pressure–strain loops analysis: an experimental evaluation. *Eur Heart J Cardiovasc Imaging* 2018;19:1372–9. Doi:10.1093/ehjci/jey024.
- [29] Boe E, Skulstad H, Smiseth OA. Myocardial work by echocardiography: A novel method ready for clinical testing. *Eur Heart J Cardiovasc Imaging* 2019;20:18–20. Doi:10.1093/ehjci/jey156.
- [30] González A, Schelbert EB, Díez J, Butler J. Myocardial Interstitial Fibrosis in Heart Failure: Biological and Translational Perspectives. *J Am Coll Cardiol* 2018;71:1696–706. Doi:10.1016/j.jacc.2018.02.021.
- [31] Mayr A, Mair J, Klug G, et al. Cardiac troponin T and creatine kinase predict mid-term infarct size and left ventricular function after acute myocardial infarction: A cardiac MR study. *J Magn Res Imaging* 2011;33:847–54. Doi:10.1002/jmri.22491.
- [32] De Jong S, Van Veen TAB, De Bakker JMT, et al. Biomarkers of Myocardial Fibrosis. *J Cardiovasc Pharmacol* 2011;57:522–35. Doi: 10.1097/FJC.0b013e31821823d9
- [33] McDonagh TA, Metra M, Adamo M, et al. 2021 ESC Guidelines for the diagnosis and treatment of acute and chronic heart failure. *Eur Heart J* 2021;42:3599–726. Doi:10.1093/eurheartj/ehab368.
- [34] Poss KD, Wilson LG, Keating MT. Heart Regeneration in Zebrafish. *Science* 2002;298:2188–90. Doi:10.1126/science.1076249.
- [35] Uygur A, Lee RT. Mechanisms of Cardiac Regeneration. *Dev Cell* 2016;36:362–74. Doi:10.1016/j.devcel.2016.01.018.
- [36] Orlic D, Kajstura J, Chimenti S, et al. Bone marrow cells regenerate infarcted myocardium. *Nature* 2001;410:701–5. Doi:10.1038/35070587.
- [37] Strauer BE, Brehm M, Zeus T, et al. Repair of infarcted myocardium by autologous intracoronary mononuclear bone marrow cell transplantation in humans. *Circulation* 2002;106:1913–8. Doi:10.1161/01.CIR.0000034046.87607.1C.
- [38] Chien KR, Frisén J, Fritsche-Danielson R, Melton DA, et al. Regenerating the field of cardiovascular cell therapy. *Nat Biotechnol* 2019;37:232–7. Doi:10.1038/s41587-019-0042-1.
- [39] Fisher SA, Brunskill SJ, Doree C, et al. Stem cell therapy for chronic ischaemic heart disease and congestive heart failure. *Cochrane Database of Syst Rev* 2014:CD007888 Doi:10.1002/14651858.CD007888.pub2.
- [40] Mira van der Naald. Enhancing quality in translational research - learning from experiences in cardiac repair. 2022. ISBN:978-94-6423-950-8

- [41] Afzal MR, Samanta A, Shah ZI, et al. Adult Bone Marrow Cell Therapy for Ischemic Heart Disease: Novelty and Significance. *Circ Res* 2015;117:558–75. Doi:10.1161/CIRCRESAHA.114.304792.
- [42] Sid-Otmane C, Perrault LP, Ly HQ. Mesenchymal stem cell mediates cardiac repair through autocrine, paracrine and endocrine axes. *J Transl Med* 2020;18. Doi:10.1186/s12967-020-02504-8.
- [43] Fernández-Avilés F, Sanz-Ruiz R, Climent AM, et al. Global position paper on cardiovascular regenerative medicine. *Eur Heart J* 2017;38:2532–46. Doi:10.1093/eurheartj/ehx248.
- [44] Gyöngyösi M, Pokushalov E, Romanov A, et al. Meta-Analysis of Percutaneous Endomyocardial Cell Therapy in Patients with Ischemic Heart Failure by Combination of Individual Patient Data (IPD) of ACCRUE and Publication-Based Aggregate Data. *J Clin Med* 2022;11. Doi:10.3390/jcm11113205.
- [45] Kastrup J, Mygind ND, Qayyum AA, et al.. Mesenchymal stromal cell therapy in ischemic heart disease. *Scand Cardiovasc J* 2016;50:293–9. Doi:10.1080/14017431.2016.1210213.
- [46] Kastrup J, Haack-Sørensen M, Juhl M, et al. Cryopreserved Off-the-Shelf Allogeneic Adipose-Derived Stromal Cells for Therapy in Patients with Ischemic Heart Disease and Heart Failure—A Safety Study. *Stem Cells Transl Med* 2017;6:1963–71. Doi:10.1002/sctm.17-0040.
- [47] Haack-Sørensen M, Follin B, Juhl M, et al. Culture expansion of adipose derived stromal cells. A closed automated Quantum Cell Expansion System compared with manual flask-based culture. *J Transl Med* 2016;14. Doi:10.1186/s12967-016-1080-9.
- [48] Haack-Sørensen M, Juhl M, Follin B, et al. Development of large-scale manufacturing of adipose-derived stromal cells for clinical applications using bioreactors and human platelet lysate. *Scand J Clin Lab Invest* 2018;78:293–300. Doi:10.1080/00365513.2018.1462082.
- [49] Møller JE, Hillis GS, Oh JK, et al. Wall motion score index and ejection fraction for risk stratification after acute myocardial infarction. *Am Heart J* 2006;151:419–25. Doi:10.1016/j.ahj.2005.03.042.
- [50] Pocock SJ, Wang D, Pfeffer MA, et al. Predictors of mortality and morbidity in patients with chronic heart failure. *Eur Heart J* 2006;27:65–75. Doi:10.1093/eurheartj/ehi555.
- [51] Solomon SD, Anavekar N, Skali H, et al. Influence of ejection fraction on cardiovascular outcomes in a broad spectrum of heart failure patients. *Circulation* 2005;112:3738–44. Doi:CIRCULATIONAHA.105.561423.
- [52] Lima MSM, Villarraga HR, Abduch MCD, et al. Global Longitudinal Strain or Left Ventricular Twist and Torsion? Which Correlates Best with Ejection Fraction? *Arq Bras Cardiol* 2017;23–9. Doi:10.5935/abc.20170085.
- [53] Barbier P, Mirea O, Cefalù C, et al. Reliability and feasibility of longitudinal AFI global and segmental strain compared with 2D left ventricular volumes and ejection fraction: Intra- and inter-operator, test-retest, and inter-cycle reproducibility. *Eur Heart J Cardiovasc Imaging* 2015;16:642–52. Doi:10.1093/ehjci/jeu274.
- [54] Mirea O, Pagourelias ED, Duchenne J, et al. Variability and Reproducibility of Segmental Longitudinal Strain Measurement. *JACC Cardiovasc Imaging* 2018;11:15–24. Doi:10.1016/j.jcmg.2017.01.027.



- [55] Cho GY, Marwick TH, Kim HS, et al. Global 2-Dimensional Strain as a New Prognosticator in Patients With Heart Failure. *J Am Coll Cardiol* 2009;54:618–24. Doi:10.1016/j.jacc.2009.04.061.
- [56] Stanton T, Leano R, Marwick TH. Prediction of all-cause mortality from global longitudinal speckle strain: Comparison with ejection fraction and wall motion scoring. *Circ Cardiovasc Imaging* 2009;2:356–64. Doi:10.1161/CIRCIMAGING.109.862334.
- [57] Duran JM, Makarewich CA, Sharp TE, et al. Bone-Derived stem cells repair the heart after myocardial infarction through transdifferentiation and paracrine signaling mechanisms. *Circ Res* 2013;113:539–52. Doi:10.1161/CIRCRESAHA.113.301202.
- [58] Herbots L, D'Hooge J, Eroglu E, et al. Improved regional function after autologous bone marrow-derived stem cell transfer in patients with acute myocardial infarction: A randomized, double-blind strain rate imaging study. *Eur Heart J* 2009;30:662–70. Doi:10.1093/eurheartj/ehn532.



# Part I

Advanced diagnostics in ischemic cardiac damage

## CHAPTER

# 2

# Global, segmental, and layer-specific two-dimensional speckle tracking echocardiography immediately after acute myocardial infarction as a predictive tool to assess myocardial viability and scar size

Van Klarenbosch BR, Driessen HE, Kirkels FP, Cramer MJ, Velthuis BK, Vos MA, Chamuleau SAJ, Ter Meulen - De Jong S, Teske AJ

## Abstract

**Aim:** The identification of myocardial scar is key in clinical decision-making after acute myocardial infarction (AMI). However, the gold standard that is cardiac magnetic resonance imaging (CMR) encounters limitations in terms of availability. Two-dimensional speckle tracking echocardiography (2D-STE) may be an accessible alternative in detecting scar and assessing scar transmural. We aim to evaluate the predictive value of 2D-STE, encompassing measures of global, segmental and layer specific strain, with respect to myocardial viability and scar size at 6 months follow up.

**Methods and results:** In 43 patients admitted for primary AMI, we conducted a comparative analysis of strain parameters (including global longitudinal strain (GLS), segmental longitudinal strain (SLS), layer-specific GLS and SLS and the transmural strain gradient from endocardium to epicardium) in relation to conventional echocardiographic parameters at baseline in predicting for scar size and the transmural index, as measured by CMR, 6 months post enrollment. We demonstrate a moderate correlation between both GLS and conventional echocardiographic parameters, and scar size as well as transmural index. Wall motion score index exhibited superior predictive performance over GLS and left ventricular ejection fraction in anticipating scar formation. At a cut-off of -13.3% for any scar and -11.5% for transmural scar, SLS can predict scar formation. Layer-specific strain did not provide added predictive value.

**Conclusion:** SLS, but not layer-specific strain, during admission after AMI is an easy and accessible quantitative tool for predicting scar formation and transmural extent at 6 months follow-up. GLS correlates well with scar size, suggesting its potential utility as a predictive tool.

**Key words:** Strain, speckle tracking, infarction, scar, transmural. cardiac magnetic resonance imaging

## INTRODUCTION

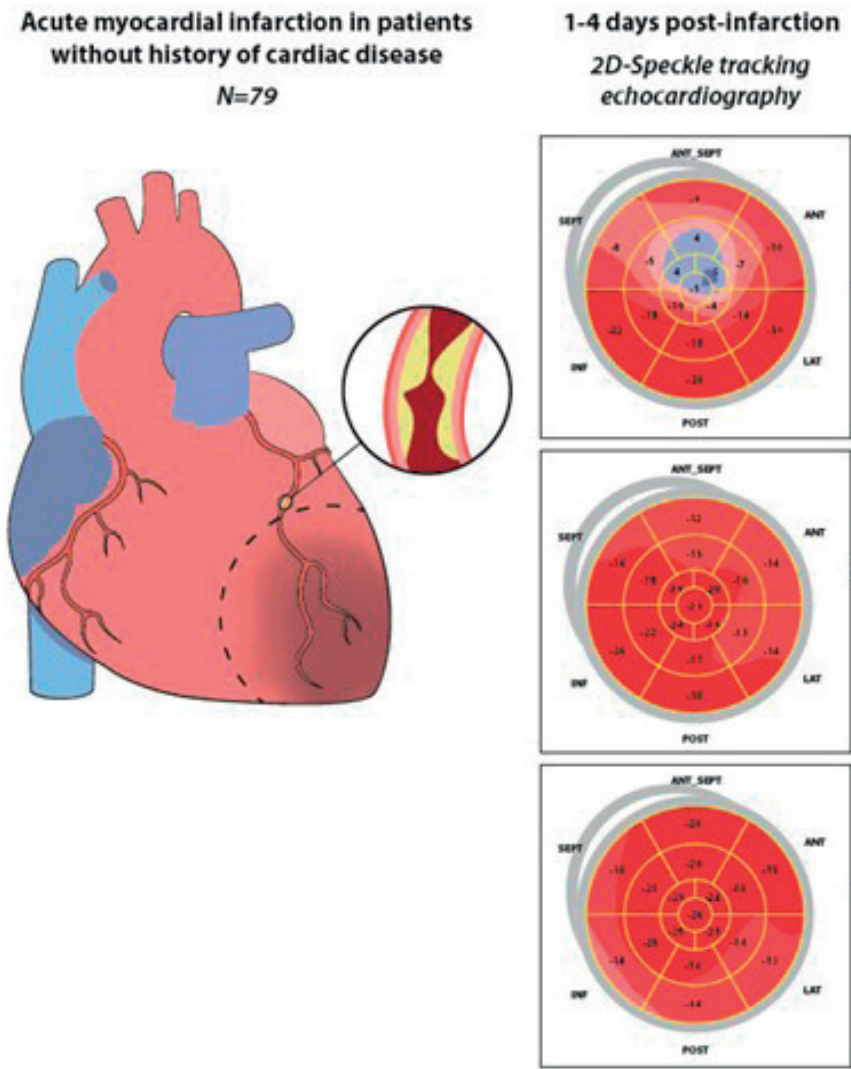
The population of patients surviving acute myocardial infarction (AMI) is on the rise, attributed to increased incidence rates of 43 to 144 per 100,000 per year [1,2], coupled with enhanced therapeutic approaches culminating in a 60% reduction in mortality over the past three decades [3]. Scar size is an important prognostic factor for cardiac events such as mortality, recurrent AMI, and congestive heart failure [4,5], understating the importance of identifying patients who stand to benefit from aggressive antifibrotic therapy. Furthermore, assessment of infarct transmural extent is important to differentiate viable from non-viable scar in individualized treatment planning for additional revascularization.

Late gadolinium enhancement (LGE) cardiac magnetic resonance imaging (CMR) is the gold standard for the assessment of scar size and transmural extent [6,7]. However, it is hampered by clinical availability, contra-indications, and substantial costs. Moreover, the exact amount of scar tissue on CMR cannot be reliably assessed directly after AMI [8]. This may potentially lead to delayed or deferred viability assessment and therefore optimal treatment, such as revascularization or optimized antifibrotic medical therapy in the post-acute setting [9]. The 2023 European Society of Cardiology (ESC) guideline for the management of acute coronary syndromes [2] advise the use of angiotensin converting enzyme inhibitors and/or mineralocorticoid receptor antagonists based on parameters of global function such as transthoracic echocardiography (TTE) derived left ventricular (LV) ejection fraction (LVEF). However, stunning in the post-acute period may lead to temporary global LV dysfunction in a situation of limited fibrosis. On the other hand, compensatory mechanisms resulting in hyperkinesia of non-infarcted myocardial regions may lead to a normal global LV function despite substantial scar burden. To address this concern, assessment of regional myocardial function using the wall motion score index (WMSI) is a possible alternative [10]. However, it is hampered by subjective interpretation, necessitating expert interpretation, and might lack sensitivity to discriminate scarred from stunned myocardium.

Two-dimensional speckle tracking echocardiography (2D-STE) derived myocardial deformation parameters may be a straightforward, accessible, and more objective alternative for scar assessment. This technique allows for discrimination between active and passive motion of the myocardial wall, thus offering the potential to discriminate between stunned myocardium and transmurally infarcted myocardium [11]. Consequently, it can provide information on infarct size and transmural extent in the days following AMI, enabling timely adoption of aggressive antifibrotic strategies. Besides full-wall myocardial deformation parameters, 2D-STE can separately provide deformation indices of endocardial, mid-myocardial, and epicardial layers [12,13]. This approach holds another potential for transmural extent assessment, given that non-transmural infarction typically first affects the subendocardial layers of the myocardium. In such cases, averaging outcomes over the full-wall thickness might underestimate endocardial functional impairment.



**Figure 1** – Schematic representation of study design and main findings. SLS = segmental longitudinal strain; TMS = transmural scar; SES = subendocardial scar.



*SLS = Segmental longitudinal strain; TMS = transmural scar; SES = subendocardial scar*

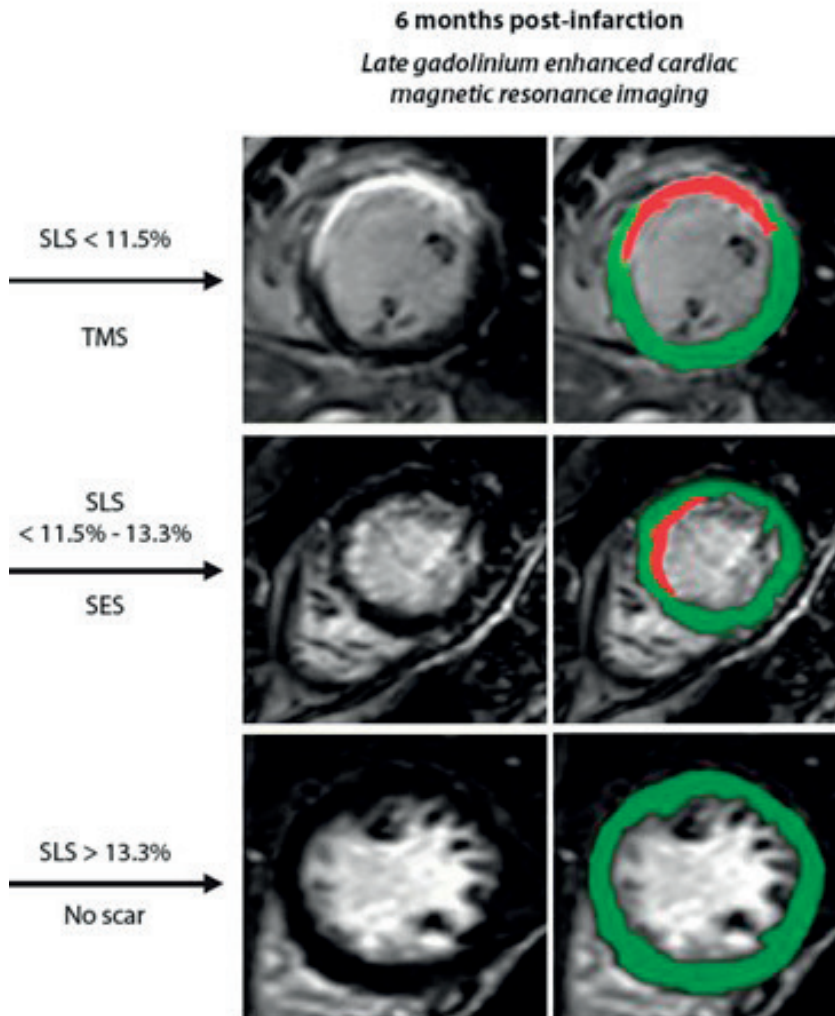


Figure 2 – Example of strain output in patient one day after acute anterior myocardial infarction

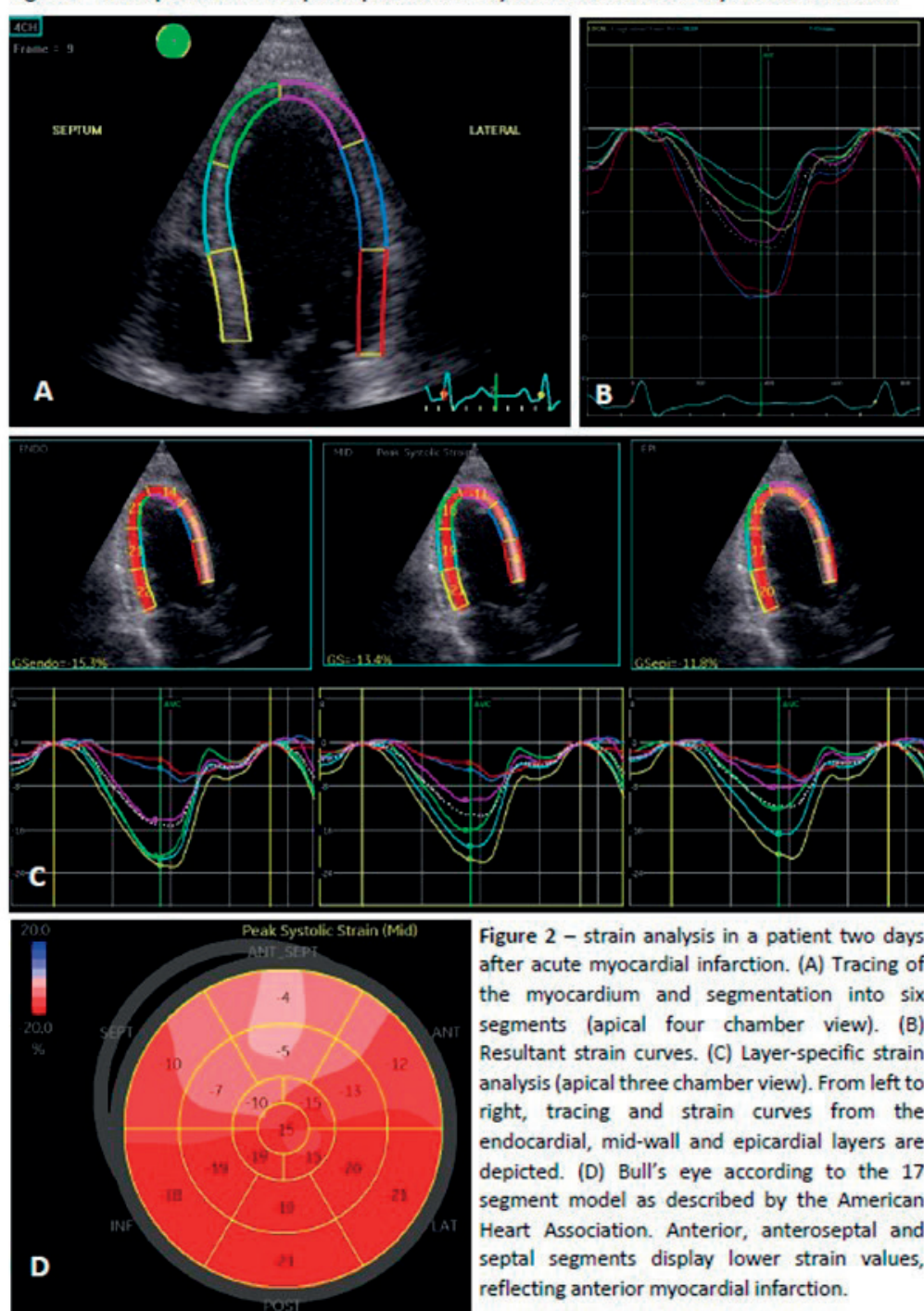


Figure 2 – strain analysis in a patient two days after acute myocardial infarction. (A) Tracing of the myocardium and segmentation into six segments (apical four chamber view). (B) Resultant strain curves. (C) Layer-specific strain analysis (apical three chamber view). From left to right, tracing and strain curves from the endocardial, mid-wall and epicardial layers are depicted. (D) Bull's eye according to the 17 segment model as described by the American Heart Association. Anterior, antero-septal and septal segments display lower strain values, reflecting anterior myocardial infarction.

The objective of this study is to explore the potential of 2D-STE derived peak-systolic global (GLS) and segmental (SLS) longitudinal strain, as well as layer-specific strain, within the immediate post-coronary reperfusion period, to predict scar size and transmural, and compare this to conventional TTE-derived indices of systolic function using LGE CMR as the gold standard.

## METHODS

### *Study population*

This prospective single center sub-study is part of the DEFI-MI study (METC: NL45241.041.13). Between March 2014 and April 2018, 89 patients without a history of cardiac disease presenting with AMI (both ST-elevation myocardial infarction (STEMI) and non-STEMI), defined as troponin I levels exceeding 60 ng/L, coupled with clinical and electrocardiographic (ECG) findings consistent with AMI, were included. 10 people were excluded from the study, making 79 patients eligible for analysis. The study was conducted according to the Declaration of Helsinki.

After informed consent, participants underwent baseline TTE within a window of one to four days after admission. At six months after inclusion, patients underwent a follow-up TTE and an LGE CMR. To avoid inter-vendor variability, only patients with a TTE on a General Electric (GE) system (n=43) were enrolled for this sub-study. Figure 1 shows the time points of the study.

### *Echocardiography*

Although TTE was performed both in the period immediately after coronary reperfusion during first admission and at follow-up, only results from the baseline examination were used to predict scar characteristics. Images were obtained with patients in left lateral decubitus position using a commercially available system (Vivid E9, GE Vingmed Ultrasound AS, Horten, Norway) fitted with a 4 MHz transducer (M5Sc). A TTE was performed, including zoomed images of the apical four-chamber, two-chamber, and long axis views, with frame rates varying from 55 to 90 frames per second. Three heart beats per image were acquired. These examinations were analyzed off-line by a single researcher (BvK) using dedicated analysis software for both standard echocardiographic parameters, including LV ejection fraction (LVEF) and WMSI, and 2D-STE analysis (EchoPAC version 20, GE Vingmed Ultrasound AS, Horten, Norway). Volumetric measurements were performed according to the current American Heart Association / European Association for Cardiovascular Imaging (AHA / EACVI) standards[14]. Segmental wall motion scoring (WMS) was scored as 1 for normokinetic, 2 for hypokinetic, 3 for akinetic, 4 for dyskinetic, and 5 for aneurysmatic segments. Wall motion scoring was indexed through dividing the sum of wall motion scores by the total number of segments. This resulted in the WMSI, a measure of global myocardial function.

Strain analysis was performed in adherence to the EACVI guidelines [15]. Both the endocardium and epicardium were manually traced and aortic valve closure time was manually set. Poorly tracked segments were excluded from analysis. Results were generated using automated frame-by-frame tracking of acoustic markers [11]. This process entailed an automatic partitioning of the myocardium into even-sized endocardial, mid-myocardial, and epicardial layers. GLS and SLS were extracted, both full-wall and layer-specific (i.e. endocardial and epicardial). Peak systolic strain was defined as the peak strain value within the time span between the R-peak on the ECG and the visually determined closure of the aortic valve. Finally, the transmural strain gradient (TSG) from the endocardial layer to the epicardial layer, according to the method described by Alcidi et al [16], was calculated. Figure 2 depicts an example of the output of strain analysis.

### *CMR*

All patients underwent follow-up contrast-enhanced 1.5 Tesla CMR imaging (Philips Healthcare, Best, The Netherlands). LGE image acquisition was performed 15 minutes after administration of 0.2 ml/kg gadobutrol (Gadovist, Bayer Vital GmbH, Leverkusen, Germany), using prospective ECG-gated sequences of the short axis views from base to apex, with a slice thickness of 5mm. Images were analyzed off-line using Philips ISP9 software (Philips Healthcare, Best, The Netherlands). By utilizing the right ventricular insertion points to the interventricular septum as anatomical landmarks, the heart was divided into 16 segments according to the model of the AHA [17], excluding the apical cap, in concordance with segmental division of the TTE examinations.

LGE was quantitatively assessed using the full width at half maximum (FWHM) method, which yields a percentage value for each of the analyzed segments, as well as a global percentage reflecting scar size of the whole LV. Instances where no scar was observed visually, FWHM results were set to zero. In two patients LGE could not be quantified due to (motion) artefacts, and only visual scar assessment was used. Qualitative assessment of scar localization and transmuralty was noted using the 16-segment AHA model by an experienced cardiovascular radiologist (BV). Transmuralty was scored for each segment, allocating 0 points for no scar, 1 point for subendocardial scar (SES) (LGE < 50% wall thickness) and 2 points for transmural scar (TMS) (LGE ≥ 50% wall thickness), in concordance with existing literature [18]. The summation of points was divided by 16 to retrieve a transmuralty index.

### *Statistical analysis*

SPSS Statistics version 25.0.0.2 (IBM, Armonk, NY, USA) and MedCalc version 19.0.5 (MedCalc Statistical Software, Ostend, Belgium) software was used. Continuous variables underwent normality assessment using the Kolmogorov-Smirnov test, and subsequently presented as mean ± standard deviation (SD) in case of normal distribution or as median [interquartile range (IQR)] in case of non-normal distribution. Categorical data were

presented as count (%).  $P < 0.05$  was considered statistically significant. Inter- and intra-observer (BvK and FK) variability was assessed for each evaluated deformation parameter. GLS, WMSI, and LVEF were compared between patients with no scar, patients with SES, and patients with TMS using the Kruskal-Wallis non-parametric one-way analysis of variance. The Dunn post-hoc analysis was applied in order to specify differences between the different scar groups when significant variance was detected across the entire cohort. Pearson's correlation coefficient was used to correlate aforementioned parameters to scar size determined by CMR, with patients lacking scar on CMR excluded from this analysis. Using the area under the curve (AUC) of receiver operating characteristics (ROC) curves, the sensitivity and specificity of these parameters for identifying patients with any type of scar and patients with TMS were determined. The Hanley & McNeil test was used to compare AUCs between studied parameters.

For segmental analysis, segments were allocated to no scar, SES, or TMS groups. Full-wall SLS, epicardial and endocardial SLS, TSG, and wall motion scoring (WMS) were compared between the scar groups using the one-way analysis of variance (ANOVA) with the Bonferroni post-hoc analysis in case of normally distributed parameters, and with the Kruskal-Wallis non-parametric one-way analysis of variance with the Dunn post-hoc analysis in case of non-normally distributed parameters. ROC-curves were generated and the AUC was calculated in order to generate sensitivity and specificity of each of these parameters for identifying any scar and TMS. AUCs were compared using the Hanley & McNeil test. Finally, SLS (full-wall, endocardial and epicardial) was correlated to the amount of LGE per segment.

## RESULTS

**Table 1 – patient characteristics**

*Patient population and baseline characteristics*

Variable	Value
<b>Age</b> (years)	58.7 ± 1.7
<b>Female sex</b> (n)	5 (11.6)
<b>STEMI</b> (n)	39 (90.7)
<b>Non-STEMI</b> (n)	4 (9.3)
<b>Culprit</b> (n)	
LAD	19 (44.2)
RCA	12 (27.9)
RCx	12 (27.9)
<b>OHCA</b> (n)	2 (4.7)
<b>Time of ischemia</b> (hours) <i>n</i> =42	2.3 [1.5 – 6.6]
<b>CK-max</b> (U/L)	1126 [633 – 2165]
<b>Medical history</b> (n)	
Diabetes	1 (2.3)
Hypertension	10 (23.3)
Hypercholesterolemia	21 (48.8)
TIA/Stroke	4 (9.3)
Smoking	20 (46.5)
<b>Medication</b> (n)	<b>Baseline / follow-up</b>
RAAS-inhibitors	5 (11.4) / 36 (83.7)
Aldosterone antagonist	1 (2.3) / 3 (7.0)
Beta-blockers	3 (7.0) / 37 (86.0)
Antiplatelet therapy	3 (7.0) / 43 (100)
Statin	7 (16.3) / 43 (100)
<b>Baseline Hemodynamics</b>	
Systolic BP (mmHg)	119 ± 24
Diastolic BP (mmHg)	68 ± 14
Heart rate (/min)	70 ± 15
<b>Baseline LV function</b>	
EDV (ml)	112.4 ± 4.5
LVEF (%)	53.9 [49.5 – 57.9]
WMSI	1.31 [1.13 – 1.56]
GLS (%)	-15.3 [-12.9 – -17.0]
<b>Follow-up LV function</b>	
EDV (ml) <i>n</i> =42	113.0 ± 5.2
LVEF (%) <i>n</i> =42	55.0 [52.1 – 59.7]
WMSI <i>n</i> =42	1.13 [1.00 – 1.27]
GLS (%) <i>n</i> =39	-17.0 [-14.5 – -18.0]
<b>Scar size</b> (%) <i>n</i> =41	8.5 ± 0.8

**TABEL 1** Data is depicted as mean ± standard deviation, median [interquartile range] or as n (%). N=43 unless stated otherwise.

STEMI = ST-elevation myocardial infarction; LAD = Left anterior descending artery; RCA = Right coronary artery; RCx = Circumflex coronary artery; OHCA = Out-of-hospital cardiac arrest; CK = creatine kinase; TIA = transient ischemic attack; RAAS = Renin angiotensin aldosterone system; BP = blood pressure; LV = left ventricle; EDV = end-diastolic volume; LVEF = left ventricular ejection fraction; WMSI = wall motion score index; GLS = global longitudinal strain



Table 1 shows the baseline characteristics. A total of 43 patients (5 females, 38 males) admitted with STEMI (n=39) or non-STEMI (n=4) were included. Forty-two patients were revascularized, after a median period of 2.3 hours after onset of complaints; one patient did not undergo percutaneous coronary intervention (PCI) due to delayed presentation missing the window for revascularization. The median highest serum creatine kinase (CK) was 1126 [IQR 633 – 2165] U/L and mean infarct size was  $8.5 \pm 0.8\%$  of the LV. Within the follow-up period, no deaths or new AMIs occurred. Eight patients presented with recurrent chest pain without signs of ischemia.

Baseline TTE was performed after a median of 2 days after admission. CMR and follow-up TTE were performed after a median of 6 months post enrollment (range 4.4 – 9.3 months). Median LVEF did not significantly improve from baseline to follow-up (53.9% to 55.0%,  $P=0.071$ ). However, median GLS (-15.3% to -17.0%,  $p=0.001$ ) and median WMSI (1.31 to 1.13,  $p<0.001$ ) did improve significantly.

### Global analysis

**Table 2 – Mean global function parameters per scar type**

	NS (n=7)	AS (n=36)	SES (n=13)	TMS (n=23)	P
<b>GLS (%)</b>	-16.3 [-17.5 – -15.3]	-14.7 [-16.9 – -12.7]	-16.2 [-17.3 – -14.1]	-14.3 [-17.0 – -9.9]	0.182
<b>LVEF (%)</b>	53.9 [52.2 – 56.8]	54.5 [48.0 – 58.1]	56.2 [50.1 – 57.9]	53.1 [45.8 – 58.2]	0.453
<b>WMSI</b>	1.06 [1 – 1.13]	1.31 [1.19 – 1.56]	1.13 [1 – 1.38]	1.38 [1.19 – 1.63]	0.005*

\*NS vs AS:  $P = 0.026$ ; NS vs SES:  $P = 1.0$ ; NS vs TMS:  $P = 0.014$ ; SES vs TMS:  $P = 0.047$

NS = no scar; AS = any scar; SES = subendocardial scar; TMS = transmural scar; GLS = global longitudinal strain; LVEF = left ventricular ejection fraction; WMSI = wall motion score index

Table 2 shows the results of global parameters per scar type. Median GLS was -16.3% in patients without any scar, compared to -16.2% in patients with subendocardial scar and -14.3 in patients with transmural scar. However, these differences did not reach statistical significance ( $P>0.05$ ). Similarly, LVEF did not display significant variations across the different scar types. Conversely, the WMSI exhibited the capacity to differentiate between patients with any scar and those without scar (1.31 vs 1.06,  $p = 0.026$ ). Furthermore, the WMSI was significantly different between patients with transmural scar and patients with subendocardial scar (1.38 vs 1.13,  $p = 0.047$ ).

Figure 3 displays correlation graphs illustrating the relationship between the global parameters and both scar size and transmural index. The WMSI exhibited the strongest correlation with scar size ( $r^2=0.32$ ,  $p<0.001$ ), followed by GLS ( $r^2=0.24$ ,  $p=0.002$ ) and LVEF ( $r^2=0.15$ ,  $p=0.016$ ). A comparable yet slightly stronger correlation was observed when using the transmural index ( $r^2=0.38$ ,  $p<0.001$  for WMSI;  $r^2=0.37$ ,  $p<0.001$  for GLS; and  $r^2=0.21$ ,  $P=0.002$  for LVEF).

Figure 3 – Correlation between global functional parameters vs scar size and transmural index

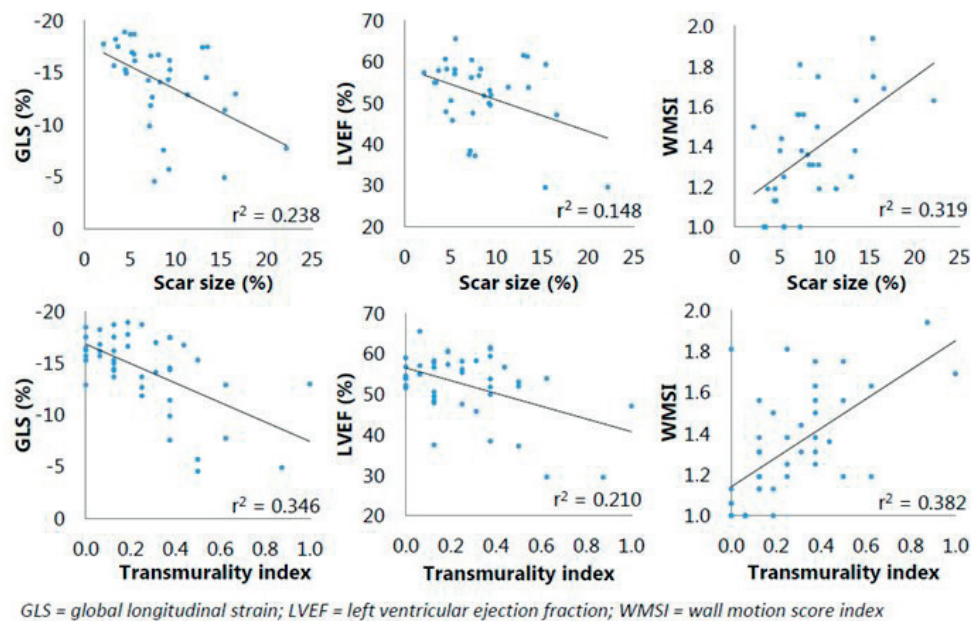
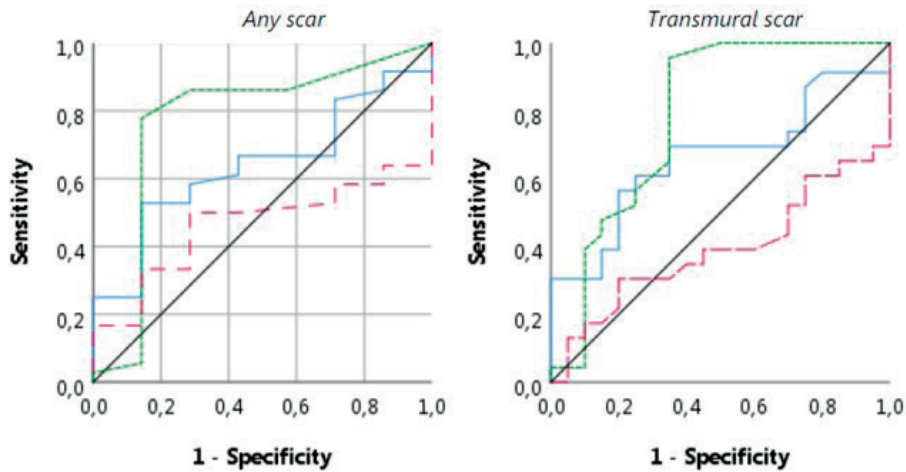


Figure 4 showcases the ROC-curves for each of the global parameters, evaluating their predictive capabilities for the presence of scar and transmural scar formation. WMSI was significantly superior to LVEF in predicting scar ( $p=0.036$ ) and predicting transmural scar ( $p=0.026$ ). Conversely, no significant difference was observed between WMSI and GLS ( $p=0.316$  for predicting any scar and  $p=0.193$  for predicting transmural scar), and GLS and LVEF ( $p=0.364$  for predicting any scar and  $p=0.459$  for predicting transmural scar).

*Segmental and layer-specific longitudinal strain*

A total of 683 segments were analyzed from the baseline TTE (99.3%). Five segments were excluded due to poor tracking or visualization. CMR revealed 571 normal segments, while 42 segments displayed subendocardial scar (SES) and 70 segments displayed transmural scar (TMS). The five segments excluded from TTE analysis showed no scar on CMR. Table 3 shows the comparison of full-wall segmental longitudinal strain (SLS), endocardial SLS, epicardial SLS, TSG and WMS per scar type.

**Figure 4 - ROC curves of segmental strain to predict for any scar and transmural scar**

Any scar	Legend	Cut-off	Sensitivity	Specificity	AUC	P
GLS	—	-15.5	58.3	71.4	0.639	0.25
LVEF	- - -	54.8	50.0	71.4	0.464	0.767
WMSI	...	1.16	77.8	85.7	0.768	0.026
Transmural scar	Legend	Cut-off	Sensitivity	Specificity	AUC	P
GLS	—	-15.5	69.6	65.0	0.662	0.07
LVEF	- - -	55.2	39.1	45.0	0.391	0.223
WMSI	...	1.16	95.7	65.0	0.783	0.002

ROC = Receiver operating characteristic; AUC = area under the curve; GLS = global longitudinal strain; WMSI = wall motion score index; LVEF = left ventricular ejection fraction

**Table 3 – Segmental deformation results**

	NS (n=571)	AS (n=112)	SES (n=42)	TMS (n=70)	P
<b>SLS Full-wall (%)</b>	-15.7 [-19.2 – -12.1]	-8.4 [-13.6 – -3.9]	-10.5 [-14.6 – -6.2]	-6.6 [-13.3 – -0.6]	<0.001*
<b>SLS Endo (%)</b>	-17.2 [-22.3 – -13.1]	-9.7 [-14.6 – -4.6]	-11.7 [-15.4 – -6.9]	-8.2 [-13.8 – -3.2]	<0.001**
<b>SLS Epi (%)</b>	-13.9 [-16.9 – -11.0]	-7.7 [-12.6 – -3.7]	-9.2 [-14.5 – -5.8]	-6.9 [-12.1 – -2.6]	<0.001†
<b>TSG</b>	-2.8 [-0.8 – -7.6]	-1.4 [-3.1 – 0.3]	-1.4 [-2.9 – 0.1]	-1.2 [-3.1 – 0.4]	<0.001††
<b>WMS</b>	1.21 ± 0.49	1.88 ± 0.77	1.67 ± 0.65	2.01 ± 0.81	<0.001‡

\*NS vs AS: P<0.001 ; NS vs SES: P<0.001; NS vs TMS: P<0.001; SES vs TMS: P=0.527

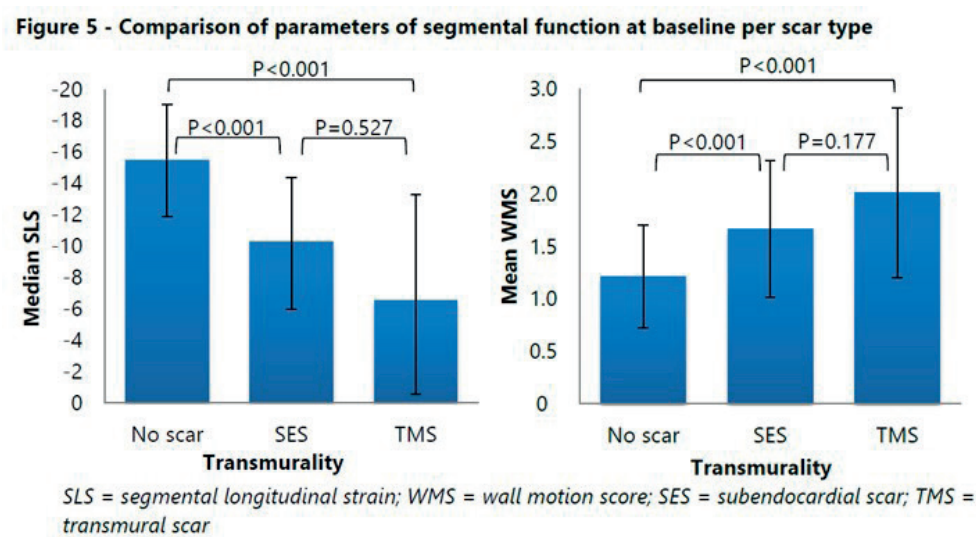
\*\*NS vs AS: P<0.001 ; NS vs SES: P<0.001; NS vs TMS: P<0.001; SES vs TMS: P=0.840

†NS vs AS: P<0.001 ; NS vs SES: P<0.001; NS vs TMS: P<0.001; SES vs TMS: P=0.261

††NS vs AS: P<0.001 ; NS vs SES: P=0.005; NS vs TMS: P<0.001; SES vs TMS: P=0.896

‡ NS vs AS: P<0.001 ; NS vs SES: P<0.001; NS vs TMS: P<0.001; SES vs TMS: P=0.177

NS = no scar; AS = any scar; SES = subendocardial scar; TMS = transmural scar; SLS = segmental longitudinal strain; TSG = transmural strain gradient; WMS = wall motion score

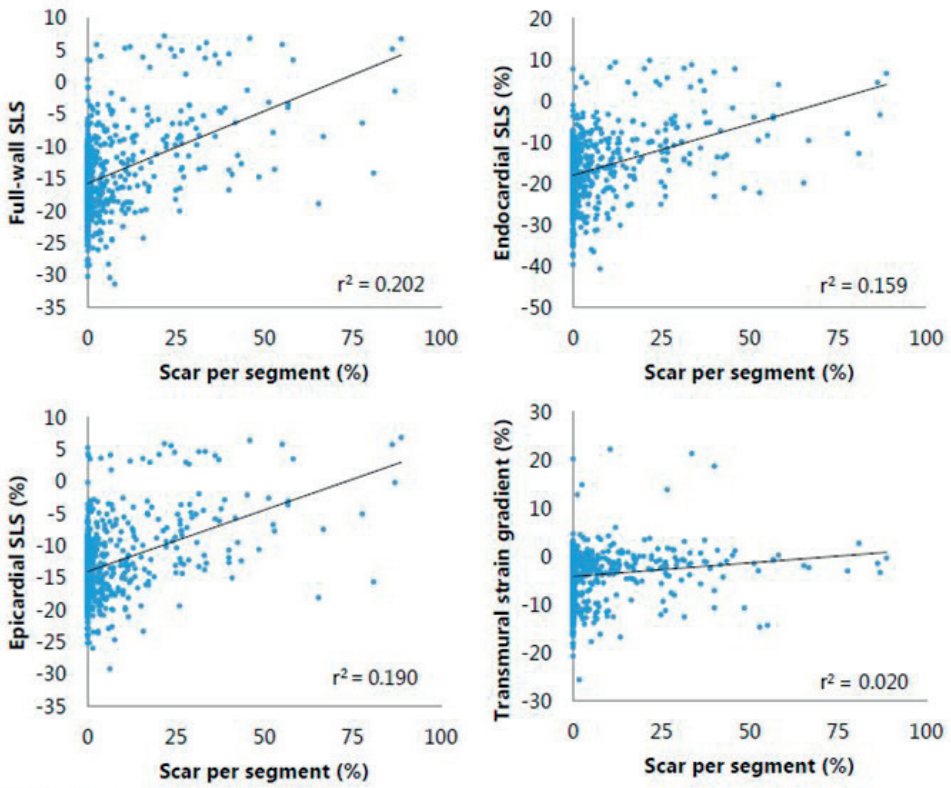


Median SLS was found to be -15.7% in non-scarred segments, compared to -8.4% in scarred segments (-10.5% for SES and -6.6% for TMS). Similar trends were noted in the evaluation of endocardial and epicardial SLS. Mean WMS was 1.21 for non-scarred segments, compared to 1.88 in scarred segments (1.67 for SES and 2.01 for TMS). TSG showed a decreasing trend from non-scarred to TMS segments. All parameters could significantly discriminate ( $P < 0.05$ ) between segments devoid of scar formation and those exhibiting either SES or TMS six months post AMI. However, it is noteworthy that there was no statistical difference between the SES and the TMS groups for each of the parameters. Bar charts of mean WMS and median full-wall SLS are shown in Figure 5.

Figure 6 depicts correlation graphs of layer-specific deformation parameters with segmental LGE percentage. Full-wall SLS exhibited the strongest correlation with LGE ( $r^2 = 0.202$ ,  $p < 0.001$ ). The TSG demonstrated a weak correlation with LGE ( $r^2 = 0.020$ ,  $p < 0.001$ ). Neither epicardial nor endocardial SLS could reliably differentiate scarred from non-scarred segments, nor discriminate between SES and TMS.

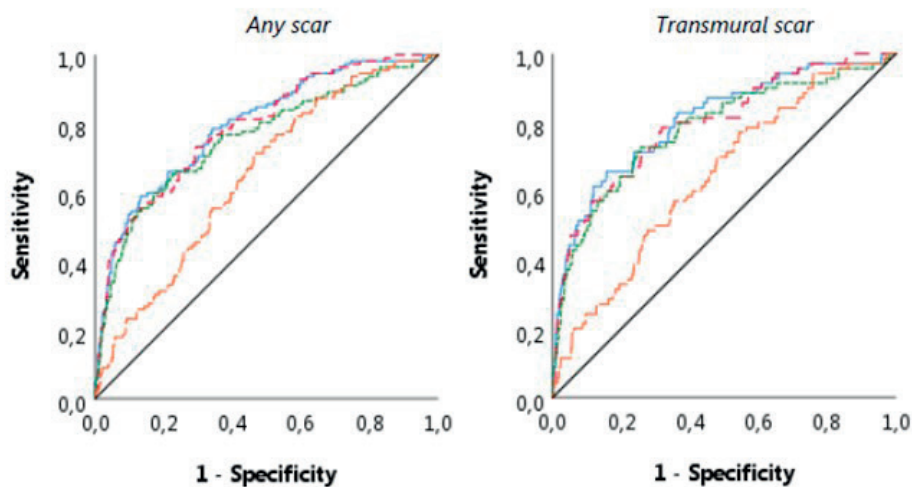
Figure 7 presents ROC-curves, along with sensitivity, specificity, and AUC for full-wall, endocardial, and epicardial SLS, as well TSG, for identifying any scar and identifying TMS. All parameters displayed fair to good accuracy. At a threshold of -13.3%, for full-wall SLS, the sensitivity and specificity were found to be 70.8% and 68.9% respectively, with an AUC of 0.791, for identifying any scarred segment. Regarding the identification of TMS segments, full-wall SLS demonstrated a sensitivity of 71.0% and a sensitivity of 76.0% at a cut-off of -11.5% (AUC 0.809). This implies that SLES of -11.5% - -13.3% predicts for SES. Figure 1 is a graphical representation of these results. Layer-specific SLS yielded similar outcomes to mid-wall SLS. The TSG showed a significantly smaller AUC compared to the other studied parameters, when predicting for either any scar or TMS formation.

Figure 6 – Correlation between segmental strain and segmental scar



SLS = segmental longitudinal strain

Figure 7 – ROC curves of segmental strain to predict for any scar and transmural scar



Any scar	Legend	Cut-off	Sensitivity	Specificity	AUC	P
SLS full-wall	————	-13.3	70.8	68.9	0.791	<0.001
SLS endo	- - - - -	-14.0	71.7	71.0	0.780	<0.001
SLS epi	. . . . .	-12.0	70.0	68.9	0.759	<0.001
TSG	- . - . -	2.01	60.2	58.4	0.635	<0.001
Transmural scar	Legend	Cut-off	Sensitivity	Specificity	AUC	P
SLS full-wall	————	-11.5	71.0	76.7	0.809	<0.001
SLS endo	- - - - -	-13.2	72.5	72.4	0.796	<0.001
SLS epi	. . . . .	-10.9	72.5	74.8	0.781	<0.001
TSG	- . - . -	2.01	59.4	59.1	0.638	<0.001

ROC = Receiver operating characteristic; AUC = area under the curve; SLS = segmental longitudinal strain; Endo = endocardial; Epi = epicardial; TSG = transmural strain gradient.

## DISCUSSION

Our study on the value of early regional assessment of myocardial function following myocardial infarction yielded four main findings: 1) SLS in the period after AMI can identify scarred segments, as well as segments in which the scar is transmural. Our data showed that segmental functional impairment with  $SLS < -13.3\%$  is predominantly due to stunning since these segments were less associated with scar formation at follow-up.  $SLS > -13.3\%$  predicts scar, and  $SLS > -11.5\%$  is associated with the formation of transmural scar at follow-up, implying that  $SLS$  of  $-11.5\% - -13.3\%$  predicts SES. 2) Layer-specific SLS and TSG do not provide incremental predictive value over full-wall SLS in the identification of scar. 3) Neither GLS nor SLS are superior to WMS in identifying segments in which scar forms after AMI. Nonetheless, SLS provides more detailed information on myocardial function than WMS and allows for determining a cut-off point for scar transmural, rendering it a more precise tool for determining scar transmural. Furthermore, it needs less of an expert eye than WMS analysis, highlighting its potential in clinical practice. 4) GLS exhibits a reasonable correlation with scar size, but its predictive performance does not surpass that of WMSI. Noteworthy, LVEF correlates weakly to scar size. GLS is not suitable to detect scar transmural.

### *Scar size*

We found a moderate correlation between GLS and scar size, as well as between WMSI and scar size. Similar research in patients with chronic ischemic heart failure has demonstrated reasonably strong correlations between GLS and scar size [19]. The first study reporting the relation between GLS shortly after AMI and subsequent scar size exhibited a strong correlation between segmental strain 1.5 hours after AMI and scar size measured with LGE CMR 8 months later. This correlation was stronger than the correlation between WMS and scar size [20]. Since then, evidence on the relation between GLS and scar size and scar transmural has expanded, showing overall moderate to good correlation between GLS and scar size and typically outperforming LVEF [21,22]. In a very similar study design as our study's, albeit conducting strain analysis some days later, Grabka et al [23] showed moderate correlations between GLS and infarct size. Interestingly, two abovementioned studies [23,24] found WMSI to reliably identify extensive infarction, whereas none correlated WMSI to infarct size, suggesting that wall motion analysis is not inferior to strain analysis with regard to scar size prediction. Finally, Trivedi et al [25] reliably correlated GLS as well as SLS to scar size measured by invasive electro-anatomical mapping in patients with chronic ischemic heart disease.

To summarize, the results of the present study are in line with the available body of evidence, although we found weaker correlations between scar size and GLS. A possible explanation could stem from the composition of our study population. A fair number of included patients suffered from small myocardial infarctions and displayed good global



LV function (mean LVEF at baseline was  $52.3 \pm 1.3\%$ ) upon enrollment. The smaller scars and fewer scarred segments possibly hampered meaningful correlations to deformation parameters. Also, previous literature was conducted in patients who underwent thrombolytic therapy instead of PCI [26]. Therefore, our study likely underestimates the utility of GLS after acute ischemic events. Nonetheless, the findings do suggest a modest diagnostic utility in patients with small myocardial infarctions. Another possible factor contributing to the discrepancy between the current study and the previously cited literature is the heterogeneity of definitions for scar transmural, as well as the diverse methodologies employed in scar size determination, which are sometimes not explicitly delineated. The FWHM method emerges as the most accurate among the assessed semi-automated infarct size quantification methods [27], but becomes less reliable when there is no or only very subtle myocardial scar. This might be of significant importance in our population of patients with relatively low CK-levels. This argument is underlined by the finding of a stronger correlation between GLS and transmural index – a semi-quantitative measure of scar size. Finally, GLS and LVEF are influenced by compensatory hypermobility of healthy segments, while WMSI is not. Consequently, this may account for the superior capability of the WMSI over LVEF in predicting cardiovascular events after AMI [28]. It is important to emphasize that WMSI is a relatively subjective parameter of systolic function and does require extensive training and experience to be reliably determined.

### *Scar transmural*

We demonstrate that GLS does not significantly differ between patients without scar, those with subendocardial scar and those with transmural scar. Global parameters are likely unsuitable for assessing scar transmural, primarily due to the previously mentioned compensatory hypermobility in non-infarcted segments, leading to an overall normal global function. As anticipated, SLS was a superior parameter in detecting scar transmural. The determined optimal cut-off points of -13.3% for predicting formation of any scar and -11.5% for transmural scar yielded sensitivities and specificities of 68.9% and 76.7% respectively. These findings underscore the potential of 2D-STE as an easy and readily available tool for identifying patients with viability in the scarred region.

Since the era of tissue Doppler strain rate imaging, efforts are made to apply this technique in determining scar transmural post AMI [29], although study designs have been heterogeneous and not all studies utilize CMR as reference modality. Literature reports cut-offs for SLS ranging from -12.3% to -13.5% for predicting any scar formation [30,31]. Cut-off values for identifying transmurally scarred segments range from -11.5% to -15.1% [31–33]. In summary, our reported cut-off values are in line with existing literature regarding scar transmural. However, since the evidence is relatively limited and strain analysis is not routinely applied in daily practice in the quest for scar assessment in the post-infarct period, this study adds to the body of evidence. Furthermore, to our

knowledge, our study is the first to investigate the value of both full-wall strain assessment as well layer-specific strain analysis in diagnosing myocardial scar.

#### *Layer-specific analysis*

Acute ischemia first affects the subendocardium but may leave the epicardium unaffected, hypothetically resulting in a loss of longitudinal systolic function of the subendocardium while leaving the epicardium unaffected. Current software facilitates the distinction of longitudinal strain parameters within these layers [34]. The subendocardium consists of obliquely oriented fibers in a clockwise direction, mainly contributing to longitudinal function [35]. Therefore, layer-specific longitudinal strain analysis is of interest in the discrimination of segments devoid of scar and those with SES, as well as between SES and TMS.

We demonstrate that both epicardial and endocardial SLS are significantly lower according to increasing scar transmural. Layer specific strain does not appear to confer incremental value beyond full-wall longitudinal strain, particularly in differentiating between SES and TMS. Moreover, the correlation between layer-specific SLS and segmental LGE is weak. These findings are of importance since the literature on layer-specific strain analysis concerning transmural assessment is ambiguous. Our findings are in line with the literature on layer-specific deformation in patients with chronic ischemic LV dysfunction [36,37]. However, in a similar study population, Becker et al [38] demonstrate that endocardial strain outperforms full wall strain in scar transmural identification, implying its potential use in non-acute evaluations. Conversely, Unlu et al [39] found no additional value of layer-specific strain over full wall strain when identifying dysfunctional segments. Notably, significant inter-vendor variability and poor reproducibility were observed. Possible explanations for our findings include the hypothesis that AMI induces transmural effects in deformation across all the myocardial layers, even when the eventual scar is not transmural after rescue PCI. Moreover, the different myocardial layers are not structurally separated from each other, and this continuity between layers could hinder the precise reflection of each layer's characteristics in layer-specific measurements. Finally, high spatial resolution is pivotal for accurate layer differentiation. Even though it is stated that layer-specific strain might independently hold prognostic value, there seems to be a discrepancy on which layer – endocardial or epicardial – gives the most relevant prognostic information [40,41].

Consistent with existing literature [42] and in line with our initial hypothesis, we found the highest transmural strain gradients in regions remote to the ischemia, while this gradient diminishes in the presence of a scar. However, despite these differences, we found that the TSG cannot reliably differentiate between SES and TMS in our population. Literature concerning this matter is ambiguous, ranging from a maintained gradient in both SES and TMS [34, 36] to a diminished gradient in patients with significant non-STEMI [43].

### *Limitations*

This study is mainly limited by its population size, resulting from both the prospective nature of the study as well as the fact that strain analysis was only possible in 43 out of 79 patients in the cohort. Five patients did not undergo TTE at baseline for logistical reasons, whereas 2 patients had insufficient TTE quality for strain analysis. The remaining patients underwent TTE on a machine from a different vendor than GE, and were excluded to avoid inter-vendor variability. However, given the prospective nature of this trial, we do not expect this to result in selection or reporting bias. Since this was a sub-study, there was no power analysis performed for this specific research question. The modest study population makes investigation of subpopulations within this study, such as a comparison of the different infarct types or regions or determining sex or age group specific cut-off values, not feasible. Furthermore, the relatively modest infarct size, probably attributed to swift revascularization in the majority of our patients, should be acknowledged. Moreover, there are considerations in the timing of the investigations. Although ideally performed immediately following AMI, the baseline TTE is performed up to four days after inclusion, for logistical reasons. Within this period, some functional recovery may have occurred, although current literature suggests that functional recovery in the days following AMI is limited [44]. Additionally, there is variation in the follow-up examinations, spanning from 4.4 to 9.3 months, although we anticipate little influence on our findings as the process of remodeling and scar stabilization mainly occurs within 2 months of AMI [44].

Additional deformation parameters, such as post-systolic shortening and pre-stretch, were not studied to ensure the practical applicability in daily practice. We only performed strain analysis using GE as the vendor of choice; other vendors that use different algorithms, especially for layer-specific analysis, might yield different results. An inherent issue when comparing TTE to CMR lies in the assumption of segment alignment, which may not be fully achieved despite maintaining anatomical landmarks for segment demarcation. Furthermore, although the FWHM method is the most reliable available technique for scar assessment, it may be prone to overestimating scar, particularly in patients with limited LGE or abundant vascular structures in the myocardium. However, error was at least partially overcome by manually setting scar size to 0% in patients in whom no scar was visible.

## **CONCLUSION AND CLINICAL IMPLICATIONS**

We demonstrate that 2D-STE derived SLS in the period following AMI is an easy and non-invasive tool with the potential to predict the transmural extent of scar six months after AMI. This holds promise for expediting clinical decision making, such as early initiation of antifibrotic therapy, by circumventing the logistical challenges of CMR. The advantage over WMS analysis, which also proved to be a good predictor for scar formation, is that strain analysis is quantitative and easily performed, and requires less of an expert eye to yield reliable results. GLS correlates well with scar size and might be used as a prognostic

tool, given that scar size is associated with adverse outcome. Within our cohort, layer-specific longitudinal strain has no incremental value over full-wall strain in predicting scar transmural. This study adds to a growing body of evidence, and is to be seen as an initiator for future research involving larger study populations to further elucidate the value of strain analysis in predicting scar formation shortly after AMI.

## ACKNOWLEDGEMENTS

The authors acknowledge Chris van Kesteren (University Medical Center Utrecht) for his help with the figure design in this manuscript, and Peter Paul Zwetsloot for his help with statistical analysis.

## DATA AVAILABILITY STATEMENT

*The data underlying this article will be shared on reasonable request to the corresponding author.*

## CONFLICTS OF INTEREST

The authors declare no conflicts of interest.

## HUMAN RIGHTS STATEMENTS AND INFORMED CONSENT

All procedures followed were in accordance with the ethical standards of the responsible committee on human experimentation (institutional and national) and with the Helsinki Declaration of 1964 and later versions. Informed consent was obtained from all patients for being included in the study.

## REFERENCES

1. Widimsky P, Wijns W, Fajadet J, et al. Reperfusion therapy for ST elevation acute myocardial infarction in Europe: description of the current situation in 30 countries. *Eur Heart J*. 2010;31:943–57. doi: 10.1093/eurheartj/ehp492
2. Ibanez B, James S, Agewall S, et al. 2017 ESC Guidelines for the management of acute myocardial infarction in patients presenting with ST-segment elevation The Task Force for the management of acute myocardial infarction. *Eur Heart J*. 2018;39:119–77. doi: 10.1093/eurheartj/ehx393
3. Hartley A, Marshall DC, Saliccioli JD, et al. Trends in Mortality From Ischemic Heart Disease and Cerebrovascular Disease in Europe: 1980 to 2009. *Circulation*. 2016;133:1916–26. doi: 10.1161/CIRCULATIONAHA.115.018931
4. Hadamitzky M, Langhans B, Hausleiter J, et al. Prognostic value of late gadolinium enhancement in cardiovascular magnetic resonance imaging after acute ST-elevation myocardial infarction in comparison with single-photon emission tomography using Tc99m-Sestamibi. *Eur Heart J Cardiovasc Imaging*. 2014;15:216–25. doi: 10.1093/ehjci/jet176
5. Greenwood JP, Herzog BA, Brown JM, et al. Prognostic value of cardiovascular magnetic resonance and single-photon emission computed tomography in suspected coronary heart disease: Long-term follow-up of a prospective, diagnostic accuracy cohort study. *Ann Intern Med*. 2016;165:1–9. doi: 10.7326/M15-1801
6. Patel MR, White RD, Abbara S, et al. 2013 ACCF/ACR/ASE/ASNC/SCCT/SCMR Appropriate Utilization of Cardiovascular Imaging in Heart failure: A joint report of the American college of Radiology appropriateness criteria committee and the American college of cardiology foundation appropriate use criteria task force. *J Am Coll Cardiol*. 2013;61:2207–31. doi: 10.1016/j.jacc.2013.02.005
7. Schwitter J, Arai AE. Assessment of cardiac ischaemia and viability: Role of cardiovascular magnetic resonance. *Eur Heart J*. 2011;32:799–809. doi: 10.1093/eurheartj/ehq481
8. Ibrahim T, Hackl T, Nekolla SG, et al. Acute myocardial infarction: Serial cardiac MR imaging shows a decrease in delayed enhancement of the myocardium during the 1st week after reperfusion. *Radiology*. 2010;254:88–97. doi: 10.1148/radiol.09090660
9. Allman KC, Shaw LJ, Hachamovitch R, et al. Myocardial viability testing and impact of revascularization on prognosis in patients with coronary artery disease and left ventricular dysfunction: A meta-analysis. *J Am Coll Cardiol*. 2002;39:1151–8. doi: 10.1016/s0735-1097(02)01726-6
10. Van Mourik MJW, Zaar DVJ, Smulders MW, et al. Adding Speckle-Tracking Echocardiography to Visual Assessment of Systolic Wall Motion Abnormalities Improves the Detection of Myocardial Infarction. *J Am Soc Echocardiogr*. 2018;32:65–73. doi: 10.1016/j.echo.2018.09.007
11. Teske AJ, De Boeck BWL, Melman PG, et al. Echocardiographic quantification of myocardial function using tissue deformation imaging, a guide to image acquisition and analysis using tissue Doppler and speckle tracking. *Cardiovasc Ultrasound*. 2007;30:5:27. doi: 10.1186/1476-7120-5-27

12. Altiok E, Neizel M, Tiemann S, et al. Layer-specific analysis of myocardial deformation for assessment of infarct transmural: Comparison of strain-encoded cardiovascular magnetic resonance with 2D speckle tracking echocardiography. *Eur Heart J Cardiovasc Imaging*. 2013;14:570–8. doi: 10.1093/ehjci/jes229
13. Nagata Y, Wu VCC, Otsuji Y, et al. Normal range of myocardial layer-specific strain using two-dimensional speckle tracking echocardiography. *PLoS One*. 2017;12:e0180584. doi: 10.1371/journal.pone.0180584.
14. Lang RM, Badano LP, Victor MA, et al. Recommendations for cardiac chamber quantification by echocardiography in adults: An update from the American Society of Echocardiography and the European Association of Cardiovascular Imaging. *Eur Heart J Cardiovasc Imaging*. 2015;16:233–70. doi: 10.1093/ehjci/jev014
15. Voigt JU, Pedrizzetti G, Lysyansky P, et al. Definitions for a common standard for 2D speckle tracking echocardiography: consensus document of the EACVI/ASE/Industry Task Force to standardize deformation imaging. *Eur Heart J Cardiovasc Imaging*. 2015;16:1–11. doi: 10.1093/ehjci/jeu184
16. Alcidì GM, Esposito R, Evola V, et al. Normal reference values of multilayer longitudinal strain according to age decades in a healthy population : A single-centre experience. *Eur Heart J Cardiovasc Imaging*. 2018;19:1390–6. doi: 10.1093/ehjci/jex306
17. Cerqueira MD, Weissman NJ, Dilsizian V, et al. Standardized Myocardial Segmentation and Nomenclature for Tomographic Imaging of the Heart: A Statement for Healthcare Professionals From the Cardiac Imaging Committee of the Council on Clinical Cardiology of the American Heart Association. *Circulation*. 2002;105:539–42. doi: 10.1161/hc0402.102975
18. Romero J, Xue X, Gonzalez W, et al. CMR imaging assessing viability in patients with chronic ventricular dysfunction due to coronary artery disease: A meta-analysis of prospective trials. *JACC Cardiovasc Imaging*. 2012;5:494–508. doi: 10.1016/j.jcmg.2012.02.009
19. Roes SD, Mollema SA, Lamb HJ, et al. Validation of Echocardiographic Two-Dimensional Speckle Tracking Longitudinal Strain Imaging for Viability Assessment in Patients With Chronic Ischemic Left Ventricular Dysfunction and Comparison With Contrast-Enhanced Magnetic Resonance Imaging. *Am J Cardiol*. 2009;104:312–7. doi: 10.1016/j.amjcard.2009.03.040
20. Vartdal T, Brunvand H, Pettersen E, et al. Early Prediction of Infarct Size by Strain Doppler Echocardiography After Coronary Reperfusion. *J Am Coll Cardiol*. 2007;49:1715–21. doi: 10.1016/j.jacc.2006.12.047
21. Sjøli B, Ørn S, Grenne B, et al. Comparison of Left Ventricular Ejection Fraction and Left Ventricular Global Strain as Determinants of Infarct Size in Patients with Acute Myocardial Infarction. *J Am Soc Echocardiogr*. 2009; 22:1232–8. doi: 10.1016/j.echo.2009.07.027
22. Huttin O, Marie PY, Benichou M, et al. Temporal deformation pattern in acute and late phases of ST-elevation myocardial infarction: incremental value of longitudinal post-systolic strain to assess myocardial viability. *Clin Res Cardiol*. 2016;105:815–26.

23. Grabka M, Wita K, Tabor Z, et al. Prediction of infarct size by speckle tracking echocardiography in patients with anterior myocardial infarction. *Coron Artery Dis.* 2013;24:127–34. doi: 10.1007/s00392-016-0989-6
24. Bendary A, Afifi M, Tawfik W, et al. The predictive value of global longitudinal strain on late infarct size in patients with anterior ST-segment elevation myocardial infarction treated with a primary percutaneous coronary intervention. *Int J Cardiovasc Imaging.* 2019;35:339–46. doi: 10.1007/s10554-018-1498-7
25. Trivedi SJ, Campbell T, Davey CJ, et al. Longitudinal strain with speckle-tracking echocardiography predicts electroanatomic substrate for ventricular tachycardia in nonischemic cardiomyopathy patients. *Heart Rhythm O2.* 2022;3:176–85. doi: 10.1016/j.hroo.2022.02.002
26. Sjøli B, Ørn S, Grenne B, et al. Comparison of Left Ventricular Ejection Fraction and Left Ventricular Global Strain as Determinants of Infarct Size in Patients with Acute Myocardial Infarction. *J Am Soc Echocardiogr.* 2009;22:1232–8. doi: 10.1016/j.echo.2009.07.027
27. Flett AS, Hasleton J, Cook C, et al. Evaluation of techniques for the quantification of myocardial scar of differing etiology using cardiac magnetic resonance. *JACC Cardiovasc Imaging.* 2011;4:150–6. doi: 10.1016/j.jcmg.2010.11.015
28. Jurado-Román A, Agudo-Quílez P, Rubio-Alonso B, et al. Superiority of wall motion score index over left ventricle ejection fraction in predicting cardiovascular events after an acute myocardial infarction. *Eur Heart J Acute Cardiovasc Care.* 2019;8:78–85. doi: 10.1177/2048872616674464
29. Zhang Y, Chan AKY, Yu CM, et al. Strain rate imaging differentiates transmural from non-transmural myocardial infarction: A validation study using delayed-enhancement magnetic resonance imaging. *J Am Coll Cardiol.* 2005;46:864–71. doi: 10.1016/j.jacc.2005.05.054
30. Rost C, Rost MC, Breithardt OA, et al. Relation of functional echocardiographic parameters to infarct scar transmural by magnetic resonance imaging. *J Am Soc Echocardiogr.* 2014;27:767–74. doi: 10.1016/j.echo.2014.02.004
31. Cimino S, Canali E, Petronilli V, et al. Global and regional longitudinal strain assessed by two-dimensional speckle tracking echocardiography identifies early myocardial dysfunction and transmural extent of myocardial scar in patients with acute ST elevation myocardial infarction and relatively. *Eur Heart J Cardiovasc Imaging.* 2013;14:805–11. doi: 10.1093/ehjci/jes295
32. Ben Driss A, Lepage C, Sfaxi A, et al. Strain predicts left ventricular functional recovery after acute myocardial infarction with systolic dysfunction. *Int J Cardiol.* 2020;307:1–7.
33. Sjøli B, Ørn S, Grenne B, et al. Diagnostic Capability and Reproducibility of Strain by Doppler and by Speckle Tracking in Patients With Acute Myocardial Infarction. *JACC Cardiovasc Imaging.* 2009;2:24–33. doi: 10.1016/j.ijcard.2020.02.039
34. Adamu U, Schmitz F, Becker M, et al. Advanced speckle tracking echocardiography allowing a three-myocardial layer-specific analysis of deformation parameters. *Eur J Echocardiogr.* 2009;10:303–8. doi: 10.1093/ejehocard/jen238
35. Greenbaum RA, Ho SY, Gibson DG, et al. Left ventricular fibre architecture in man. *Br Heart J.* 1981;45:248–63. doi: 10.1136/hrt.45.3.248

36. Tarascio M, Leo LA, Klersy C, et al. Speckle-Tracking Layer-Specific Analysis of Myocardial Deformation and Evaluation of Scar Transmurality in Chronic Ischemic Heart Disease. *J Am Soc Echocardiogr.* 2017;30:667–75. doi: 10.1016/j.echo.2017.03.015
37. Koos R, Altiok E, Doetsch J, et al. Layer-specific strain-encoded MRI for the evaluation of left ventricular function and infarct transmurality in patients with chronic coronary artery disease. *Int J Cardiol.* 2013;166:85–9. doi: 10.1016/j.ijcard.2011.10.004
38. Becker M, Ocklenburg C, Altiok E, et al. Impact of infarct transmurality on layer-specific impairment of myocardial function: A myocardial deformation imaging study. *Eur Heart J.* 2009;30:1467–76. doi: 10.1093/eurheartj/ehp112
39. Ünlü S, Mirea O, Pagourelas ED, et al. Layer-Specific Segmental Longitudinal Strain Measurements: Capability of Detecting Myocardial Scar and Differences in Feasibility, Accuracy, and Reproducibility, Among Four Vendors A Report From the EACVI-ASE Strain Standardization Task Force. *J Am Soc Echocardiogr.* 2019;32:624–32.e11. doi: 10.1016/j.echo.2019.01.010
40. Abou R, Goedemans L, Montero-Cabezas JM, et al. Prognostic Value of Multilayer Left Ventricular Global Longitudinal Strain in Patients with ST-segment Elevation Myocardial Infarction with Mildly Reduced Left Ventricular Ejection Fractions. *Am J Cardiol* 2021;152:11–8. doi: 10.1016/j.amjcard.2021.04.033
41. Liu C, Jiang SQ, Li J, et al. Prognostic potential of layer-specific global longitudinal strain in patients with non-ST-segment elevated acute coronary syndrome and preserved left ventricular ejection fraction. *Int J Cardiovasc Imaging.* 2021;37:1301–9.
42. Shi J, Pan C, Kong D, et al. Left Ventricular Longitudinal and Circumferential Layer-Specific Myocardial Strains and Their Determinants in Healthy Subjects. *Echocardiography.* 2016;33:510–8. doi: 10.1007/s10554-020-02119-6
43. Sarvari SI, Haugaa KH, Zahid W, et al. Layer-specific quantification of myocardial deformation by strain echocardiography may reveal significant CAD in patients with non-ST-segment elevation acute coronary syndrome. *JACC Cardiovasc Imaging.* 2013;6:535–44. doi: 10.1016/j.jcmg.2013.01.009
44. Ørn S, Manhenke C, Greve OJ, et al. Microvascular obstruction is a major determinant of infarct healing and subsequent left ventricular remodelling following primary percutaneous coronary intervention. *Eur Heart J.* 2009;30:1978–85. doi: 10.1093/eurheartj/ehp219



## CHAPTER

# 3

# Predicting scar transmural after acute myocardial infarction; myocardial function assessment by echocardiographic derived global and segmental myocardial work

Van Klarenbosch BR, Driessen HE, Kirkels FP, Cramer MJ, Velthuis BK,  
Vos MA, Chamuleau SAJ, Ter Meulen - De Jong S, Teske AJ

## ABSTRACT

**Purpose:** Myocardial work analysis using derived pressure-strain loops holds potential for more reliable and loading-independent assessment of myocardial function in the setting of myocardial infarction and scar. We studied 1) temporal changes of parameters of global myocardial function, global strain and global work indices between the days following acute myocardial infarction (AMI) and at follow-up after 4-6 months, and 2) the diagnostic value of both global and segmental myocardial work indices in identifying scar tissue and determining scar transmuralty.

**Methods:** Twenty patients with first time AMI were prospectively included. Echocardiography was conducted in the days following admission and 4-6 months thereafter, concurrent with cardiac magnetic resonance imaging with delayed enhancement assessment.

**Results:** Global longitudinal strain (GLS) ( $p<0.001$ ), global work index ( $p=0.011$ ), global work efficiency (GWE) ( $p=0.028$ ) and global constructive work ( $p=0.050$ ), but not global wasted work ( $p=0.165$ ), improved from days to months after AMI. No strong correlations between these parameters and myocardial scar were observed, GLS ( $R^2=0.27$ ) and GWE ( $R^2=0.27$ ) correlating the strongest. Segmental work parameters also improved from days to months after AMI ( $p<0.001$ ), even in transmurally scarred segments. Segmental work parameters could distinguish non-scarred from transmurally scarred segments ( $p<0.001$ ), but unlike segmental longitudinal strain, could not distinguish subendocardial scar from other scar groups. No relevant correlation between scar formation and myocardial work at follow-up was observed.

**Conclusion:** Myocardial work assessed in the days after myocardial infarction, but not 4-6 months after myocardial infarction, yield insights into scar extent at follow-up. In this respect, work analysis does not outperform strain analysis.

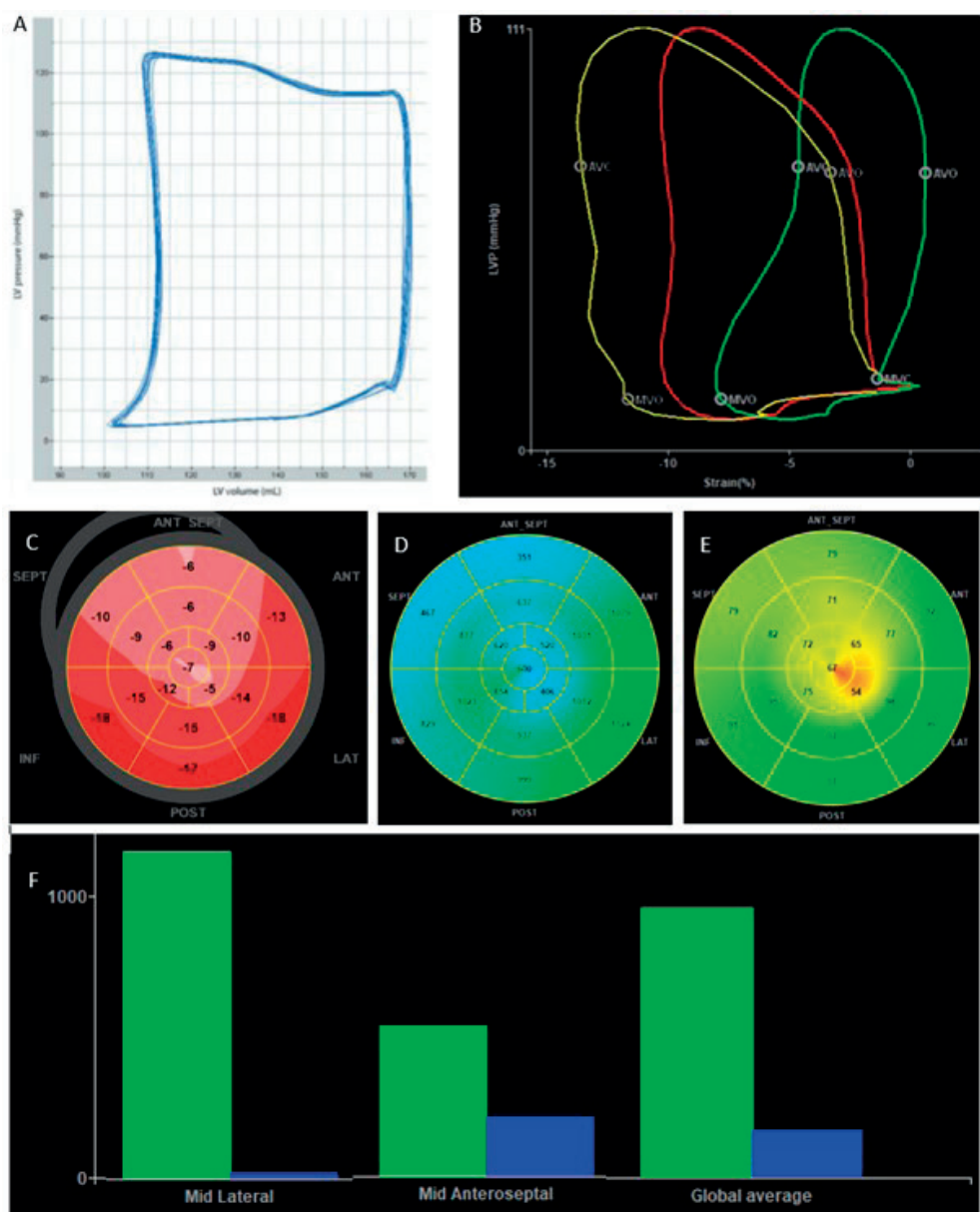
## INTRODUCTION

Acute myocardial infarction (AMI) precipitates irreversible fibrosis and scar formation, resulting in compromised function within the affected region of the heart. This might culminate in heart failure through adverse cardiac remodeling[1]. Echocardiography is the most commonly used modality for cardiac function assessment. Conventional parameters of myocardial function, such as left-ventricular ejection fraction (LVEF) and wall motion score index (WMSI), provide excellent prognostic accuracy in predicting major adverse cardiovascular endpoints[2, 3]. However, these parameters fall short of providing detailed information on myocardial function and cardiac mechanics, particularly on a segmental level. Myocardial deformation analysis has evolved to address this limitation, initially through tissue-Doppler imaging (TDI) and later via two-dimensional speckle tracking echocardiography (2D-STE)[4]. In particular, regional myocardial strain has shown to be capable of detecting areas of segmental myocardial dysfunction, as in case of AMI or the subsequent fibrous scar[5–7]. However, strain parameters are subject to load dependency and therefore may either over- or underestimate the actual myocardial contractile function[8, 9]. This consideration is particularly pertinent post myocardial infarction, where blood pressure and heart rate are altered.

Analysis of myocardial work does incorporate consideration of loading conditions, rendering it an interesting alternative for myocardial function assessment. The total area of the pressure-volume curve (figure 1a) reflects the stroke work that is performed by the myocardium. Russell et al[10] developed a method in which myocardial work is determined from 2D-STE combined with an interpolated left ventricular (LV) pressure curve derived from cuffed brachial blood pressure measurements[11–13]. The result is a pressure strain loop (figure 1b) from which the area provides a surrogate for the myocardial work performed, exhibiting a robust correlation with invasively measured pressure-volume derived work[11]. Recently, normal values for the myocardial work indices have been proposed[14, 15].

The abovementioned parameters have been studied extensively in the field of mechanical dyssynchrony and the quest for predicting response to cardiac resynchronization therapy (CRT), and has shown to be a powerful predictor of survival within these patients[16–19]. Patients who suffer from AMI or patients with a chronic fibrous scar may have a similar variation in regional myocardial conduction delay, resulting in contractile and non-contracting segments interacting at the same time during systole. This gives rise to onset of shortening before the aortic valve opening in some segments, and continuation of shortening after aortic valve closure in others, leading to significant work inefficiency. Furthermore, non-contracting segments can be either stunned or infarcted. Stunned myocardium is known to have abnormal contraction at the cellular level, which would inherently result in variation of contraction patterns between healthy, stunned and

Figure 1 – A case of myocardial work analysis after anterior myocardial infarction



**A:** Invasively measured pressure-volume loop<sup>1</sup>. **B-F:** output of myocardial work within the same patient, days after anterior myocardial infarction. **B:** Pressure strain loops. Surface area reflects work index. Red = global work index (GWI), green = segmental work index (SWI) mid-anteroseptal, yellow = SWI mid-lateral. **C-E:** Bulls-eye plots. **C:** Longitudinal strain (%). **D:** Work index (mmHg%). **E:** Work efficiency (%). **F:** Box plots of constructive work and wasted work

<sup>1</sup> Adapted from GPJ Van Hout et al, *Physiol. Rep.* 2014

transmurally scarred myocardium[20]. Finally, patients recovering from AMI are susceptible to variations in loading conditions due to decreased myocardial function. Given the consideration for loading conditions within myocardial work analysis, we hypothesize that it exhibits more reliable information on myocardial function and scar extent in comparison to 2D-STE and conventional parameters of systolic LV function in the post-AMI setting.

This study has two aims:

- 1) to investigate temporal changes of global and segmental myocardial work parameters between the days following AMI and at follow-up after 4-6 months, and compare these to conventional measures of systolic LV function and global (GLS)- and segmental longitudinal strain (SLS)
- 2) to serve as a hypothesis-generating exploration into the diagnostic value of both global- and segmental myocardial work indices in detecting scar and determining transmural extent of scar, and compare this to global and segmental strain measurements.

## METHODS

### *Study population*

This prospective, single center, post-hoc exploratory investigation is a sub-study of the DEFI-MI study (METC: NL45241.041.13). Between March 2014 and April 2018, patients (n=80) without previous cardiac disease presenting with first AMI were included. AMI, encompassing both STEMI and non-STEMI, was defined as troponin I levels > 60 ng/L along with clinical and electrocardiographic (ECG) manifestations consistent with AMI. The study was conducted according to the Declaration of Helsinki.

After written informed consent, patients underwent a baseline transthoracic echocardiography (TTE) within one to four days after admission, typically after urgent revascularization. For this sub-study, only patients receiving both baseline- and follow-up TTE on a General Electric (GE) system were included since this is currently the only vendor enabling myocardial work analysis. Blood pressure data was retrospectively collected from inpatient records for baseline TTE, and from outpatient records surrounding the follow-up examination. Patients in whom blood pressure measurements at either baseline or follow-up were not available were excluded from analysis.

### *Echocardiography*

Examinations were conducted both during the primary admission for AMI and after a follow-up period of 4-6 months. Images were obtained with patients in left lateral decubitus position using a commercially available system (Vivid E9, GE Vingmed Ultrasound AS, Horten, Norway) equipped with a 4MHz transducer (MS5c). Comprehensive ultrasound examinations, including zoomed images of the apical four-chamber, two-chamber

and long axis views, were conducted, in adherence to protocols recommended by the European Association of Cardiovascular Imaging (EACVI)[21, 22]. Frame rates ranged from 55 to 90 frames per second with three heart beats captured per image. Offline-analysis was performed by a single researcher (BvK) using dedicated analysis software for both standard echocardiographic parameters and 2D-STE analysis, including analysis of myocardial work (EchoPAC version 20, GE Vingmed Ultrasound AS, Horten, Norway). Quantification of LVEF was performed using Simpson's biplane method.

For strain analysis, manual tracing of both the endocardium and epicardium was performed, and the closure time of the aortic valve was established. The quality of tracking was checked visually, after which segments with inadequate quality of tracking were excluded from analysis. Results were generated through automated frame-by-frame tracking of acoustic markers. Segments were divided according to the 16-segment American Heart Association (AHA) model. Regarding 2D-STE, peak-systolic GLS and SLS were extracted, where the systole was defined as the interval between the electrocardiographic R-peak and the moment of aortic valve closure.

For myocardial work analysis, blood pressure readings were entered into the system. After visually determining the timing of mitral- and aortic valve closure and -opening, pressure strain loops were generated. From these, global myocardial work index (GWI) and segmental work index (SWI), global work efficiency (GWE; defined as the constructive work performed divided by the sum of constructive and wasted work performed) and segmental work efficiency (SWE), global constructive work (GCW, defined as the work performed by a segment during shortening added to the negative work performed during lengthening in isovolumetric relaxation) and global wasted work (GWW, defined as negative work performed by a segment during lengthening in systole added to the work performed during shortening in isovolumetric relaxation) were extracted[23].

#### *Cardiac magnetic resonance imaging*

Four to six months after primary AMI, on the same day as the follow-up TTE, all patients underwent contrast enhanced cardiac magnetic resonance (CMR) imaging on a Philips 1.5T scanner. Fifteen minutes after administration of 0.2ml/kg gadobutrol (Gadovist, Bayer Healthcare), delayed enhancement image acquisition was performed. These included ECG-gated sequences of the short axis views from base to apex, with slice thickness of 5mm. Images were analyzed off-line using Philips IntelliSpace Portal 9 software (Philips Medical Systems, Best, The Netherlands). Using the right ventricle insertion points as anatomic landmarks, the heart was divided into 16 segments according to the AHA model, excluding the apical cap, in concordance with segmental division of the strain results. The extent of delayed enhancement was assessed by a qualified radiologist. Each segment was scored 0 for no delayed enhancement, 1 for subendocardial scar (transmurality <50%) and 2 for transmural scar (transmurality >50%) [24]. The sum of all segments was subsequently divided by 16, to create the transmurality index.

*Statistical analysis*

For statistical analysis, SPSS Statistics version 25.0.0.2 (IBM, Armonk, NY, USA) software was used. Continuous variables were tested for normality using the Kolmogorov-Smirnov test, and subsequently depicted as mean  $\pm$  standard deviation (SD) in case of normal distribution, or as median [interquartile range (IQR)] in case of non-normality. Categorical data was depicted as count (%). A P value of  $\leq 0.05$  was deemed statistically significant.

In order to compare the behavior of indices of global myocardial function – LVEF, WMSI, GLS, GWI and GWE – between patients with recent AMI and patients with matured scar, comparison was made between baseline- and follow-up examinations using Student's paired samples T-test. Indices of global myocardial function (LVEF, GLS, GWI and GWE and WMSI) at both baseline and follow-up were correlated to the transmural index on CMR using Pearson's correlation coefficient. An  $R^2$ -value of 0-0.29 is considered a poor correlation, 0.30-0.49 is considered a moderate correlation, and 0.50 to 1 is considered a strong correlation.

For segmental analysis, all segments were allocated to no scar, subendocardial scar, or transmural scar groups. Temporal changes were compared for SLS, SWI and SWE using Student's paired samples T-test. Using one-way ANOVA (in case of no scar versus any scar) and the Bonferroni post hoc analysis (for no scar versus subendocardial scar; and for subendocardial versus transmural scar), SLS, SWE, and SWI were compared between the scar groups. Receiver operating characteristic (ROC) curves were generated for SLS, SWE, and SWI and their ability to detect transmural scar, and area under the curve (AUC) was determined for each of these. Using the Hanley & McNeil test, the AUC's of these parameters were compared.

## RESULTS

*Population characteristics*

From the total of 80 patients in the DEFI-MI study, 20 patients met our inclusion criteria. Qualitative scar assessment was available for the entire cohort, although seven segments were excluded due to poor image quality. The population characteristics are summarized in table 1. The majority of participants were male (90%), with an average age of 56.7 years, and predominantly diagnosed with ST-elevation myocardial infarction (STEMI) (90%). The extent of infarction was intermediate, as reflected by mean creatin kinase (CK)-max levels of 1305 U/L and mean scar size of 5.49% of the myocardium. Notably, despite the relatively modest mean scar size, half of the patients exhibited a transmural scar on CMR.



Table 1 – Population characteristics	
Eligible patients (n)	20
Age (years)	56.7 ± 10.9
Female sex (n)	2 (10)
Body mass index (kg/m²)	26.1 ± 3.3
Medical history (n)	
Diabetes	1 (5)
Hypertension	4 (20)
Hypercholesterolemia	11 (55)
Current smoking	10 (50)
Follow-up (months)	5.7 [5.1 – 6.1]
STEMI (n)	18 (90)
Non-STEMI (n)	2 (10)
Culprit (n)	
LAD	7 (35)
RCx	8 (40)
RCA	5 (25)
Time to revascularization (hours)	2.0 [1.5 – 6.1]
CK-max (U/L)	1305 ± 1016
CK-MB max (U/L)	160.5 ± 120.3
Scar size (%)	5.49 ± 3.18
Enhanced mass (g)	5.43 ± 3.61
Transmurality index	0.22 ± 0.17
Scar type (n)	
No scar	3 (15.0)
Subendocardial scar	7 (35)
Transmural scar	10 (50)

Data is depicted as n (%), mean ± standard deviation or median [interquartile range]. STEMI = ST-elevation myocardial infarction; LAD = left anterior descending coronary artery; RCx = circumflex coronary artery; RCA = right coronary artery; CK = creatin kinase; MB = myocardial band

Table 2 illustrates the temporal changes of each of the studied parameters of global myocardial function. With the exception of GWW, each of these parameters showed a statistically significant improvement over the follow-up period. Figure 2 presents box plots of correlation coefficients ( $R^2$ ) at both baseline and follow-up for each of the echocardiographic parameters of global function with respect to the presence of scar at follow-up. No strong or intermediate correlations were observed. Especially LVEF, both at baseline and at follow-up, demonstrated a particularly weak correlation to the transmurality index. Among the assessed parameters, GLS exhibits the most robust correlation with the transmurality index, both at baseline and at follow-up. Concerning the myocardial work parameters, GWE at baseline displayed the strongest correlation with

Global myocardial function and global work

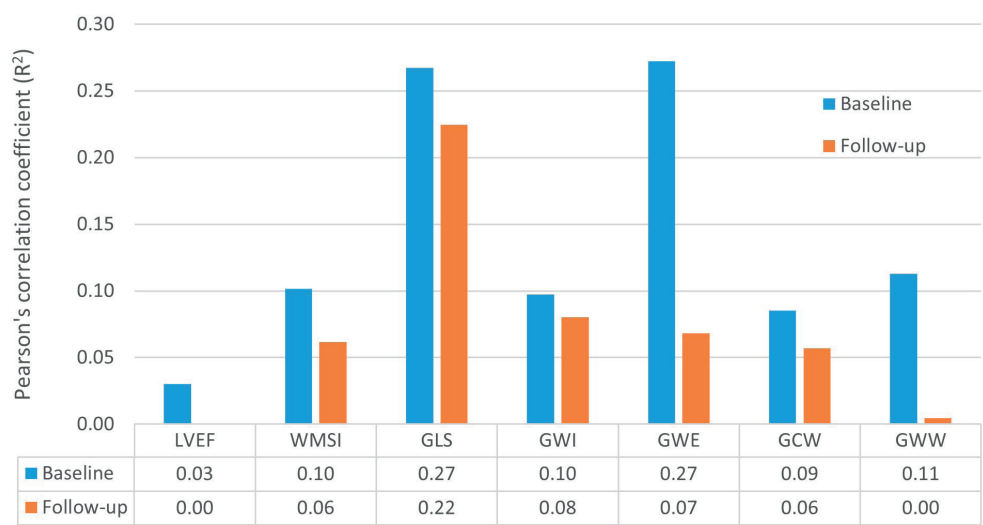
Table 2 – Temporal changes of global functional parameters

Parameter	Post-MI	Follow-up	P*
Left ventricular ejection fraction (%)	53.4 ± 7.0	56.1 ± 5.4	<0.001
Wall motion score index	1.29 ± 0.25	1.15 ± 0.15	0.014
Global longitudinal strain (%)	-14.6 ± 3.9	-16.4 ± 2.8	<0.001
Global Work Index (mmHg%)	1561 ± 345	1765 ± 370	0.011
Global Work Efficiency (%)	92.2 ± 6.8	95.5 ± 2.4	0.028
Global constructive work (mmHg%)	1780 ± 368	2020 ± 399	0.050
Global wasted work (mmHg%)	101.0 ± 75.9	76.7 ± 39.7	0.165

Data is depicted as mean ± standard deviation. MI = myocardial infarction

the transmural index at follow-up. All work parameters (GWI, GWE, GCW and GWW) at baseline displayed a stronger correlation to scar transmural index compared to the work parameters at follow-up.

Figure 2 – Box plot of correlation coefficients of global echocardiographic parameters vs. transmural index



LVEF = Left ventricle ejection fraction; WMSI = wall motion score index; GLS = global longitudinal strain; GWI = global work index; GWE = global work efficiency; GCW = global constructive work; GWW = global wasted work

### Segmental myocardial function and work

After pooling all segments of the included patients, a total of 317 segments were analyzed at baseline, and 316 segments were analyzed at follow-up. Three segments at baseline and four segments at follow-up were not eligible for analysis. Among the segments studied, 276 segments exhibited no scar, while 19 segments displayed subendocardial scar and 25 segments exhibited transmural scar. Table 3 shows mean SLS, SWI and SWE at baseline and follow-up per scar type, and the results of comparison between the different scar types as well as comparison between baseline and follow-up for each of the scar types. Figure 3 presents these results in box plots. Overall, SLS, SWI and SWE all improved significantly from baseline to follow-up ( $p < 0.001$  for each of the parameters). This pattern was also seen for SLS ( $p=0.006$ ) and SWI ( $p=0.005$ ), but not SWE ( $p=0.115$ ), in subendocardially scarred segments. Transmurally scarred segments showed improvement in each of the studied segmental parameters ( $p<0.001$ ).

**Table 3 – Mean results at baseline and follow-up for segmental parameters per scar type**

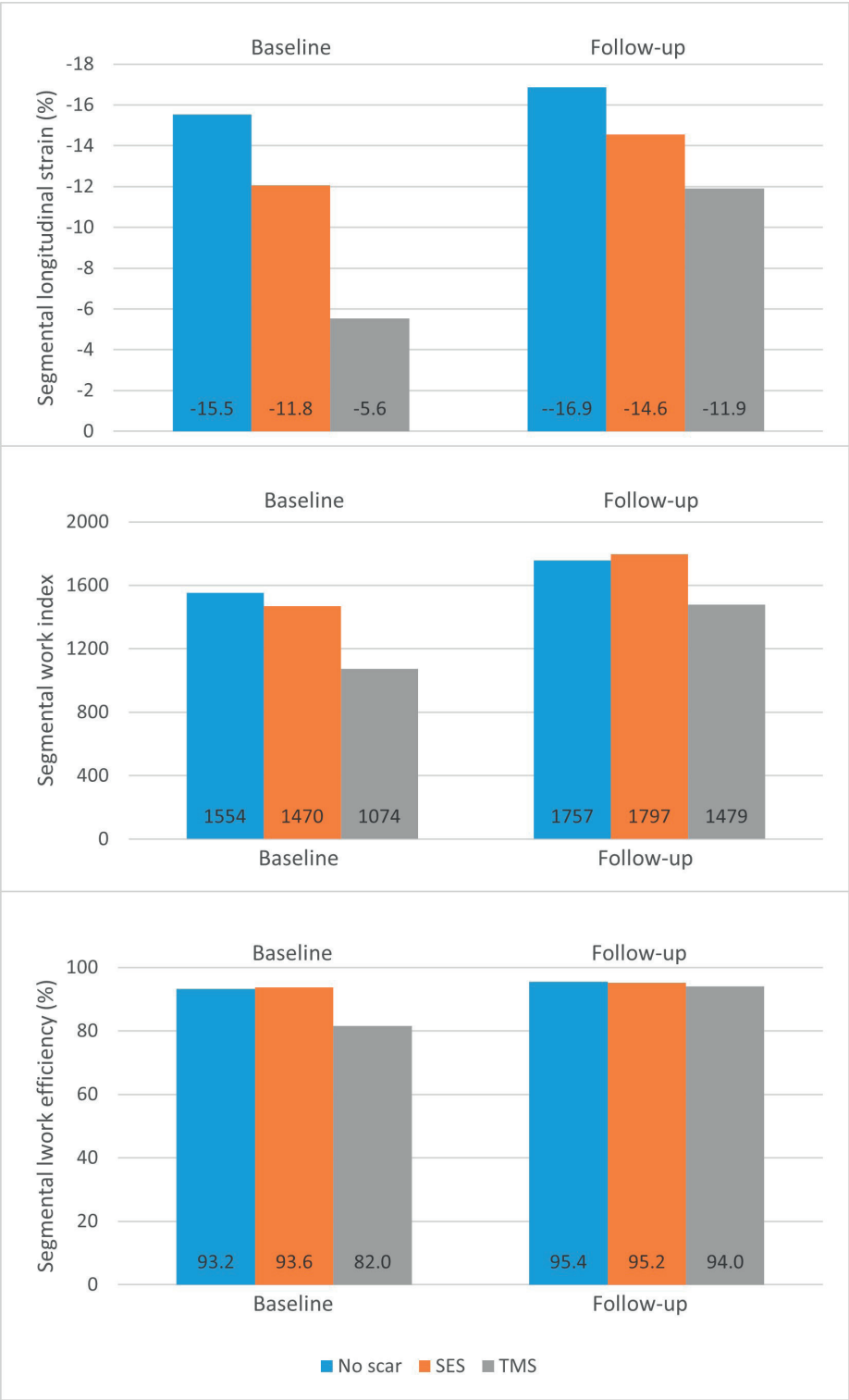
Parameter	None (n=273)	SES (n=19)	TMS (n=24)	P*
<b>SLS (%)</b>				
Baseline	-15.5 ± 6.0	-11.8 ± 4.3	-5.6 ± 9.8	<0.001 <sup>1</sup> ; 0.044 <sup>2</sup> ; <0.001 <sup>3</sup> ; 0.003 <sup>4</sup>
Follow-up	-16.9 ± 5.0	-14.6 ± 4.0	-11.9 ± 5.6	<0.001 <sup>1</sup> ; 0.179 <sup>2</sup> ; <0.001 <sup>3</sup> ; 0.122
p**	<0.001	0.006	<0.001	
<b>SWI (mmHg%)</b>				
Baseline	1543 ± 598	1438 ± 386	1098 ± 530	<0.001 <sup>1</sup> ; NS <sup>2</sup> ; <0.001 <sup>3</sup> ; NS <sup>4</sup>
Follow-up	1752 ± 547	1774 ± 530	1489 ± 448	0.071 <sup>1</sup>
p**	<0.001	0.005	0.001	
<b>SWE (%)</b>				
Baseline	93.2 ± 10.1	93.6 ± 6.4	82.0 ± 18.7	<0.001 <sup>1</sup> ; NS <sup>2</sup> ; <0.001 <sup>3</sup> ; NS <sup>4</sup>
Follow-up	95.4 ± 5.5	95.2 ± 6.6	94.0 ± 6.0	0.451 <sup>1</sup>
p**	<0.001	0.115	<0.001	

\* comparison of means between the scar groups. \*\* comparison of means from baseline to follow-up

<sup>1</sup> between either of the groups; <sup>2</sup> NS v.s. SES; <sup>3</sup> NS v.s. TMS; <sup>4</sup> SES v.s. TMS

SES = subendocardial scar; TMS = transmural scar; SLS = segmental longitudinal strain; SWI = segmental work index; SWE = segmental work efficiency; NS = not significant

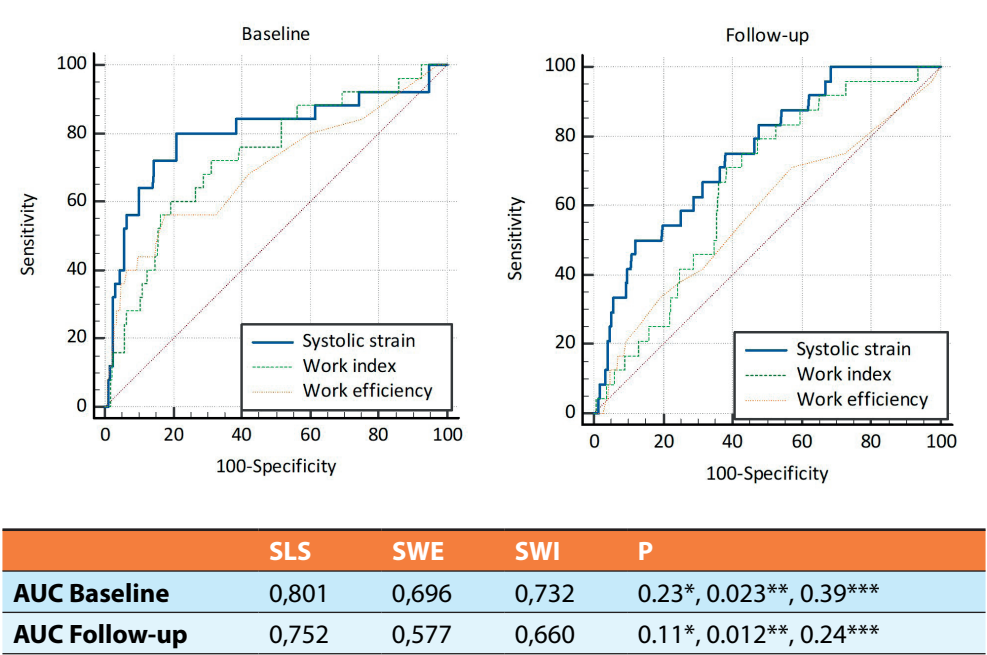
Figure 3 – temporal changes in segmental parameters per scar type



At baseline, mean SLS was statistically significantly different for each of the scar types ( $p<0.001 - p=0.044$ ). At follow up, statistically significant differences were observed between non-scarred and transmurally scarred segments ( $p<0001$ ). Mean SWI could only discriminate on a statistically significant level between non-scarred and transmurally scarred segments ( $p<0.001$ ), but not between segments with subendocardial scar and either non-scarred ( $p=0.179$ ) or transmurally scarred ( $p=0.122$ ). segments. A similar pattern was observed for SWE, which displayed significant distinction between transmurally scarred segments and non-transmurally scarred segments at baseline ( $p<0.001$ ). However, there was no difference between segments with subendocardial scar and segments with either no scar or segments with transmural scar. For SWI and SWE, no statistically significant variations between either of the scar groups was observed at follow-up.

Figure 4 illustrates ROC-curves for assessing the diagnostic performance of SLS, SWI and SWE at both baseline and follow-up in the identification of transmural scar. For each of the parameters, the AUC at baseline is greater than the AUC at follow-up. Both at baseline and at follow-up, AUC is greater for SLS than for SWI and SWE. This indicates that SLS consistently outperformed SWI and SWE in the detection of transmural scar.

Figure 4 – ROC-curves of segmental work parameters v.s. transmural scar



\*: SLS vs SWE; \*\*: SLS vs SWI; \*\*\*: SWE vs SWI  
SLS = segmental longitudinal strain; SWEW = segmental work efficiency; SWI = segmental work index; AUC = area under the curve; ROC = Receiver operating characteristics

## DISCUSSION

In this study, we studied 1) temporal changes in global and segmental echocardiographic derived myocardial work indices between the period immediately following AMI and 4-6 months thereafter, and 2) assessed the utility of myocardial work indices in predicting the extent of myocardial scarring, both when determined during the acute phase after myocardial infarction as well as at 4-6 months follow up. These are the main findings:

- 1) In concordance with LVEF, GLS and SLS, both global and segmental work indices, apart from GWW, demonstrate partial normalization in the months subsequent to AMI.
- 2) In the immediate aftermath of AMI, myocardial work parameters offer limited information on subsequent myocardial scar formation as determined by CMR. However, at follow-up, myocardial work indices do not correlate with the type and extent of chronic myocardial scar. In this respect, myocardial work parameters did not outperform GLS and SLS.

From the NORRE study, a total of 734 healthy subjects provided data for determining ranges of normal values for these parameters; normal GWI ranges from 1292-2505 mmHg% with slight variations between males and females[25]. Therefore, our reported baseline GWI of 1561mmHg% reflects that our population consists of subjects with relatively preserved global systolic myocardial function. This is underscored by the reported baseline LVEF of 53.4%.

In recent years, myocardial work has been subject of investigation in various forms of cardiac pathology, including myocardial ischemia[26]. In this field, the most research incorporating myocardial work analysis was performed in patients shortly after AMI. Although not a scope of our study, the prognostic value of myocardial work analysis has been investigated. Studies by Lustosa et al. and Meimoun et al. found that reduced GWE within 48 hours after STEMI was associated with worse long-term survival, while high segmental constructive work served as an independent predictor of functional recovery [27, 28].

### *Temporal changes and work parameters shortly after STEMI*

The temporal changes of work parameters after AMI have been reported in two other studies. Ren et al. found work indices to be decreased in non-STEMI patients (n=33), with subsequent improvement of GWI and GCW after revascularization[29]. However, GWE and GWW did not exhibit this pattern of improvement over time. In a similar study design but in a much larger population of 350 patients, Lustosa et al.[30] found GWI, GCW, and GWE, but not GWW, to improve 3 months after STEMI requiring reperfusion. This is in concordance with our results. Consequently, the authors implicate that increased GWW indicates permanent myocardial damage or scar, whereas the other myocardial work parameters reflect myocardial stunning. To our knowledge, however, there are no prior studies incorporating CMR in studying the diagnostic value of work analysis in scar

formation. Our results show that GWW directly post AMI is not a powerful predictor for myocardial scar as confirmed by CMR, which is a novel finding. More recently, in patients with preserved LVEF immediately after STEMI requiring PCI, Arnautu et al.[31] described a relationship between lower global work parameters and LV-remodeling as seen on TTE after three months follow-up. Interestingly, patients in whom LV remodeling occurred experienced a higher rate of major adverse cardiac events at four years follow-up. The temporal improvement of global parameters aligns with the expected recovery of systolic myocardial function after AMI, which likely reflects the healing process of stunned myocardium following acute revascularization. Besides, overcompensation of healthy remote segments also contributes to recovery of global function. However, GWW should not be influenced by this phenomenon and could therefore be a powerful predictor for myocardial scar. This, however, is not reflected by our results.

#### *Work parameters and chronic scar*

Segmental work parameters have been studied extensively in coronary artery disease. Studies have demonstrated their ability to reliably detect ischemic segments of the myocardium[32–34], identify the culprit vessel territory in patients with STEMI[35], and reliably distinguish acute coronary occlusion from non-occlusive coronary artery disease in patients with non-STEMI[36, 37], surpassing the efficacy of SLS. Of prognostic importance, Sun et al.[38] found regional myocardial work to serve as a predictor for functional recovery, as assessed with echocardiographic wall motion scoring, at 3 months follow-up after reperfused STEMI. The collective findings of the abovementioned studies underscore the potential utility of myocardial work analysis in identifying coronary artery disease and determining its extent, while also serving as a predictor of long-term outcome. However, we are the first to report on the value of segmental work parameters in predicting for scar formation at six months follow-up as determined by the non-invasive gold standard of late gadolinium enhancement CMR. The most noteworthy result is that, similar to SLS, SWE at baseline is significantly reduced in transmural scar. However, as shown in the ROC-curve and contrary to our hypothesis, GWE does not outperform GLS. Interestingly, in transmurally scarred segments, segmental work parameters exhibit function recovery over time, which would not be expected from non-viable transmurally scarred myocardium. An explanation would be that scarred myocardium is surrounded by the infarct border zone, which is prone to stunning and therefore likely to show functional improvement over time.

In comparison to the relatively substantial body of evidence in acute myocardial ischemia, myocardial work has been studied less extensively in the setting of a chronic scar. Coisne et al.[39] found a GWE of <91% one month after AMI to be a predictive marker for major adverse cardiovascular events after a median follow-up of nearly two years. Additionally, El Mahdiui et al.[40] have studied GWE in a cohort of patients after STEMI and noted a statistically significantly reduced work efficiency. However, it is noteworthy that this

reduction was relatively modest when compared to the reduction in work efficiency observed in patients with heart failure. In a subsequent investigation, El Mahdiui et al. retrospectively analysed 53 patients who had undergone CMR after a median period of 2 months following STEMI. They showed that lower values of myocardial work indices, when performed within a one-month period from the CMR, were associated with increased hyperenhancement on CMR[41]. It is important to mention that this study utilized a dataset in which patients were included at a time prior to our study, when revascularization methods were less advanced than they are today. This presumably explains the larger infarct size (mean CK-max of 2665 U/L, compared to 1269 in our study).

Our findings are consistent with current literature, suggesting the potential value of myocardial work analysis in patients with myocardial ischemia or AMI. However, unlike Lustosa et al[30], we were unable to differentiate whether the parameters were reflective of myocardial stunning or scarring. Interestingly, our study indicates that work indices directly after AMI can forecast the development of a transmural scar, although our results do not demonstrate additional value over conventional strain analysis. In contrast, in the setting of a chronic scar without concurrent acute ischemia, we demonstrate myocardial work indices to be unreliable parameters for detecting myocardial scar. We hypothesize that, in the acute setting, the intricate interplay of myocardial mechanics between scarred and stunned myocardium is reflected in the work parameters. Interestingly, the resolution of stunned myocardium in the setting of scar at six months after the infarction, alongside the improvement in global function, presumably alters the regional mechanics within the scar area to a degree that work analysis is unable to differentiate healthy from scarred myocardium. Another explanation for the abovementioned findings might be that scar size plays a role, with a larger scar leading to a more extensive area of stunned myocardium and, consequently, greater regional impairment. In this matter, it is important to consider that our analysis is based on three two-dimensional cross-sections of the heart which may not necessarily encompass the most affected region of the heart.

#### *Limitations and future perspectives*

This sub-study faced limitations stemming from its retrospective design, leading to the inclusion of only 20 out of 80 patients originally included in the DEF-AMI trial. This was primarily due to unavailability of consecutive ultrasound examinations eligible for work analysis, for example when another vendor than GE was used for image acquisition, or when image quality was insufficient. Moreover, absence of coinciding blood pressure measurements from the initial study design further reduced the amount of eligible patients. Consequently, the potential for comparing subgroups was impaired and therefore not extensively performed, and determining cut-off points for optimal sensitivity and specificity for the studied indices was deemed unfeasible. The small study population introduced a heterogeneity among our patients, including variations in culprit lesion and scar size, possibly impacting our results. Another limitation when



correlating echocardiographic parameters to CMR is the potential lack of overlap between the analysed segments, potentially leading to underestimation of the true correlation and predictive value. However, care was taken in optimal image acquisition of echo images and segmentation of CMR images. Taking these factors into account, the results of this study should be viewed as hypothesis-generating data, and clinical implications are limited.

Future studies, ideally with larger study populations, should explore whether myocardial work analysis has a place in the detection of scar. This is of particular interest, since it offers a more easily performed and readily available alternative to the current CMR golden standard for myocardial scar detection. In addition, larger study cohorts could facilitate the analysis of specific subgroups, for example by scar size, culprit lesion, extent of functional impairment or the presence of comorbidities, potentially identifying scenarios where the specific advantages of work analysis could translate into clinically relevant benefits. Currently, efforts are made to elaborate on the value of myocardial work parameters[42, 43].

## **CONCLUSION**

Like conventional LV systolic function parameters, including LVEF, WMSI and 2D-STE, myocardial work indices are generally impaired shortly after AMI and subsequently improve over the following months. In the post-acute setting after AMI requiring PCI, myocardial work parameters provide information on myocardial scar formation in a similar way to, but not outperforming, conventional strain parameters. However, when assessed in the months after myocardial infarction, myocardial work analysis does not provide information on myocardial scar characteristics. To gain a more comprehensive understanding of the application of this technique in the context of myocardial infarction, future research should utilize larger cohorts. This could lead to the identification of patients who could benefit from the application of this technique to assess scar extent, particularly in the days after sustaining AMI.

## **FUNDING AND CONFLICTS OF INTEREST**

The authors declare that no funds, grants or other support were received during the preparation of this manuscript. The authors have no relevant financial or non-financial interests to disclose.

## REFERENCES

1. Jenča D, Melenovský V, Stehlik J, et al. Heart failure after myocardial infarction: incidence and predictors. *ESC Heart Fail* 2022;8:222–37. doi:10.1002/ehf2.13144
2. Curtis JP, Sokol SI, Wang Y, et al. The association of left ventricular ejection fraction, mortality, and cause of death in stable outpatients with heart failure. *J Am Coll Cardiol* 2003;42:736–42. doi:10.1016/S0735-1097(03)00789-7
3. Savarese G, Vedin O, D'Amario D, et al. Prevalence and Prognostic Implications of Longitudinal Ejection Fraction Change in Heart Failure. *JACC Heart Fail* 2019;7:306–17. doi:10.1016/j.jchf.2018.11.019
4. Teske AJ, De Boeck BWL, Melman PG, et al. Echocardiographic quantification of myocardial function using tissue deformation imaging, a guide to image acquisition and analysis using tissue Doppler and speckle tracking. *Cardiovasc Ultrasound* 2007;5:27. doi:10.1186/1476-7120-5-27
5. Kwon DH, Hachamovitch R, Popovic ZB, et al. Survival in patients with severe ischemic cardiomyopathy undergoing revascularization versus medical therapy: Association with end-systolic volume and viability. *Circulation* 2012;126:83-8. doi:10.1161/CIRCULATIONAHA.111.084434
6. Maffessanti F, Nesser HJ, Weinert L, et al. Quantitative Evaluation of Regional Left Ventricular Function Using Three-Dimensional Speckle Tracking Echocardiography in Patients With and Without Heart Disease. *Am J Cardiol* 2009;104:1755–62. doi:10.1016/j.amjcard.2009.07.060
7. Popović ZB, Benejam C, Bian J, et al. Speckle-tracking echocardiography correctly identifies segmental left ventricular dysfunction induced by scarring in a rat model of myocardial infarction. *Am J Physiol Heart Circ Physiol* 2007;292:2809–16. doi:10.1152/ajpheart.01176.2006
8. Murai D, Yamada S, Hayashi T, et al. Relationships of left ventricular strain and strain rate to wall stress and their afterload dependency. *Heart Vessels* 2017;32:574–83. doi:10.1007/s00380-016-0900-4
9. Donal E, Bergerot C, Thibault H, et al. Influence of afterload on left ventricular radial and longitudinal systolic functions: A two-dimensional strain imaging study. *Eur J Echocardiogr* 2009;10:914–21. doi:10.1093/ejechocard/jep095
10. Russell K, Eriksen M, Aaberge L, et al. Assessment of wasted myocardial work: A novel method to quantify energy loss due to uncoordinated left ventricular contractions. *Am J Physiol Heart Circ Physiol* 2013;305:996–1003. doi:10.1152/ajpheart.00191.2013
11. Russell K, Eriksen M, Aaberge L, et al. A novel clinical method for quantification of regional left ventricular pressure-strain loop area: A non-invasive index of myocardial work. *Eur Heart J* 2012;33:724–33. doi:10.1093/eurheartj/ehs016
12. Hubert A, Le Rolle V, Leclercq C, et al. Estimation of myocardial work from pressure–strain loops analysis: an experimental evaluation. *Eur Heart J Cardiovasc Imaging* 2018;19:1372–79. doi:10.1093/ehjci/jey024

13. Boe E, Skulstad H, Smiseth. Myocardial work by echocardiography: A novel method ready for clinical testing. *Eur Heart J Cardiovasc Imaging* 2019;20:18–20. doi:10.1093/ehjci/jez156
14. Olsen FJ, Skaarup KG, Lassen MCH, et al. Normal Values for Myocardial Work Indices Derived From Pressure–Strain Loop Analyses: From the CCHS. *Circ Cardiovasc Imaging* 2022;15:316–27. doi:10.1161/circimaging.121.013712
15. Truong VT, Vo HQ, Ngo TNM, et al. Normal Ranges of Global Left Ventricular Myocardial Work Indices in Adults: A Meta-Analysis. *J Am Soc Echocardiogr* 2022;35:369–77.e8. doi:10.1016/j.echo.2021.11.010
16. Van Der Bijl P, Vo NM, Kostyukevich MV, et al. Prognostic implications of global, left ventricular myocardial work efficiency before cardiac resynchronization therapy. *Eur Heart J Cardiovasc Imaging* 2019;20:1388–94. doi:10.1093/ehjci/jez095
17. Manganaro R, Marchetta S, Dulgheru R, et al. Correlation between non-invasive myocardial work indices and main parameters of systolic and diastolic function: results from the EACVI NORRE study. *Eur Heart J Cardiovasc Imaging* 2020;21:533–41. doi:10.1093/ehjci/jez203
18. Galli E, Hubert A, Le Rolle V, et al. Myocardial constructive work and cardiac mortality in resynchronization therapy candidates. *Am Heart J* 2019;212:53–63. doi:10.1016/j.ahj.2019.02.008
19. Duchenne J, Larsen CK, Cvijic M, et al. Mechanical Dyssynchrony Combined with Septal Scarring Reliably Identifies Responders to Cardiac Resynchronization Therapy. *J Clin Med* 2019;12:6108. doi:10.3390/jcm12186108
20. Gao WD, Atar D, Backx PH, Marban E. Relationship Between Intracellular Calcium and Contractile Force in Stunned Myocardium. *Circ Res* 1995;76:1036–48. doi:10.1161/01.res.76.6.1036
21. Lang RM, Badano LP, Victor MA, et al. Recommendations for cardiac chamber quantification by echocardiography in adults: An update from the American Society of Echocardiography and the European Association of Cardiovascular Imaging. *J Am Soc Echocardiogr* 2015;28:1–39.e14. doi:10.1016/j.echo.2014.10.003
22. Voigt JU, Pedrizzetti G, Lysyansky P, et al. Definitions for a common standard for 2D speckle tracking echocardiography: consensus document of the EACVI/ASE/Industry Task Force to standardize deformation imaging. *Eur Heart J Cardiovasc Imaging* 2015;16:1–11. doi:10.1093/ehjci/jeu184
23. Samset E (2017) Evaluation of segmental myocardial work in the left ventricle. <https://www.gehealthcare.com/-/media/8cab29682ace4ed7841505f813001e33.pdf>. Accessed 24 October 2023
24. Cho GY, Marwick TH, Kim HS, et al. Global 2-Dimensional Strain as a New Prognosticator in Patients With Heart Failure. *J Am Coll Cardiol* 2009;54:618–24. doi:10.1016/j.jacc.2009.04.061
25. Manganaro R, Marchetta S, Dulgheru R, et al. Echocardiographic reference ranges for normal non-invasive myocardial work indices: Results from the EACVI NORRE study. *Eur Heart J Cardiovasc Imaging* 2019;20:582–90. doi:10.1093/ehjci/jez188

26. Moya A, Buytaert D, Penicka M, et al. State-of-the-Art: Noninvasive Assessment of Left Ventricular Function Through Myocardial Work. *J Am Soc Echocardiogr* 2023;36:1027-42. doi:10.1016/j.echo/2023/07.002
27. Lustosa RP, Butcher SC, van der Bijl P, et al. Global Left Ventricular Myocardial Work Efficiency and Long-Term Prognosis in Patients After ST-Segment-Elevation Myocardial Infarction. *Circ Cardiovasc Imaging* 2021;14:247-55. doi:10.1161/circimaging.120.012072
28. Meimoun P, Abdani S, Stracchi V, et al. Usefulness of Noninvasive Myocardial Work to Predict Left Ventricular Recovery and Acute Complications after Acute Anterior Myocardial Infarction Treated by Percutaneous Coronary Intervention. *J Am Soc Echocardiogr* 2020;33:1180-90. doi:10.1016/j.echo.2020.07.008
29. Ren F, Xue T, Tang G, et al. Assessment of Myocardial Work of the Left Ventricle before and after PCI in Patients with Non-ST-Segment Elevation Acute Coronary Syndrome by Pressure-Strain Loop Technology. *Comput Math Methods Med* 2022;8026689. doi:10.1155/2022/8026689
30. Lustosa RP, Fortuni F, van der Bijl P, et al. Changes in Global Left Ventricular Myocardial Work Indices and Stunning Detection 3 Months After ST-Segment Elevation Myocardial Infarction. *Am J Cardiol* 2021;157:15-21. doi:10.1016/j.amjcard.2021.07.012
31. Arnautu DA, Gheorghiu A, Arnautu SF, et al. Subtle Changes in Myocardial Work Indices Assessed by 2D-Speckle Tracking Echocardiography Are Linked with Pathological LV Remodeling and MACEs Following an Acute Myocardial Infarction Treated by Primary Percutaneous Coronary Intervention. *Diagnostics* 2023;13:3108. doi:10.3390/diagnostics13193108
32. Guo Y, Yang C, Wang X, et al. Regional Myocardial Work Measured by Echocardiography for the Detection of Myocardial Ischemic Segments: A Comparative Study With Invasive Fractional Flow Reserve. *Front Cardiovasc Med* 2022;9:813710. doi:10.3389/fcvm.2022.813710
33. Sabatino J, De Rosa S, Leo I, et al. Prediction of Significant Coronary Artery Disease Through Advanced Echocardiography: Role of Non-invasive Myocardial Work. *Front Cardiovasc Med* 2021;8:719603. doi:10.3389/fcvm.2021.719603
34. Sabatino J, De Rosa S, Leo I, et al. Non-invasive myocardial work is reduced during transient acute coronary occlusion. *PLoS One* 2020;15:e0244397. doi:10.1371/journal.pone.0244397
35. Lustosa RP, Fortuni F, Van Der Bijl P, et al. Left ventricular myocardial work in the culprit vessel territory and impact on left ventricular remodelling in patients with ST-segment elevation myocardial infarction after primary percutaneous coronary intervention. *Eur Heart J Cardiovasc Imaging* 2021;22:339-347. doi:10.1093/ehjci/jeaa175
36. Boe E, Russell K,EEK C, et al. Non-invasive myocardial work index identifies acute coronary occlusion in patients with non-STsegment elevation-acute coronary syndrome. *Eur Heart J Cardiovasc Imaging* 2015;16:1247-55. doi:10.1093/ehjci/jev078
37. Qin YY, Wu XP, Wang JT, et al. Value of territorial work efficiency estimation in non-ST-segment-elevation acute coronary syndrome: a study with non-invasive left ventricular pressure-strain loops. *Int J of Cardiovasc Imaging* 2020;37:1255-65. doi:10.1007/s10554-020-02110-1
38. Sun S, Chen N, Sun Q, et al. Association Between Segmental Noninvasive Myocardial Work and Microvascular Perfusion in ST-Segment Elevation Myocardial Infarction: Implications for Left

- Ventricular Functional Recovery and Clinical Outcomes. *J Am Soc Echocardiogr* 2023;10:1055-63. doi:10.1016/j.echo.2023.04.017
39. Coisne A, Fourdinier V, Lemesle G, et al. Clinical significance of myocardial work parameters after acute myocardial infarction. *Eur Heart J Open* 2022;2:oeac037. doi:10.1093/ehjopen/oeac037
  40. El Mahdiui M, van der Bijl P, Abou R, et al. Global Left Ventricular Myocardial Work Efficiency in Healthy Individuals and Patients with Cardiovascular Disease. *J Am Soc Echocardiogr* 2019;32:1120–7. doi:10.1016/j.echo.2019.05.002
  41. Mahdiui M El, van der Bijl P, Abou R, et al. Myocardial Work, an Echocardiographic Measure of Post Myocardial Infarct Scar on Contrast-Enhanced Cardiac Magnetic Resonance. *Am J of Cardiol* 2021;151:1–9. doi:10.1016/j.amjcard.2021.04.009
  42. Daios S, Anastasiou V, Moysidis DV, et al. Prognostic Implications of Clinical, Laboratory and Echocardiographic Biomarkers in Patients with Acute Myocardial Infarction—Rationale and Design of the “CLEAR-AMI Study”. *J Clin Med* 2023;12:5726. doi:10.3390/jcm12175726
  43. Moysidis DV, Daios S, Anastasiou V, et al. Association of clinical, laboratory and imaging biomarkers with the occurrence of acute myocardial infarction in patients without standard modifiable risk factors – rationale and design of the “Beyond-SMuRFs Study”. *BMC Cardiovasc Disord* 2023;23:149. doi:10.1186/s12872-023-03180-4



# CHAPTER

# 4

# Correlation between circulating biomarkers of collagen homeostasis and scar size using magnetic resonance imaging in patients after acute myocardial infarction

Van Klarenbosch BR, Driessen HE, Kok GJM, Vos MA, Cramer MJ, Teske AJ, Van Veen TAB, Velthuis BK, Ter Meulen – De Jong S



## ABSTRACT

### *Introduction*

Myocardial fibrosis as a result of acute myocardial infarction (AMI) can lead to adverse remodeling and heart failure. Assessment of cardiac fibrosis, such as by late gadolinium-enhanced cardiac magnetic resonance (LGE CMR) imaging, has limitations, especially in the direct postoperative period. Circulating biomarkers of collagen homeostasis have emerged as potential alternatives, but their clinical utility remains unclear.

### *Methods*

The prospective DEFI-MI trial enrolled 76 patients with AMI, excluding those with prior heart disease or other conditions affecting collagen homeostasis. At baseline, 1<sup>st</sup> follow-up (approximately six weeks after AMI) and 2<sup>nd</sup> follow-up (approximately five months after AMI), blood samples were drawn and levels of procollagen type I C-terminal propeptide (PICP) and C-terminal telopeptide of type I collagen (ICTP) were measured. LGE CMR for scar assessment and T<sub>1</sub> mapping for extracellular volume (ECV) estimation were performed at the 2<sup>nd</sup> follow-up moment.

### *Results*

PICP levels increased significantly from baseline to the 1<sup>st</sup> follow-up moment ( $p < 0.001$ ). PICP level ( $p = 0.020$ ,  $R = 0.274$ ) and  $\Delta$ PICP from baseline to first follow-up ( $p = 0.006$ ,  $R = 0.324$ ) correlated weakly with scar size. ICTP decreased significantly from baseline to both 1<sup>st</sup> and 2<sup>nd</sup> follow-up ( $p < 0.001$  and  $p = 0.007$  respectively), and decreased ICTP levels at 1<sup>st</sup> follow-up ( $p = 0.039$ ,  $R = 0.327$ ) and 2<sup>nd</sup> follow-up ( $p = 0.012$ ,  $R = 0.381$ ) correlated weakly scar size. There were no significant correlations between PICP/ICTP and scar size, or between ECV and circulating biomarkers.

### *Conclusion*

After AMI, increased PICP levels at 6 weeks, and decreased ICTP levels at 6 weeks and 5 months, correlate weakly but on a statistically significant level to scar size. The clinical utility does not seem obvious due to the many factors influencing the results, such as baseline collagen turnover, medication use, and timing of sampling. Further investigation seems warranted to establish potentially useful patient groups or better timing of measurements.

## INTRODUCTION

The mortality as a consequence of acute myocardial infarction (AMI) has decreased in western Europe since 2003, due to several innovations in clinical practice [1]. Despite slightly decreasing incidence rates of AMI over the past years, the improved survival combined with an increase in the prevalence of cardiovascular risk factors will lead to an increasing prevalence of ischemic heart disease [1–3]. Therefore, adverse cardiac remodeling eventually resulting in heart failure is a growing socio-economic burden.

Fibrosis in the heart is most commonly the result of AMI, which may ultimately culminate into contractile dysfunction and arrhythmogenicity [4,5]. It is caused by a disturbed equilibrium between the synthesis and breakdown of collagen fibres, a process that is mainly regulated by cardiac fibroblasts [6]. The most abundant collagen type in the heart is collagen type I (85%), followed by collagen type III (11%). The collagen fibres create a thinly weaved network of collagen fibres that provides mechanical strength to the myocardium [7]. Collagen turnover is relatively slow and estimated to be between 80-120 days [8]. In myocardial damage, the balance shifts towards fibroblast activation and increased collagen type I production, leading to fibrosis. Three types of fibrosis are distinguished: 1) reactive fibrosis where there is collagen deposition without the loss of cardiomyocytes, such as in pressure overload, that may result in cardiomyopathy, 2) infiltrative fibrosis, such as in infiltrative heart disease, and 3) replacement fibrosis, where apoptotic cardiomyocytes are replaced by predominantly collagen type I, such as in myocardial damage. Furthermore, the texture of fibrosis varies between disease aetiologies [9,10], ranging from interstitial fibrosis (accumulation of collagens between cells) as seen in heart failure, compact fibrosis (accumulation of large collagenous structures) as in myocardial scar, diffuse fibrosis (short stretches of fibrosis) as seen for example in chronic overloading and patchy fibrosis (long strands of collagen fibres between the cardiomyocytes) as seen in infiltrative heart disease. After AMI, timely observation of increased cardiac fibrosis could lead to therapy adjustments, thereby preventing further functional deterioration. The current gold standard to assess cardiac fibrosis is late gadolinium enhancement cardiac magnetic resonance imaging (LGE CMR) [11], which utilises the fact that the washout of gadolinium in fibrotic myocardium is slower than the washout in healthy myocardium. On  $T_1$  weighted CMR, performed 10-15 minutes after intravenous administration of gadolinium, scar can be visualised, since the remaining gadolinium within scarred tissue is reflected as an enhanced signal. The clinical availability, costs, and need for contrast agents that are associated with LGE CMR are major drawbacks that limit its application in the setting of AMI. Furthermore, myocardial inflammation which is often seen after AMI but which is not necessarily related to fibrosis, also yields an enhanced  $T_1$  weighted signal that leads to an overestimation of scar [12]. Finally, interstitial fibrosis such as seen in heart failure, which might be a result of AMI and adverse remodeling, is challenging to establish by LGE CMR.  $T_1$  mapping, by which native and post-contrast  $T_1$  mappings are used to acquire a

quantitative estimation of extracellular volume (ECV), is an alternative imaging technique that has previously been related to interstitial fibrosis in a range of cardiac pathologies [13–15]. However, the aforementioned limitations concerning LGE CMR in the quest for fibrosis detection in general make that alternative methods for fibrosis monitoring might improve clinical decision-making.

Circulating biomarkers of collagen homeostasis could pose as alternatives for fibrosis assessment after AML. Multiple of these biomarkers have been identified in the past decades. Peptides that derive from the synthesis and breakdown of collagen and are stabilised in the bloodstream are of specific interest. Synthesis of collagen type I starts with fibroblasts producing procollagen I. When the procollagen is transported into the intercellular space, the pro-peptides at the amino (N)- and carboxy (C)-terminus are cleaved and released into the blood, as PINP and PICP respectively [8]. Furthermore, the C-terminal telopeptide of type I collagen (ICTP) is a stable degradation peptide that is also eliminated via the bloodstream. This peptide might therefore serve as a biomarker of cardiac collagen breakdown [16,17]. PICP is considered to be associated with collagen synthesis, whereas ICTP is associated with collagen breakdown. The ratio PICP/ICTP (collagen synthesis corrected for collagen degradation) is associated with increased collagen turnover. These biomarkers have been related to histologically confirmed myocardial fibrosis in patients with chronic heart failure and hypertension [18,19].

In current clinical practice, creatine kinase (CK) and its myocardial fraction (CK-MB) are used abundantly, since they are strong predictors of scar size and myocardial function, stronger than cardiac troponin [20]. However, these markers reflect the degradation of cardiomyocytes and do not necessarily reflect the formation of fibrosis. Biomarkers of collagen turnover have been studied before, showing their relation to fibrosis in various cardiac pathologies and even predicting clinical outcomes [17,21,22]. However, the results are conflicting. A possible reason for this is that collagen turnover is not limited to the heart, so alterations in concentrations of these biomarkers may not reflect changes that occur in the heart. Furthermore, methodological issues with the immunoassays may arise, as they are not fully standardised. Finally, there are concerns about the reference standards used in prior research that correlate concentrations of collagen turnover biomarkers to cardiac fibrosis, such as sampling error in endocardial biopsy, and only a few studies use non-invasive techniques for fibrosis detection to validate the value of the studied biomarkers [23].

To address these issues, we explore the behaviour of PICP, ICTP, and the ratio between ICTP/PICP, and their relation to non-invasive measurements of fibrosis using LGE CMR in patients after AML, in whom alterations of myocardial collagen homeostasis are expected. In addition, we explore their relation to ECV measurement using T1-mapping CMR as a marker for interstitial fibrosis. We thereby investigate whether these biomarkers could be used for fibrosis detection in a clinical setting. We hypothesise that PICP as a direct marker for collagen I synthesis will especially be useful in the post-acute period, whereas ICTP as

a marker of increased collagen catabolism is expected to relate to scar size in the setting of a mature scar. The ratio between these two biomarkers (PICP/ICTP), as a marker for collagen turnover, might be useful both in the post-acute setting as well as in the setting of chronic scar.

## MATERIALS AND METHODS

### *Study population and study protocol*

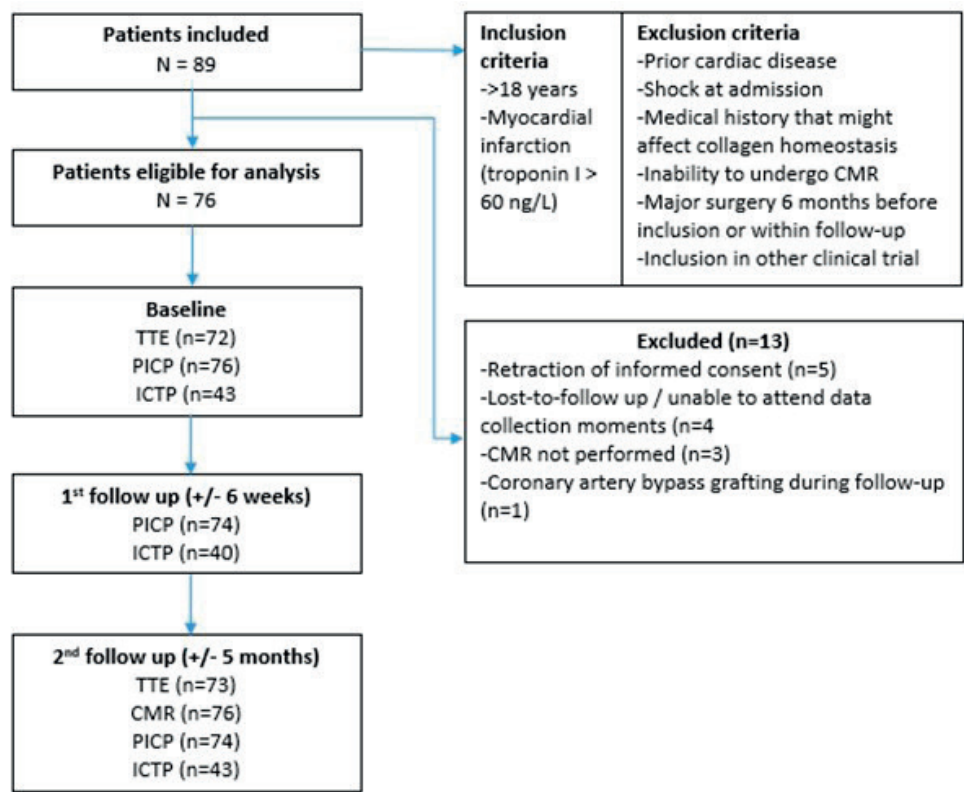
The DEFI-MI study is a prospective single-centre study (METC UMCU: NL45241.041.13). Patients of age >18 years presenting with an AMI, both ST-elevation (STEMI) and non-ST-elevation (non-STEMI) were included. AMI was defined as troponin I levels >60 ng/L together with clinical and electrocardiographic (ECG) findings consistent with AMI. Exclusion criteria were prior cardiac disease, patients presenting with cardiac shock, any other disease which may influence collagen homeostasis such as malignancy, chronic liver disease or inflammatory disease, kidney failure defined as glomerular filtration rate (GFR) <30ml/min/1.73m<sup>2</sup>, inability to undergo CMR (for example due to claustrophobia or metalloprotheses), surgery or major trauma in the 6 months before inclusion or within the study period, the need for surgical revascularisation, or inclusion in another clinical trial. A total of 89 patients were enrolled between March 2014 and April 2018, of whom 13 patients were excluded after inclusion due to loss to follow-up (for example, due to transfer to another clinic), or because of the emerging of additional medical information that met exclusion criteria, such as the need for thoracotomy within the follow-up period. In conclusion, a total of 76 patients were included in this study. The study was conducted according to the Declaration of Helsinki.

Figure 1 visualises the study flow chart. At baseline, during admission for AMI, blood samples were drawn and a TTE (transthoracic echocardiography) examination was performed. Coinciding with their first outpatient clinic visit, usually six weeks after AMI, blood samples were drawn again (deemed 1<sup>st</sup> follow-up). Finally, approximately 5 months after inclusion and ideally coinciding with an outpatient clinic visit (deemed 2<sup>nd</sup> follow-up), blood was collected, follow-up TTE was performed and a CMR was made.

### *Circulating biomarker analysis*

The collected plasma samples (using heparin and EDTA as anticoagulants) were stored at -80°C at the biobank of the University Medical Centre Utrecht. PICP pro-peptides were measured using a commercially available enzyme-linked immunosorbent assay (ELISA) from MicroVue, Quidel (MicroVue Bone, CACP, product number 8005). ICTP was measured using a commercially available radioimmunoassay (RIA) (UniQ®, Orion Diagnostica, product number 68601). PICP and ICTP levels are indicated in ng/ml. Collagen turnover was determined as the ratio of PICP/ICTP levels. Since there is a significant spread in

Figure 1 – Study flow chart



baseline values of these biomarkers between patients [24,25], for each of the parameters and at each of the follow-up time points, a change in concentration ( $\Delta$ ) was determined to correct for this variation.  $\Delta$ ICTP has been shown to correlate with a reduced left ventricular (LV) mass index in patients using antifibrotic therapy [21].

*TTE*

At both baseline and the 2<sup>nd</sup> follow-up moment, patients underwent a standard TTE exam. Images were obtained with patients in left lateral decubitus position using a commercially available system (Vivid E9, GE Vingmed Ultrasound AS, Horten, Norway) fitted with a 4 MHz transducer (M5Sc). Three heart beats per image were acquired. A standard TTE protocol was performed, including zoomed images of the apical four-chamber, two-chamber, and long-axis views. Baseline- and follow-up LV ejection fraction (LVEF) measurements and 2D-speckle tracking analysis resulting in a global longitudinal strain value were performed in adherence to the concurrent guidelines [26,27].

### CMR

During the 2<sup>nd</sup> follow-up visit, patients underwent contrast-enhanced 1.5 Tesla CMR imaging (Philips Healthcare, Best, The Netherlands). LGE image acquisition was performed 15 minutes after administration of 0.2 ml/kg gadobutrol (Gadovist, Bayer Healthcare, Berlin, Germany) with an infusion rate of 1.5ml/s. Prospective ECG-gated sequences of the short axis views from base to apex, with a slice thickness of 5mm were acquired. Images were analysed using the Philips ISP9 software (Philips Healthcare). The amount of LGE was quantitatively assessed using the full-width-at-half-maximum (FWHM) method [11], providing a percentage for scar size in relation to the whole left ventricle. For patients in whom no scar was observed visually, FWHM results were manually set to zero to avoid false positive outcomes, to which this technique is prone in the absence of scar. Finally, both native T<sub>1</sub> and contrast-enhanced T<sub>1</sub> mappings were acquired at the base, midventricular, and apical levels. Using Medis Suite 3.1 analysis software (Medis, Leiden, The Netherlands), the endocardium and epicardium at each level for both native and contrast-enhanced images were traced, as well as a tracing of the blood pool to retrieve an estimation of ECV of the whole left ventricle.

### Statistical analysis

For statistical analysis, SPSS Statistics version 25.0.0.2 (IBM, Armonk, NY, USA) software was used. Continuous parameters were tested for normal distribution using the Kolmogorov-Smirnov test. Student's paired samples T-test was used to compare the mean concentrations of the studied biomarkers between each of the time points. Since scar size was normally distributed, correlation analysis was performed using Pearson's correlation coefficient. Differences and correlations were deemed significant if  $p < 0.05$ . Correlations were considered weak between 0.10 and 0.40, moderate between 0.40 and 0.70, strong between 0.70 and 0.80, and very strong between 0.80 and 1.00. To correct for the spread of both PICP and ICTP concentrations at baseline, for both follow-up time points  $\Delta$ PICP and  $\Delta$ ICTP relative to the measurement at baseline were determined, and subsequently correlated with scar size.

Because of the substantial spread in the timing of measurements at each of the follow-up moments, a sub-analysis within the different blood sampling moments was performed, to serve as hypothesis generating data regarding the ideal timing of biomarker measurement to identify these biomarkers with relation to myocardial fibrosis. For baseline, a division was made between sampling <3 days from admission, versus >4 days from admission. For 1<sup>st</sup> follow-up, data was divided between blood sampling performed <6.6 weeks (which was the median period from baseline to 1<sup>st</sup> follow-up) after hospital admission and blood sampling performed  $\geq 6.6$  weeks after admission. For 2<sup>nd</sup> follow-up, patients were divided into follow-up performed before and after 5.8 months (which is the median period from baseline to 2<sup>nd</sup> follow-up) after admission.

In order to compare the performance of the novel biomarkers between patients with smaller and larger myocardial infarctions, the patients were divided into tertiles based on the maximum recorded CK-MB value. CK-MB is a powerful predictor of scar size and is therefore used in clinical practice [28]. Using non-parametric one-way ANOVA with the Kruskal-Wallis test, the measured levels of biomarkers were compared between the tertiles.

RESULTS

Patient characteristics

Figure 1 represents the study flow chart. Informed consent was signed by 89 patients. Thirteen patients dropped out due to retraction of the informed consent, absence at data collection time points, failure to undergo CMR due to claustrophobia, not having the ability to attend follow-up appointments, or the need for coronary artery bypass grafting (CABG) within the follow-up period. As such, a total of 76 patients were eligible for analysis. There is some missing data, especially for ICTP analysis. This proved to be a less robust parameter than PICP, which required more material to be used in the analysis process. In a substantial amount of patients, there was insufficient blood material available, resulting in missing ICTP data. Furthermore, there is a substantial spread in the timing of data collection points (Table 1).

Table 1 – Timing of data acquisition, measured from day of admission

	n	Median [IQR]	Range
<b>Blood samples</b>			
Baseline (days)	76	2 [2 – 3.75]	1 – 7
1 <sup>st</sup> follow-up (weeks)	74	6.6 [5.9 – 7.7]	4.0 – 13.0
2 <sup>nd</sup> follow-up (months)	74	5.9 [5.0 – 6.1]	4.0 – 9.7
<b>TTE</b>			
Baseline (days)	72	3 [2 – 4]	0 - 84
2 <sup>nd</sup> follow-up (months)	73	5.9 [5.0 – 6.0]	3.8 – 8.8
<b>CMR</b>			
2 <sup>nd</sup> follow-up (months)	76	5.9 [5.0 – 6.0]	3.8 – 9.7

IQR = interquartile range. TTE = trans-thoracic echocardiography. CMR = cardiac magnetic resonance

The population characteristics are displayed in Table 2. The mean age was 57.2 years, and 85.5% of participants were male. Cardiovascular risk factors were very frequently present. The use of antifibrotic medication at baseline was 10.5%; one patient used both renin-angiotensin-aldosterone system (RAAS) inhibitors and mineralocorticoid receptor antagonists (Table 3). Overall, patients suffering from STEMI were typically included (81.6%). Out-of-hospital cardiac arrest (OHCA) occurred in 7.9% of patients. The median

time from onset of complaints to revascularization was 2.5 hours. Median creatine kinase (CK)-max was 987 U/L. Baseline LVEF and global longitudinal strain (GLS) were slightly impaired (52.4% and -14.9% respectively). At 2<sup>nd</sup> follow-up, median infarct size was 5.1% of the total LV mass.

**Table 2 – Patient characteristics**

<b>Age (years)</b>	57.2 ± 11.0
<b>Female sex (n)</b>	11 (14.5)
<b>Medical history (n)</b>	
Diabetes	4 (5.3)
Hypertension	19 (25.0)
Hypercholesterolemia	34 (44.7)
TIA/Stroke	5 (6.6)
Smoking	37 (48.7)
<b>STEMI (n)</b>	62 (81.6)
<b>Non-STEMI (n)</b>	14 (17.9)
<b>Culprit (n = 74)</b>	
LAD	35 (46.1)
RCA	20 (26.3)
RCx	19 (25.0)
<b>OHCA (n)</b>	6 (7.9)
<b>Time to revascularisation (hours, n=74)</b>	2.5 [1.5 – 7.0]
<b>CK-max (U/L)</b>	987 [476 – 1777]
<b>CK-MB max (U/L)</b>	113 [47 – 239]
<b>Troponin max (ng/mL)</b>	9435 [2825 – 34168]
<b>LVEF (%)</b>	
<b>Baseline (n=70)</b>	52.4 ± 8.0
<b>2<sup>nd</sup> follow-up (n=71)</b>	54.2 ± 5.9
<b>GLS (%)</b>	
<b>Baseline (n=44)</b>	-14.9 ± 3.6
<b>2<sup>nd</sup> follow-up (n=61)</b>	-16.0 ± 2.9
<b>Scar size (%) (n=75)</b>	5.1 [2.1 – 8.1]

Data is depicted as mean ± standard deviation, n (%), or median [interquartile range]. N=76 unless stated otherwise.

TIA = transient ischemic attack; STEMI = ST-elevation myocardial infarction; LAD = Left anterior descending artery; RCA = Right coronary artery; RCx = Circumflex coronary artery; OHCA = Out-of-hospital cardiac arrest; CK = creatine kinase; CK-MB = myocardial fraction of CK; LV = left ventricle; EDV = end-diastolic volume; LVEF = left ventricular ejection fraction; GLS = global longitudinal strain

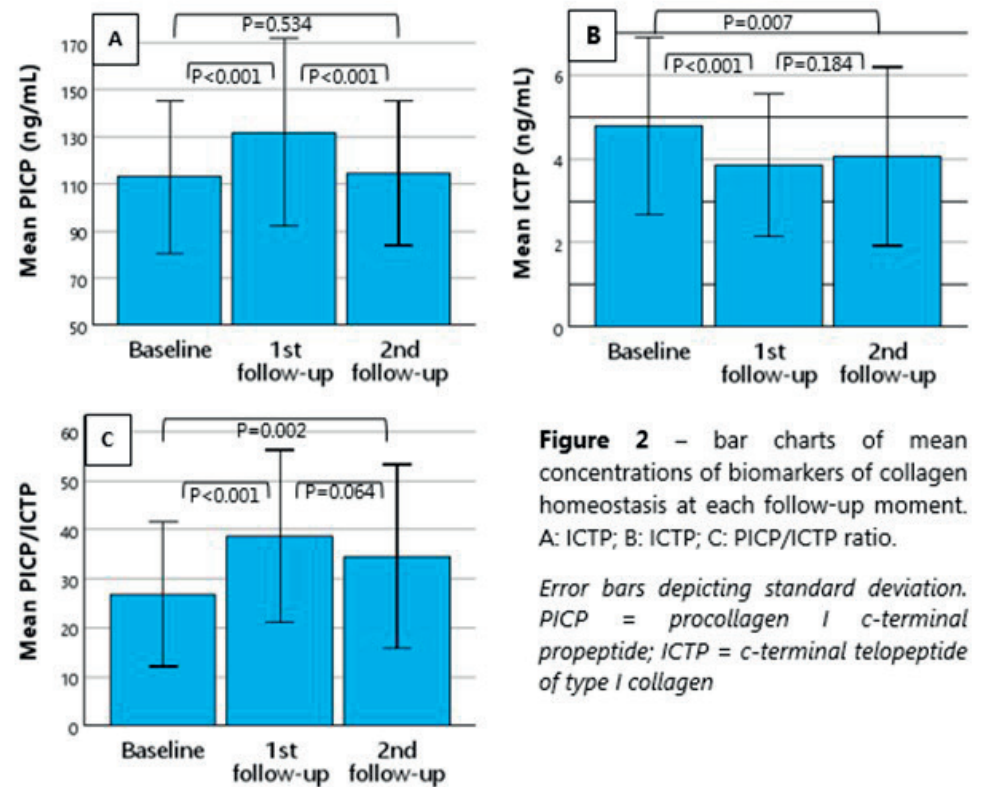


Table 3 – Medication use

	Baseline (n=76)	1 <sup>st</sup> follow-up (n=76)	2 <sup>nd</sup> follow-up (n=75)
Platelet inhibitors	6 (7.9)	76 (100)	77 (100)
Beta blocker	3 (3.9)	69 (90.8)	67 (89.3)
RAAS inhibitor	8 (10.5)	70 (92.1)	67 (89.3)
MR antagonist	1 (1.3)	13 (17.1)	10 (13.3)
Calcium channel blocker	1 (1.3)	5 (6.6)	6 (8.0)
Statin	9 (11.8)	73 (96.1)	75 (100)

N (%). RAAS = Renin angiotensin aldosterone system; MR = mineralocorticoid receptor

Collagen synthesis and correlation with scar size



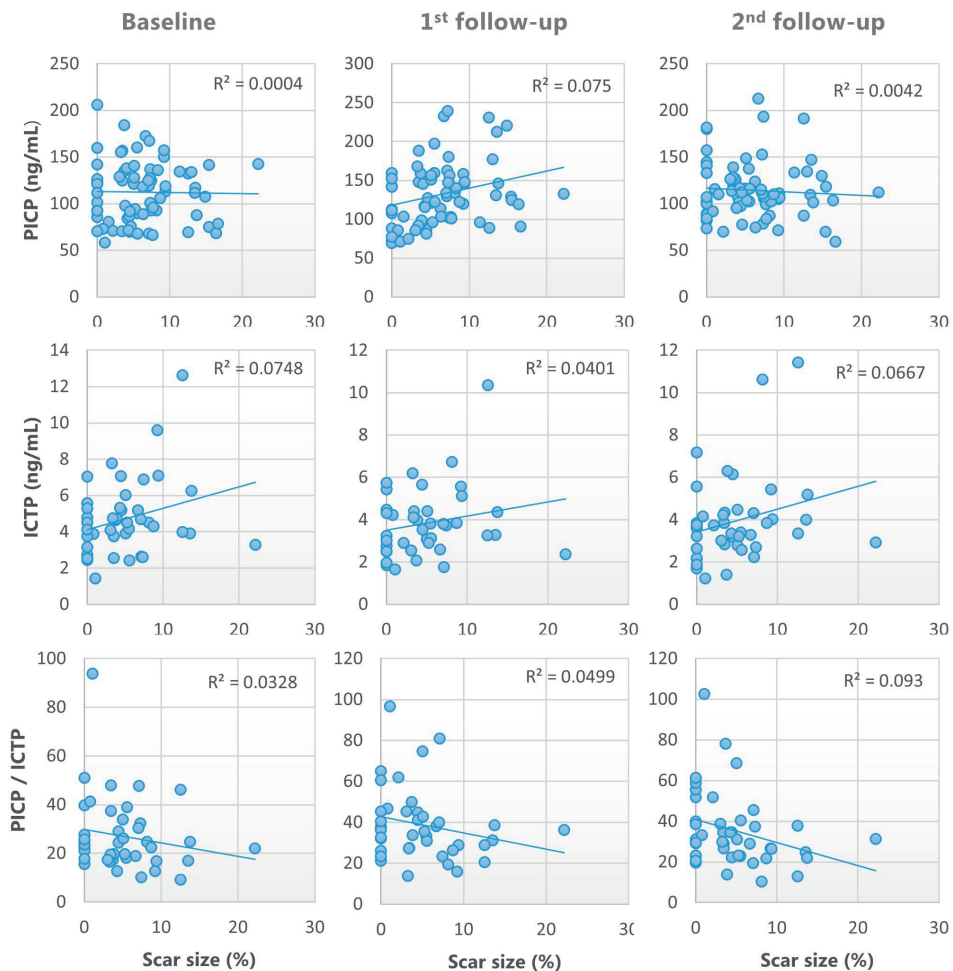
**Figure 2** – bar charts of mean concentrations of biomarkers of collagen homeostasis at each follow-up moment. A: ICTP; B: ICTP; C: PICP/ICTP ratio.

Error bars depicting standard deviation. PICP = procollagen I c-terminal propeptide; ICTP = c-terminal telopeptide of type I collagen

Baseline PICP concentrations (as a marker for collagen synthesis) ranged from 58.4 ng/mL to 206.0 ng/mL. Mean PICP levels increase significantly from baseline ( $111.7 \pm 32.4$  ng/mL) to 1<sup>st</sup> follow-up ( $131.3 \pm 39.7$  ng/mL,  $p < 0.001$ ), and subsequently decrease to 2<sup>nd</sup> follow-up ( $114.3 \pm 30.3$  ng/mL,  $p < 0.001$ ) (Figure 2A). The correlation between circulating

biomarkers and LGE CMR-derived scar size is depicted in Table 4 and Figure 3. PICP levels at six weeks show a statistically significant ( $p = 0.020$ ) but weak ( $R = 0.274$ ) correlation to scar size measured by the FWHM method. At other time points, PICP concentrations showed no statistically significant relation to scar size. When correlating the  $\Delta$ PICP at 1<sup>st</sup> follow-up to scar size, a statistically significant but weak correlation was found ( $R = 0.324$ ,  $p = 0.006$ ) (figure 4). No statistically significant correlations between PICP concentrations and ECV results were found (table 5).

**Figure 3 – Correlation graphs of circulating biomarker concentrations at each time point to scar size**



### Collagen degradation and collagen turnover

ICTP concentrations (as a marker for collagen degradation) at baseline ranged from 1.44 to 12.63 ng/mL. Collagen degradation, as reflected by ICTP, decreased significantly ( $p < 0.001$ ) from baseline to 1<sup>st</sup> follow-up, and remained decreased towards 2<sup>nd</sup> follow-up ( $P = 0.007$  compared to baseline) (figure 2B). Weak but statistically significant correlations between ICTP concentrations at both 1<sup>st</sup> ( $R = 0.327$ ,  $p = 0.039$ ) and 2<sup>nd</sup> ( $R = 0.381$ ,  $p = 0.012$ ) follow-up and scar size were observed (Table 4 and Figure 3). However,  $\Delta$ ICTP at both follow-up moments did not correlate to scar size (Table 4, Figure 4), and no significant correlations between ICTP concentrations and ECV were found (Table 5). Collagen synthesis (represented by PICP) corrected for collagen degradation (represented by ICTP), or PICP/ICTP, serves as a marker for total collagen turnover. This parameter showed a significant increase ( $p < 0.01$ ) from baseline to 1<sup>st</sup> follow-up and remained elevated at 2<sup>nd</sup> follow-up ( $p = 0.002$  compared to baseline) (figure 2C). There was no statistically significant relation between scar size and ECV, neither at the 1<sup>st</sup> nor at the 2<sup>nd</sup> follow-up moment (Table 5).

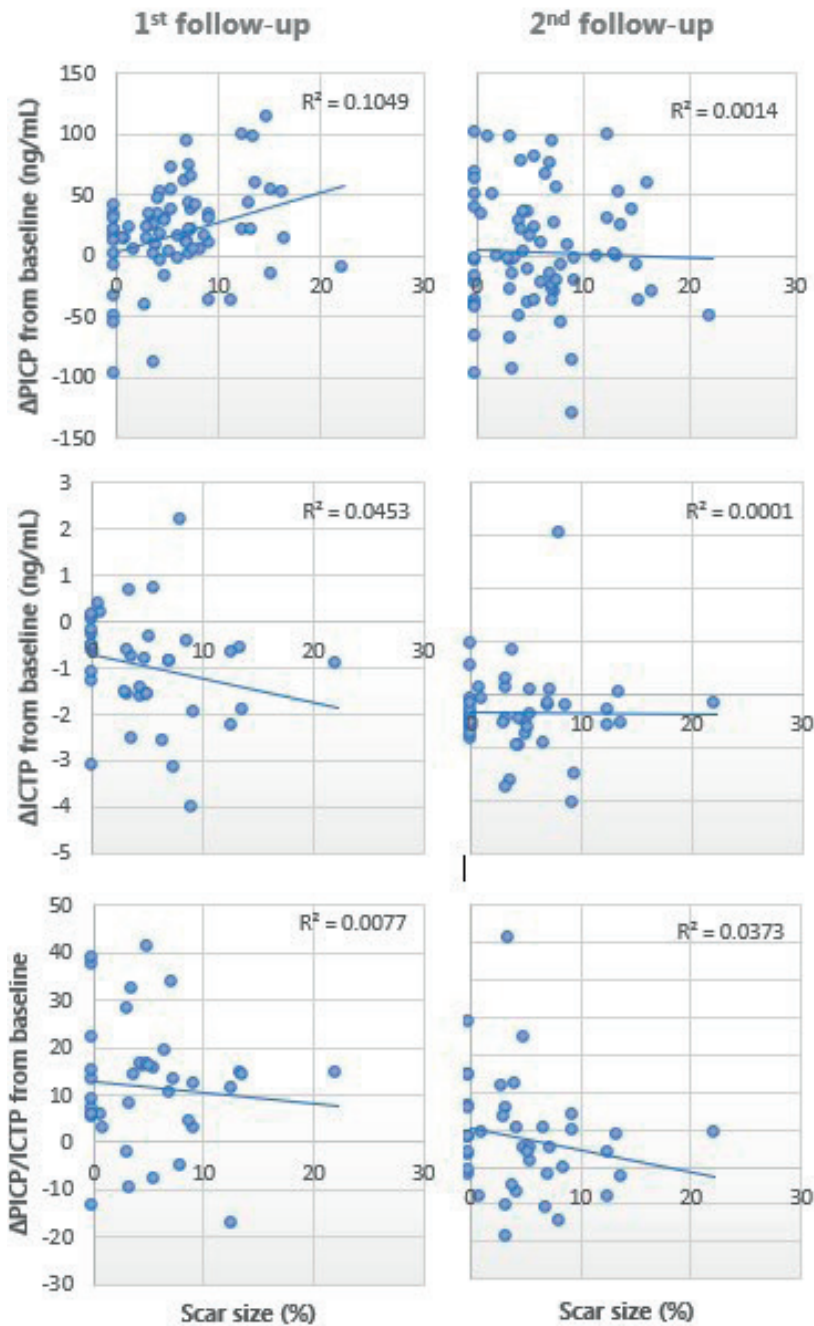
**Table 4 - Correlation between circulating biomarkers and scar size measured by LGE CMR**

	Baseline			1 <sup>st</sup> follow-up			2 <sup>nd</sup> follow-up		
	n	R	p-value	n	R	p-value	n	R	p-value
<b>PICP</b>	74	-0.019	0.873	72	0.274	0.020	72	-0.065	0.589
<b><math>\Delta</math>PICP</b>	-	-	-	72	0.324	0.006	72	-0.037	0.759
<b>ICTP</b>	43	0.184	0.237	40	0.327	0.039	43	0.381	0.012
<b><math>\Delta</math>ICTP</b>	-	-	-	39	0.219	0.181	42	0.238	0.129
<b>PICP/ICTP</b>	43	-0.204	0.189	40	-0.018	0.910	43	-0.230	0.137
<b><math>\Delta</math>PICP/ICTP</b>	-	-	-	39	0.127	0.442	42	-0.085	0.591

*LGE CMR = late gadolinium enhancement cardiac magnetic resonance imaging; R = Pearson's correlation coefficient; PICP = C-terminal propeptide of procollagen type I;  $\Delta$  = change in biomarker concentration compared to baseline; ICTP = C-terminal telopeptide of collagen type I*

**Table 5 - Correlation between circulating biomarkers and ECV measured by T1 mapping**

	Baseline			1 <sup>st</sup> follow-up			2 <sup>nd</sup> follow-up		
	n	R	p-value	n	R	p-value	n	R	p-value
<b>PICP</b>	66	-0.017	0.892	65	0.165	0.188	64	0.017	0.892
<b><math>\Delta</math>PICP</b>	-	-	-	65	0.170	0.176	64	0.014	0.912
<b>ICTP</b>	37	0.206	0.222	34	0.201	0.254	37	0.143	0.398
<b><math>\Delta</math>ICTP</b>	-	-	-	33	-0.089	0.623	36	-0.026	0.879
<b>PICP/ICTP</b>	37	-0.151	0.372	34	-0.069	0.698	37	-0.111	0.515
<b><math>\Delta</math>PICP/ICTP</b>	-	-	-	33	-0.097	0.592	36	-0.012	0.944

**Figure 4 – Correlation graphs of  $\Delta$ PICP,  $\Delta$ ICTP, and  $\Delta$ PICP/ICTP to scar size at 1<sup>st</sup> and 2<sup>nd</sup> follow-up**

ECV = extracellular volume; CMR = cardiac magnetic resonance imaging;  $R$  = Pearson's correlation coefficient; PICP = C-terminal propeptide of procollagen type I;  $\Delta$  = change in biomarker concentration compared to baseline; ICTP = C-terminal telopeptide of collagen type I

*Effect of timing of follow-up measurements*

An explorative sub-analysis into the effect of variation within blood sampling time points was performed by dividing patients for PICP, PICP/ICTP, or ICTP between early (<3 days) and late (>3 days) baseline measurement, early (<6.5 weeks) and late (>6.5 weeks) 1<sup>st</sup> follow-up and early (<5.8 months) and late (>5.8 months) 2<sup>nd</sup> follow-up. For  $\Delta$ PICP at 1<sup>st</sup> follow-up, a stronger Pearson's correlation to scar size of 0.411 ( $p = 0.002$ ) was found for patients with early baseline measurement compared to the whole study population ( $R = 0.324$ ). Patients with late baseline measurement ( $n = 19$ ) showed no significant correlation of  $\Delta$ PICP to scar size. This was not observed for  $\Delta$ ICTP and  $\Delta$ PICP/ICTP. At 1<sup>st</sup> follow-up, the correlation of PICP to scar size was stronger for early 1<sup>st</sup> follow-up compared to the whole study population ( $R = 0.421$  for PICP and  $R = 0.472$  for  $\Delta$ PICP, compared to  $R = 0.274$  and  $R = 0.324$  respectively), but patients with late 1<sup>st</sup> follow-up showed no statistically significant correlations between any biomarker result and scar size. When exploring 2<sup>nd</sup> follow-up, no stronger correlations were observed for any of the biomarkers compared to the correlations reported for the whole study population.

*Relation with CK-MB*

To investigate the circulating biomarker levels in relation to the current clinical practice of infarct size estimation using biomarkers, table 6 shows concentrations of the investigated biomarkers according to a division of subjects into tertiles according to the highest measured CK-MB concentration [low – intermediate – high]. Low CK-MB was defined as a concentration < 60.8 U/L ( $n = 25$ ), high CK-MB was defined as >189.7 U/L ( $n = 25$ ), and patients with CK-MB concentrations 60.8 – 189.7 U/L were categorised as intermediate CK-MB ( $n = 26$ ). No statistically significant differences were observed between the CK-MB groups regarding their circulating biomarker levels, indicating that the values of these biomarker concentrations probably hold limited value for clinical use regarding scar size estimation. Indeed, CK-MB concentrations at baseline showed a moderate correlation to scar size ( $R = 0.50$ ,  $P < 0.001$ ), stronger than any of the investigated biomarkers.

**Table 6 - Change in circulating biomarker concentration per CK-MB tertile**

Biomarker	Median CK-MB level (U/L)			P-value
	Low (n=25)	Intermediate (n=26)	High (n=25)	
<b>ΔPICP</b>				
1 <sup>st</sup> follow-up	16.1 [5.0 – 26.9]	-26.6 [11.8 – 53.4]	19.3 [5.0 – 36.6]	0.473
2 <sup>nd</sup> follow-up	-8.1 [-32.5 – 35.4]	0.1 [-19.1 – 29.5]	4.1 [-12.0 – 33.1]	0.679
<b>ΔICTP</b>				
1 <sup>st</sup> follow-up	-1.3 [-2.4 – -0.7]	-0.7 [-1.6 – 0.2]	-0.6 [-0.8 – -0.3]	0.145
2 <sup>nd</sup> follow-up	-1.1 [-1.6 – -0.5]	-0.9 [-1.7 – 0.3]	-0.5 [-1.1 – 0.2]	0.089
<b>ΔPICP / ICTP</b>				
1 <sup>st</sup> follow-up	9.7 [4.4 – 23.7]	15.5 [3.2 – 18.0]	12.2 [3.9 – 14.3]	0.650
2 <sup>nd</sup> follow-up	7.6 [-2.5 – 14.5]	4.9 [-7.1 – 13.7]	7.4 [-0.5 – 9.7]	0.651

Low CK-MB is defined as < 60.8 ng/mL; high CK-MB is defined as >189.7; intermediate CK-MB is defined as 60.8 – 189.7

CK-MB = creatin kinase-myocardial band; Δ = Change in biomarker concentration, compared to baseline; PICP = procollagen I c-terminal propeptide; ICTP = c-terminal telopeptide of type I collagen

## DISCUSSION

### Main findings

In this study, we explored the potential value of circulating biomarkers involved in collagen homeostasis and their value in diagnosing myocardial scar. The main findings of this study are 1) the concentration of the circulating collagen synthesis product PICP increases from days to weeks after myocardial infarction and normalises to levels similar to baseline after months, whereas the concentration of circulating collagen breakdown product ICTP decreases from days to weeks after myocardial infarction and remains decreased when measured months after AMI; 2) PICP, measured approximately six weeks after AMI as well as its change from baseline to six weeks thereafter, correlates weakly with scar size measured 5 months after AMI; and 3) ICTP, measured approximately 6 weeks and approximately 5 months after AMI correlates weakly with scar size measured at 5 months after AMI.

### Markers of collagen turnover

In current clinical practice, diagnosis of myocardial fibrosis remains a challenge. CK-MB is used frequently and is indeed a strong predictor of infarct size after AMI [28]. However, it reflects the breakdown of cardiomyocytes and is not involved in the fibrosis cascade. Since myocardial fibrosis, as occurs after AMI, is associated with adverse outcomes like heart failure and arrhythmogenicity, efforts are made to identify alternative methods of predicting fibrosis. Promising advances are made in cardiac fibroblast activation imaging in identifying early evidence of fibrosis [29], but most modalities for diagnosing fibrosis

remain logistically challenging. As an alternative to imaging, because of their ease of use, biomarkers are studied. Once robust biomarkers of myocardial fibrosis are identified, these could be applied in any other myocardial disease in which fibrosis manifests.

PICP, as a collagen synthesis marker, has been studied previously in the setting of chronic heart failure, diastolic dysfunction, and hypertensive cardiomyopathy, finding elevated levels in all of these settings and also predicting long-term all-cause- and cardiovascular mortality [30,31]. ICTP, as a marker of collagen breakdown, also shows increased levels in patients with dilated- and hypertrophic cardiomyopathy [32].

In the setting of AMI, these biomarkers have been studied as well. McGavigan et al. described an increase in both ICTP and PICP after AMI [33]. Cerisano et al. found a correlation between ICTP and brain natriuretic peptide (BNP), but not with PICP and BNP, at 1-4 days, 6 weeks, and 6 months after AMI [16]. On the contrary, in the study of Ren et al. late revascularisation, compared to early revascularisation, was found to be associated with an increased PICP level at 90 and 180 days after PCI [34]. Moreover, Radovan et al. observed that patients with unsuccessful PCI express higher levels of PICP and ICTP 6 months after MI [35] compared to patients with successful revascularisation. Similarly, Poulsen et al. observed that lower levels of circulating PICP were associated with improvement in LVEF measured up to a year after AMI [36]. Finally, ICTP measured shortly after AMI has been shown to predict all-cause death and the development of symptoms of heart failure [37].

Although there are studies that correlate PICP and ICTP to LV volume indices [38], to our knowledge, there are no studies on the association of these biomarkers to the gold standard of non-invasive fibrosis detection which is CMR in patients after AMI. We found only a weak correlation between PICP measured in the weeks after AMI and scar size at months follow-up, and a similar weak but statistically significant correlation between scar size and ICTP at both 1<sup>st</sup> follow-up  $\pm$  6 weeks after AMI, and 2<sup>nd</sup> follow-up  $\pm$  5 months after AMI. This indicates that these biomarkers, to a limited extent, bear information on scar size after AMI. However, the fact that there seems to be an important variation in circulating levels between patients, makes it hard to determine solid cut-off points that apply to the entire patient population. This can partly be solved by serial measurements since  $\Delta$ PICP correlates slightly stronger to infarct size than PICP concentrations alone. However, adopting such a strategy in clinical practice is impractical compared to a single-measurement parameter.

In the current study, we observe lower correlations of collagen turnover biomarkers to scar size than what was expected based on the aforementioned studies. One possible reason for this is that our study population consists of people who generally were revascularised quickly, a strategy aimed at limiting scar size. A substantial amount of patients with small or no detectable scar will inherently hamper correlation analysis. Furthermore, a vast number of patients were treated with RAAS inhibitors or mineralocorticoid receptor antagonists. These medications have a profound effect on collagen turnover and fibrosis

formation [21]. On the other hand, the use of antifibrotic therapy before admission was sparse. For this reason, a comparative analysis between antifibrotic therapy naïve patients and patients who already used a RAAS inhibitor or a mineralocorticoid receptor antagonist was not feasible.

#### *Factors influencing collagen turnover*

Collagen type I is expressed in almost all connective tissues. It is the major collagen isoform in the heart, bone, skin, and ligaments [39,40]. The scar formed after AMI will only marginally affect the grand scheme of collagen type I homeostasis within the entire body. Furthermore, collagen type I has a long turnover time of 80-120 days, leading to a slow translation of altered fibrosis homeostasis into circulating biomarkers of synthesis or breakdown. While it could be hypothesised that these two factors combined make it unlikely to reliably detect a very profound effect on PICP and ICTP levels when a stable scar has been generated, we do think there is a role for these circulating biomarkers in the setting of acute AMI. The initial need for increased collagen synthesis directly after AMI, and the remodeling of collagen deposition in the period needed to create a stable scar, does lead to detectable changes in PICP and ICTP.

Other processes affecting collagen turnover might also affect the clinical applicability of collagen turnover markers as a biomarker for cardiac fibrosis. Age, especially in women, can affect PICP and ICTP levels due to menopause-related osteoporosis [41,42]. Furthermore, immobility can increase collagen degradation, and thereby ICTP levels, significantly [43]. This could partly explain why ICTP baseline levels are not suitable for fibrosis detection. Although our study excludes these patients, systemic inflammatory diseases like active Crohn's disease and rheumatoid arthritis affect ICTP and PICP plasma levels in various ways [44–47]. Furthermore, collagen metabolism markers are known to show a circadian rhythm [24,48], but unfortunately, we could not standardise the time of blood collection of all patients due to logistical reasons. This aspect tentatively could have affected the obtained results.

#### *Timing of blood sampling*

We performed a sub-analysis in which patients were divided into groups according to the timing of blood sampling. We observed that the strength of correlation for PICP improved when baseline measurements were performed earlier, as well as when 1<sup>st</sup> follow-up occurred early compared to when it occurred late. Ideally, meticulous explorative studies should be performed including repeated measurement of collagen turnover biomarkers at multiple time points in patients after AMI, in order to clarify the behaviour of these biomarkers over time. Literature on this matter is limited; Cerisano et al. [16] measured ICTP and PICP 1 day, 3 days, 1 month, and 6 months after AMI. Indeed, a significant increase in PICP levels was already observed from 1 day to 3 days after AMI. Contrary to our results, no normalisation to baseline levels was found. ICTP increased slightly from 1



day to 3 days after AMI, and similar to our results, subsequently decreased to significantly lower concentrations than at baseline.

### *Strengths and limitations*

The main strength of this study is that a population was included in whom utmost effort was made to exclude bias by other factors that influence collagen turnover than the myocardial infarction that the patients suffered from. Furthermore, biomarkers of fibrosis were correlated to the gold standard for fibrosis detection, which has to our knowledge not been studied before in the setting of AMI. In addition, we applied the current gold standard for non-invasive interstitial fibrosis detection,  $T_1$  mapping.

This study also has some limitations. First of all, measurements of collagen turnover are easily confounded and hard to standardise, which should always be considered when comparing results to prior literature. This problem is also a limitation for clinical applicability. The current study has considerable variation in the timing of follow-up data collection, mainly because the study protocol adhered to existing outpatient clinic visits to pose the least burden on patients as well as medical personnel during the admission. Indeed, in our sub-analysis into the timing of blood sampling, we showed that this variation is likely to have a relevant impact on our results. Due to an excellent and timely protocol for acute revascularisation, infarct size in our population is usually limited, which inherently hampers correlation analysis leading to a possible underestimation of the true relation of the studied biomarkers to myocardial fibrosis. This might also be the reason that ECV estimation was less robust than scar size estimation with regards to correlating to circulating biomarkers since there are no patients with symptomatic heart failure within our study cohort, which would lead to increased interstitial fibrosis. Regarding inclusion, there might be a potential risk for inclusion bias since there were more studies regarding patients with AMI that were conducted within our centre during the acquisition period.

## **CONCLUSION**

To conclude, levels of circulating PICP are increased and levels of ICTP are decreased approximately six weeks after AMI, and correlate weakly with scar size. PICP levels normalise months after AMI, but ICTP levels remain significantly decreased. PICP/ICTP does not relevantly correlate to scar. From our results, clinical implications of the studied biomarkers seem limited, although our results need to be validated in larger studies in which some of our important study limitations are mitigated.

## ACKNOWLEDGEMENTS

The authors thank Dr T. Mast and Dr F. Arslan for their critical input during the design of the DEFI-MI study and their contribution to the initial inclusion. We would also like to thank Mr M.D.A. Araya Roos for mentoring during the initial data analysis using Philips ISP9 software.

## FUNDING

This work was supported by a grant from the Netherlands Cardio Vascular Research Initiative (CVON): the Dutch Heart Foundation, Dutch Federation of University Medical Centres, the Netherlands Organization for Health Research and Development and the Royal Netherlands Academy of Sciences (CVON-eDETECT 2015-12, to HED&TABvV).

## REFERENCES

- [1] Timmis A, Vardas P, Townsend N, et al. European Society of Cardiology: cardiovascular disease statistics 2021. *Eur Heart J* 2022;43:716–99. Doi:10.1093/eurheartj/ehab892.
- [2] Mohebi R, Chen C, Ibrahim NE, et al. Cardiovascular Disease Projections in the United States Based on the 2020 Census Estimates. *J Am Coll Cardiol* 2022;80:565–78. Doi:10.1016/j.jacc.2022.05.033.
- [3] Roth GA, Mensah GA, Johnson CO, et al. Global Burden of Cardiovascular Diseases and Risk Factors, 1990-2019: Update From the GBD 2019 Study. *J Am Coll Cardiol* 2020;76:2982–3021. Doi:10.1016/j.jacc.2020.11.010.
- [4] Stein M, Boulaksil M, Jansen JA, et al. Reduction of fibrosis-related arrhythmias by chronic renin-angiotensin-aldosterone system inhibitors in an aged mouse model. *Am J Physiol Heart Circ Physiol* 2010;299:H310-21. Doi:10.1152/ajpheart.01137.2009.
- [5] Burlew BS, Weber KT. Cardiac fibrosis as a cause of diastolic dysfunction. *Herz* 2002;27:92–8. Doi:10.1007/s00059-002-2354-y
- [6] Hinderer S, Schenke-Layland K. Cardiac fibrosis – A short review of causes and therapeutic strategies. *Adv Drug Deliv Rev* 2019;146:77–82. <https://doi.org/10.1016/j.addr.2019.05.011>.
- [7] Eghbali M, Weber KT. Collagen and the myocardium: fibrillar structure, biosynthesis and degradation in relation to hypertrophy and its regression. *Mol Cell Biochem* 1990;96:1–14. Doi:10.1007/BF00228448
- [8] de Jong S, van Veen TAB, van Rijen HVM, de Bakker JMT. Fibrosis and Cardiac Arrhythmias. *J Cardiovasc Pharmacol* 2011;57:630–8. Doi:10.1097/FJC.0b013e318207a35f.
- [9] González A, Schelbert EB, Díez J, Butler J. Myocardial Interstitial Fibrosis in Heart Failure: Biological and Translational Perspectives. *J Am Coll Cardiol* 2018;71:1696–706. Doi:10.1016/j.jacc.2018.02.021.
- [10] De Jong S, Van Veen TAB, De Bakker JMT, et al. Biomarkers of Myocardial Fibrosis. *J Cardiovasc Pharmacol* 2011;57(5):522-35. Doi:10.1097/FJC.0b013e31821823d9.
- [11] Flett AS, Hasleton J, Cook C, et al. Evaluation of techniques for the quantification of myocardial scar of differing etiology using cardiac magnetic resonance. *JACC Cardiovasc Imaging* 2011;4:150-6. Doi:10.1016/j.jcmg.2010.11.015
- [12] Doltra A, Amundsen BH, Gebker R, et al. Emerging concepts for myocardial late gadolinium enhancement MRI. *Curr Cardiol Rev* 2013;9:185–90. Doi:10.2174/1573403X113099990030.
- [13] Begg GA, Swoboda PP, Karim R, et al. Imaging, biomarker and invasive assessment of diffuse left ventricular myocardial fibrosis in atrial fibrillation. *J Cardiovasc Magn Res* 2020;22:13. Doi:10.1186/s12968-020-0603-y.
- [14] Barison A, Grigoratos C, Todiere G, Aquaro GD. Myocardial interstitial remodelling in non-ischaemic dilated cardiomyopathy: insights from cardiovascular magnetic resonance. *Heart Fail Rev* 2015;20:731–49. Doi:10.1007/s10741-015-9509-4.
- [15] Taylor AJ, Salerno M, Dharmakumar R, Jerosch-Herold M. T1 Mapping Basic Techniques and Clinical Applications 2016;9:67-81. Doi:10.1016/j.jcmg.2015.11.005.

- [16] Cerisano G, Pucci PD, Sulla A, et al. Relation Between Plasma Brain Natriuretic Peptide, Serum Indexes of Collagen Type I Turnover, and Left Ventricular Remodeling After Reperfused Acute Myocardial Infarction. *Am J Cardiol* 2007;99:651–6. Doi:10.1016/j.amjcard.2006.09.114.
- [17] López B, González A, Díez J. Circulating biomarkers of collagen metabolism in cardiac diseases. *Circulation* 2010;121:1645–54. Doi:10.1161/CIRCULATIONAHA.109.912774.
- [18] Querejeta R, Varo N, López B, et al. Serum Carboxy-Terminal Propeptide of Procollagen Type I Is a Marker of Myocardial Fibrosis in Hypertensive Heart Disease. *Circulation* 2000;101:1729–35. Doi:10.1161/01.cir.101.14.1729
- [19] López B, Querejeta R, González A, et al. Effects of loop diuretics on myocardial fibrosis and collagen type I turnover in chronic heart failure. *J Am Coll Cardiol* 2004;43:2028–35. Doi:10.1016/j.jacc.2003.12.052.
- [20] Hartman MHT, Eppinga RN, Vlaar PJJ, et al. The contemporary value of peak creatine kinase-MB after ST-segment elevation myocardial infarction above other clinical and angiographic characteristics in predicting infarct size, left ventricular ejection fraction, and mortality. *Clin Cardiol* 2017;40:322–8. Doi:10.1002/clc.22663.
- [21] Iraqi W, Rossignol P, Angioi M, et al. Extracellular cardiac matrix biomarkers in patients with acute myocardial infarction complicated by left ventricular dysfunction and heart failure: Insights from the Eplerenone Post-Acute Myocardial Infarction Heart Failure Efficacy and Survival Study (EPHESUS) study. *Circulation* 2009;119:2471–9. Doi:10.1161/CIRCULATIONAHA.108.809194.
- [22] Van der Voorn SM, Bourfiss M, te Riele ASJM, et al. Exploring the Correlation Between Fibrosis Biomarkers and Clinical Disease Severity in PLN p.Arg14del Patients. *Front Cardiovasc Med* 2022;13:8:802998. Doi:10.3389/fcvm.2021.802998.
- [23] López B, González A, Ravassa S, et al. Circulating Biomarkers of Myocardial Fibrosis The Need for a Reappraisal. *J Am Coll Cardiol* 2015;65:2449–56. Doi:10.1016/j.jacc.2015.04.026
- [24] Hassager C, Risteli J, Risteli L, et al. Diurnal Variation in Serum Markers of Type I Collagen Synthesis and Degradation in Healthy Premenopausal Women. *J Bone Miner Res* 1992;7:1307–11. Doi:10.1002/jbmr.5650071110
- [25] Ravassa S, Lupón J, López B, et al. Prediction of Left Ventricular Reverse Remodeling and Outcomes by Circulating Collagen-Derived Peptides. *JACC Heart Fail* 2023;11:58–72. Doi:10.1016/j.jchf.2022.09.008.
- [26] Lang RM, Badano LP, Victor MA, et al. Recommendations for cardiac chamber quantification by echocardiography in adults: An update from the American Society of Echocardiography and the European Association of Cardiovascular Imaging. *J Am Soc Echocardiogr* 2015;28:1–39.e14. Doi:10.1016/j.echo.2014.10.003.
- [27] Voigt JU, Pedrizzetti G, Lysyansky P, et al. Definitions for a common standard for 2D speckle tracking echocardiography: consensus document of the EACVI/ASE/Industry Task Force to standardize deformation imaging. *Eur Heart J Cardiovasc Imaging* 2015;16:1–11. Doi:10.1093/ehjci/jeu184.

- [28] Pöyhönen P, Kylmälä M, Vesterinen P, et al. Peak CK-MB has a strong association with chronic scar size and wall motion abnormalities after revascularized non-transmural myocardial infarction-A prospective CMR study. *BMC Cardiovasc Disord* 2018;18:27. Doi:10.1186/s12872-018-0767-7.
- [29] Bengel FM, Diekmann J, Hess A, Jerosch-Herold M. Myocardial Fibrosis: Emerging Target for Cardiac Molecular Imaging and Opportunity for Image-Guided Therapy. *J Nucl Med* 2023;64:49S-58S. Doi:10.2967/jnumed.122.264867.
- [30] Löfsjögård J, Kahan T, Díez J, et al. Usefulness of Collagen Carboxy-Terminal Propeptide and Telo peptide to Predict Disturbances of Long-Term Mortality in Patients  $\geq 60$  Years With Heart Failure and Reduced Ejection Fraction. *Am J Cardiol* 2017;119:2042–8. Doi:10.1016/j.amjcard.2017.03.036.
- [31] Lijnen PJ, Maharani T, Finahari N, Prihadi JS. Serum Collagen Markers and Heart Failure. *Cardiovascular & Hematological Disorders-Drug Targets* 2012;12:51–5. Doi:10.2174/187152912801823147.
- [32] Raafs AG, Verdonschot JAJ, Henkens MTHM, et al. The combination of carboxy-terminal propeptide of procollagen type I blood levels and late gadolinium enhancement at cardiac magnetic resonance provides additional prognostic information in idiopathic dilated cardiomyopathy – A multilevel assessment of myocardial fibrosis in dilated cardiomyopathy. *Eur J Heart Fail* 2021;23:933–44. Doi:10.1002/ehf.2201.
- [33] McGavigan AD, Maxwell PR, Dunn FG. Serological evidence of altered collagen homeostasis reflects early ventricular remodeling following acute myocardial infarction. *Int J Cardiol* 2006;111:267–74. Doi:10.1016/j.ijcard.2005.08.045.
- [34] Ren HZ, Zhang XS, Wang LX. Effect of coronary revascularization on serum collagen biomarkers and left ventricular remodeling in patients with acute myocardial infarction. *Heart Lung* 2012;41:344–9. Doi:10.1016/j.hrtlng.2011.09.013.
- [35] Radovan J, Vaclav P, Petr W, et al. Changes of collagen metabolism predict the left ventricular remodeling after myocardial infarction. *Mol Cell Biochem* 2006;293:71–8. Doi:10.1007/s11010-006-2955-5.
- [36] Poulsen SH, Høst NB, Egstrup K. Long-Term Changes in Collagen Formation Expressed by Serum Carboxyterminal Propeptide of Type-I Procollagen and Relation to Left Ventricular Function after Acute Myocardial Infarction. *Cardiology* 2001;96:45-50. Doi:10.1159/000047385
- [37] Manhenke C, Ørn S, Squire I, et al. The prognostic value of circulating markers of collagen turnover after acute myocardial infarction. *Int J Cardiol* 2011;150:277–82. Doi:10.1016/j.ijcard.2010.04.034.
- [38] Murakami T, Kusachi S, Murakami M, et al. Time-dependent changes of serum carboxy-terminal peptide of type I procollagen and carboxy-terminal telopeptide of type I collagen concentrations in patients with acute myocardial infarction after successful reperfusion: correlation with left ventricular volume indices. *Clin Chem* 1998;44:2453-61. Doi not available.
- [39] Henriksen K, Karsdal MA. Type I Collagen. *Biochemistry of Collagens, Laminins and Elastin: Structure, Function and Biomarkers*, Elsevier Inc.; 2016. 1–11. Doi:10.1016/B978-0-12-809847-9.00001-5.

- [40] Vasikaran S, Eastell R, Bruyère O, et al. Markers of bone turnover for the prediction of fracture risk and monitoring of osteoporosis treatment: A need for international reference standards. *Osteoporos Int* 2011;22:391–420. Doi:10.1007/s00198-010-1501-1.
- [41] Hannon R, Eastell R. Preanalytical Variability of Biochemical Markers of Bone Turnover. *Osteoporos Int* 2000;11:Suppl 6:S30-44. Doi:10.1007/s001980070004.
- [42] Hlaing TT, Compston JE. Biochemical markers of bone turnover – uses and limitations. *Ann Clin Biochem* 2014;51:189–202. Doi:10.1177/0004563213515190.
- [43] Zerwekh JE, Ruml LA, Gottschalk F, Pak CYC. The Effects of Twelve Weeks of Bed Rest on Bone Histology, Biochemical Markers of Bone Turnover, and Calcium Homeostasis in Eleven Normal Subjects. *J Bone Miner Res* 2009;13:1594–601. Do:10.1359/jbmr.1998.13.10.1594.
- [44] Kjeldsen J, Rasmussen M, Schaffalitzky de Muckadell OB, et al. Collagen metabolites in the peripheral and splanchnic circulation of patients with Crohn disease. *Scand J Gastroenterol* 2001;36:1193–7. Doi:10.1080/00365520152584833.
- [45] Kjeldsen J, Schaffalitzky De Muckadell B, Junker P. Seromarkers of collagen I and III metabolism in active Crohn's disease. Relation to disease activity and response to therapy. *Gut* 1995;37:805–10. Doi:10.1136/gut.37.6.805.
- [46] Falcini F, Ermini M, Bagnoli F. Bone turnover is reduced in children with juvenile rheumatoid arthritis. *J Endocrinol Invest* 1998;21:31–6. Doi:10.1007/BF03347283.
- [47] Matuszewska A, Szechiński J. Evaluation of Selected Bone Metabolism Markers in Rheumatoid Arthritis Patients. *Adv Clin Exp Med* 2013;22:193-202. Doi not available.
- [48] Pedersen BJ, Schlemmer A, Rosenquist C, et al. Circadian Rhythm in Type I Collagen Formation in Postmenopausal Women With and Without Osteopenia. *Osteoporos Int* 1995;5:472-7. Doi:10.1007/BF01626611.



# Part II

Application of advanced imaging in cell based therapeutic strategies



## CHAPTER

# 5

# Deformation imaging to assess global and regional effects of cardiac regenerative therapy in ischemic heart disease - a systematic review

Van Klarenbosch BR, Chamuleau SAJ, Teske AJ

## ABSTRACT

### *Background*

Currently, left ventricular ejection fraction (LVEF) is the most common endpoint in cardiovascular stem cell therapy research. However, this global measure of cardiac function might not be suitable to detect the regional effects sorted by this therapy, and is hampered by high operator variability and loading dependency. Deformation imaging might be more accurate in detecting potential regional functional improvements by cardiac regenerative therapy.

### *Objective*

The aim of this systematic review is to provide a comprehensive overview of current literature on the value of deformation imaging in cardiac regenerative therapy.

### *Methods*

A systematic review of current literature available on PubMed, Embase, Cochrane databases was performed regarding both animal- and patient studies in which deformation imaging was used to study cardiac cell therapy. After critical appraisal, outcomes regarding study design, type of cell therapy, procedural characteristics, outcome measure, method for measuring strain and efficacy on both LVEF and deformation parameters were depicted.

### *Results*

A total of 30 studies, 15 preclinical and 15 clinical, were included for analysis. Deformation outcomes improved significantly in 14 out of 15 preclinical studies and in 10 out of 15 clinical studies, whilst LVEF improved in 12 and 4 articles respectively. Study designs and used deformation outcomes varied significantly among the included papers.

### *Conclusion*

6 studies found a positive effect on deformation outcomes without LVEF improvement. Hence, deformation imaging seems at least equal, and perhaps superior, to LVEF measurement in the assessment of cardiac regenerative therapy. However, strategies varied substantially and call for a standardized approach.

### *Keywords*

Stem cells; myocardial infarction; coronary artery disease; echocardiography; strain; deformation imaging; 2D speckle tracking; left ventricular ejection fraction

## INTRODUCTION

Ischemic heart disease concerns an important health issue in modern-day medicine. Reperfusion of ischemic myocardium by catheter-based- and surgical treatment has proven to be successful in both the treatment of acute myocardial infarction (AMI) in order to limit infarct size, as well as in chronic ischemic cardiomyopathy (ICMP) in order to protect the heart from further deterioration [1]. Since the regenerative capacity of the human heart is intrinsically limited, ischemic left ventricular (LV) dysfunction currently is a chronic condition. The ability to regenerate infarcted myocardium can be seen as the holy grail within cardiovascular research. Since 2002, when the first clinical trial [2] on the effect of cell therapy on the failing heart was published, clinical research makes effort into regenerating the damaged myocardium [3]. Unfortunately, myocardial regeneration has not found its way into the routine clinical setting. However, transfer of progenitor cells into infarcted myocardium has shown to sort a positive, albeit modest, effect on cardiac function [4]. The most commonly used functional outcome measure in cardiac regenerative research is the LV ejection fraction (LVEF) as measured by echo or MRI, which is easy to perform and effective for measuring global cardiac function changes. In the clinical setting, LVEF has been shown to be a powerful predictor of outcome [5–7]. Notwithstanding these advantages, the technique is hampered by high inter- and intra-operator variability and is dependent on loading conditions [8,9]. Furthermore, LVEF measurement may be less suitable to detect regional function changes potentially sorted by cardiac regenerative therapy. Keeping the high operator variability in mind, LVEF is arguably a suboptimal endpoint.

Cardiac deformation, expressed as strain ( $\epsilon$ ), is defined as the magnitude of deformation of a segment of myocardium during a cardiac cycle relative to the original length of this segment, and is expressed as a percentage. It can be measured using either tissue Doppler echocardiography (TDI), two-dimensional speckle-tracking echocardiography (2DSTE) and magnetic resonance (MR) tagging and tracking. Deformation is measured in either direction in which the myocardium deforms: longitudinal (shortening), circumferential (shortening) and radial (thickening) [10]. Peak systolic strain correlates well with LVEF, but unlike LVEF, is more likely to detect regional attenuations of cardiac function [11,12]. Deformation imaging is a noninvasive, quantitative, largely operator-independent and therefore reproducible and objective means of measuring both global and regional cardiac function, which at least in the longitudinal direction seems to outperform standard LVEF measurement regarding feasibility, accuracy and test-retest and inter-operator variability [13,14]. It therefore is a promising new technique, especially in the field of cardiac regenerative research. However, the additional value of this technique compared to current endpoint measurement within this field is currently inadequately understood. We hypothesize that deformation imaging will be effective in detecting the potential effects in regional cardiac function sorted by cardiac stem cell therapy. Hence, efficacy

of cell therapy can be assessed more precisely. The aim of this systematic review is to identify the added value of strain analysis over standard echocardiography in cardiac regenerative therapy for ischemic heart disease by providing a comprehensive overview of current literature on cardiac stem cell therapy in which deformation endpoints were used as outcome measures.

## METHODS

### *Search strategy*

According to PRISMA (Preferred Reporting Items for Systematic review and Meta Analyses) guidelines [15], a systematic search was performed on PubMed, Embase and Cochrane database. The search consisted of a combination of three main key terms: “stem cell”, “strain” and “ischaemia”, with their respective synonyms and related terms (Appendix 1). Using Covidence systematic review software (Veritas Health Innovation, Melbourne, Australia), duplicates were removed. Two authors (BvK and AT) separately assessed each of the identified records for eligibility based on title and abstract. Disagreements were discussed and consensus was reached, after which the remaining publications were independently assessed on full text by the stated in- and exclusion criteria. In addition, references from the identified publications were manually screened in order to identify relevant articles missing from our search.

### *In- and exclusion criteria*

Inclusion criteria were the use of stem cell therapy in ischemic heart disease, both acute and chronic, and deformation outcomes in either human or large- or small animal studies. Exclusion criteria were no 1) full text available, 2) language other than English/Dutch, 3) study design other than randomized controlled trial, randomized trial, case-control study or cohort study, 4) ex-vivo studies, 5) non-ischemic cardiac disease, 6) the use of surgically placed sheets as a delivery method since this is inherently expected to alter deformation parameters, 7) growth factor therapy and intervention and 8) assessment of diastolic deformation parameters only.

### *Study characteristics and quality assessment*

Of the included articles, the following data on study characteristics were collected: Study design (randomized controlled trial, randomized trial, case-control study, cohort study), population size, setting (acute infarction defined as infusion within a week of myocardial infarction or during the same hospitalization as opposed to ischemic cardiomyopathy, defined as diminished LVEF  $\leq 45\%$  at least 4 weeks after myocardial infarction) and model used (murine, canine or porcine). The cell type used (e.g. bone-marrow derived stem cells, mesenchymal stem cells, cardiac stem cells, umbilical cord-derived stem cells, pluripotent stem cells) and origin of these cells (either autologous or allogeneic) were

identified, as well as the used delivery method (intramyocardial delivery either surgical or percutaneous, intracoronary delivery, retrograde coronary sinus infusion). As for outcome measures, we assessed the deformation imaging modality utilized (TDI, 2DSTE, MR tagging or MR feature tracking) and the regional deformation outcomes (regional strain in either longitudinal, circumferential or radial direction), global deformation outcomes (global longitudinal strain (GLS), global circumferential strain (GCS) or global radial strain (GRS) ), strain rate (SR) outcomes (either in the longitudinal or radial direction) and LVEF measurements. When possible, within-group changes of the above mentioned outcome parameters were derived.

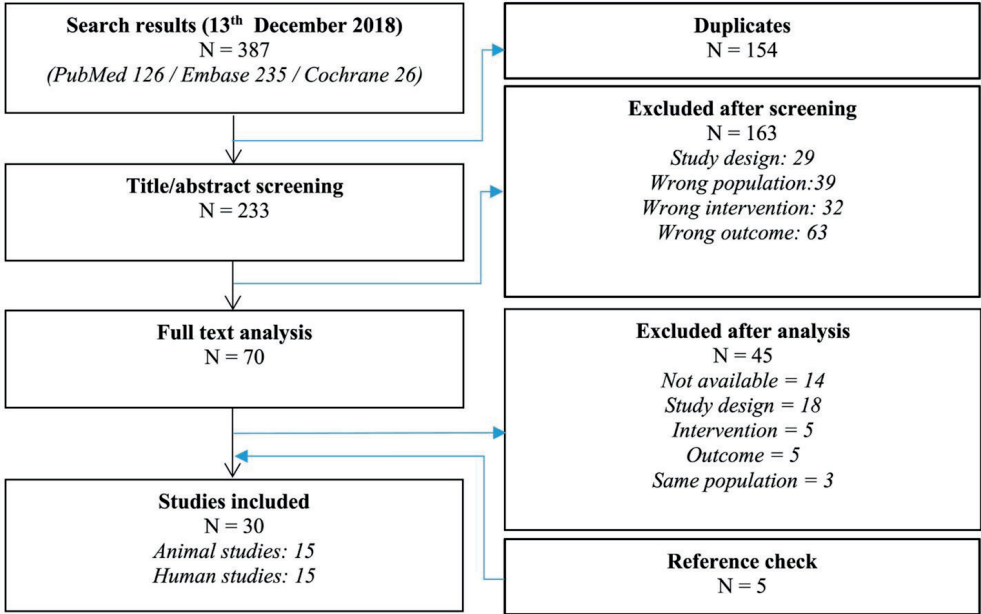
Using the Cochrane risk of bias tool [16], individual studies were assessed for quality. Since data were not pooled, no data synthesis and statistical analyses were performed. In order to provide results in a comprehensive manner, absolute improvement in longitudinal or circumferential strain were depicted as a positive numeral.

## RESULTS

### *Search results*

The final search (figure 1) was performed on December 13<sup>th</sup>, 2018. A total of 126 papers were identified from PubMed database, 235 papers were identified from Embase and 26 papers were identified from Cochrane database. After removal of 154 duplicates, 233 titles and abstracts were screened. After exclusion of 163 papers based on title and abstract, 70 papers were selected for full-text screening. An additional 45 papers were excluded, after which five papers were included after checking cross-references. Finally, a total of 30 [17–46] papers were included, of which fifteen papers were based on preclinical research and fifteen papers were based on clinical research.

Figure 1 – Study flowchart



*Quality assessment and study characteristics*

Quality of the included studies was assessed using the Cochrane risk of bias tool [16]. Results are shown in table 1. Five of the included papers, all of these performed in the clinical setting, were double-blind placebo-controlled randomized trials where a risk of bias could not be identified. In the remaining 25 studies, a risk of one or more types of bias could not be excluded.

*Preclinical study results*

Results are shown in table 2. The following paragraph portrays the heterogeneity of the included articles, due to which pooled analysis or assessment was not feasible. Of the fifteen identified papers, seven were based on a porcine model, six on a murine model and two a canine model. AMI was studied in eleven papers, the remaining studied animals with ICMP. Sample sizes ranged from ten to 184 subjects. A total of nine different cell products were used, mesenchymal stem cells (MSC's) being the most common studied cell type. Only three papers use autologous cell types; intramuscular delivery of stem cells was the most commonly used delivery method. Strain was measured using 2DSTE in seven papers, using either longitudinal, radial, or circumferential strain as an outcome measure. Four of these papers reported both global and regional deformation outcomes, one paper mentioned both global strain and SR, and the other two papers used SR respectively regional strain only. MR tagging was used in eight papers, all of these using regional circumferential strain as outcome measure. One paper used TDI, reporting

**TABLE 1** Quality assessment according to Cochrane risk of bias tool (Higgins et al., 2011)

Study	Study design	Selection bias		Performance bias	Detection bias	Attrition bias	Reporting bias	Other bias
		ASM	ACM					
Preclinical studies								
Amado et al. (2006)	RCT	+	+	-	?	+	+	+
Bonios et al. (2011)	RCT	+	+	?	?	+	+	+
Cal et al. (2015)	RCT	+	+	?	+	+	+	+
Chen et al. (2015)	RCT	+	+	-	?	+	-	+
Duran et al. (2013)	RCT	+	+	-	+	+	-	+
Jaussaud et al. (2013)	RCT	+	+	?	+	+	-	+
Karantalis et al. (2015)	RCT	+	+	?	?	+	+	+
Miao et al. (2014)	RCT	+	+	?	?	+	+	+
Quevedo et al. (2009)	RCT	+	+	?	?	?	-	+
Rickers et al. (2004)	RCT	+	+	?	?	?	-	+
Schneider et al. (2008)	RCT	+	+	?	+	+	-	+
Schuleri et al. (2008)	RCT	+	+	?	?	+	+	+
Schuleri et al. (2009)	RCT	+	+	+	?	+	+	+
Sun et al. (2016)	RCT	+	+	?	?	+	+	+
Yamada et al. (2013)	RCT	+	+	?	+	-	-	+
Clinical studies								
Beitnes et al. (2011)	RCT	+	+	-	+	+	+	+
Bhatti et al. (2013)	RCT	+	+	-	+	-	+	+
Heldman et al. (2014)	RCT	+	+	+	+	+	+	+
Herbots et al. (2009)	RCT	+	+	+	+	+	+	+
Hopp et al. (2011)	RCT	+	+	-	+	+	+	+
Karatasakis et al. (2010)	OCS	-	-	-	-	+	+	+
Lebrun et al. (2006)	OCS	-	-	-	-	+	+	+
Malliaras et al. (2014)	RCT	+	+	-	+	+	+	+
Nasseri et al. (2009)	OCS	-	-	-	-	+	+	+
Nasseri et al. (2014)	RCT	+	+	+	+	+	+	+
Plewka et al. (2009)	RCT	+	+	-	?	+	-	+
Qi et al. (2015)	RCT	+	+	+	+	+	+	+
Williams et al. (2011)	RT	?	-	-	?	+	+	+
Van Ramshorst et al. (2009)	CCS	-	-	-	+	+	+	+
Van Ramshorst et al. (2011)	RCT	+	+	+	+	+	+	+

Abbreviations: +, no risk of bias assumed; -, possible risk of bias; ?, not reported; CCS, case-control study; OCS, observational cohort study; RCT, randomized controlled trial; RT, randomized trial.

regional radial strain and radial strain rate. Three papers performed SR analysis. All but one paper reported a statistically significant effect of cell therapy on deformation parameters. Of these, eleven papers also demonstrated a significant positive effect of cell therapy on LVEF. One of these papers, however, only showed a significant effect on regional radial strain whilst no significant effect on global longitudinal-, circumferential- and radial strain was seen. Two papers identified significant changes in regional deformation, whilst LVEF and global strain were not affected by cell therapy or were not reported.



**TABLE 2** Studies reporting effect of stem cell therapy on deformation parameters in a preclinical setting

Study	Model	N	Cell type	Cell origin	Delivery method	Imaging modality	Endpoint			Effect			Effect LVEF
							Reg	Glo	SR	Reg	Glo	SR	
No significant effect of stem cell therapy on deformation parameters, no significant effect on LVEF													
Sun et al. (2016)	Canine, AMI	28	MSC	NR	RCSI	2DSTE	εL	GLS GCS GRS	-	-	-	-	-
Significant effect of stem cell therapy on deformation parameters, no significant effect on LVEF/LVEF not reported													
Miao et al. (2014)	Murine, AMI	24	MSC	Allo	IM	2DSTE	εL εC εR	GLS GCS GRS	-	↑ ↑ ↑	- - -	- - -	-
Rickers et al. (2004)	Canine, AMI	10	NR	Allo	IM	MR tag	εC	-	-	↑	-	-	-
Significant effect of stem cell therapy on deformation parameters, significant effect on LVEF													
Amado et al. (2006)	Porcine, AMI	14	MSC	Allo	IM	MR tag	εC	-	-	↑	-	-	↑
Bonios et al. (2011)	Murine, AMI	14	CDC	Allo	IM	2DSTE	εC	GCS	-	↑	↑	-	↑
Cai et al. (2015)	Murine, AMI	41	H-CSC	Allo	IM	2DSTE	-	-	dεL/dt	-	-	↑	↑
Chen et al. (2015)	Murine, AMI	12	UCBSC	Allo	IM	MR tag	εC εR	-	-	↑ ↑	-	-	↑
Duran et al. (2013)	Murine, AMI	184	CBSC CSC	Allo	IM	2DSTE	-	GLS GRS	dεL/dt dεR/dt	-	↑ ↑	↑ ↑	↑
Jaussaud et al. (2013)	Porcine, ICMP	18	BM-MS	Allo	IM	2DSTE	εL	-	-	↑	-	-	↑
Karantalis et al. (2015)	Porcine, ICMP	28	CSC + MSC MSC	Allo	IM	MR tag	εC	-	-	↑ ↑	-	-	↑ -
Quevedo et al. (2009)	Porcine, ICMP	10	MSC	Allo	IM	MR tag	εC	-	-	↑	-	-	↑
Schneider et al. (2008)	Porcine, AMI	23	MSC MSC mBMC	Auto Allo Allo	IM	TDI	εR	-	dεR/dt	↑ ↑ ↑	-	↑ ↑ ↑	↑ ↑ ↑
Schuleri et al. (2008)	Porcine, AMI	21	MSC	Auto	IM	MR tag	εC	-	-	↑	-	-	↑
Schuleri et al. (2009)	Porcine, ICMP	15	MSC	Auto	IM	MR tag	εC	-	-	↑	-	-	↑
Yamada et al. (2013)	Murine, AMI	12	IPSC	Allo	IM	2DSTE	εR	GLS GCS GRS	-	↑ - -	-	-	↑ - -

Sun et al. [17] report a non-significant absolute increase of 2.5% and 3.6% respectively in both global and regional deformation outcomes for MSC treated subjects, compared to 0.66% and 0.69% for saline treated controls. LVEF improved non-significantly by 1.98% in controls and decreased non-significantly by 0.06% in MSC treated subjects. The two papers reporting a significant effect of cardiac stem cell therapy on deformation but not on LVEF measurement did not allow for within-group analysis. In the studies with a significant effect of cell therapy on both deformation and LVEF which allowed for within-group analysis, absolute regional strain improvement ranged from 1.1% to 6.3% [20,21,26,29,30], compared to -0.6% - 1.3% for control groups. LVEF improvement ranged from 6.9% - 29.8% [21,26,28,29,31] for intervention subjects, compared to -7.6% - 2.5% for control subjects.

**TABLE 3** Studies reporting effect of stem cell therapy on deformation parameters in a clinical setting

Study	Setting	N	Cell type	Delivery method	Imaging modality	Endpoint			Effect			Effect LVEF	
						Reg	Glo	SR	Reg	Glo	SR		
No significant effect of stem cell therapy on deformation parameters, no significant effect on LVEF													
Beitnes et al. (2011)	AMI	100	mBMC	IC	2DSTE	eL	GLS	-	-	-	-	-	
Bhatti et al. (2013)	AMI	23	BMC	IC	MR FT	eC	GCS	-	-	-	-	-	
Lebrun et al. (2006)	ICMP	11	mBMC	IC	TDI	eL	-	deL/dt	-	-	-	-	
Nasseri et al. (2014)	ICMP (pre-CABG)	52	BMC	IM	2DSTE	eL	-	-	-	-	-	-	
Significant effect of stem cell therapy on deformation parameters, no significant effect on LVEF/LVEF not reported													
Heldman et al. (2014)	ICMP	65	mBMC MSC	IM	MR tag	eC	-	-	↑ ↑	-	-	- -	
Herbots et al. (2009)	AMI	67	BMC	IC	TDI	eL	-	deL/dt	↑	-	↑	-	
Hopp et al. (2011)	AMI	28	mBMC	IC	MR tag	eC	GCS	-	↓	↓	-	-	
Karatasakis et al. (2010)	ICMP	10	MSC	IC	TDI	eL	-	deL/dt	↑	-	↑	-	
Malliaras et al. (2014)	ICMP	25	CDC	IC	MR tag	eC	-	-	↑	-	-	-	
Nasseri et al. (2009)	ICMP	12	BMC	IM	2DSTE	eL	-	-	↑	-	-	-	
Williams et al. (2011)	ICMP	8	mBMC BM-MS	IM	MR tag	eC	-	-	↑	-	-	-	
Significant effect of stem cell therapy on deformation parameters, significant effect on LVEF													
Plewka et al. (2009)	AMI	60	BMC	IC	2DSTE	eL	-	-	↑	-	-	↑	
Qi et al. (2015)	ICMP (pre-CABG)	42	mBMC	IC (graft)	2DSTE	eL eC	GLS GCS	-	- -	↑ -	-	↑	
Van Ramshorst et al. (2009)	ICMP	24	mBMC	IM	2DSTE	-	GLS	-	-	↑	-	↑	
Van Ramshorst et al. (2011)	ICMP	50	mBMC	IM	2DSTE	eL	GLS	deL/dt	↑	↑	↑	↑	

### Clinical study results

Results are shown in table 3. Similar to preclinical study results, identified articles were markedly heterogeneous in their study design, making the results unsuitable for pooled analysis. Of the fifteen identified papers, ten papers studied patients with ICMP, whereas five studies were carried out in patients with AMI. Sample sizes ranged from eight to 100 patients. The majority of papers studied bone-marrow derived cells (of which eight studied mononuclear bone marrow cells), while three papers studied MSC's and one paper studied cardiosphere-derived stem cells. Six papers delivered the cells intramyocardially, nine performed intracoronary cell infusion. Seven papers measured strain by 2DSTE, where four papers determined strain by TDI. MR-derived strain was reported in five papers, four of which using MR tagging and one using feature tracking. All but one paper measured regional deformation endpoints, either longitudinal or circumferential. Four papers additionally demonstrated global deformation outcomes, as did four papers additionally show longitudinal strain rate. One paper expressed global longitudinal strain only.

Four papers [32–35] found no significant effect of cell therapy on either regional strain (range -0.2 – 2.6% for the intervention groups compared to 3.0 – 3.3% for the control groups), global strain (range 2.1 – 2.5% vs. 0.4 – 2.4%) or LVEF (range 1.8 – 2.5% vs. -0.1 – 1.0%), implying no statistically significant beneficial effect of cell therapy on cardiac

function. On the contrary, four papers [43–46] show a positive effect of cardiac stem cell therapy on both regional (range 1% – 3-2% for the intervention groups vs. 0 – 2.3% for the control groups) and global (range 0.8% – 5.5% vs -1.2% – 2.3%) deformation outcomes, as well as LVEF measurement (range 4% – 13% vs -3 – 6.7%). Qi et al. [44] showed a beneficial effect of cell therapy on LVEF, but only found global longitudinal strain to show a significant positive effect of cell therapy, as opposed to global circumferential strain and regional longitudinal- and circumferential strain. Three papers [43,45,46] showed regional- and global longitudinal strain as a positive outcome measurement of cardiac cell therapy. A total of six papers [36,37,39–42] found a significant positive effect of cell therapy on regional longitudinal- (range 3.7% – 7.5% for cell treatment groups, no within-group analyses of control groups supplied) or circumferential (range 2.9% – 4.9% vs 0.03% in control patients) strain, whereas an effect on LVEF (range 2.5% – 5.4% vs -5.0% – 5.8%) was not detected (n=5) or was not mentioned (n=1). In addition, two of these papers [37,39] also found a positive effect of cell therapy on longitudinal strain rate, and one found a positive effect of cell therapy on global longitudinal strain [39]. Contrary to expectation, one paper [38] found a significant negative effect of mononuclear bone marrow cell therapy on both regional and global circumferential strain, but not on LVEF.

## DISCUSSION

One of the main conclusions that can be drawn from this review is that the use of deformation outcome measures within cardiac cell therapy research is very heterogeneous. The included studies varied substantially in their choice of patient setting or animal model, type of cardiac stem cell and method of administration. To add to the heterogeneity of our results, the method of deformation measurement (either 2DSTE, TDI or MR feature tracking or tagging) and the outcome measure of choice (global or regional strain in the longitudinal, radial or circumferential direction) varied distinctively between the different included studies. Comparing results of different studies or performing meta-analyses was therefore not feasible.

Notwithstanding the heterogeneity in deformation imaging within cardiac regenerative medicine, this article provides an insight into the value of strain analysis within this field of research. The results show that in thirteen out of fifteen preclinical papers and in nine out of fifteen clinical papers deformation imaging results followed the results of LVEF outcome measurement, either both showing a significant effect of cardiac cell therapy on LV function or both showing a non-significant effect of cardiac cell therapy on LV function. There are no papers that reported a significant effect of cell therapy on LVEF measurement without deformation outcomes doing so. Importantly, and fitting with our main hypothesis, two out of fifteen preclinical papers and seven out of fifteen clinical papers showed a significant effect of cell therapy on cardiac deformation, whereas LVEF was not improved significantly

in these studies. These results advocate a potential added value of deformation imaging within cardiac regenerative medicine for ischaemic heart disease.

Although experience with cardiac stem cell therapy shows a positive effect on cardiac function, underlying mechanisms are not fully elucidated. It is believed to be based on paracrine effects, leading to 1) neo-vascularization into regions affected by ischaemia [29], 2) modulation of inflammatory effects [47,48], 3) modulation of ventricular remodeling and extracellular matrix homeostasis [49,50] and 4) enhancement of cardiac repair by host resident cardiac progenitors [51]. Currently effort is put into optimizing the effect of cardiac regenerative therapy. Indeed, this is reflected by the large heterogeneity in research strategies of the studies included in this article. In addition to these necessary efforts for improving cardiac cell therapy, however, we suggest assessing new outcome measures. This is because effects of cell therapy on global cardiac function as measured by LVEF are limited. In a meta-analysis assessing the effect of adult bone-marrow cardiac cell therapy (Afzal et al., 2015), the authors presented a beneficial effect of bone-marrow derived cell therapy on LVEF of merely 2.92%. Of importance, the results of papers included in our systematic review are of similar magnitude. Keeping in mind the high inter- and intra-operator variability and loading dependency of LVEF measurement [8,9], leading to variations of up to 18% for 2D LVEF measurement by Simpson's rule [52], LVEF is in our opinion not suitable for endpoint measurement in cardiac regenerative medicine in individual cases.

Deformation imaging has already proven its value in for example hypertrophic cardiomyopathy [53] and valvular heart disease [54,55], in which deterioration of deformation parameters can be observed before LVEF decreases. This apparent superior sensitivity for changes in cardiac function makes deformation imaging of great potential use within cardiac regenerative medicine. Besides being less operator dependent compared to LVEF, strain analysis allows for assessment of regional cardiac function, making this technique especially suitable for therapies in which a regional effect is expected to be sorted. Regional strain is indeed analyzed in all but two included studies in this article, of which seven studies suggest an improved sensitivity to changes in LV function compared to LVEF measurement. There are however no studies reporting on significantly increased global strain while LVEF was not altered. Furthermore, from the results it is not clear which type of regional strain parameter is best used. As an additional advantage, 2D-STE seems more accurate, also in direct comparison with LVEF measurement [13,56].

The effect of stem cell therapy varies strikingly between preclinical and clinical research: preclinical papers show a positive effect on deformation parameters more often than clinical studies do. This 'translational failure' is a known phenomenon, due to which preclinical results may not always be applicable to the clinical setting. A possible explanation can be found in the risk of bias analysis, showing a higher risk for performance bias, detection bias and reporting bias in preclinical studies. Also, study models might be more heterogeneous in the patient setting.

*Limitations*

This aim of this study was to investigate whether deformation imaging could provide added value over conventional endpoint measurement in stem cell research. Although evidence is not scarce, and data indeed do suggest added value of deformation imaging, articles that were related to in this study were too heterogeneous in their study design for pooled analysis. Therefore we could not provide a statistical analysis on deformation imaging as a diagnostic tool over conventional functional imaging. In addition, deformation imaging was not compared to other methods of endpoint measurement, such as myocardial perfusion imaging, so the value compared to these remains to be elucidated. Moreover, the relevance of so-called surrogate endpoints in stem cell research needs to be addressed. We aimed to investigate deformation imaging as a new surrogate endpoint for stem cell research. However, regardless of the probable additional value of deformation imaging over conventional endpoint measurement, we are unsure how this relates to clinical endpoints such as mortality, hospital admissions, quality of life or recovery from myocardial infarction. This remains to be studied. To conclude, the conventional echocardiography endpoint used in the included papers was 2-dimensional LVEF, of which diagnostic accuracy is inferior compared to 3-dimensional assessment. Therefore, results might not be applicable to the current situation in which 3-dimensional LVEF assessment is common practice.

*Future perspectives*

In order to be able to compare deformation outcomes within cardiac regenerative medicine, the methods of performing this should be standardized. We propose to use the 'Definitions for a common standard for 2D speckle tracking echocardiography: consensus document of the EACVI/ASE/Industry Task Force to standardize deformation imaging' [57] as a guide for standardized deformation imaging within cardiac regenerative research. This provides guidance into both image acquisition and image processing. Preferably, deformation should be measured using 2DSTE or MRI tagging or feature tracking; TDI-derived strain is arguably too laborious and complicated for common clinical use. Future efforts of this task force might further enhance diagnostic performance of 2DSTE and allow for more inter-study comparison. Future research might provide insight into which of the deformation parameters is most sensitive to LV functional change after regenerative therapy. Also, newer strategies such as 3-dimension speckle tracking echocardiography might provide additional diagnostic accuracy.

## **CONCLUSION**

Deformation imaging shows to be a promising new endpoint measure in cardiac stem cell research, which is at least equally, and possibly more, effective than LVEF assessment in the detection of changes in cardiac function, and may provide research with a more objective measure of response to therapy. However, current use is diverse and needs standardization in order to compare results between studies.

## **CONFLICTS OF INTEREST**

None declared.

## REFERENCES

1. Windecker S, Stortecky S, Stefanini GG, et al. Revascularisation versus medical treatment in patients with stable coronary artery disease: network meta-analysis. *BMJ*. 2014;348:g3859. doi: 10.1136/bmj.g3859
2. Strauer BE, Brehm M, Zeus T, et al. Repair of infarcted myocardium by autologous intracoronary mononuclear bone marrow cell transplantation in humans. *Circulation*. 2002;106:1913–8. doi: 10.1161/01.cir.0000034046.87607.1c
3. Fernández-Avilés F, Sanz-Ruiz R, Climent AM, et al. Global position paper on cardiovascular regenerative medicine. *Eur Heart J*. 2017;38:2532–46. doi: 10.1093/eurheartj/ehx248
4. Afzal MR, Samanta A, Shah ZI, et al. Adult Bone Marrow Cell Therapy for Ischemic Heart Disease: Novelty and Significance. *Circ Res*. 2015;117:558–75. doi: 10.1161/CIRCRESAHA.114.304792
5. Pocock SJ, Wang D, Pfeffer MA, et al. Predictors of mortality and morbidity in patients with chronic heart failure. *Eur Heart J*. 2006;27:65–75. doi: 10.1093/eurheartj/ehi555
6. Solomon SD, Anavekar N, Skali H, et al. Influence of ejection fraction on cardiovascular outcomes in a broad spectrum of heart failure patients. *Circulation*. 2005;112:3738–44. doi: 10.1161/CIRCULATIONAHA.105.561423
7. Møller JE, Hillis GS, Oh JK, et al. Wall motion score index and ejection fraction for risk stratification after acute myocardial infarction. *Am Heart J*. 2006;151:419–25. doi: 10.1016/j.ahj.2005.03.042
8. Wood PW, Choy JB, Nanda NC, Becher H. Left ventricular ejection fraction and volumes: It depends on the imaging method. *Echocardiography*. 2014;31:87–100.
9. Dorosz JL, Lezotte DC, Weitzenkamp DA, Allen LA, Salcedo EE. Performance of 3-dimensional echocardiography in measuring left ventricular volumes and ejection fraction: A systematic review and meta-analysis. *J Am Coll Cardiol*. 2012;59:1799–808. doi: 10.1111/echo.12331
10. Teske AJ, De Boeck BWL, Melman PG, et al. Echocardiographic quantification of myocardial function using tissue deformation imaging, a guide to image acquisition and analysis using tissue Doppler and speckle tracking. *Cardiovasc Ultrasound*. 2007;5:27. doi: 10.1186/1476-7120-5-27
11. Lima MSM, Villarraga HR, Abduch MCD, et al. Global Longitudinal Strain or Left Ventricular Twist and Torsion? Which Correlates Best with Ejection Fraction? *Arq Bras Cardiol*. 2017;23–9. doi: 10.5935/abc.20170085
12. Weidemann F, Jamal F, Sutherland GR, et al. Myocardial function defined by strain rate and strain during alterations in inotropic states and heart rate. *Am J Physiol Heart Circ Physiol*. 2002;283:H792–9. doi: 10.1152/ajpheart.00025.2002.
13. Barbier P, Mirea O, Cefalù C, et al. Reliability and feasibility of longitudinal AFI global and segmental strain compared with 2D left ventricular volumes and ejection fraction: Intra- and inter-operator, test-retest, and inter-cycle reproducibility. *Eur Heart J Cardiovasc Imaging*. 2015;16:642–52. doi: 10.1093/ehjci/jeu274

14. Mirea O, Pagourelas ED, Duchenne J, et al. Variability and Reproducibility of Segmental Longitudinal Strain Measurement. *JACC: Cardiovascular Imaging*. 2018;11:15–24. doi: 10.1016/j.jcmg.2017.01.027
15. Moher D, Liberati A, Tetzlaff J, Altman DG. Preferred reporting items for systematic reviews and meta-analyses: the PRISMA statement. *BMJ*. 2009;339:b2535. doi: 10.1136/bmj.b2535
16. Higgins JPT, Altman DG, Gøtzsche PC, et al. The Cochrane Collaboration's tool for assessing risk of bias in randomised trials. *BMJ*. 2011;343:d5928. doi: 10.1136/bmj.d5928
17. Sun QW, Zhen L, Wang Q, et al. Assessment of Retrograde Coronary Venous Infusion of Mesenchymal Stem Cells Combined with Basic Fibroblast Growth Factor in Canine Myocardial Infarction Using Strain Values Derived from Speckle-Tracking Echocardiography. *Ultrasound Med Biol*. 2016;42:272–81. doi: 10.1016/j.ultrasmedbio.2015.09.010
18. Miao Q, Shim W, Tee N, et al. iPSC-derived human mesenchymal stem cells improve myocardial strain of infarcted myocardium. *J Cell Mol Med*. 2014;18:1644–54. doi: 10.1111/jcmm.12351
19. Rickers C, Gallegos R, Seethamraju RT, et al. Catheter Interventions in Congenital Heart Disease—Part I Applications of Magnetic Resonance Imaging for Cardiac Stem Cell Therapy. *J Interv Cardiol*. 2004;17:37–46. doi: 10.1111/j.1540-8183.2004.01712.x
20. Amado LC, Schuleri KH, Saliaris AP, et al. Multimodality Noninvasive Imaging Demonstrates In Vivo Cardiac Regeneration After Mesenchymal Stem Cell Therapy. *J Am Coll Cardiol*. 2006;48:2116–24. doi: 10.1177/1531003507308791.
21. Bonios M, Chang CY, Pinheiro A, et al. Cardiac resynchronization by cardiosphere-derived stem cell transplantation in an experimental model of myocardial infarction. *J Am Soc Echocardiogr*. 2011;24:808–14. doi: 10.1016/j.echo.2011.03.003
22. Cai C, Guo Y, Teng L, et al. Preconditioning Human Cardiac Stem Cells with an HO-1 Inducer Exerts Beneficial Effects after Cell Transplantation in the Infarcted Murine Heart. *Stem Cells*. 2015;33:3596–607. doi: 10.1002/stem.2198
23. Chen Y, Ye L, Zhong J, et al. The Structural Basis of Functional Improvement in Response to Human Umbilical Cord Blood Stem Cell Transplantation in Hearts with Post-Infarct LV Remodeling HHS Public Access. *Cell Transplant*. 2015;24:971–83. doi: 10.3727/096368913X675746
24. Duran JM, Makarewich CA, Sharp TE, et al. Bone-Derived stem cells repair the heart after myocardial infarction through transdifferentiation and paracrine signaling mechanisms. *Circ Res*. 2013;113:539–52. doi: 10.1161/CIRCRESAHA.113.301202
25. Jaussaud J, Biais M, Calderon J, et al. Hypoxia-preconditioned mesenchymal stromal cells improve cardiac function in a swine model of chronic myocardial ischaemia. *Eur J of Cardiothorac Surg*. 2013;43:1050–7. doi: 10.1093/ejcts/ezs549
26. Karantalis V, Suncion-Loescher VY, Bagno L, et al. Synergistic effects of combined cell therapy for chronic ischemic cardiomyopathy. *J Am Coll Cardiol*. 2015;66:1990–9. doi: 10.1016/j.jacc.2015.08.879
27. Quevedo HC, Hatzistergos KE, Oskouei BN, et al. Allogeneic mesenchymal stem cells restore cardiac function in chronic ischemic cardiomyopathy via trilineage differentiating capacity. *Proc Natl Acad Sci U S A*. 2009;106:14022–7. doi: 10.1073/pnas.0903201106



28. Schneider C, Krause K, Jaquet K, et al. Intramyocardial Transplantation of Bone Marrow-Derived Stem Cells: Ultrasonic Strain Rate Imaging in a Model of Hibernating Myocardium. *J Card Fail.* 2008;14:861–72. doi: 10.1016/j.cardfail.2008.08.005
29. Schuleri KH, Amado LC, Boyle AJ, et al. Early improvement in cardiac tissue perfusion due to mesenchymal stem cells. *Am J Physiol Heart Circ Physiol.* 2008;294:H2002–2011. doi: 10.1152/ajpheart.00762.2007
30. Schuleri KH, Feigenbaum GS, Centola M, et al. Autologous mesenchymal stem cells produce reverse remodelling in chronic ischaemic cardiomyopathy. *Eur Heart J.* 2009;30:2722–32. doi: 10.1093/eurheartj/ehp265
31. Yamada S, Nelson TJ, Kane GC, et al. Induced pluripotent stem cell intervention rescues ventricular wall motion disparity, achieving biological cardiac resynchronization post-infarction. *J Physiol.* 2013;591:4335–49. doi: 10.1113/jphysiol.2013.252288
32. Beitnes JO, Gjesdal O, Lunde K, et al. Left ventricular systolic and diastolic function improve after acute myocardial infarction treated with acute percutaneous coronary intervention, but are not influenced by intracoronary injection of autologous mononuclear bone marrow cells: A 3 year serial echocardiographic sub-study of the randomized-controlled ASTAMI study. *Eur J Echocardiogr.* 2011;12:98–106. doi: 10.1093/ejechocard/jeq116
33. Bhatti S, Al-Khalidi H, Hor K, et al. Assessment of Myocardial Contractile Function Using Global and Segmental Circumferential Strain following Intracoronary Stem Cell Infusion after Myocardial Infarction: MRI Feature Tracking Feasibility Study. *ISRN Radiol.* 2013;371028. doi: 10.5402/2013/371028
34. Lebrun F, Berchem G, Delagardelle C, et al.. Improvement of exercise-induced cardiac deformation after cell therapy for severe chronic ischemic heart failure. *J Card Fail.* 2006;12:108–13. doi: 10.1016/j.cardfail.2005.10.011
35. Nasser BA, Ebell W, Dandel M, et al. Autologous CD133+ bone marrow cells and bypass grafting for regeneration of ischaemic myocardium: The Cardio133 trial. *Eur Heart J.* 2014;35:1263–74. doi: 10.1093/eurheartj/ehu007
36. Heldman AW, DiFede DL, Fishman JE, et al. Transendocardial mesenchymal stem cells and mononuclear bone marrow cells for ischemic cardiomyopathy: The TAC-HFT randomized trial. *JAMA.* 2014;311:62–73. doi: 10.1001/jama.2013.282909
37. Herbots L, D'Hooge J, Eroglu E, et al. Improved regional function after autologous bone marrow-derived stem cell transfer in patients with acute myocardial infarction: A randomized, double-blind strain rate imaging study. *Eur Heart J.* 2009;30:662–70. doi: 10.1093/eurheartj/ehn532
38. Hopp E, Lunde K, Solheim, et al. Regional myocardial function after intracoronary bone marrow cell injection in reperfused anterior wall infarction - A cardiovascular magnetic resonance tagging study. *J Cardiovasc Magn Reson.* 2011;13:22. doi: 10.1186/1532-429X-13-22
39. Karatasakis G, Leontiadis E, Peristeri I, et al. Intracoronary infusion of selected autologous bone marrow stem cells improves longitudinal myocardial strain and strain rate in patients with old anterior myocardial infarction without recent revascularization. *Eur J Echocardiogr.* 2010;11:440–5. doi: 10.1093/ejechocard/jep235

40. Malliaras K, Makkar RR, Smith RR, et al. Intracoronary cardiosphere-derived cells after myocardial infarction: Evidence of therapeutic regeneration in the final 1-year results of the CADUCEUS trial (Cardiosphere-derived aUtologous stem CELls to reverse ventricular dysfunction). *J Am Coll Cardiol.* 2014;63:110–22. doi: 10.1016/j.jacc.2013.08.724
41. Nasser BA, Kukucka M, Dandel M, et al. Two-Dimensional Speckle Tracking Strain Analysis for Efficacy Assessment of Myocardial Cell Therapy. *Cell Transplant.* 2009;18:361–70. doi: 10.3727/096368909788534924
42. Williams AR, Trachtenberg B, Velazquez DL, et al. Intramyocardial stem cell injection in patients with ischemic cardiomyopathy: Functional recovery and reverse remodeling. *Circ Res.* 2011;108:792–6. doi: 10.1161/CIRCRESAHA.111.242610
43. Plewka M, Krzemińska-Pakuła M, Lipiec P, et al. Effect of Intracoronary Injection of Mononuclear Bone Marrow Stem Cells on Left Ventricular Function in Patients With Acute Myocardial Infarction. *Am J Cardiol.* 2009;104:1336–42. doi: 10.1016/j.amjcard.2009.06.057
44. Qi Z, Duan F, Liu S, et al. Effectiveness of bone marrow mononuclear cells delivered through a graft vessel for patients with previous myocardial infarction and chronic heart failure: An echocardiographic study of left ventricular remodeling. *Echocardiography.* 2015;32:937–46. doi: 10.1111/echo.12787
45. Van Ramshorst J, Atsma DE, Beeres SLMA, et al. Effect of intramyocardial bone marrow cell injection on left ventricular dyssynchrony and global strain. *Heart.* 2009;95:119–24. doi: 10.1136/hrt.2007.129569
46. Van Ramshorst J, Antoni ML, Beeres SLMA, Roes SD, Delgado V, Rodrigo SF, et al. Intramyocardial bone marrow-derived mononuclear cell injection for chronic myocardial ischemia: The effect on diastolic function. *Circ Cardiovasc Imaging.* 2011;4:122–9. doi: 10.1161/CIRCIMAGING.110.957548
47. Van Den Akker F, Deddens JC, Doevendans PA, Sluijter JPG. Cardiac stem cell therapy to modulate inflammation upon myocardial infarction. *Biochim Biophys Acta Gen Subj.* 2013;1830:2449–58. doi: 10.1016/j.bbagen.2012.08.026
48. Luger D, Lipinski MJ, Westman PC, et al. Intravenously delivered mesenchymal stem cells. *Circ Res.* 2017;120:1598–613. doi: 10.1161/CIRCRESAHA.117.310599
49. Laflamme MA, Zbinden S, Epstein SE, Murry CE. Cell-Based Therapy for Myocardial Ischemia and Infarction: Pathophysiological Mechanisms. *Ann Rev Pathol.* 2007;2:307–39.
50. Xu X, Xu Z, Xu Y, Cui G. Effects of mesenchymal stem cell transplantation on extracellular matrix after myocardial infarction in rats. *Coron Artery Dis.* 2005;16:245–55. doi: 10.1146/annurev.pathol.2.010506.092038
51. Etzion S, Battler A, Barbash IM, et al. Influence of embryonic cardiomyocyte transplantation on the progression of heart failure in a rat model of extensive myocardial infarction. *J Mol Cell Cardiol.* 2001;33:1321–30. doi: 10.1006/jmcc.2000.1391
52. Jensen-Urstad K, Bouvier F, Höjer J, et al. Comparison of Different Echocardiographic Methods With Radionuclide Imaging for Measuring Left Ventricular Ejection Fraction During Acute

- Myocardial Infarction Treated by Thrombolytic Therapy. *Am J Cardiol.* 1998;81:538–44. doi: 10.1016/s0002-9149(97)00964-8
53. Fuster V, Van Der Zee S, Miller MA. Evolving anatomic, functional, and molecular imaging in the early detection and prognosis of hypertrophic cardiomyopathy. *J Cardiovasc Transl Res.* 2009;2:398–406. doi: 10.1007/s12265-009-9133-6
54. Gunjan M, Kurien S, Tyagi S. Early prediction of left ventricular systolic dysfunction in patients of asymptomatic chronic severe rheumatic mitral regurgitation using tissue Doppler and strain rate imaging. *Indian Heart J.* 2012;64:245–8. doi: 10.1016/S0019-4832(12)60080-7
55. Casas-Rojo E, Fernández-Golfin C, Moya-Mur JL, et al. Area strain from 3D speckle-tracking echocardiography as an independent predictor of early symptoms or ventricular dysfunction in asymptomatic severe mitral regurgitation with preserved ejection fraction. *Int J Cardiovasc Imaging.* 2016;32:1189–98. doi: 10.1007/s10554-016-0904-2
56. Mirea O, Pagourelias ED, Duchenne J, et al. Variability and Reproducibility of Segmental Longitudinal Strain Measurement. *JACC: Cardiovascul Imaging.* 2018;11:15–24. doi: 10.1016/j.jcmg.2017.01.027
57. Voigt JU, Pedrizzetti G, Lysyansky P, et al. Definitions for a common standard for 2D speckle tracking echocardiography: consensus document of the EACVI/ASE/Industry Task Force to standardize deformation imaging. *Eur Heart J Cardiovasc Imaging.* 2015;16:1–11. doi: 10.1093/ehjci/jeu184

## APPENDIX – SEARCH SYNTAX

### *Pubmed*

((((((((((Stem cell [title/abstract]) OR stem cells [title/abstract]) OR progenitor [title/abstract]) OR mother cell [title/abstract]) OR mother cells [title/abstract]) OR colony forming [title/abstract]) OR colony-forming [title/abstract]) OR regeneration [title/abstract]) OR regenerative therapy [title/abstract]) OR bone marrow [title/abstract])) AND (((((((Strain [title/abstract]) OR deformation [title/abstract]) OR regional myocardial function [title/abstract]) OR speckle tracking [title/abstract]) OR tissue Doppler [title/abstract]) OR tissue velocity [title/abstract])) AND (((((((((((((((Myocardial infarction [title/abstract]) OR myocardial infarctions [title/abstract]) OR myocardial infarct [title/abstract]) OR myocardial infarcts [title/abstract]) OR myocardial ischaemia [title/abstract]) OR myocardial ischemia [title/abstract]) OR cardiac ischemia [title/abstract]) OR cardiac ischaemia [title/abstract]) OR cardiovascular stroke [title/abstract]) OR heart attack [title/abstract]) OR heart attacks [title/abstract]) OR coronary [title/abstract]) OR ischemic cardiomyopathy [title/abstract]) OR ischaemic cardiomyopathy [title/abstract]) OR ischemic heart failure [title/abstract]) OR ischaemic heart failure [title/abstract]) OR ischemic heart disease [title/abstract]) OR ischaemic heart disease [title/abstract]) OR CAD [title/abstract]) OR IHD [title/abstract]) OR STEMI [title/abstract]) OR NSTEMI [title/abstract]) OR CHD [title/abstract]) OR AMI [title/abstract]) OR ACS [title/abstract]))

### *Embase*

('stem cell':ti,ab OR 'stem cells':ti,ab OR 'progenitor':ti,ab OR 'mother cell':ti,ab OR 'mother cells':ti,ab OR 'colony forming':ti,ab OR 'colony-forming':ti,ab OR 'regeneration':ti,ab OR 'regenerative therapy':ti,ab OR 'bone marrow':ti,ab) AND ('strain':ti,ab OR 'deformation':ti,ab OR 'regional myocardial function':ti,ab OR 'speckle tracking':ti,ab OR 'tissue doppler':ti,ab OR 'tissue velocity':ti,ab) AND ('myocardial infarction':ti,ab OR 'myocardial infarctions':ti,ab OR 'myocardial infarct':ti,ab OR 'myocardial infarcts':ti,ab OR 'myocardial ischaemia':ti,ab OR 'myocardial ischemia':ti,ab OR 'cardiac ischemia':ti,ab OR 'cardiac ischaemia':ti,ab OR 'cardiovascular stroke':ti,ab OR 'heart attack':ti,ab OR 'heart attacks':ti,ab OR 'coronary':ti,ab OR 'ischemic cardiomyopathy':ti,ab OR 'ischaemic cardiomyopathy':ti,ab OR 'ischemic heart failure':ti,ab OR 'ischaemic heart failure':ti,ab OR 'ischemic heart disease':ti,ab OR 'ischaemic heart disease':ti,ab OR 'CAD':ti,ab OR 'IHD':ti,ab OR 'STEMI':ti,ab OR 'NSTEMI':ti,ab OR 'CHD':ti,ab OR 'AMI':ti,ab OR 'ACS':ti,ab)

### *Cochrane*

("stem cell":ti,ab,kw OR "stem cells":ti,ab,kw OR "progenitor":ti,ab,kw OR "mother cell":ti,ab,kw OR "mother cells":ti,ab,kw OR "colony forming":ti,ab,kw OR "colony-forming":ti,ab,kw OR "regeneration":ti,ab,kw OR "regenerative therapy":ti,ab,kw OR "bone marrow":ti,ab,kw) AND ("strain":ti,ab,kw OR "deformation":ti,ab,kw OR "regional

myocardial function":ti,ab,kw OR "speckle tracking":ti,ab,kw OR "tissue doppler":ti,ab,kw OR "tissue velocity":ti,ab,kw) AND ("myocardial infarction":ti,ab,kw OR "myocardial infarctions":ti,ab,kw OR "myocardial infarct":ti,ab,kw OR "myocardial infarcts":ti,ab,kw OR "myocardial ischaemia":ti,ab,kw OR "myocardial ischemia":ti,ab,kw OR "cardiac ischaemia":ti,ab,kw OR "cardiac ischemia":ti,ab,kw OR "cardiovascular stroke":ti,ab,kw OR "heart attack":ti,ab,kw OR "heart attacks":ti,ab,kw OR "coronary":ti,ab,kw OR "ischemic cardiomyopathy":ti,ab,kw OR "ischaemic cardiomyopathy":ti,ab,kw OR "ischemic heart failure":ti,ab,kw OR "ischaemic heart failure":ti,ab,kw OR "ischemic heart disease":ti,ab,kw OR "ischaemic heart disease":ti,ab,kw OR "CAD":ti,ab,kw OR "IHD":ti,ab,kw OR "STEMI":ti,ab,kw OR "NSTEMI":ti,ab,kw OR "CHD":ti,ab,kw OR "AMI":ti,ab,kw OR "ACS":ti,ab,kw)



# CHAPTER

# 6

# Rationale and design of the European multicentre study on Stem Cell therapy in Ischemic Non-treatable Cardiac disease (SCIENCE)

Paitazoglou C, Bergmann MW, Vrtovec B, Chamuleau SAJ, Van Klarenbosch BR, Wojakowski W, Michalewska-Wludarczyk A, Gyöngyösi M, Ekblond A, Haack-Sørensen M, Jaquet K, Vrangbæk K, Kastrup J, on behalf of the SCIENCE investigators



## ABSTRACT

### *Aim*

Ischaemic heart failure (IHF) patients have a poor prognosis even with current guideline-derived therapy. Intramyocardial injections of autologous or allogeneic mesenchymal stromal cells might improve cardiac function leading to better clinical outcome.

### *Methods*

The SCIENCE (Stem Cell therapy in IschEmic Non-treatable Cardiac disease) consortium has initiated a Horizon2020 funded multi-centre phase II study in six European countries. It is a double-blind, placebo-controlled trial testing the safety and efficacy of allogeneic Cardiology Stem Cell Centre Adipose-derived Stromal Cells (CSCC\_ASC) from healthy donors or placebo in 138 symptomatic IHF patients. Main inclusion criteria are New York Heart Association class II–III, left ventricular ejection fraction < 45% and N-terminal pro-B-type natriuretic peptide levels > 300 pg/mL. Patients are randomized in a 2:1 pattern to receive intramyocardial injections of either CSCC\_ASC or placebo. CSCC\_ASC and placebo treatments are prepared centralized at Rigshospitalet in 5 mL vials as an off-the-shelf product. Vials are distributed to all clinical partners and stored in nitrogen vapour tanks ready to be used directly after thawing. A total of  $100 \times 10^6$  CSCC\_ASC or placebo are injected directly into viable myocardium in the infarct border zone using the NOGA XP system (BDS, Cordis, Johnson & Johnson, USA). Primary endpoint is a centralized core-laboratory assessed change in left ventricular end-systolic volume at 6-month follow-up measured by echocardiography. The trial started in January 2017, 58 patients were included and treated until July 2018.

### *Conclusion*

The SCIENCE trial will provide clinical data on efficacy and safety of intramyocardial cell therapy of allogeneic adipose-derived stromal cells from healthy donors in patients with IHF.

## INTRODUCTION

Regenerative heart failure (HF) therapy might repair damaged heart muscle tissue [1]. Several randomized clinical trials over recent years found the therapy to be safe but so far not effective, and clinical data remain conflicting. In particular, intramyocardial injection might reduce patient's HF symptoms [2–5]. Fluoroscopy-guided intramyocardial injection of bone marrow (BM)-derived progenitor cells (CD133+cells) in ischaemic refractory cardiomyopathy recently showed improved myocardial perfusion and improved angina symptoms [6]. Mesenchymal stromal cells (MSC) have migratory abilities, can secrete protective factors, and act as a primary matrix for tis-sue regeneration [7]. Furthermore, MSC possess immunosuppressive capacities, evade being recognized by a recipient immune system and can therefore be used as allogeneic therapy without eliciting an immune response [8,9]. The presence of MSC-like cells in different tissues (adipose tissue, BM, peripheral blood, etc.) indicates their importance and pre-clinical studies indicate that these cells have regenerative capacity regardless of tissue origin [7]. Adipose-derived stromal cells (ASC) are very promising since their tissue concentration is 100–300 times higher than the MSC concentration in the BM [10]. Adipose-derived stromal cells are capable of secreting a large number of angiogenesis-related cytokines, including vascular endothelial growth factor, granulocyte/macrophage colony stimulating factor and stromal-derived factor-1 $\alpha$  [11]. They showed greater pro-angiogenic action compared to BM-MSC and can be an ideal source for therapeutic angiogenesis in ischaemic disease in terms of efficacy, accessibility and available tissue amounts [12]. The production of allogeneic Cardiology Stem Cell Centre Adipose-derived Stromal Cells (CSCC\_ASC) from healthy donors was established at Rigshospitalet Copenhagen. CSCC\_ASC are stored in nitrogen vapour containers as an off-the-shelf product in the hospital ready to be used without any delay. In a phase I study, this newly developed cryopreserved CSCC\_ASC product from healthy donors was proven safe. Furthermore, feasibility of the treatment concept was demonstrated [13]. The SCIENCE trial is a phase II, prospective, randomized, European multicentre, placebo-controlled, double-blind, investigator-initiated clinical trial with NOGA-guided intramyocardial injection of CSCC\_ASC vs. placebo in patients with chronic ischaemic HF (IHF).

## STUDY DESIGN

### *Study population*

The SCIENCE trial has passed the Voluntary Harmonization process through Clinical Trials Facilitation Groups, European Medicines Agency. It was approved by the National Competent Authorities and Ethics Committees in Denmark, Germany, The Netherlands, Austria, Slovenia and Poland at the end of 2016. The study is conducted according to Good Clinical Practice and follows the latest version of the Helsinki Declaration adopted

in 2013 at the 64<sup>th</sup> World Medical Association Assembly, Brazil. The study is registered in ClinicalTrials.gov (NCT02673164).

A total of 138 patients will be enrolled in the SCIENCE study. Key inclusion criteria are patients aged 30–80 years with chronic IHF, impaired left ventricular ejection fraction (LVEF < 45% measured by echocardiography), symptomatic HF (New York Heart Association (NYHA) class II–III), plasma N-terminal pro-B-type natriuretic peptide (NT-proBNP) > 300 pg/mL (> 35 pmol/L). All included patients should be on maximal tolerable standard HF medication and without further treatment options like valvular intervention/surgery or revascularization or implantation of a cardiac resynchronisation therapy (CRT) device. CRT device implantation between baseline and the 6-month follow-up exams will lead to study exclusion due to a possible effect of CRT on the primary end-point of left ventricular end-systolic volume (LVESV). All inclusion and exclusion criteria are listed in Table 1.

**Table 1** Inclusion and exclusion criteria of the SCIENCE trial

Inclusion criteria	Exclusion criteria
<ul style="list-style-type: none"> <li>• 30–80 years of age</li> <li>• Signed informed consent</li> <li>• Chronic stable ischaemic heart disease</li> <li>• Symptomatic HF (NYHA class II–III)</li> <li>• LVEF ≤ 45% on echocardiography, CT or MRI scan</li> <li>• Plasma NT-proBNP &gt; 300 pg/mL (&gt; 35 pmol/L)</li> <li>• Maximal tolerable HF medication unchanged 2 months prior to inclusion</li> <li>• No option for PCI or CABG</li> <li>• Patients who have had PCI or CABG within 6 months of inclusion must have a new coronary angiography to rule out early restenosis</li> <li>• Patients cannot be included until 3 months after implantation of a CRT-D and until 1 month after an ICD unit</li> </ul>	<ul style="list-style-type: none"> <li>• HF NYHA class I or IV</li> <li>• Acute coronary syndrome within 6 weeks of inclusion</li> <li>• Other revascularization treatment within 4 months of treatment</li> <li>• Moderate to severe aortic stenosis (valve area &lt; 1.3 cm<sup>2</sup>) or valvular disease with option for surgery or interventional therapy</li> <li>• Aortic valve replacement with an artificial heart valve. However, a trans-septal treatment approach can be considered in these patients</li> <li>• If the patient is expected to be candidate for MitraClip therapy</li> <li>• Diminished functional capacity for other reasons such as COPD with FEV<sub>1</sub> &lt; 1 L/min, moderate to severe claudication or morbid obesity</li> <li>• Clinical significant anaemia (Hb &lt; 6 mmol/L), leukopenia (leucocytes &lt; 2 × 10<sup>9</sup>/L), leukocytosis (leucocytes &gt; 14 × 10<sup>9</sup>/L) or thrombocytopenia (thrombocytes &lt; 50 × 10<sup>9</sup>/L)</li> <li>• Reduced kidney function (eGFR &lt; 30 mL/min)</li> <li>• Left ventricular thrombus</li> <li>• Anticoagulation treatment that cannot be paused during cell injections</li> <li>• Patients with reduced immune response or known anti-HLA antibodies</li> <li>• History with malignant disease within 5 years of inclusion or suspected malignancy – except treated skin cancer other than melanoma</li> <li>• Pregnant women</li> <li>• Other experimental treatment within 4 weeks of baseline tests</li> <li>• Life expectancy &lt; 1 year</li> <li>• Participation in another intervention trial</li> <li>• Known hypersensitivity to DMSO, penicillin and streptomycin</li> </ul>

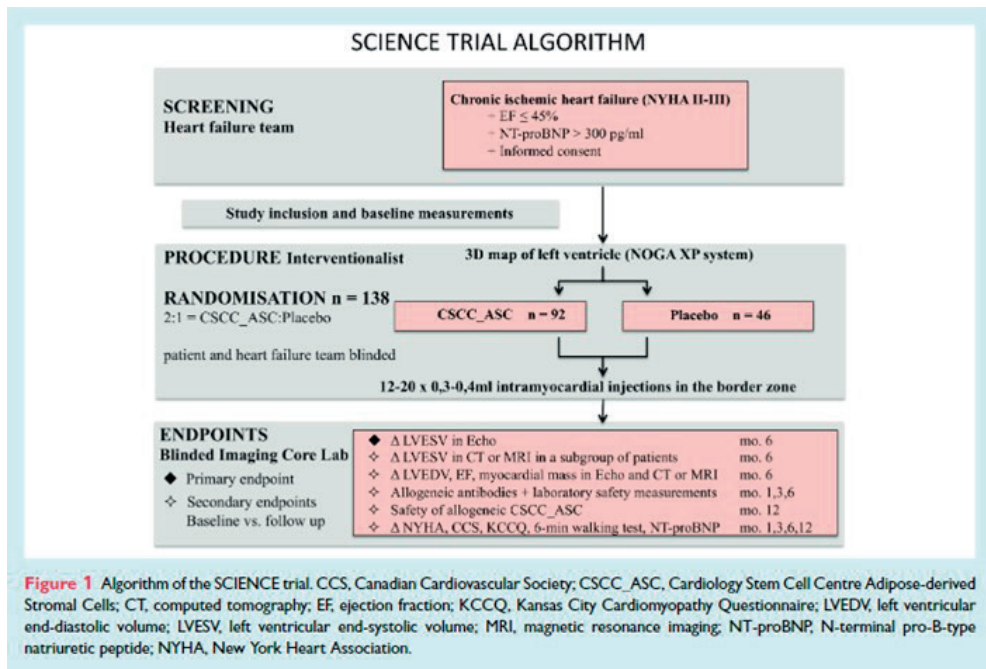
CABG, coronary artery bypass graft; COPD, chronic obstructive pulmonary disease; CRT-D, cardiac resynchronization therapy with defibrillation; CT, computed tomography; DMSO, dimethyl sulfoxide; eGFR, estimated glomerular filtration rate; FEV<sub>1</sub>, forced expiratory volume in 1 s; Hb, haemoglobin; HF, heart failure; HLA, human leucocyte antigen; ICD, implantable cardioverter defibrillator; LVEF, left ventricular ejection fraction; MRI, magnetic resonance imaging; NT-proBNP, N-terminal pro-B-type natriuretic peptide; NYHA, New York Heart Association; PCI, percutaneous coronary intervention.

### Overview of the study flow

Patients are screened for trial eligibility, treated and followed in six European HF centers. Patients with signed informed consent approved for the study are randomized 2:1 to receive intramyocardial injections of CSCC\_ASC or placebo (isotonic saline) in a double-blind design. Randomization is performed by personnel at the Cardiology Stem Cell Centre (CSCC) cell-processing unit before shipment of treatment doses to clinical sites. To assure blinding of the treatment, the clinical teams, which are responsible for screening

and follow-up of the patients will not participate in the treatment procedure or be in the catheterization laboratory during the treatment. Follow-up visits will be 1, 3, 6 and 12 months after treatment for safety and efficacy evaluation. The study algorithm and visit schedule are summarized in Figure 1.

**Figure 1 – Study algorithm**



### Cell production

CSCC\_ASC and placebos (saline) are manufactured at CSCC, Rigshospitalet, University Hospital Copenhagen. The CSCC holds a manufacturing authorization (no. 23909) and a tissue establishment authorization (no. 32298) issued and inspected every second year by Danish Medicines Agency and Danish Patient Safety Authority, respectively. The manufacturing procedure is in compliance with the EU Guidelines for Good Manufacturing Practice (GMP) of Medicinal Products for Human Use (certificate of GMP compliance no. DK IMP 92217). The cells are gained from abdominal adipose tissue after lipo-suction from healthy donors. A donor is eligible only if screening shows that the donor is healthy and free from risk factors and laboratory tests for relevant infectious disease agents are negative. Liposuction is performed according to CSCC Standard Operating Procedures. Approximately 100–150 mL lipoaspirate is obtained from each donor from the abdomen under local anaesthesia by a plastic surgeon. Animal-free expansion is performed with human platelet lysate (Cook Regentec) in automated closed bioreactor systems (Quantum Cell Expansion System, Terumo BCT) [14]. The final cell product has had two passages in

**Table 2** Release criteria of the final Cardiology Stem Cell Centre Adipose-derived Stromal Cells product

Attribute	Acceptance criteria
Number of cells	100–120 million cells
ASC viability	>80%
Donor serology	Negative for anti-antibody + Ag) Negative for anti-HCV Negative for HBsAg Negative for anti-HBc Negative for syphilis Negative for HTLV I/II
Sterility	
Bacteria/fungi	Negative/negative
Endotoxin level	< 70 EU/mL
Mycoplasma	Negative
Characterization (Immunophenotype)	CD90 > 80% CD105 > 80% CD73 > 80% CD45 < 3% HLA-DR < 5%

ASC, adipose-derived stromal cells; HBsAg, hepatitis B surface antigen; HBc, hepatitis B core; HCV, hepatitis C virus; HIV, human Immunodeficiency virus; HLA, human leucocyte antigen; HTLV, human T-lymphotropic virus.

the bioreactor system. CSCC\_ASC is cryopreserved in CellSeal vials (COOK Regentec) (110 million cells 5 mL) in CryoStor CS10 (BioLife Solutions). The concentration is a little higher than the intended  $100 \times 10^6$  for the treatment. There is an estimated loss of  $10 \times 10^6$  cells during handling of the cells. The cell doses  $100 \times 10^6$  CSCC\_ASC is based on the experience from our previous HF trial where we could see a dose titrating effect. Patients treated with  $>84 \times 10^6$  cells had the highest improvement in LVEF and LVESV [4]. CSCC\_ASC is stored below  $-180^\circ\text{C}$  in nitrogen vapour or dry-storage until clinical use. Release criteria are sterility, viability ( $>80\%$ ) and

immunophenotype (stable positive markers CD90, CD105, CD73  $> 80\%$  and negative markers  $< 3\%$  CD45,  $< 5\%$  human leucocyte antigen (HLA)-DR) and are listed in Table 2. The presence of mycoplasma is tested from all bioreactor expansions immediately prior to cell harvest, and the presence of bacteria, fungi and endotoxins is tested on the final product, immediately prior to cryopreservation. Purity, differentiation capacity (adipose, bone, cartilage), and full phenotyping consistent with ISCT/IFATS standards for the ASC phenotype as well as genomic stability has been determined during manufacturing process development [14–16]. Stability studies have been established, and currently 24-month stability demonstrating sterility, viability, recovery, ASC immunophenotype, and cell potency as defined by in vitro cell adherence and proliferation, after thawing of the final product, has been documented and approved by competent authorities. Cell delivery is recommended within 1 hour after thawing (5 minutes in sterile water and temperature set at  $37^\circ\text{C}$ ). Samples from each batch of CSCC\_ASC are stored at CSCC for future analyses of correlations between cell function and clinical efficacy as well as for statutory reference samples. CSCC\_ASC vials are shipped in a qualified portable nitrogen dry-shipper to the trial participating HF units in Europe by WorldCourier, in accordance with European rules for Good Distribution Practices. The randomization code for each delivered vial is available in a sealed envelope at each site if there is an acute need for breaking the code in a case of an unexpected serious adverse event.

## *Safety*

### Allogeneic treatment

The final CSCC\_ASC product is intended for allogeneic treatment. Each vial will only contain cells from one donor. A total of 6–8 donors will be used to produce the vials for the clinical trial. There will be no HLA tissue type matching between the donor and the patients. Allogeneic cell therapy generally poses a risk for graft-versus-host reaction or host-versus-graft reaction. A graft-versus-host reaction is considered insignificant from a safety perspective given the lack of immunologically active cells in the graft (< 3% CD45 positive cells, < 5% HLA-DR cells). MSC not only inhibit B-cell proliferation, but also the cytokine-induced proliferation of natural killer (NK) cells. Furthermore, they prevent cytotoxic activity and cytokine production due to a sharp downregulation of surface expression of the activating NK receptors [8]. MSC are also able to suppress proliferation of stimulated peripheral blood mononuclear cells and to inhibit differentiation of monocyte-derived dendritic cells. However, ASC show more potent immunomodulatory effects compared to BM-MSC, which is related to higher levels of cytokine secretion [9]. Furthermore, ASC express only low levels of major histocompatibility complex (MHC) class I (HLA-ABC) and no MHC class II (HLA-DR) or co-stimulatory molecules, making them less likely to interact with recipient immune cells [8,9]. Although very low levels of antibody titers toward CSCC\_ASC were detected in the phase I safety study with CSCC\_ASC, these titers were not correlated with clinical events [13].

### Viral screening

Each donor is tested for human immunodeficiency virus, hepatitis B and C, syphilis and human T-lymphotropic virus type I/II serology by serum analysis within 30 days prior to liposuction and on the day of donation. Donor testing is performed by the Virus Laboratory, The Blood Bank, Department of Clinical Immunology, Rigshospitalet, Copenhagen, as authorized by The Danish Patient Safety Authority.

### Tissue typing and alloantibodies

Tissue typing (low HLA I and II genotyping) is performed of all donors for the purpose of alloantibody screening in patients after cell treatment; in The Netherlands it was requested by the Medical Research Ethics Committee (METC) to perform such analysis before randomization and allocate accordingly the correct donor samples at randomization. Blood samples of all patients in this trial will be stored for later centralized analyses of tissue antibodies and biomarkers.

### *NOGA-guided injection*

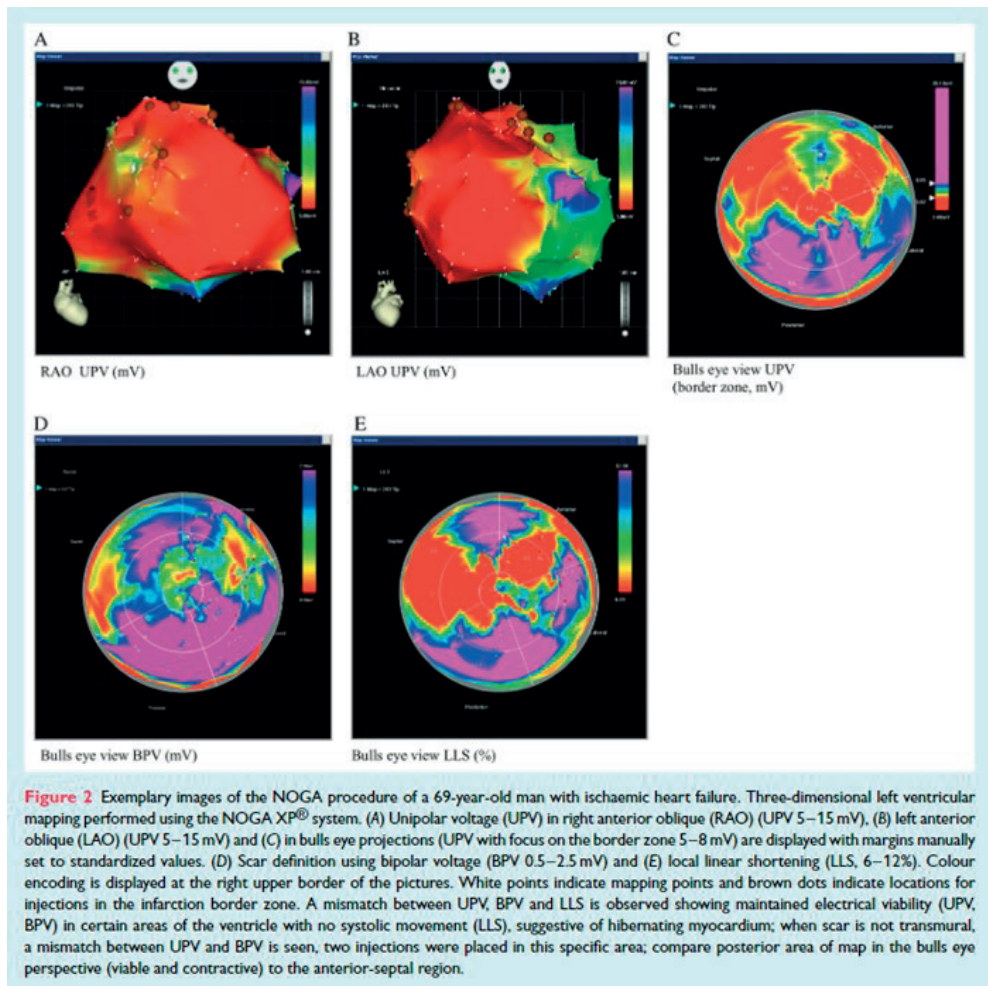
Three-dimensional left ventricular (LV) mapping is performed using the NOGA XP® system (BDS, Cordis, Johnson & Johnson, USA). Intramyocardial injection of stem cells using the NOGA platform in patients with ischaemic disease has proven to be safe and feasible

[4,17,18]. It reduces the likelihood of systemic toxicity of the injected substance, resulting in minimal washout, limited exposure of non-target organs and precise placement of the cells to peri-ischaemic regions (border zone) of the myocardium. Every patient receives an electromechanical three-dimensional LV map by point-by-point measurement. Usually > 100 verified points are necessary to obtain a complete LV map. The system distinguishes between viable (unipolar voltage > 12mV, bipolar voltage > 2.5 mV, local linear shortening (LLS) > 6%), non-viable-myocardium (unipolar voltage < 6 mV, bipolar voltage < 1.5 mV, LLS < 4%) and border zone (unipolar voltage 6–12 mV, bipolar voltage 1.5–2.5 mV, LLS 4–6%) around myocardial scar tissue. Cut-off values may vary in the literature, because borders are not exactly defined [19]. Mismatch between unipolar and bipolar signals is observed when the myocardial scar is not transmural. Border zones are defined after interpretation of all mapping data and 12–20 injections of 0.3–0.4 mL CSCC\_ASC (in total 100 Mio cells) or placebo are performed with MYOSTAR® injection catheters (BDS, Cordis, Johnson & Johnson, USA) with 3D computer aided navigation precisely in this region. The number of injections may vary, depending on the scar size and the decision to split the injected volume to cover all areas of the border zone, with adequate distance between the injection points. Laboratory measurements of plasma creatine kinase-MB and troponin will be made before treatment, 6 hours and 1 day after to assess possible myocardial effects. Additionally, echocardiographic assessment is performed after the procedure to exclude pericardial effusion. Exemplary images of the NOGA procedure of a 69-year-old patient with IHF are shown in Figure 2.

### *Endpoints*

Primary endpoint is a centralized core-laboratory assessed change in LVESV at 6-month follow-up measured in all patients by echocardiography. Secondary endpoints are safety evaluated by development of donor-specific de novo HLA antibodies and laboratory safety measurements 1, 3, and 6 months after treatment. Other endpoints are changes in LVEF, end-diastolic volume and myocardial mass at 6-month follow-up measured by echocardiography. Computed tomography (CT) and magnetic resonance imaging (MRI) will be performed in a subgroup of patients at baseline and 6 months after treatment to evaluate further cardiac function and LVESV. Other secondary endpoints are changes in NYHA class, Canadian Cardiovascular Society class, Kansas City Cardiomyopathy Questionnaire, Seattle Angina Questionnaire, 6-minute walking test, additional echocardiographic measurements, and NT-proBNP levels. In addition, safety of CSCC\_ASC with respect to incidence and severity of serious adverse events and suspected unrelated serious adverse events will be evaluated at 12-month follow-up. A combined endpoint will be assessed of 1) death, hospitalization for worsening HF, including insertion of a biventricular pacemaker, hospitalization due to ventricular tachycardia or fibrillation 1, 2, and 3 years after treatment, and 2) death, hospitalization for any cardiovascular reason, hospitalization for worsening HF, including insertion of a biventricular pacemaker, hospitalization due to ventricular tachycardia or fibrillation 1, 2, and 3 years after treatment.



**Figure 2 – Example of NOGA procedure**

### Cardiac imaging analysis

All patients will have echocardiographic assessment at baseline and in follow-up visits 3, 6, and 12 months after treatment to evaluate cardiac parameters for primary and secondary endpoints. Patients with a plasma creatinine < 130  $\mu\text{mol/L}$  may also undergo CT scan or MRI (only in patients without implantable cardioverter defibrillator or pacemaker) to determine the effect of regenerative therapy on myocardial function at baseline and 6-month follow-up. Echocardiographic scans will be without contrast and assess LV end-systolic and end-diastolic volumes, myocardial mass, LVEF, radial and longitudinal global and segmental strain by two-dimensional speckle-tracking echocardiography, left atrial volume, valvular function, and tissue Doppler parameters ( $e'$ ,  $s'$ ); this will be independently and blinded assessed using Philips Intellispace Software. Regarding reproducibility for every individual patient, all exams will be performed using the same ultrasound machine



preferably operated by the same technician. The inclusion scans will be investigated before treatment to ensure a proper quality of imaging before randomization. Endocardial and epicardial borders will be traced manually in end-diastole and end-systole and the mitral plane set to define the basal border of the left ventricle. Study sites electronically transmit all imaging data to a central server at Netherlands Heart Institute & Lygature/TraIT, Amsterdam, The Netherlands. All image data are analyzed blinded with the cvi post-processing tool (for CT and MRI: Circle Cardiovascular Imaging, Calgary, Alberta, Canada). Also, NOGA data will be used to crosscheck and fuse with other imaging modalities to investigate its value in accurately pointing out the target border zone for treatment planning using the Cartbox-2 software platform [20,21].

### *Power calculation and statistics*

A total of 138 patients, randomized in a 2:1 pattern, with a maximum dropout rate of 15% before the 6-month follow-up, will be required to have a statistical power of > 90% to detect an absolute change in LVESV of 9.5 mL (estimated standard deviation (SD) 15mL) and 12.7 mL (estimated higher SD of 20 mL). Change in LVEF of 3.2% (estimated SD 5%) and of 5.1% (estimated higher SD of 8%) results in a statistical power of > 90%. An alpha value of 5% was used in all calculations. The power calculation of this trial is based on the results of the MSC-HF trial, a placebo-controlled comparison of intramyocardial injection of BM-MS (randomized in a 2:1 pattern) in patients with IHF [4]. In this previous trial, the primary endpoint of LVESV measured with MRI or CT was significantly reduced in the BM-MS group (between-group difference of  $13.0 \pm 12.9$  mL,  $P = 0.001$ ). There was also a significant improvement in LVEF measured with MRI or CT (between-group difference of  $6.2 \pm 3.8\%$ ,  $P < 0.0001$ ). SD in the MSC-HF trial was 12.9% for LVESV and 3.8% for LVEF. Since the SD is higher if echocardiography is employed compared to CT or MRI, we did the power calculation of this trial with two SD's higher than in the MSC-HF trial. Statistical analyses will be performed using SAS 9.4 (SAS Institute Inc., Cary, NC, USA) and SPSS 22 (SPSS Inc., Chicago, IL, USA). For baseline characteristic comparison and follow-up data between and within groups, an independent samples t-test and paired t-test for normally distributed continuous data will be used, respectively. Mann-Whitney U test will be used for between-group comparisons of continuous non-normally distributed data. For baseline categorical data, Pearson's chi-square or Fisher's exact test will be used, as appropriate. For follow-up data with more than two time-points, repeated measures with autoregressive covariance structure will be used. For nominal repeated data, generalized estimating equations will be used. Fisher's exact test will be used for comparison of occurrences of serious adverse events between groups. A two sided P-value of  $< 0.05$  is considered statistically significant. When data are ready for analysis, our statistician will evaluate missing data, whether the data are missing completely at random (MCAR) or missing at random (MAR). We will then decide about handling of missing values.

*Current status*

Patients will be enrolled during a recruitment phase of 24 months. The trial has been delayed due to different approval processes in the involved countries and implementation of new regulations for clinical use of human platelet lysate in the production of stem cell products. The trial started January 2017 and 58 patients have been enrolled until July 2018 without safety events. Since minimum study duration for one patient is 12 months, the overall study duration will be 4 years.

## DISCUSSION

The SCIENCE trial is the first European multicenter randomized phase II trial testing the safety and efficacy of allogeneic CSCC\_ASC from healthy donors or placebo (saline) in 138 patients with symptomatic IHF. Presently, there is no established and approved regenerative therapy for patients with heart disease. Our hypothesis is that cell therapy leads to myocardial regeneration and improvement of LV parameters. Therefore, the primary endpoint in this phase II trial is the centralized core-laboratory assessed change in LVESV at 6-month follow-up. In the MSC-HF trial, a significant improvement of LVESV and LVEF was observed after 6 months [4]. LVESV is considered superior to LVEF when LVEF is low (<50%) or when end-systolic volume is high (>100 mL) [22]. Furthermore, LVESV is a simple yet powerful echocardiographic marker of LV remodeling that can be measured easily and is an independent predictor of hospitalization for HF in patients with stable coronary heart disease [23]. A limitation of the study is that not all patients can have measurements from echocardiography, CT and MRI. However, all patients receive measurements by echocardiography. Additionally, MRI or CT scans will be performed in a subgroup of patients without the possibility of establishing an equal distribution in the treatment and control group. Not all patients will undergo CT imaging due to different European radiation protection guidelines in the participating centers. Additionally, many HF patients have implantable cardioverter defibrillator or CRT devices and cannot undergo MRI imaging. Cardiac cell therapy employing autologous BM cells applied via the intracoronary route was previously shown to be safe but not sufficiently effective [24]. Intracoronary delivery may result in many cells directly lost to the systemic circulation. The transendocardial delivery route on the other hand, allows precise placement of cells in the border zone of ischaemic heart regions. Table 3 lists pertinent trials with cell treatment via the intramyocardial delivery route [2–5,17,18,25–30]. Previous randomized clinical trials with different cell types suggest that cell-based therapy via the intramyocardial route of acute and chronic cardiomyopathy is safe, feasible and possibly effective in improving various surrogate markers of LV function and symptoms [3–5,17]. Discrepancies in previous trials were seen between LV function improvement and reduction in clinical endpoints. Improvement in LV function not always goes hand in hand with improvement of clinical outcome. In the recent IxCELL-DCM trial, mortality and cardiovascular

**Table 3** Stem cell trials with intramyocardial delivery route in patients with ischaemic cardiomyopathy

Author/acronym, publication dates, number of patients (trial design)	Disease and delivery route	Cell type and dose	Methods for efficacy measurement	Phase, results
FOCUS-HF <sup>27</sup> : 06/2011, 30 (randomized 2:1)	CICM (EF < 40%), IM (NOGA)	Autologous BM-MC (30 × 10 <sup>6</sup> ± 0 cells) vs. control	Symptom reduction, Echo, SPECT	Phase II, quality of life improved at 6 months (P = 0.009), no effect on cardiac function
TABMMI <sup>5</sup> : 11/2011, 20 (non-randomized)	CICM (EF ≤ 40%), IM (TESI)	Autologous BM-MC, CD34+, CD133+ (96 ± 29 × 10 <sup>6</sup> cells)	Symptom reduction, Echo	Phase II, exercise tolerance test improved (P < 0.01), EF improved (from 34.9 ± 4.3 to 41.9 ± 5.1 at 12 months and 42.2 ± 7.1% at 24 months, P = 0.00005)
ALSTER-Stem Cell <sup>17</sup> : 10/2012, 23 (non-randomized)	3–4 weeks after acute myocardial infarction (EF < 45%), IM (NOGA)	Autologous BM-MC (220 ± 42 × 10 <sup>6</sup> cells)	MRI	Phase II, EF (+7.9 ± 1.5%, P = 0.001) at 6 months, no effect on scar volume
POSEIDON <sup>2</sup> : 12/2012, 30 (randomized, 5 patients each dose level and cell type)	CICM (EF < 50%), IM (TESI)	Autologous vs. allogeneic BM-MSC (20, 100, 200 × 10 <sup>6</sup> cells)	Symptom reduction, ESP, CT	Phase I/II, reduced infarct scar and end-diastolic diameter (P = 0.001) at 13 months in both groups, no effect on EF. Symptom reduction in the autologous cell group. Inverse dose response to EF and LVESV
MSC-HF <sup>4</sup> : 07/2015, 60 (randomized 2:1, double-blind, placebo-controlled)	CICM (EF < 45%), IM (NOGA)	Autologous BM-MSC (77.5 ± 67.9 × 10 <sup>6</sup> cells) vs. placebo	Symptom reduction, MRI, CT	Phase II, improvement of LVESV -7.6 ± 13.2 mL (P = 0.001), EF +5.0 ± 3.8% and stroke volume +15.6 ± 14.6 mL (P < 0.0001) at 6 months in the cell group, no significant symptom reduction
Perin et al. <sup>3</sup> : 08/2015, 60 (20 randomized patients each dose, 2:1 vs. control)	CICM (EF < 40%), IM (NOGA)	Allogeneic BM-MSC (25, 75, 150 × 10 <sup>6</sup> cells)	Symptom reduction, Echo, SPECT	Phase II, HF-MACE reduced at 36 months in 150 × 10 <sup>6</sup> cell group (P = 0.025)
MyStromalCell <sup>18</sup> : 11/2017, 10 (non-randomized)	CICM (EF ≤ 45%), IM (NOGA)	Autologous ASC (100 × 10 <sup>6</sup> cells)	Safety Labs, Echo, CT	Phase II, tendency towards efficacy
TRIDENT <sup>29</sup> : 11/2017, 30 (randomized 1:1, double-blind)	CICM (EF ≤ 50%), IM (TESI)	Allogeneic BM-MSC (20 or 100 × 10 <sup>6</sup> cells)	Symptom reduction, CT, ESP	Phase II, reduced scar size in both groups (20 × 10 <sup>6</sup> P = 0.001, 100 × 10 <sup>6</sup> P = 0.0002), EF increased only in 100 × 10 <sup>6</sup> cell group at 12 months (+3.7 U; IQR 1.1–6.1; P = 0.04)
Kastrup et al. <sup>30</sup> : ongoing, 81 (randomized 2:1, double-blind, placebo-controlled)	CICM (EF ≤ 45%), IM (NOGA)	CSCC_ASC (110 × 10 <sup>6</sup> cells) vs. placebo	Echo, MRI, CT	Phase II
ixCELL-DCM <sup>25</sup> : 04/2016, 126 (randomized 1:1, double-blind, placebo-controlled)	CICM (EF ≤ 35%), IM (NOGA)	Autologous iXmyelocel-T cell product (CD90+ MSC and CD45+, CD14+ auto-fluorescent+ activated macrophages, cell)	Symptom reduction, Echo	Primary endpoint (composite number of deaths, cardiovascular hospitalizations during 12-month follow-up) significantly reduced (P = 0.03), no effect on EF or LVESV
CHART-1 <sup>28</sup> : 12/2016, 315 (randomized 1:1, double-blind, sham-controlled)	CICM (EF ≤ 35%), IM (C-Catheter <sup>TM</sup> )	Autologous BM-derived cardiopoietic cells (>24 × 10 <sup>6</sup> cells)	Symptom reduction, Echo	Hierarchical composite (mortality, worsening HF, Minnesota Living with Heart Failure Questionnaire score, 6-minute walk test, LVESV, and EF) at 9 months neutral (P = 0.27)
ATHENA <sup>26</sup> : 02/2017, 31, (randomized 2:1, double-blind, placebo-controlled)	CICM (EF 20–45%), IM (NOGA)	Autologous ASC (n = 28: 40 × 10 <sup>6</sup> and n = 3: 80 × 10 <sup>6</sup> cells)	Symptom reduction, Echo, ESP	VO <sub>2</sub> max favoured ASC, fewer hospitalizations and symptom reduction in the ASC arm, no difference in EF and LVESV

ASC, adipose-derived mesenchymal stromal cells; BM, bone marrow; BM-MC, bone marrow mononuclear cells; BM-MSC, bone marrow-derived mesenchymal stem cells; CICM, chronic ischaemic cardiomyopathy; CSCC\_ASC, Cardiology Stem Cell Centre Adipose-derived Stromal Cells; CT, computed tomography; Echo, echocardiography; EF, ejection fraction; ESP, ergospirometry; HF, heart failure; IM, intramyocardial; IQR, interquartile range; LVESV, left ventricular end-systolic volume; MACE, major adverse cardiac events; MRI, magnetic resonance imaging; VO<sub>2</sub>, oxygen uptake; SPECT, single photon emission computed tomography.

hospitalization rates were reduced, without significant effect on LV function [25]. Patients in the ATHENA trials also had fewer hospitalizations and improvement in HF symptoms, but no improvement in LVEF [26]. Additionally, age and medical comorbidities from HF may decrease the number, quality, and potency of autologous cells. Stratifying cell results by age in the FOCUS-HF trial showed that younger patients (< 60 years) had more BM mononuclear cells than older patients (> 60 years), which may be one of the main reasons for contradictory results in autologous regenerative therapy [27]. The largest trial so far (CHART-1) with intramyocardial autologous BM cardiopoietic cells demonstrated safety but the primary endpoint (hierarchical composite of all-cause mortality, worsening HF, LVESV and ejection fraction) was neutral [28]. Based on the collected experience from previous clinical trials, the lack of an efficient homogeneous cell product prevents repeatability and dissemination of regenerative therapy. Therefore, a switch from autologous to allogeneic treatment is necessary to establish a standardized effective therapy option for patients with IHF. Allogeneic MSC and ASC have already been used in previous clinical trials without any side effects [3,13,29]. The TRIDENT trial compared two doses of allogeneic MSC, directly injected intramyocardially in patients with ischaemic cardiomyopathy [29]. Although both cell doses (20 and  $100 \times 10^6$  cells) decreased scar size, only the  $100 \times 10^6$  dose increased ejection fraction. Improvement of clinical outcomes and LV parameters following treatment with an allogeneic cell product of the BM is currently also investigated in a large phase III trial (DREAM HF-1, NCT02032004). The Cardiology Stem Cell Centre, Rigshospitalet, University Hospital Copenhagen, has established new cultivation protocols for the production of allogeneic CSCC\_ASC from healthy donors, which can be stored in nitrogen vapour containers as an off-the-shelf product ready to be used. In a phase I study, the newly developed cryopreserved product CSCC\_ASC was safe and demonstrated feasibility and efficacy in 10 patients with IHF [13]. Ongoing is a phase II Danish multicenter study with CSCC\_ASC in 81 patients with IHF parallel to the SCIENCE trial to provide further data on safety and regenerative efficacy. The cell product and eligibility criteria are similar to the SCIENCE trial [30]. The SCIENCE trial will provide further clinical data from six large European sites on efficacy and safety of intramyocardial cell therapy of allogeneic treatment with this newly developed cell product. To analyze the economic impact of clinical application of regenerative stem cell technology for myocardial function at the societal level and within the health organizations using the present technology, data related to social aspects of ASC therapy, relating to resource use and to health-related quality of life, are collected in the trial, so as to create a solid base for more advanced economic analyses and approaches.

## ACKNOWLEDGEMENTS

Joanna Ciosek, Sebastian Dworowy, Tomasz Jadczyk, Michal Kozłowski, Pawel Nadrowski, Ronja Sagalski, Esther Schlegel, Annette Schmidt, Anna Sikora, Dorota Skiba and Denise Traxler, Abbas Ali Qayyum, and Anders B. Mathiasen are all actively involved in the conduction of the SCIENCE trial.

## FUNDING

This work was supported by an EU funding as part of the Horizon2020 program to conduct this randomized multicenter clinical trial (SCIENCE grant no. 643478). The multinational SCIENCE consortium consists of heart failure units from Denmark, Germany, The Netherlands, Austria, Slovenia and Poland, coordinated by Prof. Jens Kastrup, Rigshospitalet, Copenhagen University Hospital, Denmark. Conflict of interest: A.E., M.H-S. and J.K. are inventors of a patent application ['Stem Cell Therapy Based on Adipose-Derived Stem Cells' (20440PCT00 - Publication WO 2017-068140 -1005171105501)] owned by the Capital Region of Denmark and Rigshospitalet, Copenhagen University Hospital. The other authors declare no conflicts of interest.

## REFERENCES

1. Burchfield JS, Dimmeler S. Role of paracrine factors in stem and progenitor cell mediated cardiac repair and tissue fibrosis. *Fibrogenesis Tissue Repair* 2008;1:4. Doi:10.1186/1755-1536-1-4
2. Hare JM, Fishman JE, Gerstenblith G, et al. Comparison of allogeneic vs autologous bone marrow-derived mesenchymal stem cells delivered by transendocardial injection in patients with ischemic cardiomyopathy: the POSEIDON randomized trial. *JAMA* 2012;308:2369–79. Doi:10.1001/jama.2012.25321
3. Perin EC, Borow KM, Silva GV, et al. A phase II dose-escalation study of allogeneic mesenchymal precursor cells in patients with ischemic or nonischemic heart failure. *Circ Res* 2015;117:576–84. Doi:10.1161/CIRCRESAHA.115.306332
4. Mathiasen AB, Qayyum AA, Jorgensen E, et al. Bone marrow-derived mesenchymal stromal cell treatment in patients with severe ischaemic heart failure: a randomized placebo-controlled trial (MSC-HF trial). *Eur Heart J* 2015;36:1744–53. Doi:10.1093/eurheartj/ehv136
5. De la Fuente LM, Stertzer SH, Argentieri J, et al. Transendocardial autologous bone marrow in myocardial infarction induced heart failure, two-year follow-up in an open-label phase I safety study (the TABMMI study). *EuroIntervention* 2011;7:805–12. doi:10.4244/EIJV7I7A127
6. Bassetti B, Carbucicchio C, Catto V, et al. Linking cell function with perfusion: insights from the transcatheter delivery of bone marrow-derived CD133(+) cells in ischemic refractory cardiomyopathy trial (RECARDIO). *StemCell Res Ther* 2018;9:235. Doi:10.1186/s13287-018-0969-z
7. Hass R, Kasper C, Bohm S, Jacobs R. Different populations and sources of human mesenchymal stem cells (MSC): a comparison of adult and neonatal tissue-derived MSC. *Cell Commun Signal* 2011;9:12. Doi:10.1186/1478-811X-9-12
8. Spaggiari GM, Capobianco A, Abdelrazik H, et al. Mesenchymal stem cells inhibit natural killer-cell proliferation, cytotoxicity, and cytokine production: role of indoleamine 2,3-dioxygenase and prostaglandin E2. *Blood* 2008;111:1327–33. Doi:10.1182/blood-2007-02-074997
9. Melief SM, Zwaginga JJ, Fibbe WE, Roelofs H. Adipose tissue-derived multipotent stromal cells have a higher immunomodulatory capacity than their bone marrow-derived counterparts. *Stem Cells Transl Med* 2013;2:455–63. Doi:10.5966/sctm.2012-0184
10. Helder MN, Knippenberg M, Klein-Nulend J, Wuisman PI. Stem cells from adipose tissue allow challenging new concepts for regenerative medicine. *Tissue Eng* 2007;13:1799–1808. Doi:10.1089/ten.2006.0165
11. Meliga E, Strem BM, Duckers HJ, Serruys PW. Adipose-derived cells. *Cell Transplant* 2007;16:963–70. Doi:10.3727/096368907783338190
12. Kim Y, Kim H, Cho H, et al. Direct comparison of human mesenchymal stem cells derived from adipose tissues and bone marrow in mediating neovascularization in response to vascular ischemia. *Cell Physiol Biochem* 2007;20:867–76. Doi:10.1159/000110447

13. Kastrup J, Haack-Sorensen M, Juhl M, et al. Cryopreserved off-the-shelf allogeneic adipose-derived stromal cells for therapy in patients with ischemic heart disease and heart failure – a safety study. *Stem Cells Transl Med* 2017;6:1963–71. Doi:10.1002/sctm.17-0040
14. Haack-Sorensen M, Juhl M, Follin B, et al. Development of large-scale manufacturing of adipose-derived stromal cells for clinical applications using bioreactors and human platelet lysate. *Scand J Clin Lab Invest* 2018;17:1–8. Doi:10.1080/00365513.2018.1471618
15. Haack-Sorensen M, Follin B, Juhl M, et al. Culture expansion of adipose derived stromal cells. A closed automated Quantum Cell Expansion System compared with manual flask-based culture. *J Transl Med* 2016;14:319. Doi:10.1186/s12967-016-1080-9
16. Bourin P, Bunnell BA, Casteilla L, et al. Stromal cells from the adipose tissue-derived stromal vascular fraction and culture expanded adipose tissue-derived stromal/stem cells: a joint statement of the International Federation for Adipose Therapeutics and Science (IFATS) and the International Society for Cellular Therapy (ISCT). *Cytotherapy* 2013;15:641–48. Doi:10.1016/j.jcyt.2013.02.006
17. Heeger CH, Jaquet K, Thiele H, et al. Percutaneous, transendocardial injection of bone marrow-derived mononuclear cells in heart failure patients following acute ST-elevation myocardial infarction: ALSTER-Stem Cell trial. *EuroIntervention* 2012;8:732–42. Doi:10.4244/EIJV8I6A113
18. Qayyum AA, Mathiasen AB, Mygind ND, et al. Adipose-derived stromal cells for treatment of patients with chronic ischemic heart disease (MyStromalCell trial): a randomized placebo-controlled study. *Stem Cells Int* 2017;2017:5237063. Doi:10.1155/2017/5237063
19. Gyongyosi M, Dib N. Diagnostic and prognostic value of 3D NOGA mapping in ischemic heart disease. *Nat Rev Cardiol* 2011;8:393–404. Doi:10.1038/nrcardio.2011.64
20. Pavo N, Jakab A, Emmert MY, et al. Comparison of NOGA endocardial mapping and cardiac magnetic resonance imaging for determining infarct size and infarct transmuralty for intramyocardial injection therapy using experimental data. *PLoS One* 2014;9:e113245. Doi:10.1371/journal.pone.0113245
21. Van Slochteren FJ, van Es R, Gyongyosi et al. Three dimensional fusion of electromechanical mapping and magnetic resonance imaging for real-time navigation of intramyocardial cell injections in a porcine model of chronic myocardial infarction. *Int J Cardiovasc Imaging* 2016;32:833–43. Doi:10.1007/s10554-016-0852-x
22. White HD, Norris RM, Brown MA, et al. Left ventricular end-systolic volume as the major determinant of survival after recovery from myocardial infarction. *Circulation* 1987;76:44–51. Doi:10.1161/01.cir.76.1.44
23. McManus DD, Shah SJ, Fabi MR, et al. Prognostic value of left ventricular end-systolic volume index as a predictor of heart failure hospitalization in stable coronary artery disease: data from the Heart and Soul Study. *J Am Soc Echocardiogr* 2009;22:190–7. Doi:10.1016/j.echo.2008.11.005
24. Gyongyosi M, Wojakowski W, Lemarchand P, et al. Meta-Analysis of Cell-based Cardiac Studies (ACCRUE) in patients with acute myocardial infarction based on individual patient data. *Circ Res* 2015;116:1346–60. Doi:10.1161/CIRCRESAHA.116.304346

25. Povsic TJ, Zeiher AM. IxCELL-DCM: rejuvenation for cardiac regenerative therapy? *Lancet* 2016;387:2362–3. Doi:10.1016/S0140-6736(16)30138-6
26. Henry TD, Pepine CJ, Lambert CR, et al. The Athena trials: autologous adipose-derived regenerative cells for refractory chronic myocardial ischemia with left ventricular dysfunction. *Catheter Cardiovasc Interv* 2017;89:169–77. Doi:10.1002/ccd.26601
27. Perin EC, Silva GV, Henry TD, et al. A randomized study of transendocardial injection of autologous bone marrow mononuclear cells and cell function analysis in ischemic heart failure (FOCUS-HF). *Am Heart J* 2011;161:1078–87-e3. Doi:10.1016/j.ahj.2011.01.028
28. Bartunek J, Terzic A, Davison BA, et al. CHART Program. Cardiopoietic cell therapy for advanced ischaemic heart failure: results at 39 weeks of the prospective, randomized, double blind, sham-controlled CHART-1 clinical trial. *Eur Heart J* 2017;38:648–60. Doi:10.1093/eurheartj/ehw543
29. Florea V, Rieger AC, DiFede DL, et al. Dose comparison study of allogeneic mesenchymal stem cells in patients with ischemic cardiomyopathy (the TRIDENT study). *Circ Res* 2017;121:1279–90. Doi:10.1161/CIRCRESAHA.117.311827
30. Kastrup J, Schou M, Gustafsson I, et al. Rationale and design of the first double-blind, placebo-controlled trial with allogeneic adipose tissue-derived stromal cell therapy in patients with ischemic heart failure: a phase II Danish multicentre study. *Stem Cells Int* 2017;2017:8506370. Doi:10.1155/2017/8506370



# 7

**CHAPTER**

# Effect of allogeneic adipose tissue-derived mesenchymal stromal cell treatment in chronic ischaemic heart failure with reduced ejection fraction – the SCIENCE trial

Qayyum AA, Van Klarenbosch BR, Frljak S, Cerar A, Poglajen G, Traxler-Weidenauer D, Nadrowski P, Paitazoglou C, Vrtovec B, Bergmann MW, Chamuleau SAJ, Wojakowski W, Gyöngyösi M, Kraaijeveld AO, Hansen KS, Vrangbæk K, Jørgensen E, Helqvist S, Joshi FR, Johansen EM, Follin B, Juhl M, Højgaard LD, Mathiasen AB, Ekblond A, Haack- Sørensen M, Kastrup J, on behalf of the SCIENCE investigators

## ABSTRACT

### *Aims*

The aim of the SCIENCE trial was to investigate whether a single treatment with direct intramyocardial injections of adipose tissue-derived mesenchymal stromal cells (CSCC\_ASCs) was safe and improved cardiac function in patients with chronic ischaemic heart failure with reduced ejection fraction (HFrEF).

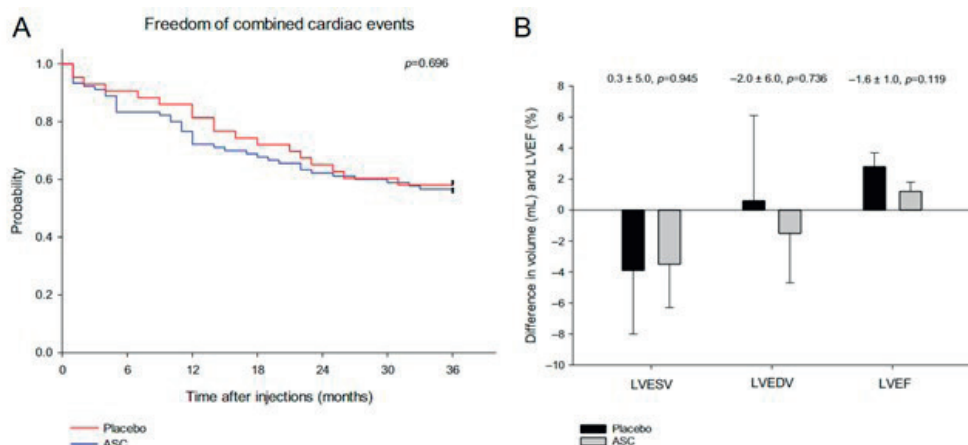
### *Methods and results*

The study was a European multi-centre, double-blind, placebo-controlled phase II trial using allogeneic CSCC\_ASCs from healthy donors or placebo (2:1 randomization). Main inclusion criteria were New York Heart Association (NYHA) class II–III, left ventricular ejection fraction (LVEF) < 45%, and N-terminal pro-B-type natriuretic peptide (NT-proBNP) levels > 300 pg/ml. CSCC\_ASCs or placebo (isotonic saline) were injected directly into viable myocardium. The primary endpoint was change in left ventricular end-systolic volume (LVESV) at 6-month follow-up measured by echocardiography. A total of 133 symptomatic HFrEF patients were included. The treatment was safe without any drug-related severe adverse events or difference in cardiac-related adverse events during a 3-year follow-up period. There were no significant differences between groups during follow-up in LVESV ( $0.3 \pm 5.0$  ml,  $p = 0.945$ ), nor in secondary endpoints of left ventricular end-diastolic volume ( $-2.0 \pm 6.0$  ml,  $p = 0.736$ ) and LVEF ( $-1.6 \pm 1.0\%$ ,  $p = 0.119$ ). The NYHA class improved slightly within the first year in both groups without any difference between groups. There were no changes in 6-min walk test, NT-proBNP, C-reactive protein or quality of life the first year in any groups.

### *Conclusion*

The SCIENCE trial demonstrated safety of intramyocardial allogeneic CSCC\_ASC therapy in patients with chronic HFrEF. However, it was not possible to improve the pre-defined endpoints and induce restoration of cardiac function or clinical symptoms.

## Graphical abstract



Treatment of chronic ischaemic heart failure with reduced ejection fraction (HFrEF) patients with allogeneic adipose tissue-derived stromal cells (ASC) was safe but without any demonstrable restoration of cardiac function or clinical symptoms. (A) Kaplan–Meier plot of freedom of cumulative combined cardiac-related adverse events during a 3-year follow-up period. (B) Differences in baseline to 6-month follow-up in left ventricular end-systolic volume (LVESV), left ventricular end-diastolic volume (LVEDV) and left ventricular ejection fraction (LVEF) in ASC treated compared to placebo patients.

## INTRODUCTION

Ischaemic heart failure with reduced ejection fraction (HFrEF) is a serious clinical condition with a poor prognosis despite improvements in medical therapies, cardiac rehabilitation and device-based therapies [1,2]. Cell therapies can potentially be an adjunct approach for improvement of cardiac function and heart failure (HF) symptoms. Several smaller randomized clinical trials have been conducted with different cell populations in both patients with ischaemic HF and refractory angina [3–13]. They have all demonstrated safety but so far, the clinical efficacy data have been conflicting. Many research groups and companies are now focusing on mesenchymal stromal cell (MSC) as the cell of choice for regeneration in many disease indications [6–10]. MSCs can be isolated from several different tissues (adipose tissue, bone marrow, umbilical cord, etc.) and culture expanded in large quantities. The MSCs have unique immunomodulatory traits since they evade being recognized by a recipient immune system and can modulate the function of host immune system – most intriguingly by suppressing it [14–20]. Allogeneic cell products have several advantages compared to autologous cell products. It is a much more homogeneous cell product, which can be better characterized with potency tests and stored to be used as an off-the-shelf product. Therefore, it is easy to deliver a standardized cell dose to all patients. Moreover, by using healthy donors, the cell product has not been exposed to the risk factors of the patients. Moreover, the MSC regenerative capacity is further related to reduction in fibrosis, anti-apoptosis, and initiation of endogenous tissue regeneration [18]. We have established a production of clinical grade allogeneic adipose tissue-derived MSCs (CSCC\_ASCs) from healthy donors [21–23]. The CSCC\_ASCs are stored in sealed vials in nitrogen dry containers as an off-the-shelf product in the hospital ready to be used without any delay. In a phase I study, this cell product demonstrated safety in patients with ischaemic HF and a clinical treatment feasibility concept [24]. The aim of the SCIENCE trial was to investigate the safety and clinical efficacy of a single treatment with direct intramyocardial injections of CSCC\_ASCs versus placebo in patients with symptomatic chronic ischaemic HFrEF without further treatment options.

## METHODS

### *Study design*

The SCIENCE trial is an investigator-initiated, randomized, European multicenter, placebo-controlled, double-blind, phase II clinical trial described in detail previously [25]. The study was conducted in Denmark, Germany, The Netherlands, Austria, Slovenia, and Poland after a Voluntary Harmonization Procedure approval through the Clinical Trials Facilitation Groups, European Medicines Agency, EudraCT No:2015–002929-19. Moreover, it was then approved by the National Competent Authorities and Ethics Committees in the participating countries. The study was conducted according to Good Clinical Practice

and follows the latest version of the Helsinki Declaration adopted in 2013 at the 64th World Medical Association Assembly, Brazil. The study is registered in ClinicalTrials.gov (NCT02673164).

### Study population

The study included patients between 30 and 80 years with chronic ischaemic HFrEF, impaired left ventricular ejection fraction (LVEF <45% measured by echocardiography), symptomatic HF (New York Heart Association (NYHA) class II–III), and plasma N-terminal pro-B-type natriuretic peptide (NT-proBNP) > 300 pg/ml (> 35 pmol/L). All included patients had to be on maximal tolerated doses of guideline-recommended HF medications without indications for further invasive treatment, such as revascularization and mechanical circulatory support. All inclusion and exclusion criteria are listed in Appendix 1 and in the design publication [25].

### Overview of the study flow

Patients were screened for trial eligibility, included, treated, and followed for 12 months in six European HF centers. Patients were randomized 2:1 to receive intramyocardial injections of CSCC\_ASC or placebo (isotonic saline). Treatment randomization was

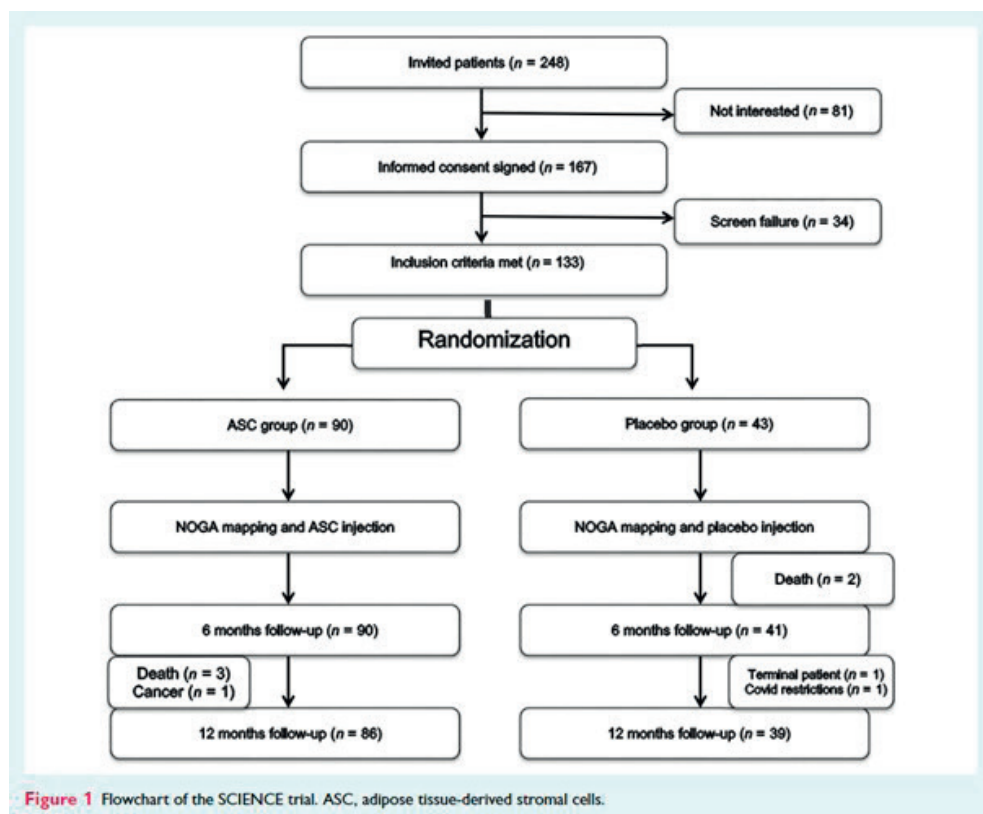


Figure 1 Flowchart of the SCIENCE trial. ASC, adipose tissue-derived stromal cells.

performed by personnel at the Cardiology Stem Cell Centre (CSCC) cell-manufacturing unit before shipment of the treatment vials to the clinical sites. The randomization was for each site performed in blocks of six (four CSCC\_ASC and two placebo) to avoid bias in randomization between sites. The vials were stored locally until treatment of patients with direct intramyocardial injections of either  $110 \times 10^6$  CSCC\_ASCs in 5 ml CryoStor or 5 ml saline (placebo). There was no human leucocyte antigen (HLA) tissue type matching between the donor and the patients except for the site in The Netherlands. Here, it was requested by the Medicinal Research Ethics Committee (METC) to perform HLA antibody screening in all patients before randomization and allocate accordingly a donor to which no specific alloantibodies were present, if randomized to CSCC\_ASC treatment. To assure blinding of outcome ascertainment, the clinical teams performing screening and follow-up of the patients were not allowed to participate in the treatment procedure or be in the catheterization laboratory during the treatment. Follow-up visits were conducted 1, 3, 6, and 12 months after treatment for safety and efficacy evaluation. The study algorithm and visit schedule are summarized in Figure 1.

### *Cell production*

The CSCC\_ASC and placebo (saline) vials were manufactured at CSCC, Rigshospitalet, University Hospital Copenhagen, Denmark. CSCC holds a manufacturing authorization (no. 23909) and a tissue establishment authorization (no. 32298) issued and inspected every second year by the Danish Medicines Agency and the Danish Patient Safety Authority, respectively. The manufacturing procedure is following the EU Guidelines for Good Manufacturing Practice (GMP) of Medicinal Products for Human Use (certificate of GMP compliance no. DK IMP 92217). Six healthy volunteer donors, five female (age 26–34 years) and one male (age 30 years), were included in the study. Donors signed an informed consent in compliance with the Declaration of Helsinki. Donors were tested for human immunodeficiency virus 1/2, hepatitis B and C, syphilis, and human T-cell lymphotropic virus I/II serology by serum analysis within 30 days prior to liposuction and by repeated serology and/or nucleic acid testing on the day of donation. Liposuction was performed under local anaesthesia from abdominal subcutaneous adipose tissue in donors by an experienced plastic surgeon (Printzlau Private Hospital, Denmark) in full compliance with surgical procedures for sterile cosmetic surgery. Approximately 100 – 150 ml lipoaspirate was obtained from each donor, followed by a xeno-free cell expansion performed with human platelet lysate (Cook Regentec/Sexton Biotechnologies) as a growth supplement in semi-automated and functionally closed bioreactor systems (Quantum Cell Expansion System, Terumo BCT) [21–23]. The final cell product was on two passages in the bioreactor system. Harvested CSCC\_ASCs were cryopreserved in CellSeal vials (COOK Regentec/Sexton Biotechnologies) at doses of  $110 \times 10^6$  cells in 5 ml CryoStor CS10 (BioLife Solutions) and were stored below  $-180^\circ\text{C}$  in nitrogen dry storage until clinical use. Release criteria were sterility, endotoxin  $<70$  IU/ml, viability ( $>80\%$ ) and identity (stable positive markers CD90,

CD105, and CD73; and negative markers CD45 and HLA-DR) (Appendix 2). Mycoplasma testing was performed on the supernatant from all bioreactor expansions immediately prior to cell harvest. The presence of bacteria, fungi, and endotoxins was tested on the final product, immediately prior to cryopreservation [21–23]. A total of 24-month stability has been documented by analyses for sterility, viability, recovery, CSCC\_ASC identity, and proliferation potential after thawing of the final product. Each final CSCC\_ASC product vial contained cells from a single donor. Patients randomized to placebo received injections of isotonic saline from a vial stored identical to the CSCC\_ASC vials. World courier shipped the CSCC\_ASC and placebo vials to each site in Europe in a qualified portable nitrogen dry shipper, in accordance with the European rules for Good Distribution Practices. The randomization code for each delivered vial was available in a sealed envelope at each site in case there was an acute need to break the code in situations with a serious unexpected serious adverse event (SAE).

#### *Cardiac echocardiographic scans and analyses*

The investigation is described in detail in the design publication [25]. The echocardiographic (ECHO) scans were performed at each site following the same ECHO site instruction manual. Patients had an ECHO scan at baseline and after 6 months for inclusion and evaluation of the primary endpoint. All ECHO imaging data were stored in a central server at the Netherlands Heart Institute & Lygature/TraIT, Durrer Center, Amsterdam, The Netherlands. The baseline and 6-month ECHO investigations were analysed blinded by two independent groups at the Stem Cell Imaging Core Lab, University Medical Center Utrecht, Utrecht, The Netherlands, and at the Advanced Heart Failure and Transplantation Centre, University Medical Centre, Ljubljana, Slovenia. The two groups did not have any access to each other's analyses. If a difference between the two observers of more than  $\pm 2$  standard deviations (SD) in left ventricular end-systolic volume (LVESV) and left ventricular end-diastolic volume (LVEDV) existed, then data were re-analysed by a third observer from another group. The mean values between the two/three observers of the measurements were used for further statistical analysis.

#### *NOGA-guided injection*

A three-dimensional (3D) left ventricular mapping was created with the NOGA® system (Biologics Delivery Systems). Point by point measurement generates an electromechanical 3D left ventricular map. The system distinguishes between viable (unipolar voltage > 12 mV, bipolar voltage > 2.5 mV, local linear shortening (LLS) > 6%), non-viable-myocardium (unipolar voltage < 6 mV, bipolar voltage < 1.5 mV, LLS < 4%) and border zone (unipolar voltage 6–12 mV, bipolar voltage 1.5 – 2.5 mV, LLS 4–6%) around myocardial scar tissue. To ensure appropriate injection into the ventricle wall, the injection catheter tip was located perpendicular to the ventricle wall and a ventricular extrasystole was elicited when extending the needle into the wall before any injection. Approximately 15 injections of



0.3 ml CSCC\_ASC CryoStor solution (total cell dose  $100 \times 10^6$ ) or placebo were performed into the viable myocardium judged by the 3D map in the border zone of infarcted tissue using the NOGA Myostar® catheter (Biological Delivery System, Cordis, Johnson & Johnson) [8-10, 24].

#### *Quality of life*

Quality of life was evaluated by the Kansas City Cardiomyopathy Questionnaire (KCCQ) and EQ-5D-3L Questionnaire. The KCCQ is a self-administered questionnaire with 23 items addressing specific HF health domains: physical limitation, symptoms, quality of life, social limitation, symptom stability, and self-efficacy. The first four domains combine into a clinical summary score. Scores range from 0 to 100, and higher scores point to lower symptom burden and better quality of life. The EQ-5D-3L Questionnaire focuses on mobility, self-care, usual activities, discomfort, and anxiety. These five elements can be ranged from no, some, and extreme problems. Each element results in a score and all scores can be combined into one, which express the health status of the patient.

#### *Endpoints*

The primary endpoint was change in LVESV at 6-month follow-up measured by ECHO [25]. Safety of CSCC\_ASC treatment was registered as incidence and severity of SAEs and suspected unrelated SAEs at 12-month follow-up. Secondary endpoints were changes in LVEF and LVEDV, NYHA class, KCCQ, EQ-5D-3L Questionnaire, 6-min walk test (6MWT) and NT-proBNP-levels at 6-month follow-up. In addition, we analyzed a composite endpoint of death, HF hospitalization, cardiac resynchronization therapy device implantation, ventricular tachycardia, or aborted sudden cardiac death 1, 2, and 3 years after treatment.

#### *Power calculation and statistics*

Power calculation has been described previously [25]. In short, it was based on the MSC-HF trial, a placebo-controlled comparison of intramyocardial injections of autologous bone marrow-derived MSCs (randomized in a 2:1 pattern) in patients with ischaemic HFrEF [9]. It was estimated that with a maximum dropout rate of 15% before the 6-month follow-up, then it would be possible to detect an absolute difference between the two groups in LVESV of 9.5 ml (estimated SD 15ml) and 12.7 ml (estimated higher SD of 20ml) by including 138 patients, a difference in LVEF of 3.2% (estimated SD 5%) and of 5.1% (estimated higher SD of 8%) with a statistical power of >90%. An alpha value of 5% was used in all calculations [24]. Statistical analyses were performed using SPSS 25 (SPSS Inc., Chicago, IL, USA). For baseline characteristic comparison and follow-up data between and within groups, an independent sample t-test and paired t-test for normally distributed continuous data was used, respectively. Mann-Whitney U test was used for between-group comparisons of continuous non-normally distributed data. For baseline categorical data, we used Pearson's chi-square or Fisher's exact test, as appropriate. For

follow-up data with more than two time-points, we used repeated measures analysis with autoregressive covariance structure. For nominal repeated data, we used generalized estimating equations. Person's chi-square or Fisher's exact test was used for comparison of occurrences of SAEs between groups. Kaplan–Meier curves using log-rank test was used to analyze the incidence of combined cardiac endpoint. A two-sided p-value < 0.05 was considered statistically significant.

## RESULTS

### *Patients*

A total of 133 patients (122 men and 11 women) with stable symptomatic chronic ischaemic HFrEF were included in the study. Demographic data are presented in Table 1. The ASC and placebo groups were comparable at baseline regarding cardiovascular risk factors, medication, and medical history except for a higher systolic blood pressure and a more frequent use of diuretics in the ASC group. Approximately two-thirds of the patients were in NYHA class II and one-third in NYHA class III in both groups. There was no significant difference between groups in LVESV, LVEDV, or LVEF. In the 6MWT, the ASC patients walked  $402 \pm 104$  meters (mean  $\pm$  SD) and the placebo group  $393 \pm 107$  meters. There was no difference in blood NT-proBNP, C-reactive protein (CRP), or renal function between the groups.

### *Safety*

A small pericardial effusion was detected by ECHO after the NOGA procedure in one patient, which was treated with diuretics. During the movement of the catheter in the left ventricle, one patient developed ventricular tachycardia, which was converted to sinus rhythm with direct current cardioversion and the treatment was continued. Beside this event, no procedure-related complications were seen to the direct intra-myocardial injections. The SAEs reported within the first year are outlined in Table 2. There was no significant difference in occurrence of events between the two groups. There were three deaths due to progression of HF in the ASC group and two in the placebo group. One patient in the ASC group was diagnosed with B-cell lymphoma with large pelvic tumor 10 months after CSCC\_ASC treatment, which was judged not to be related to the treatment. The overall mean time to occurrence of combined cardiac adverse event during the 3-year follow-up period was  $26 \pm 1$  months in the ASC group and  $27 \pm 2$  months in the placebo group ( $p = 0.696$ ) (Figure 2).

**Table 1** Baseline characteristics in the adipose tissue-derived stromal cell and placebo groups

Parameter	ASC group (n = 90)	Placebo group (n = 43)	p-value
<b>Patient profile</b>			
Age (years)	66.4 ± 8.1	64.0 ± 8.8	0.122
Male sex	84 (93.3)	38 (88.4)	0.233
Smoking			
Current	15 (16.7)	5 (11.6)	0.447
Former	60 (66.7)	29 (67.4)	0.930
Diabetes mellitus			
Type I	1 (1.1)	1 (2.3)	0.544
Type II	37 (41.1)	16 (37.2)	0.667
Stroke	7 (7.8)	5 (11.6)	0.472
TIA	8 (8.9)	5 (11.6)	0.622
PAD	14 (15.6)	7 (16.3)	0.915
Pulmonary disease	18 (20.0)	10 (23.3)	0.667
BMI (kg/m <sup>2</sup> )	28.5 ± 4.6	29.9 ± 3.8	0.084
Blood pressure			
Systolic (mmHg)	125 ± 17	118 ± 18	0.033
Diastolic (mmHg)	77 ± 11	74 ± 11	0.190
Heart rate (bpm)	68 ± 10	71 ± 12	0.089
6-min walk test (m)	402 ± 104	393 ± 107	0.656
<b>Cardiac history</b>			
Previous MI	69 (76.7)	39 (90.7)	0.053
Previous PCI	68 (75.6)	34 (79.1)	0.654
Previous CABG	44 (48.9)	15 (34.9)	0.128
Hypertension	72 (80.0)	29 (67.4)	0.115
Hypercholesterolaemia	81 (90.0)	39 (90.7)	0.113
Family history of premature IHD	36 (40.0)	15 (34.9)	0.538
Cardiac device implant	53 (58.9)	27 (62.8)	0.667
Cardiac valve operation	3 (3.3)	4 (9.3)	0.212
<b>Baseline endpoints</b>			
LVESV (ml)	154.5 ± 54.8	150.0 ± 57.7	0.567
LVEDV (ml)	221.8 ± 63.0	214.1 ± 65.8	0.460
LVEF (%)	31.6 ± 7.2	32.0 ± 8.9	0.712
NYHA class	2.3 ± 0.5	2.3 ± 0.5	0.919
II	62 (68.9)	30 (69.8)	0.918
III	28 (31.1)	13 (30.2)	
CCS class	1.7 ± 0.6	1.3 ± 0.5	0.258
I	6 (6.7)	4 (9.3)	0.497
II	8 (8.9)	2 (4.7)	
III	1 (1.1)	0 (0.0)	
<b>Medication</b>			
Acetylsalicylic acid	48 (53.3)	29 (67.4)	0.123
Clopidogrel	9 (10.0)	6 (14.0)	0.562
Prasugrel	3 (3.3)	2 (4.7)	0.658
Ticagrelor	7 (7.8)	5 (11.6)	0.523
Warfarin	35 (38.9)	11 (25.6)	0.131
Angiotensin-converting enzyme inhibitor	41 (45.6)	18 (41.9)	0.688
Angiotensin II receptor blocker	40 (44.4)	24 (55.8)	0.220
β-blocker	87 (96.7)	41 (95.3)	0.685
Calcium channel blocker	11 (12.2)	2 (4.7)	0.222
Diuretic agent	68 (75.6)	25 (58.1)	0.041
Aldosterone	53 (58.9)	30 (69.8)	0.226
Statins	81 (90.0)	41 (95.3)	0.502
Non-statin cholesterol-lowering drug	10 (11.1)	8 (18.6)	0.237
Nitrate	15 (16.7)	9 (20.9)	0.550
Insulin	12 (13.3)	5 (11.6)	0.783

Table 1 (Continued)

Parameter	ASC group (n = 90)	Placebo group (n = 43)	p-value
Liraglutide	3 (3.3)	1 (2.3)	1.000
Oral anti-diabetic	27 (30.0)	10 (23.3)	0.417
Biochemical profile			
NT-proBNP (pg/ml)	1495 ± 2242	1828 ± 2376	0.503
Total cholesterol (mg/dl)	133 ± 52	136 ± 68	0.833
HDL-cholesterol (mg/dl)	39 ± 20	47 ± 17	0.195
Creatinine (μmol/L)	111.3 ± 39.0	106.3 ± 32.9	0.585
CRP (mg/L)	8.7 ± 13.3	7.4 ± 8.5	0.690
KCCQ			
Total symptom score	70 ± 22	74 ± 20	0.241
Clinical summary score	68 ± 19	65 ± 21	0.585
Overall summary score	64 ± 19	65 ± 21	0.671
Physical limitation	67 ± 20	66 ± 21	0.820
Symptom stability	51 ± 14	49 ± 8	0.549
Symptom frequency	67 ± 21	71 ± 20	0.292
Symptom burden	72 ± 26	78 ± 24	0.243
Self-efficacy	78 ± 20	78 ± 16	0.840
Quality of life	60 ± 23	60 ± 25	0.898
Social limitation	58 ± 24	59 ± 27	0.790
EQ-SD-3L score	59 ± 17	63 ± 19	0.221

Values are mean ± standard deviation, or n (%).

ASC, adipose tissue-derived stromal cell; BMI, body mass index; CABG, coronary artery bypass graft; CCS, Canadian Cardiovascular Society; CRP, C-reactive protein; eGFR, estimated glomerular filtration rate; HDL, high density lipoprotein; IHD, ischaemic heart disease; KCCQ, Kansas City Cardiomyopathy Questionnaire; LVEDV, left ventricular end-diastolic volume; LVESV, left ventricular end-systolic volume; MI, myocardial infarction; NT-proBNP, N-terminal pro-B-type natriuretic peptide; NYHA, New York Heart Association; PAD, peripheral arterial disease; PCI, percutaneous coronary intervention; TIA, transient ischaemic attack.

### Cardiac function

The LVESV, LVEDV and the LVEF did not change from baseline to 6-month follow-up between the two groups (Table 3). Change in the primary endpoint of LVESV from baseline to follow-up was  $-3.5 \pm 2.8$  ml ( $p = 0.216$ ) in the ASC group and  $-3.9 \pm 4.1$  ml ( $p = 0.358$ ) in the placebo group (Table 3). The change in LVEDV was  $-1.5 \pm 3.2$  ml ( $p = 0.646$ ) in the ASC group and  $0.6 \pm 5.5$  ml ( $p = 0.919$ ) in the placebo group. There was a significant increase in LVEF from baseline to 6-month follow-up in the ASC ( $1.2 \pm 0.6\%$ ,  $p = 0.044$ ) and placebo ( $2.8 \pm 0.9\%$ ,  $p = 0.003$ ) group, respectively. There were no significant differences between groups during follow-up in LVESV ( $0.3 \pm 5.0$  ml,  $p = 0.945$ ), LVEDV ( $-2.0 \pm 6.0$  ml,  $p = 0.736$ ), or LVEF ( $-1.6 \pm 1.0\%$ ,  $p = 0.119$ ) (Figure 3).

### Functional status and quality of life

There were no changes in 6MWT, NT-proBNP, or the inflammatory marker CRP during the first year in any of the two groups (Table 4). The NT-proBNP level was significantly higher in the placebo group, compared to the ASC group at 12-month follow-up ( $p = 0.034$ , online supplementary Figure S2). However, no differences in response between the two groups were detected for 6MWT and CRP at follow-up (online supplementary Figure S1). The NYHA class did not change in the two groups or between groups (Table 5).

The KCCQ quality of life evaluation demonstrated significant improvements in total symptoms, clinical summary and total summary scores in both the ASC and placebo groups within the 1-year follow-up. However, there were no differences between groups

**Table 2** Serious adverse events within the first year in the adipose tissue-derived stromal cell and placebo groups

	ASC group (n = 90)	Placebo group (n = 43)	p-value
Death	3 (3.3)	2 (4.7)	1.000
<b>Hospitalizations for:</b>			
Cancer	1 (1.1)	0	1.000
Heart failure worsening	14 (15.5)	7 (16.3)	1.000
VT/VF	6 (6.6)	0	0.177
MI	4 (4.4)	1 (2.3)	1.000
PCI or CABG	2 (2.2)	0	1.000
Stroke or TIA	1 (1.1)	1 (2.3)	1.000
Angina worsening	1 (1.1)	1 (2.3)	1.000
Pneumonia	4 (4.4)	2 (4.7)	1.000
Syncope non-cardiac	1 (1.1)	0	1.000
Cutaneous abscess	2 (2.2)	1 (2.3)	1.000
Pulmonary embolism	1 (1.1)	0	1.000
Epididymitis	2 (2.2)	0	1.000
Cholecystitis	1 (1.1)	0	1.000
Colon perforation	1 (1.1)	0	1.000
Incarcerated abdominal hernia	1 (1.1)	0	1.000
Diabetic foot amputation	1 (1.1)	0	1.000
Acute ischaemic leg	0	1 (2.3)	0.331
Aortic valve operation	1 (1.1)	0	1.000
Ulcer ventriculi	0	1 (2.3)	0.331
Gout	1 (1.1)	0	1.000
Severe headache	0	1 (2.3)	0.331
Struma multinodular	1 (1.1)	0	1.000
Costa fracture - bicycle accident	1 (1.1)	0	1.000
Depression	1 (1.1)	0	1.000
Diabetic derailment	1 (1.1)	0	1.000

Values are  $n$  (%).

ASC, adipose tissue-derived stromal cell; CABG, coronary artery bypass graft; MI, myocardial infarction; PCI, percutaneous coronary intervention; TIA, transient ischaemic attack; VF, ventricular fibrillation; VT, ventricular tachycardia.

**Table 3** Changes in left ventricular end-systolic volume, left ventricular end-diastolic volume and left ventricular ejection fraction at baseline and 6-month follow-up in the adipose tissue-derived stromal cell- and placebo-treated groups

	ASC group				Placebo group			
	Baseline	6-month FU	Change from baseline to 6-month FU	p-value	Baseline	6-month FU	Change from baseline to 6-month FU	p-value
LVESV (ml)	154.5 ± 54.8	151.0 ± 55.2	-3.5 ± 2.8	0.216	150.0 ± 57.7	146.2 ± 70.5	-3.9 ± 4.1	0.358
LVEDV (ml)	221.8 ± 63.0	220.3 ± 63.6	-1.5 ± 3.2	0.646	214.1 ± 65.8	214.6 ± 83.5	0.6 ± 5.4	0.919
LVEF (%)	31.6 ± 7.2	32.8 ± 7.5	1.2 ± 0.6	0.044	32.0 ± 8.9	34.7 ± 9.7	2.8 ± 0.9	0.003

Values are mean ± standard deviation.

FU, follow-up; LVEDV, left ventricular end-diastolic volume; LVEF, left ventricular ejection fraction; LVESV, left ventricular end-systolic volume.

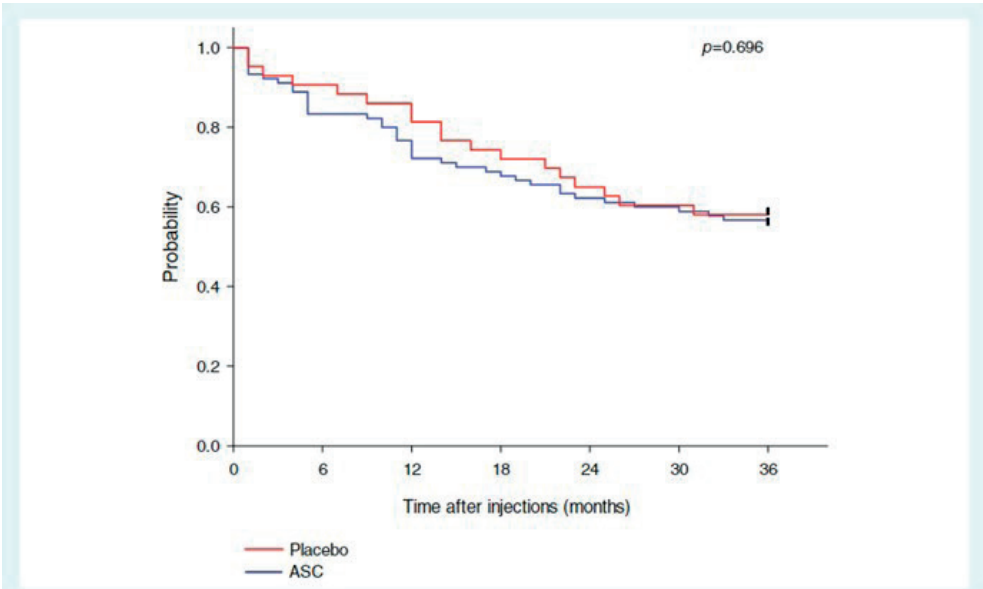


**Figure 2** Freedom of combined cardiac events. Combined cardiac events: death, hospitalization for worsening heart failure including inserting biventricular pacemaker, and hospitalization for ventricular tachycardia or fibrillation 1, 2, and 3 years after treatment. ASC, adipose tissue-derived stromal cells.

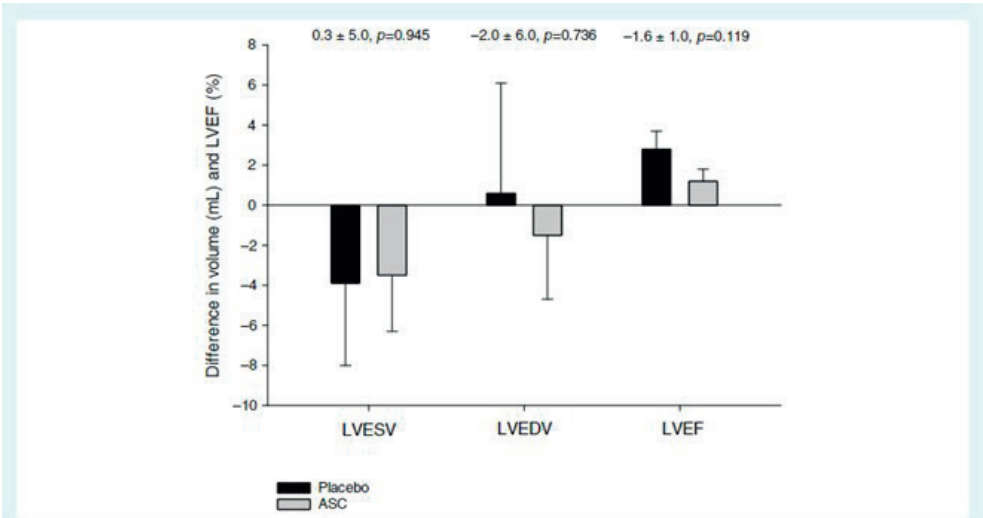


**Figure 3** Difference between groups from baseline to 6-month follow-up in left ventricular end-systolic volume (LVESV), left ventricular end-diastolic volume (LVEDV), and left ventricular ejection fraction (LVEF). ASC, adipose tissue-derived stromal cells.



**Table 4** Changes in 6-min walk test, N-terminal pro-B-type natriuretic peptide and C-reactive protein within the first year in the adipose tissue-derived stromal cell and placebo groups

	n	ASC group	p-value baseline to FU	p-value overall	n	Placebo group	p-value baseline to FU	p-value overall	p-value for between-group differences baseline to FU
<b>6MWT</b>									
Baseline	90	419 ± 12			43	423 ± 18			
6 months	90	422 ± 13	0.676		41	450 ± 20	0.040		0.089
12 months	86	432 ± 13	0.092	0.372	39	451 ± 19	0.051	0.183	0.097
<b>NT-proBNP</b>									
Baseline	90	1907 ± 381			43	1329 ± 419			
6 months	90	1687 ± 281	0.485		41	1875 ± 486	0.227		0.403
12 months	86	1607 ± 274	0.759	0.429	39	1652 ± 595	0.495	0.079	0.033
<b>CRP</b>									
Baseline	90	5.5 ± 0.8			43	5.8 ± 1.5			
6 months	90	5.1 ± 0.7	0.428		41	5.7 ± 1.4	0.341		0.952
12 months	86	5.5 ± 0.5	0.438	0.483	39	5.0 ± 0.5	0.377	0.489	0.711

Values are mean ± standard deviation.

6MWT, 6-min walk test; CRP, C-reactive protein; FU, follow-up; NT-proBNP, N-terminal pro B-type natriuretic peptide.

**Table 5** Changes in New York Heart Association class between baseline and follow-up in the adipose tissue-derived stromal cell and placebo groups

NYHA class	ASC group			Placebo			p-value for between-group differences	
	Baseline	6-month FU	12-month FU	Baseline	6-month FU	12-month FU	Baseline to 6-month FU	Baseline to 12-month FU
I		11 (12.2)	11 (12.2)		7 (16.3)	9 (20.9)		
II	62 (68.9)	62 (68.9)	59 (65.6)	30 (69.8)	26 (60.5)	23 (53.5)		
III	28 (31.1)	15 (16.7)	16 (17.8)	13 (30.2)	8 (18.6)	6 (14.0)		
IV		1 (1.1)				1 (2.3)	0.632	0.341

ASC, adipose tissue-derived stromal cell; FU, follow-up; NYHA, New York Heart Association.

for any parameter (online supplementary Figure S2). All KCCQ parameters are outlined in online supplementary Table S1. The EQ-5D-3L quality of life evaluation demonstrated improvement in the ASC group from  $60 \pm 2$  to  $66 \pm 2$  ( $p < 0.001$ ) and no change in the placebo group ( $64 \pm 3$  to  $66 \pm 4$ ;  $p < 0.09$ ) (online supplementary Table S2). However, there were no significant differences between groups.

## DISCUSSION

We have previously demonstrated that direct intramyocardial injections of autologous bone marrow-derived MSCs in patients with ischaemic HFrEF were safe and improved cardiac function [8–10]. However, to use a more standardized and quality-controlled cell product, we have established production of an allogeneic CCCC\_ASC product obtained from healthy donors stored in nitro-gen dry container as an off-the-shelf product ready to be used without any time delay. It has proven safety and indications of efficacy in phase I clinical trials in patients with ischaemic HFrEF, dry eyes caused by Sjogren's syndrome and radiation-induced xerostomia with reduced saliva production [24,26,27].

The SCIENCE trial is the first European multicenter randomized phase II trial testing the safety and efficacy of direct intramyocardial injections of allogeneic CCCC\_ASC product or saline in 133 patients with symptomatic chronic ischaemic HFrEF without any further treatment options. Our hypothesis was that the cell therapy would lead to improvement of left ventricular volumes and function.

The study demonstrated that it was safe to inject CCCC\_ASC intramyocardially in patients with chronic ischaemic HFrEF. However, it was not possible to detect any improvement in the primary endpoint of LVESV. Moreover, we did not find any significant beneficial effect of the treatment on the secondary endpoints evaluating cardiac function, HF symptoms or quality of life (Graphical Abstract). These findings were very surprising based on our previous studies with autologous MSC and allogeneic CCCC\_ASC in patients with ischaemic HFrEF [8,10,24]. However, the present results are in line with the results from a parallel conducted single site national Danish CCCC\_ASC phase II study with the same CCCC\_ASC product and dose in 81 patients with chronic ischaemic HFrEF (unpublished data).

It was very surprising that the use of a more homogeneous and functional proven allogeneic cell product was without any clinical effect. It can be speculated whether an autologous mesenchymal cell product would be more effective than an allogeneic mesenchymal cell product. When changing the production from autologous to allogeneic production, we performed in vitro comparison studies, which demonstrated that the cell markers and functional tests were identical. However, the allogeneic cell product was much more homogeneous in characteristics and functional tests compared to autologous cell products from patients. Based on the accumulating evidence for the potential immunomodulatory and inflammatory regulation mode of action of ASC in different diseases, our hypothesis was probably wrong [28]. The ASCs seem not to be able to restore cardiac function by inducing the creation of new cardiomyocytes by the cell's paracrine secretion.

The discrepancy with the previous study could also be due the use of magnetic resonance/computed tomography scans which were more accurate and with less variability than ECHO. With the implementation of prophylactic implantable cardioverter-defibrillator treatment in patients with HFrEF, magnetic resonance scans were no longer an option. Moreover, we were not allowed to use computed tomography scans with contrast by the competent authorities in all countries. Therefore, we decided to use ECHO and perform the analyses by two independent groups in the Netherlands and Slovenia to minimize the variation in analyses.

Allogeneic MSCs and ASCs have already been used in small clinical trials without any side effects [29,30]. The TRIDENT trial compared two doses of allogeneic MSCs, injected directly into the myocardium in 30 patients with ischaemic cardiomyopathy [30]. The treatment was safe. Both cell doses ( $20 \times 10^6$  and  $100 \times 10^6$  cells) decreased scar size, but only the  $100 \times 10^6$  dose increased LVEF. In the present trial, we only used one total dose of



CSCC\_ASCs ( $100 \times 10^6$ ). Therefore, we can only speculate on whether another dose would have changed the results of the study.

Worldwide, there are still no approved stem cell products on the market for HF. Mesoblast Ltd has an allogeneic bone marrow-derived mesenchymal cell product, rexlemestrocel-L, being used in an event-driven study finalized approximately 2 years ago, the phase III DREAM-HF trial in 537 patients with ischaemic and non-ischaemic HFrEF in the US [31]. Our findings are in accordance with some of the results announced by Mesoblast on 15 November 2020 demonstrating that the study did not reach the primary endpoint – time to recurrent non-fatal HF-related major adverse cardiac events [32].

We have included chronic ischaemic HF patients with no further treatment options. The CSCC\_ASC products regenerative mechanisms of action are through paracrine trophic, antifibrotic, angiogenetic, and immunomodulatory processes [18]. In a pre-clinical model of ischaemic cardiomyopathy, we found that immune cell activation was the most prominent effect in the myocardium after cell therapy [33]. Some patients with ischaemic HF do also have increased immunological activity in the myocardium [34]. In chronic HFrEF patients with no further treatment options, the micromilieu in the myocardium may not be able to benefit from the cells delivered. Early cell treatment after presentation of HFrEF may be more effective, which the preliminary data from the DREAM-HF trial also indicate. It can be discussed whether the cell dose in this study was high enough and whether the delivered cell product remains in the myocardium for enough time to initiate clinically meaningful improvement [35–38]. Injection of combined cell and hydrogel solutions may improve efficacy [39]. More than one treatment session could potentially also increase efficacy. Many of the cells will pass through the capillaries in the myocardium by time and migrate to the lungs and spleen. Therefore, the cell retention may be too short to initiate the paracrine effects. Also, the number of resident primitive cells in the chronic myocardium may be too low to be stimulated sufficiently by the delivered cells.

In conclusion, the SCIENCE trial demonstrated that the direct injection with allogeneic CSCC\_ASCs into the myocardium of patients with chronic ischaemic HFrEF was safe during a 3-year follow-up period. However, it was not possible to detect any significant improvement of left ventricular volumes or function, or clinical symptoms 6 months after treatment. Also, in comparison to placebo there was no significant improvement in 6MWT, NYHA class and self-reported indices of quality of life during the follow-up. It has not been tested whether autologous ASCs would be more effective than the present used allogeneic ASCs. However, the clinical effect of autologous ASCs should be highly significant to justice the very expensive production of the inhomogeneous cell product and invasive treatment, which can be difficult to get re-imbursed. Therefore, there is a need for new potential effective treatment strategies and hypotheses to justify clinical trials in this HFrEF patient population.

## ACKNOWLEDGEMENTS

Joanna Ciosek, Sebastian Dworowy, Tomasz Jadczyk, Kai Jaquet, Michal Kozłowski, Aleksandra Michalewska-Włodarczyk, Mira van der Naald, Kasper Westinga, Karin Vlaardingerbroek, Ronja Sagalski, Esther Schlegel, Annette Schmidt, Anna Sikora, Dorota Skiba, Mojdeh Lofti, Kirstine Joo Andresen, Rebekka Harary Søndergaard, Louise Frandsen, and Anne Lavigne were actively involved in the conduction of the SCIENCE trial.

## FUNDING

This work was supported by an EU funding as part of the Horizon 2020 program to conduct this randomized multicenter clinical trial (SCIENCE grant no. 643478). The Innovation Fund Denmark grant (CSCC grant no. 6153-00002A), and Aase and Ejnar Danielsens Foundation. Conflict of interest: A.E., M.H.S. and J.K. are inventors of a granted patent ('STEM CELL THERAPY BASED ON ADIPOSE-DERIVED STEM CELLS') (WO2017068140A1EP3365432A1) owned by the Capital Region of Denmark and Rigshospitalet, Copenhagen University Hospital, Denmark. The patent is granted in Europe and Australia. Applications are submitted in Canada, China, Hong Kong, Japan, Korea, and USA. A.E., M.H.S. and J.K. are founder of Cell2Cure ApS, which has a license to commercialize the patent. All other authors have nothing to disclose.

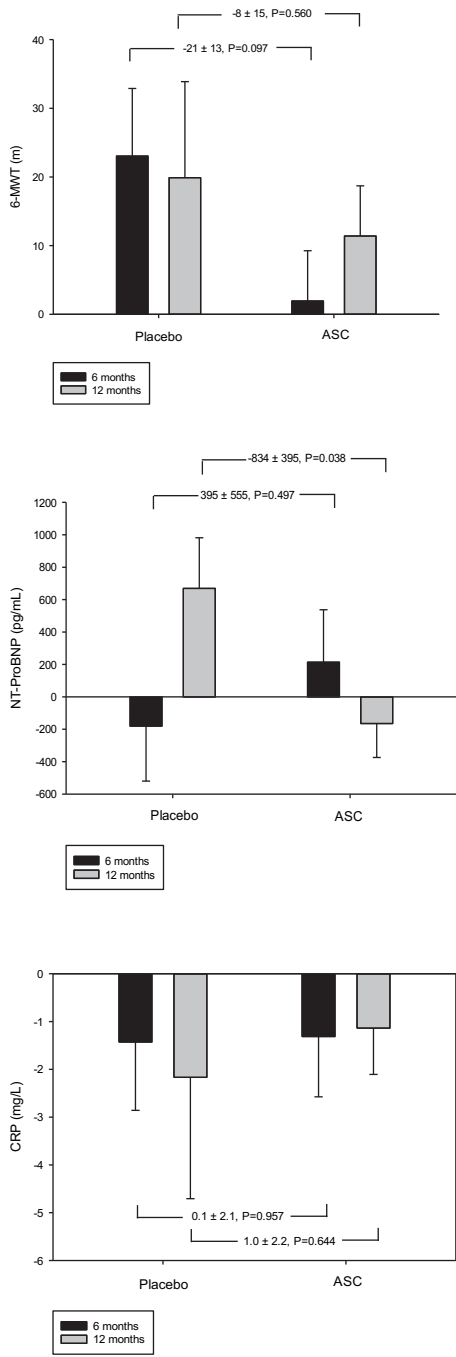
## REFERENCES

31. Metra M, Teerlink JR. Heart failure. *Lancet* 2017;390:1981–95. Doi:10.1155/2017/8506370
32. Ambrosy AP, Fonarow GC, Butler J, et al. The global health and economic burden of hospitalizations for heart failure: lessons learned from hospitalized heart failure registries. *J Am Coll Cardiol* 2014;63:1123–33. Doi:10.1016/j.jacc.2013.11.053
33. Fernández-Avilés F, Sanz-Ruiz R, Climent AM, et al. TACTICS (Transnational Alliance for Regenerative Therapies in Cardiovascular Syndromes) Writing Group; Authors/Task Force Members. Chairpersons, Basic Research Subcommittee, Translational Research Subcommittee, Challenges of Cardiovascular Regenerative Medicine Subcommittee, Tissue Engineering Subcommittee, Delivery, Navigation, Tracking and Assessment Subcommittee, Clinical Trials Subcommittee, Regulatory and Funding Strategies Subcommittee, Delivery, Navigation, Tracking and Assessment Subcommittee. Global position paper on cardiovascular regenerative medicine. *Eur Heart J* 2017;38:2532–46. Doi:10.1093/eurheartj/ehx248
34. Grigorian SL, Sanz-Ruiz R, Climent A, et al. Insights into therapeutic products, preclinical research models and clinical trials in cardiac regenerative and reparative medicine: where are we now and the way ahead. Current opinion paper of the ESC Working Group on Cardiovascular Regenerative and Reparative Medicine. *Cardiovasc Res* 2021;117:1428–33. Doi:10.1093/cvr/cvaa337
35. Povsic TJ, Sanz-Ruiz R, Climent AM, et al. Reparative cell therapy for the heart: critical internal appraisal of the field in response to recent controversies. *ESC Heart Fail* 2021;8:2306–9. Doi:10.1002/ehf2.13256
36. Liang P, Ye F, Hou CC, et al. Mesenchymal stem cell therapy for patients with ischemic heart failure – past, present, and future. *Curr Stem Cell Res Ther* 2021;16:608–21. Doi:10.2174/1574888X15666200309144906
37. Shen T, Xia L, Dong W, et al. A systematic review and meta-analysis: safety and efficacy of mesenchymal stem cells therapy for heart failure. *Curr Stem Cell Res Ther* 2021;16:354–65. Doi: 10.2174/1574888X15999200820171432
38. Qayyum AA, Mathiasen AB, Helqvist S, et al. Autologous adipose-derived stromal cell treatment for patients with refractory angina (MyStromalCell trial): 3-years follow-up results. *J Transl Med* 2019;17:360. Doi:10.1186/s12967-019-2110-1
39. Mathiasen AB, Qayyum AA, Jorgensen E, et al. Bone marrow-derived mesenchymal stromal cell treatment in patients with severe ischaemic heart failure: a randomized placebo-controlled trial (MSC-HF trial). *Eur Heart J* 2015;36:1744–53. Doi:10.1093/eurheartj/ehv136
40. Mathiasen AB, Qayyum AA, Jørgensen E, et al. Bone marrow-derived mesenchymal stromal cell treatment in patients with ischaemic heart failure: final 4-year follow-up of the MSC-HF trial. *Eur J Heart Fail* 2020;22:884–92. Doi:10.1002/ehf.1700
41. Vrtovec B, Poglajen G, Sever M, et al. Effects of repetitive transendocardial CD34+ cell transplantation in patients with non-ischemic dilated cardiomyopathy. *Circ Res* 2018;123:389–96. Doi:10.1161/CIRCRESAHA.117.312170

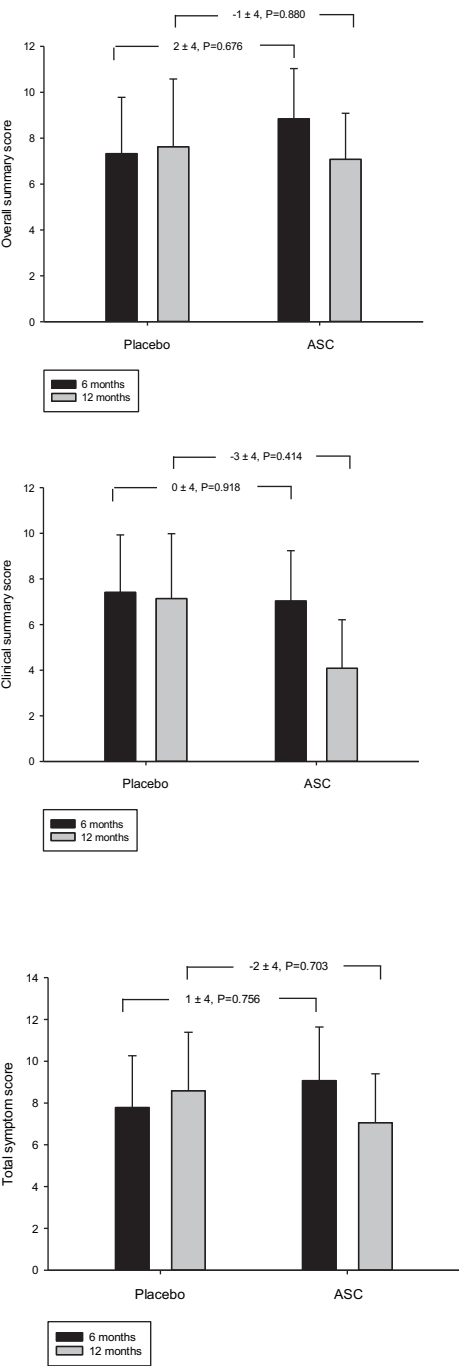
42. Žorž N, Poglajen G, Frljak S, et al. Transendocardial CD34+ cell therapy improves local mechanical dyssynchrony in patients with non-ischemic dilated cardiomyopathy. *Cell Transplant* 2022;31:9636897221080384. Doi:10.1177/09636897221080384
43. Gyöngyösi M, Pokushalov E, Romanov A, et al. Meta-analysis of percutaneous endomyocardial cell-therapy in patients with ischemic heart failure by combination of individual patient data (IPD) of ACCRUE and publication-based aggregate data. *J Clin Med* 2022;11:3205. Doi:10.3390/jcm11113205
44. Weiss AR, Dahlke MH. Immunomodulation by mesenchymal stem cells (MSCs): mechanisms of action of living, apoptotic, and dead MSCs. *Front Immunol* 2019;10:1191. Doi:10.3389/fimmu.2019.01191
45. Gebler A, Zabel O, Seliger B. The immunomodulatory capacity of mesenchymal stem cells. *Trends Mol Med* 2012;18:128–34. Doi:10.1016/j.molmed.2011.10.004
46. Hoeeg C, Frljak S, Qayyum AA, et al. Efficacy and mode of action of mesenchymal stem cells in non-ischemic dilated cardiomyopathy: a systematic review. *Biomedicines* 2020;8:570. Doi:10.3390/biomedicines8120570
47. Le Blanc K, Davies LC. Mesenchymal stromal cells and the innate immune response. *Immunol Lett* 2015;168:140–6. Doi:10.1016/j.imlet.2015.05.004
48. Pittenger MF, Discher DE, Péault BM, et al. Mesenchymal stem cell perspective: cell biology to clinical progress. *NPJ Regen Med* 2019;4:22. Doi:10.1038/s41536-019-0083-6
49. Spaggiari GM, Capobianco A, Abdelrazik H, et al. Mesenchymal stem cells inhibit natural killer-cell proliferation, cytotoxicity, and cytokine production: role of indoleamine 2,3-dioxygenase and prostaglandin E2. *Blood* 2008;111:1327–33. Doi:10.1182/blood-2007-02-074997
50. Melief SM, Zwaginga JJ, Fibbe WE, Roelofs H. Adipose tissue-derived multipotent stromal cells have a higher immunomodulatory capacity than their bone marrow-derived counterparts. *Stem Cells Transl Med* 2013;2:455–46. Doi:10.5966/sctm.2012-0184
51. Haack-Sørensen M, Follin B, Juhl M, et al. Culture expansion of adipose derived stromal cells. A closed automated quantum cell expansion system compared with manual flask-based culture. *J Transl Med* 2016;14:319. Doi:10.1186/s12967-016-1080-9
52. Haack-Sørensen M, Juhl M, Follin B, et al. Development of large-scale manufacturing of adipose-derived stromal cells for clinical applications using bioreactors and human platelet lysate. *Scand J Clin Lab Invest* 2018;78:293–300. Doi:10.1080/00365513.2018.1462082
53. Haack-Sørensen M, Johansen EM, Højgaard LD, et al. GMP compliant production of a cryo-preserved adipose-derived stromal cell product for feasible and allogeneic clinical use. *Stem Cells Int* 2022;2022:4664917. Doi:10.1155/2022/4664917
54. Kastrup J, Haack-Sørensen M, Juhl M, et al. Cryopreserved off-the-shelf allogeneic adipose-derived stromal cells for therapy in patients with ischemic heart disease and heart failure – a safety study. *Stem Cells Transl Med* 2017;6:1963–71. Doi:10.1002/sctm.17-0040
55. Paitazoglou C, Bergmann MW, Vrtovec B, et al. Rationale and design of the European multicenter study on Stem Cell therapy in IschEmic Non-treatable Cardiac disease (SCIENCE). *Eur J Heart Fail* 2019;21:1032–41. Doi:10.1002/ehf.1412

56. Møller-Hansen M, Larsen AC, Toft PB, et al. Safety and feasibility of mesenchymal stem cell therapy in patients with aqueous deficient dry eye disease. *Ocul Surf* 2021;19:43–52. Doi:10.1016/j.jtos.2020.11.013
57. Lynggaard CD, Grønhøj C, Christensen R, et al. Intraglandular off-the-shelf allogeneic mesenchymal stem cell treatment in patients with radiation-induced xerostomia – a safety study (MESRIX-II). *Stem Cells Transl Med* 2022;11:szac011. Doi:10.1093/stcltm/szac011
58. Adamo L, Rocha-Resende C, Prabhu SD, Mann DL. Reappraising the role of inflammation in heart failure. *Nat Rev Cardiol* 2020;17:269–85. Doi:10.1038/s41569-019-0315-x
59. Perin EC, Borow KM, Silva GV, et al. A phase II dose-escalation study of allogeneic mesenchymal precursor cells in patients with ischemic or nonischemic heart failure. *Circ Res* 2015;117:576–84. Doi:10.1161/CIRCRESAHA.115.306332
60. Florea V, Rieger AC, DiFede DL, et al. Dose comparison study of allogeneic mesenchymal stem cells in patients with ischemic cardiomyopathy (the TRIDENT study). *Circ Res* 2017;121:1279–90. Doi:10.1161/CIRCRESAHA.117.311827
61. Borow KM, Yaroshinsky A, Greenberg B, Perin EC. Phase 3 DREAM-HF trial of mesenchymal precursor cells in chronic heart failure. A review of biological plausibility and implementation of flexible clinical trial design. *Circ Res* 2019;125:265–81. Doi:10.1161/CIRCRESAHA.119.314951
62. Late breaking presentation at American Heart Association Annual meeting of landmark phase 3 trial of Rexlemestrol-L in chronic heart failure. <https://www.mesoblast.com/>
63. Follin B, Hoeeg C, Højgaard LD, et al. The initial cardiac tissue response to cryopreserved allogeneic adipose tissue-derived mesenchymal stromal cells in rats with chronic ischemic cardiomyopathy. *Int J Mol Sci* 2021;22:11758. Doi:10.3390/ijms222111758
64. Mann DL. Innate immunity and the failing heart: the cytokine hypothesis revisited. *Circ Res* 2015;116:1254–68. Doi:10.1161/CIRCRESAHA.116.302317
65. Bagno LL, Salerno AG, Balkan W, Hare JM. Mechanism of action of mesenchymal stem cells (MSCs): impact of delivery method. *Expert Opin Biol Ther* 2022;22:449–63. Doi:10.1080/14712598.2022.2016695
66. Vekstein AM, Wendell DC, DeLuca S, et al. Targeted delivery for cardiac regeneration: comparison of intra-coronary infusion and intra-myocardial injection in porcine hearts. *Front Cardiovasc Med* 2022;9:833335. Doi:10.3389/fcvm.2022.833335
67. Van der Spoel TIG, Le JCT, Vrijnsen K, et al. Non-surgical stem cell delivery strategies and in vivo cell tracking to injured myocardium. *Int J Cardiovasc Imaging*. 2011;27:367–83. Doi:10.1007/s10554-010-9658-4
68. Van den Akker F, Feyen DAM, van den Hoogen P, et al. Intramyocardial stem cell injection: go(ne) with the flow. *Eur Heart J* 2017;38:184–6. Doi:10.1093/eurheartj/ehw056
69. Hoeeg C, Dolatshahi-Pirouz A, Follin B. Injectable hydrogels for improving cardiac cell therapy- in vivo evidence and translational challenges. *Gels* 2021;7:7. Doi:10.3390/gels7010007

**Supplementary Figure 1** - Changes in 6-MWT, NT-ProBNP, and CRP in the ASC and Placebo group in the 6- and 12-months follow-up period.



**Supplementary Figure 2** - Changes in Kansas City Cardiomyopathy Questionnaire between baseline and 6- and 12-months follow-up in the Placebo and ASC group.



**Supplementary Table 1** - KCCQ Questionnaire evaluation at baseline and follow-up.

	<i>n</i>	ASC group	P-value Baseline - FU	P-value Overall	<i>n</i>	Placebo group	P-value Baseline - FU	P-value Overall
<b>Total Symptom</b>								
Baseline	90	72.5 (2.3)			43	75.7 (3.2)		
3 months	90	81.7 (2.5)	<0.001		41	82.4 (3.7)	0.013	
6 months	90	83.1 (2.2)	<0.001		41	83.0 (4.0)	0.010	
12 months	86	79.4 (2.5)	0.006	<0.001	39	85.1 (3.8)	0.002	0.016
<b>Overall Summary</b>								
Baseline	90	66.1 (2.0)			43	67.5 (3.2)		
3 months	90	74.7 (2.2)	<0.001		41	74.2 (3.5)	0.014	
6 months	90	76.0 (2.0)	<0.001		41	74.4 (3.7)	0.014	
12 months	86	73.1 (2.2)	0.001	<0.001	39	75.8 (3.6)	0.008	0.048
<b>Clinical Summary</b>								
Baseline	90	71.2 (2.0)			43	71.5 (3.0)		
3 months	90	77.6 (2.3)	0.004		41	78.6 (3.2)	0.008	
6 months	90	79.3 (2.0)	<0.001		41	79.0 (3.7)	0.011	
12 months	86	75.2 (2.2)	0.073	<0.001	39	79.5 (3.6)	0.007	0.038
<b>Physical Limitation</b>								
Baseline	90	70.1 (2.0)			43	67.3 (3.4)		
3 months	90	73.4 (2.3)	0.135		41	74.8 (3.3)	0.014	
6 months	90	75.2 (2.1)	0.017		41	74.9 (3.6)	0.024	
12 months	86	71.1 (2.3)	0.677	0.016	39	74.0 (3.7)	0.060	0.108
<b>Symptom Stability</b>								
Baseline	90	51.9 (1.6)			43	50.7 (1.3)		
3 months	90	58.0 (2.0)	0.012		41	54.3 (2.2)	0.134	
6 months	90	57.7 (2.0)	0.017		41	55.7 (3.1)	0.128	
12 months	86	54.6 (2.0)	0.288	0.027	39	56.4 (3.0)	0.044	0.117
<b>Symptom Frequency</b>								
Baseline	90	70.0 (2.1)			43	72.8 (3.0)		
3 months	90	77.9 (2.2)	0.001		41	76.9 (3.6)	0.117	
6 months	90	79.5 (1.8)	<0.001		41	77.9 (3.7)	0.059	
12 months	86	74.8 (2.2)	0.036	<0.001	39	81.0 (3.1)	0.003	0.029

Symptom Burden								
Baseline	90	75.0 (2.8)			43	78.7 (3.8)		
3 months	90	85.6 (3.0)	<0.001		41	88.0 (4.1)	0.005	
6 months	90	86.7 (2.8)	<0.001		41	88.2 (4.6)	0.006	
12 months	86	83.9 (2.9)	0.002	0.001	39	89.1 (4.7)	0.006	0.014
Self-Efficacy								
Baseline	90	77.5 (2.1)			43	79.6 (2.5)		
3 months	90	83.0 (2.1)	0.003		41	85.7 (2.5)	0.009	
6 months	90	85.2 (2.2)	<0.001		41	87.1 (2.3)	0.004	
12 months	86	84.0 (2.1)	0.001	0.002	39	88.2 (2.6)	<0.001	0.005
Social Limitation								
Baseline	90	59.4 (2.8)			43	60.0 (4.3)		
3 months	90	71.4 (2.9)	<0.001		41	66.1 (4.7)	0.129	
6 months	90	72.7 (2.5)	<0.001		41	67.2 (4.5)	0.056	
12 months	86	69.5 (2.6)	0.001	<0.001	39	70.7 (4.6)	0.015	0.123

Values are mean ± SD  
FU = Follow-up.

Supplementary Table 2. Changes in EQ-5D-3L Questionnaire within the first year.

EQ-5D-3L		Mean	Std. Error	95% Confidence Interval		P-value Overall	P-value Baseline - FU
				Lower Bound	Upper Bound		
ASC group	Baseline	60.225	1.805	56.633	63.817	<0.001	
	3 months	63.950	1.833	60.301	67.599		0.080
	6 months	68.075	1.559	64.971	71.179		<0.001
	12 months	66.088	1.682	62.739	69.436		0.001
Placebo group	Baseline	63.694	3.067	57.468	69.921	0.093	
	3 months	69.444	2.935	63.485	75.404		0.028
	6 months	70.361	2.843	64.589	76.133		0.012
	12 months	67.583	3.660	60.153	75.014		0.219



## APPENDIX 1 - Inclusion- and exclusion criteria of the SCIENCE trial

No.	Inclusion criteria	Exclusion criteria
1.	30 to 80 years of age	Symptomatic heart failure (NYHA class I or IV)
2.	Signed informed consent	Acute coronary syndrome within 6 weeks of inclusion
3.	Chronic stable ischaemic heart disease	Other revascularization treatment within 4 months of treatment
4.	Symptomatic NYHA class II–III	Moderate to severe aortic stenosis (valve area $<1.3 \text{ cm}^2$ ) or valvular heart disease with option for surgery or interventional therapy
5.	LVEF $\leq 45\%$ on echocardiography	Aortic valve replacement with an artificial heart valve. However, a trans-septal treatment approach can be considered in these patients
6.	Plasma NT-proBNP $>300 \text{ pg/ml}$ ( $>35 \text{ pmol/L}$ )	If the patient is expected to be candidate for MitraClip therapy
7.	Maximal tolerated heart failure medication unchanged 2 months prior to inclusion	Diminished functional capacity for other reasons such as reduced lung function with FEV $<1 \text{ L/min}$ , moderate to severe claudication or morbid obesity
8.	No option for PCI or CABG	Clinically significant anaemia (Hb $<6 \text{ mmol/L}$ ), leukopenia (leucocytes $<2 \cdot 10^9/\text{L}$ ), leukocytosis (leucocytes $>14 \cdot 10^9/\text{L}$ ) or thrombocytopenia (thrombocytes $<50 \cdot 10^9/\text{L}$ )
9.	Patients who have had PCI or CABG within 6 months of inclusion must have a new coronary angiography to rule out early restenosis	Reduced kidney function (eGFR $<30 \text{ ml/min}$ )
10.	Patients cannot be included until 3 months after implantation of a CRT-D and until 1 month after an ICD unit	Left ventricular thrombus
11.		Anticoagulation treatment that cannot be paused during cell injections
12.		Patients with reduced immune response or known anti-HLA antibodies
13.		History with malignant disease within 5 years of inclusion or suspected malignancy – except treated skin cancer other than melanoma
14.		Pregnant women
15.		Other experimental treatment within 4 weeks of baseline tests
16.		Life expectancy $<1 \text{ year}$
17.		Participation in another intervention trial
18.		Known hypersensitivity to DMSO, penicillin and streptomycin

CABG, coronary artery bypass graft; CRT-D, cardiac resynchronization therapy-defibrillator; DMSO, dimethyl sulfoxide; eGFR, estimated glomerular filtration rate; FVC, forced vital capacity; Hb, haemoglobin; HLA, human leucocyte antigen; ICD, implantable cardioverter-defibrillator; LVEF, left ventricular ejection fraction; NT-proBNP, N-terminal pro-B-type natriuretic peptide; NYHA, New York Heart Association; PCI, percutaneous coronary intervention.

APPENDIX 2 – Release criteria for the clinical stem cell product CSCC\_ACC

Attribute	Acceptance criteria
No. of cells	100–120 × 10 <sup>6</sup> cells
CSCC_ASC viability	>80%
Donor serology	Negative for anti-HIV 1/2 (antibody + Ag) Negative for anti-HCV Negative for HBsAg Negative for anti-HBc Negative for syphilis Negative for HTLV I/II
Sterility	
Bacteria/fungi	Negative/negative
Endotoxin level	<70 EU/ml
Mycoplasma	Negative
Characterization	CD90 >80%
(Immunophenotype)	CD105 >80% CD73 >80% CD 45 <3% HLA-DR <5%

# CHAPTER



# General discussion

## GENERAL DISCUSSION

Advances in cardiovascular risk management and medical and catheter-based therapies have led to a decrease in disease-specific mortality of cardiovascular disease from 2007 to 2017 [1–4]. However, cardiovascular disease, with ischemic heart disease as its most prevalent entity, remains the leading cause of morbidity worldwide [1]. A main cause for this is that the human heart inherently lacks the capacity to regenerate itself; myocardium that is lost remains lost [5]. The quest for myocardial regeneration as of yet remains one of the holy grails in cardiovascular research. Furthermore, advances in diagnostics into myocardial scar after myocardial infarction are of great importance to identify patients who stand to benefit from aggressive therapeutic regimens.

This thesis is divided into two parts. In part one, we explored novel diagnostic strategies for detection of myocardial scar and myocardial fibrosis after acute myocardial infarction (AMI). We investigated the value of 2D-speckle tracking analysis derived global and regional myocardial deformation, and its novel applications of layer-specific strain analysis and myocardial work analysis, in the prediction for, and assessment of, myocardial scar size and transmuralty. This was done both in the days following myocardial infarction as well as in the setting of a chronic scar months after AMI. Furthermore, we assessed the behavior of circulating biomarkers of collagen synthesis and breakdown and their role in myocardial scar assessment. In part two, the current status of the use of deformation imaging, an investigation endpoint that is potentially superior over the widely used conventional imaging endpoint that is left ventricular ejection fraction, in cardiac regenerative therapy is assessed. Finally, we report on the rationale, study design, and results of the SCIENCE trial [6], a double-blind placebo-controlled randomized trial into the therapeutic efficacy of allogeneic adipose-tissue-derived mesenchymal stromal cells in patients with symptomatic ischemic heart failure.

### PART ONE – ADVANCED DIAGNOSTICS IN ISCHEMIC MYOCARDIAL DAMAGE

#### *Advanced imaging in the assessment of scar after AMI*

In chapter one, we present an investigation into the value for the prediction of scar size and scar transmuralty of early global and regional assessment of myocardial function after AMI. Scar size is an important prognostic factor regarding mortality, recurrent AMI, and congestive heart failure [7,8]. It is therefore of key importance to identify patients at risk for developing a large scar after myocardial infarction, in order to install aggressive antifibrotic medical therapy. Furthermore, early differentiation between viable and non-viable scar may prompt early aggressive revascularization. Although being the gold standard for scar assessment, late gadolinium-enhanced cardiac magnetic resonance imaging (LGE CMR) in the days after myocardial infarction [9] is seldom performed. This is mainly because of logistical challenges and the fact that myocardial edema and

inflammation result in delayed enhancement, mimicking scar. An easy and readily available alternative for scar assessment would aid clinical decision-making. We demonstrated that when transthoracic echocardiography (TTE) incorporating two-dimensional speckle tracking echocardiography (2D-STE), performed in the days following AMI, yields segmental longitudinal strain (SLS)  $> -13.3\%$ , the formation of scar in this area is likely. SLS of  $> -11.5\%$  predicts for transmural scar, implying that SLS between  $-11.5\%$  and  $-13.3\%$  predicts subendocardial scar. This confirms and adds to the existing and relatively limited body of evidence on this matter [10–13]. However, from our data, global longitudinal strain (GLS) does not significantly vary between patients with or without scar detectable from CMR and seems to not hold a relevant place in transmural detection. There is, however, a moderate correlation between GLS and scar size. Likewise, conventional parameters of global function such as the wall motion score index (WMSI) and left ventricular (LV) ejection fraction (LVEF) show a correlation with scar size. From our data, GLS performed in the days after AMI does not bear any advantages over conventional echocardiography in scar size prediction. This is not fully in line with existing literature, where GLS seems to outperform LVEF in the estimation of scar size after AMI [14–17]. We hypothesize that the relatively small infarct size as seen in the study cohort hampers a meaningful correlation between scar size and deformation parameters, and our results might underestimate the value of GLS when applied to patients with a larger myocardial infarction. Although interesting from a theoretical standpoint into the assessment of scar transmural, layer-specific myocardial strain analysis, at least when performed with the available General Electric (GE) software, does not appear to confer incremental value beyond full wall longitudinal strain. This is an important addition to the existing ambiguous literature on layer-specific strain analysis [18,19].

Although it provides a detailed insight into myocardial function, 2D-STE is influenced by loading conditions [20,21]. This consideration is particularly pertinent post myocardial infarction, which in itself will affect blood pressure and heart rate and prompts the initiation of medication that reduces afterload. Recently, myocardial work analysis has emerged as a 2D-STE derived imaging technique that overcomes this issue [22–25]. It incorporates the generation of a pressure-strain curve, the area of which resembles the area of invasively measured pressure-volume loops. In chapter two, we first studied the temporal changes of myocardial work parameters between the immediate post-infarction period and four to six months thereafter. Global work index, global work efficiency, and global constructive work significantly improved over time, whereas no significant changes were observed in global wasted work. These results are in concordance with the evolving body of evidence [26,27] and the determined range of normal values for work parameters, as reported in the NORRE study [28]. Second, we explored the value of these indices in both the direct post-infarct period and the setting of chronic myocardial scar. We found that In the immediate aftermath of AMI, myocardial work analysis exhibits the potential of reliably distinguishing non-scarred from transmurally scarred segments. However,

four to six months after AMI, work parameters did not correlate with scar transmuralty or scar size. Importantly, no apparent benefit over strain analysis was found. Although the value of myocardial work analysis has been studied in the setting of ischemic heart disease before [29–36], there is no prior investigation that correlates work parameters to scar as determined by CMR. The results of our small study should be seen as hypothesis-generating data that might initiate further research.

Although LVEF is by far the most commonly used parameter for myocardial function assessment in clinical practice. However, its sensitivity for early or regional myocardial dysfunction compared to GLS is worse [37], and it is hampered by significant intra-operator variability [38]. However, strain analysis also has its limitations. For example, it requires excellent image quality. Furthermore, there is significant variation in strain results between different vendors, hampering standardization [39,40]. Although offering the availability assessment of regional LV function, there is considerable inter-operator, intra-operator, inter-cycle, and test-retest variability in strain results [41]. Literature has shown that the reliability of regional strain in the setting of scar detection is variable [39], hampering its routine clinical application. Our results understate this finding. Future research should focus on specific subpopulations in which reliable scar assessment using strain analysis could be reliable and feasible. A promising future perspective lies within three-dimensional regional strain assessment, which overcomes the problem of segment alignment between TTE and CMR and the possible sampling error that is inherent with two-dimensional TTE. Finally, strain derived from feature-tracking CMR overcomes the limitation of image quality that frequently hampers TTE. However, similar to 2D-STE, this technique encounters inter-vendor variability, although inter- and intra-observer variability was excellent [42].

#### *The role of circulating biomarkers in myocardial fibrosis after AMI*

Whereas chapters two and three focus on the role of imaging in myocardial scarring, chapter four describes the role of circulating biomarkers of collagen homeostasis in the process of remodeling and scar formation after AMI. In current clinical practice, the use of creatine kinase and troponin is widespread. However, these biomarkers are reflective of myocardial cell loss, not necessarily of collagen deposition as seen in myocardial fibrosis and remodeling. In chapter 4, we study C-terminal propeptide of procollagen type I (PICP) which is a cleavage product of procollagen I and therefore a marker of collagen type I synthesis, and C-terminal telopeptide of type I collagen (ICTP) which serves as a marker of collagen type I degradation [43,44]. We found that collagen synthesis, as reflected by levels of circulating PICP, increases from baseline to approximately six weeks after AMI. Concentrations of circulating PICP six weeks after AMI correlate weakly to scar size. At follow-up approximately five months after AMI, levels of PICP decrease to levels similar to the level at baseline. In a similar fashion, collagen degradation, as reflected by circulating levels of ICTP, decreases from baseline to six weeks after AMI, but contrary to PICP,

concentrations remain decreased compared to baseline at approximately five months follow-up. Circulating ICTP concentrations at both six weeks and five months follow-up correlate weakly with scar size. PICP and ICTP have been studied before [45–50]. Similar to our results, there seems to be a trend towards increasing circulating PICP levels according to larger myocardial infarction. Moreover, both PICP and ICTP are independent predictors of mortality in patients with heart failure with reduced LVEF [51]. Although PICP and ICTP have been correlated to LV volume indices [52], we present a novel finding that PICP and ICTP correlate, although weakly, to the gold standard of myocardial fibrosis imaging which is late gadolinium-enhanced cardiac magnetic resonance imaging. Our results might trigger further investigation into PICP as a marker of collagen deposition, because of the correlation to scar size. However, the studied biomarkers of collagen homeostasis do not seem promising for application in the clinical setting. There are questions regarding the robustness and standardization of the measurements. Furthermore, robust biomarkers like creatine kinase (CK) and troponin are already available. An explanation for this limited applicability might be sought in that fibrosis turnover is a process that is not limited to the heart but occurs through the whole body. Therefore, results might be influenced by processes that take place outside of the heart, whereas the release of these biomarkers from the heart may have limited influence on systemic concentrations. Although our study sought to exclude patients in whom confounding might be expected, this feature further limits the clinical application of these biomarkers.

### *Future perspectives*

The LVEF is one of the ‘sacred cows’ of cardiology. Although myocardial strain analysis is a novel means of myocardial function assessment that seems to be more reproducible and reliable than LVEF assessment has been available for some time now, the mainstream use of this technique has not yet caught on. This is a pity because both the clinician and the patient will benefit from improvements in diagnostic capabilities. By expanding the body of evidence on its potential use in various clinical settings this paradigm might shift. This indeed was the aim of our contributions to the value of strain analysis, as well as work analysis and novel biomarkers, in the assessment of myocardial scar size and scar transmural. However, our data is to be seen as hypothesis-generating, and our results should be validated in future, larger studies. Furthermore, our results can be used to guide therapy, and it would be very interesting to compare the administration of antifibrotic medication or the need for additional revascularization as guided by strain results or circulating biomarker concentrations to conventional treatment standards. Ultimately, it would be interesting to investigate whether the prognosis of patients suffering from AMI regarding survival or major adverse cardiac events would actually improve when adapting strain-guided therapy compared to conventional therapy.



## PART TWO – APPLICATION OF ADVANCED IMAGING IN NOVEL THERAPEUTIC STRATEGIES FOR ISCHEMIC HEART FAILURE

### *Deformation imaging in cell-based cardiac regenerative research*

Since the clinical cardiac regenerative field of research emerged, surrogate endpoints for determining the efficacy of the cell product have been used. The main reason for this is the subtle effect of cell-based therapies requires large patient cohorts to investigate their efficacy concerning end-points in clinical parameters, such as mortality and rehospitalization. Indeed, praiseworthy efforts were made by the BAM1-trial investigators to elucidate the effect of bone marrow-derived mononuclear cells on all-cause mortality, but the immense lack of included patients is exemplary of the non-feasibility to use such endpoints in clinical cell-based therapy research [53]. Imaging endpoints are among the most common of these surrogates. This mainly involves conventional echocardiography by which LV dimensions, LVEF, or the WMSI are determined. These parameters indeed prove to be powerful predictors of clinical outcomes [54–56]. However, these parameters are hampered by significant error and inter- and intra-operator variability [38,57,58]. As LVEF is concerned, when one considers the inter-operator variability of up to 10% for two-dimensional biplane measurements, the subtle effect sorted by cell-based therapies on global LV function of approximately 2.9% (despite statistical significance) triggers skepticism towards the clinical significance and relevance of these results. Therefore, these parameters of global LV function are not suitable for detecting the subtle and regional effects that are sorted by cell-based therapies [59]. Deformation imaging is a technique that provides a much more detailed insight into cardiac function, especially on a regional level, deeming it an interesting alternative to conventional echocardiography in evaluating the efficacy of cell-based regenerative therapy [60]. Indeed, GLS correlates well with LVEF, and similar to LVEF, has risk stratification potential [61–64].

In chapter 5, a systematic review of the use of deformation imaging in the cardiac regenerative field is presented. A total of 15 preclinical [65–79] and 15 clinical [80–94] papers were found, inherently with very heterogeneous study characteristics. Of the preclinical studies, 12 out of 15 found cell-based regenerative therapy to sort a statistically significant effect on both LVEF and deformation parameters; two papers found deformation parameters but not LVEF to be statistically significantly different in the subjects treated with cell-based therapy, and one study was negative for both deformation and LVEF. Of the 15 clinical studies, only four papers showed a statistically significant effect of cell-based therapy on both strain outcomes and LVEF. A further four studies were negative for both deformation endpoints and LVEF. Finally, six studies reported significant benefits regarding deformation parameters but no significantly different LVEF, whereas one study reported deterioration in global and regional circumferential strain, but not LVEF. The results underscore the hypothesis that deformation imaging is a more suitable endpoint for clinical regenerative therapy investigations. Future studies planning to use imaging

endpoints in the cardiac regenerative field should therefore employ deformation imaging endpoints as well as conventional echocardiography. Besides this hypothesis-generating result, this systematic review displays one of the main problems of cardiac regenerative research, which is the failure of translation from pre-clinical to clinical research [95]. Currently, efforts are made to attend to this, for example by pre-registration of preclinical trials [96].

#### *The effect of allogeneic adipose tissue-derived mesenchymal stromal cells*

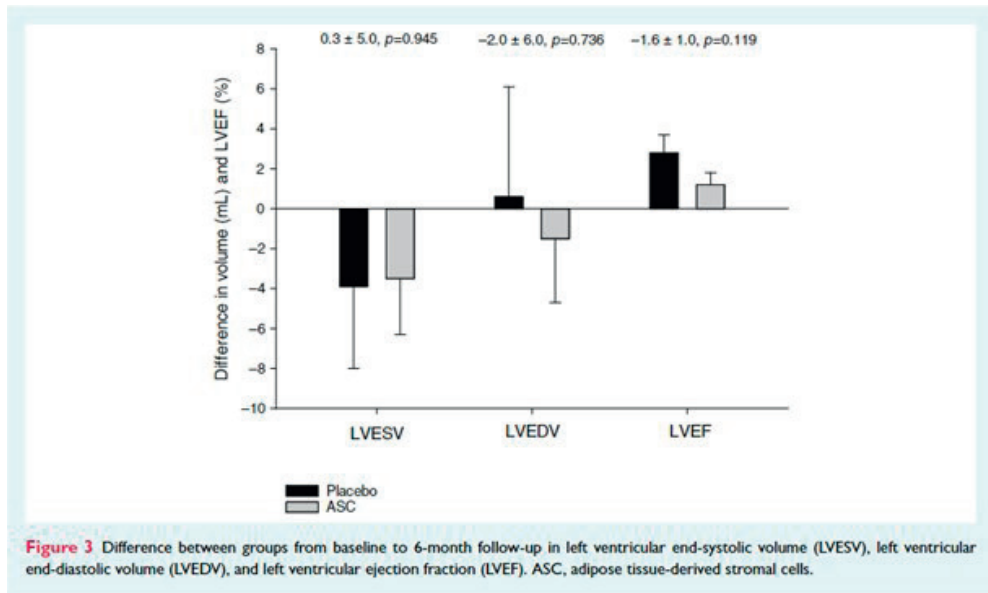
In chapters six and seven, the rationale, study design, and results of the Cell therapy in IschEmic Non-treatable Cardiac disease (SCIENCE) trial are Stem elaborated upon. In this double-blind placebo-controlled randomized trial, the safety and efficacy of CSCC\_ASC were studied. This is an allogeneic, adipose-tissue-derived mesenchymal stromal cell product derived from healthy donors that was developed in the Rigshospitalet, Copenhagen, Denmark. In recent years, the focus of regenerative therapy research has switched from hematopoietic stem cells to mesenchymal stem cells for their presumed superior effect [97,98]. The advantage of utilizing allogeneic cells is that there is a presumed increased immunomodulatory effect, as well as improved availability, less logistical challenges, and dosage standardization. Prior to the SCIENCE trial, the MSC-HF trial that studied bone-marrow-derived mesenchymal stem cells showed promising results. CSCC\_ASC was proven safe, and the feasibility of the treatment concept was proven [99]. A total of 133 patients with symptomatic ischemic heart failure were randomized in a 2:1 fashion to receive either intra-myocardial injection of CSCC\_ASC using the NogaXP guided injection system [100], or saline placebo.

In chapter 6, we elaborate on the study protocol. This was published [101] ahead of the completion of the trial to provide insight into the study rationale, improve study quality, and strive for uniformity in study design and data reporting within the field. In Utrecht, a central imaging core lab was set up to analyze the performed images TTE, computed tomography (CT), and CMR images. The primary imaging endpoint for the SCIENCE study is the change in 2D TTE derived, biplane measured LV end-systolic volume (LVESV) at 6 months after the administration of study product. LVESV is a good predictor of mortality and heart failure hospitalization, with a reported hazard ratio of 4.4 for a combined endpoint of these two outcomes in patients with stable coronary artery disease and an indexed LVESV of  $> 50 \text{ ml/m}^2$  [102]. Moreover, LVESV indexed to body surface area (BSA) was independently associated with mortality in patients with ischemic heart failure ( $p = 0.0017$ ) [103]. It has previously been successfully applied in the MSC-HF trial [104]. Secondary endpoints were changes in biplane LVEF and end-diastolic volume, as well as the non-imaging endpoints NYHA-class, 6-minute walk test, and serum n-terminal propeptide of brain natriuretic peptide (NT-proBNP) levels. Although volume data from 3D TTE, CT, and CMR were acquired, these images could not be acquired for all patients. The same limitation holds true for deformation imaging due to images being collected

from different vendors and insufficient image quality for reliable 2D-STE analysis. To avoid error by pooling data from different modalities [105,106] and to avoid losing the equal distribution between intervention- and control groups, only 2D TTE-derived volumetric measures were used in the results. However, data allows for the analysis of more imaging endpoints such as CT- and CMR-derived volumetric measures, 3D LVEF, diastolic function [94], and deformation parameters [107]. Moreover, the electromechanical map from the NogaXP injection system provides information on scar transmural and can determine regional viability in the infarct border zone [108–110], which can be correlated to, for example, deformation parameters. Due to the lack of time to finalize measurement and analysis for the main paper of the SCIENCE trial, the value of these imaging end-points will be the subject of a future sub-study.

Data transfer is a specific challenge in international multicenter trials in the era of the European Union's General Data Protection Regulation (GDPR) [111]. Specific software is required to extensively anonymize or pseudonymize the shared images, since simple anonymization within image analysis software does not anonymize hidden DICOM headers or metadata incorporated within the files, we used the Radiological Society of North America (RSNA) Clinical Trial Processor (CTP) software. Images were subsequently stored in the National Biomedical Imaging Archive (NBIA), a repository developed by the National Cancer Institute (NCI). The limitation of this extensive anonymization process is that certain software, for example, GE EchoPAC, will not allow for analysis of the anonymized image. To optimize data quality, images were analyzed in a standardized manner, adhering to available guidelines [112,113], by a single researcher who was supervised by an imaging cardiologist. Inter-operator variability of the primary endpoint was assessed through analysis by a single researcher in one of the other participating centers, and in case of significant discrepancy, data analysis by a third reviewer was performed and mean values between these measurements were used for further analysis. In chapter 7, the results from the SCIENCE trial are shown. There were no significant differences in response between the treatment arm and the placebo arm in any of the studied endpoints, apart from circulating NT-proBNP levels being lower in the treatment arm at 12 months follow-up compared to the placebo arm. Across the whole study population, LVESV showed no statistically significant difference between baseline and follow. Interestingly, LVEF significantly improved from baseline to follow-up in both the treatment arm ( $+1.2 \pm 0.6\%$ ,  $p = 0.044$ ) and the placebo arm ( $+2.8 \pm 0.9\%$ ,  $p = 0.003$ ) (figure 1).

**Figure 1 – Graphical representation of primary and secondary imaging endpoints in the SCIENCE trial**



These results are surprising since similar research conducted with autologous bone-marrow-derived cell products did show a benefit of the cell product compared to placebo [114], and the CSCC\_ASC was hypothesized to sort a similar or more profound effect based on in-vitro comparison between autologous and allogeneic MSCs. However, the results are in line with a recently published parallel national Danish phase II study with the same product [115]. This leads to the conclusion that the CSCC\_ASC is less potent in stimulating the paracrine effects that are thought to be the main mode of action of cell-based cardiac regenerative therapy. However, as stated before in this thesis, the selected primary and secondary imaging end points may not be suitable for reliably detecting the very subtle changes in myocardial function sorted by cell-based therapies. Moreover, in the era of widespread implantable cardioverter defibrillator use in patients with ischemic cardiomyopathy, CMR is equally not suitable for endpoint measurement, and the use of CCT could raise ethical questions concerning radiation exposure. Nonetheless, the neutral result of the SCIENCE trial combined with the generally small effect – if any – of cell-based therapeutic agents that has been observed over the past years, makes one question whether clinically relevant results will ever be achieved by optimizing the currently applied treatment strategies.

#### *Controversy and future perspectives in the field of cardiac regenerative therapy*

Because differentiation into cardiomyocytes could never be reproducibly established in vivo [116], the field of cardiac regeneration has remained controversial. Initially, this did

not lead to less research, since the consensual hypothesis of cellular transdifferentiation was abandoned for the aforementioned hypothesis of paracrine and endocrine effects. However, from 2015 onwards, progress in the field was slow [117,118]. The DAMASCENE trial shook the field in 2014, showing that factual and methodological discrepancies were abundant in cardiac regenerative therapy trials. Furthermore, they cynically reported that the papers that contained the most inconsistencies were in fact the papers that reported the largest effect of the studied cell-based therapeutic agent [119]. However, the big shock was yet to come. In 2018, the field was startled by several cases of scientific misconduct [120]. This led to many early papers from 2001 onward from the research group of Anversa et al. being retracted. It is disheartening to realize what scientific effort, financial investment, and above all sacrifice by study participants has been lost due to a conceptually flawed and, in retrospect, presumably unjustly hyped scientific concept. The problem reflects the vulnerability of medical research in general to the perverse incentives of both investigators and scientific journals. Since the retractions, which were also reported upon in mainstream media [121], skepticism towards cardiac regenerative therapy is common. New clinical trials into the effects of cell-based therapeutic agents seem to have become extinct.

However, contemporary science still does not allow for the cure of ischemic heart failure, understating the importance of the continuance of this quest. Perhaps, now is the time to abandon the endeavors towards optimizing cell-based therapies that allegedly have a paracrine mechanism of action, and instead focus on true myocardial regeneration. This should be considered as the replacement of scar tissue by cardiomyocytes that are electromechanically coupled to the rest of the heart. Promising preclinical research has been conducted on cells derived from the human pluripotent stem cell, tissue-engineered heart patches, and therapeutic agents such as miRNAs that sort a regenerative paracrine effect, but as of yet, the cure for ischemic heart failure does not lurk over the horizon [122].

### FINAL REMARKS

With part I of this thesis, we aim to improve diagnostic strategies for scar characteristics and myocardial fibrosis assessment in patients after AMI, hopefully resulting in altered therapeutic strategies that ultimately reduce the, as of yet still significant, burden of ischemic heart disease. 2D-STE derived strain measurement holds potential for improved diagnostic capabilities for scar formation in patients after AMI. It seems to be a more precise and reliable parameter than LVEF, and as such, it should become part of a routine TTE examination, especially in patients after AMI. Although circulating biomarkers of collagen homeostasis are reflective of myocardial fibrosis after AMI, the clinical value seems to be limited, and the application of these biomarkers probably will not find a foothold in clinical practice. From part II of this thesis, we conclude that advanced imaging is a promising technique that is more sensitive in detecting the subtle and regional effects of cell-based cardiac regenerative therapy. We plea for incorporating strain analysis into the study

protocol, should future cell-based therapies be initiated, to improve our understanding of the effects of these therapies on myocardial function. However, the neutral results of the SCIENCE trial are in line with the existing and growing body of evidence that shows that there is no clinical benefit of cell-based therapeutics in ischemic heart failure. In the quest of curing the failing ischemic heart, the field of cardiac regenerative research should focus its efforts towards true myocardial regeneration, that is the replacement of scar by functional cardiomyocytes that are electromechanically coupled to the rest of the heart alternative methods of curing the failing ischemic heart.

## REFERENCES

- [1] GBD 2017 Causes of Death Collaborators. Global, regional, and national age-sex-specific mortality for 282 causes of death in 195 countries and territories, 1980-2017: a systematic analysis for the Global Burden of Disease Study 2017. *Lancet* 2018;392:1736-88. Doi:10.1016/S0140-6736(18)32203-7
- [2] McDonagh TA, Metra M, Adamo M, et al. 2021 ESC Guidelines for the diagnosis and treatment of acute and chronic heart failure. *Eur Heart J* 2021;42:3599–726. Doi:10.1093/eurheartj/ehab368.
- [3] Visseren F, Mach F, Smulders YM, et al. 2021 ESC Guidelines on cardiovascular disease prevention in clinical practice. *Eur Heart J* 2021;42:3227–337. Doi:10.1093/eurheartj/ehab484.
- [4] Byrne RA, Rossello X, Coughlan JJ, et al. 2023 ESC Guidelines for the management of acute coronary syndromes. *Eur Heart J* 2023;44:3720–826. Doi:10.1093/eurheartj/ehad191.
- [5] Uygur A, Lee RT. Mechanisms of Cardiac Regeneration. *Dev Cell* 2016;36:362–74. Doi:10.1016/j.devcel.2016.01.018.
- [6] Qayyum AA, van Klarenbosch B, Frljak S, et al. Effect of allogeneic adipose tissue-derived mesenchymal stromal cell treatment in chronic ischaemic heart failure with reduced ejection fraction – the SCIENCE trial. *Eur J Heart Fail* 2023;25:576–87. Doi:10.1002/ehjhf.2772.
- [7] Hadamitzky M, Langhans B, Hausleiter J, et al. Prognostic value of late gadolinium enhancement in cardiovascular magnetic resonance imaging after acute ST-elevation myocardial infarction in comparison with single-photon emission tomography using Tc99m-Sestamibi. *Eur Heart J Cardiovasc Imaging* 2014;15:216–25. Doi:10.1093/ehjci/jet176.
- [8] Greenwood JP, Herzog BA, Brown JM, et al. Prognostic value of cardiovascular magnetic resonance and single-photon emission computed tomography in suspected coronary heart disease: Long-term follow-up of a prospective, diagnostic accuracy cohort study. *Ann Intern Med* 2016;165:1–9. Doi:10.7326/M15-1801.
- [9] Patel MR, White RD, Abbara S, et al. 2013 ACCF/ACR/ASE/ASNC/SCCT/SCMR Appropriate Utilization of Cardiovascular Imaging in Heart failure: A joint report of the American college of Radiology appropriateness criteria committee and the American college of cardiology foundation appropriate use criteria task force. *J Am Coll Cardiol* 2013;61:2207–31. Doi:10.1016/j.jacc.2013.02.005.
- [10] Rost C, Rost MC, Breithardt OA, et al. Relation of functional echocardiographic parameters to infarct scar transmural by magnetic resonance imaging. *J Am Soc Echocardiogr* 2014;27:767–74. Doi:10.1016/j.echo.2014.02.004.
- [11] Cimino S, Canali E, Petronilli V, et al. Global and regional longitudinal strain assessed by two-dimensional speckle tracking echocardiography identifies early myocardial dysfunction and transmural extent of myocardial scar in patients with acute ST elevation myocardial infarction and relatively. *Eur Heart J Cardiovasc Imaging* 2013;14:805–11. Doi:10.1007/978-3-642-45068-6\_34.

- [12] Ben Driss A, Lepage C, Sfaki A, et al. Strain predicts left ventricular functional recovery after acute myocardial infarction with systolic dysfunction. *Int J Cardiol* 2020;307:1–7. Doi:10.1016/j.ijcard.2020.02.039.
- [13] Sjøli B, Ørn S, Grenne B, et al. Diagnostic Capability and Reproducibility of Strain by Doppler and by Speckle Tracking in Patients With Acute Myocardial Infarction. *JACC Cardiovasc Imaging* 2009;2:24–33. Doi:10.1016/j.jcmg.2008.10.007.
- [14] Sjøli B, Ørn S, Grenne B, et al. Comparison of Left Ventricular Ejection Fraction and Left Ventricular Global Strain as Determinants of Infarct Size in Patients with Acute Myocardial Infarction. *J Am Soc Echocardiogr* 2009;22:1232–8. Doi:10.1016/j.echo.2009.07.027.
- [15] Huttin O, Marie PY, Benichou M, et al. Temporal deformation pattern in acute and late phases of ST-elevation myocardial infarction: incremental value of longitudinal post-systolic strain to assess myocardial viability. *Clin Res Cardiol* 2016;105:815–26. Doi:10.1007/s00392-016-0989-6.
- [16] Bendary A, Afifi M, Tawfik W, et al. The predictive value of global longitudinal strain on late infarct size in patients with anterior ST-segment elevation myocardial infarction treated with a primary percutaneous coronary intervention. *Int J Cardiovasc Imaging* 2019;35:339–46. Doi:10.1007/s10554-018-1498-7.
- [17] Grabka M, Wita K, Tabor Z, et al. Prediction of infarct size by speckle tracking echocardiography in patients with anterior myocardial infarction. *Coron Artery Dis* 2013;24:127–34. Doi:10.1097/MCA.0b013e32835b6798.
- [18] Becker M, Hoffmann R, Kühl HP, et al. Analysis of myocardial deformation based on ultrasonic pixel tracking to determine transmural extent in chronic myocardial infarction. *Eur Heart J* 2006;27:2560–6. Doi:10.1093/eurheartj/ehl288.
- [19] Ünlü S, Mirea O, Pagourelas ED, et al. Layer-Specific Segmental Longitudinal Strain Measurements: Capability of Detecting Myocardial Scar and Differences in Feasibility, Accuracy, and Reproducibility, Among Four Vendors A Report From the EACVI-ASE Strain Standardization Task Force. *J Am Soc Echocardiogr* 2019;32:624–632.e11. Doi:10.1016/j.echo.2019.01.010.
- [20] Murai D, Yamada S, Hayashi T, et al. Relationships of left ventricular strain and strain rate to wall stress and their afterload dependency. *Heart Vessels* 2017;32:574–83. Doi:10.1007/s00380-016-0900-4.
- [21] Donal E, Bergerot C, Thibault H, et al. Influence of afterload on left ventricular radial and longitudinal systolic functions: A two-dimensional strain imaging study. *Eur J Echocardiogr* 2009;10:914–21. Doi:10.1093/ejechocard/jep095.
- [22] Russell K, Eriksen M, Aaberge L, et al. Assessment of wasted myocardial work: A novel method to quantify energy loss due to uncoordinated left ventricular contractions. *Am J Physiol Heart Circ Physiol* 2013;305:996–1003. Doi:10.1152/ajpheart.00191.2013.
- [23] Russell K, Eriksen M, Aaberge L, et al. A novel clinical method for quantification of regional left ventricular pressure-strain loop area: A non-invasive index of myocardial work. *Eur Heart J* 2012;33:724–33. Doi:10.1093/eurheartj/ehs016.



- [24] Hubert A, Le Rolle V, Leclercq C, et al. Estimation of myocardial work from pressure–strain loops analysis: an experimental evaluation. *Eur Heart J Cardiovasc Imaging* 2018;19:1372–9. Doi:10.1093/ehjci/jeu024.
- [25] Boe E, Skulstad H, Smiseth OA. Myocardial work by echocardiography: A novel method ready for clinical testing. *Eur Heart J Cardiovasc Imaging* 2019;20:18–20. Doi:10.1093/ehjci/jeu156.
- [26] Ren F, Xue T, Tang G, et al. Assessment of Myocardial Work of the Left Ventricle before and after PCI in Patients with Non-ST-Segment Elevation Acute Coronary Syndrome by Pressure-Strain Loop Technology. *Comput Math Methods Med* 2022;80:26689 Doi:10.1155/2022/8026689.
- [27] Lustosa RP, Fortuni F, van der Bijl P, et al. Changes in Global Left Ventricular Myocardial Work Indices and Stunning Detection 3 Months After ST-Segment Elevation Myocardial Infarction. *AM J Cardiol* 2021;157:15–21. Doi:10.1016/j.amjcard.2021.07.012.
- [28] Manganaro R, Marchetta S, Dulgheru R, et al. Correlation between non-invasive myocardial work indices and main parameters of systolic and diastolic function: results from the EACVI NORRE study. *Eur Heart J Cardiovasc Imaging* 2020;21:533–41. Doi:10.1093/ehjci/jez203.
- [29] Arnautu DA, Gheorghiu A, Arnautu SF, et al. Subtle Changes in Myocardial Work Indices Assessed by 2D-Speckle Tracking Echocardiography Are Linked with Pathological LV Remodeling and MACEs Following an Acute Myocardial Infarction Treated by Primary Percutaneous Coronary Intervention. *Diagnostics* 2023;13:3108. Doi:10.3390/diagnostics13193108.
- [30] Guo Y, Xia Z, Li Q, et al. Motion and removal behavior of inclusions in electrode tip during magnetically controlled electrosag remelting: X-ray microtomography characterization and modeling verification. *J Mater Sci Technol* 2022;96:1–10. Doi:10.1016/j.jmst.2021.05.003.
- [31] Sabatino J, De Rosa S, Leo I, et al. Non-invasive myocardial work is reduced during transient acute coronary occlusion. *PLoS One* 2020;15:e0244397 Doi:10.1371/journal.pone.0244397
- [32] Sabatino J, De Rosa S, Leo I, et al. Prediction of Significant Coronary Artery Disease Through Advanced Echocardiography: Role of Non-invasive Myocardial Work. *Front Cardiovasc Med* 2021;8:719603. Doi:10.3389/fcvm.2021.719603.
- [33] Lustosa RP, Fortuni F, Van Der Bijl P, et al. Left ventricular myocardial work in the culprit vessel territory and impact on left ventricular remodelling in patients with ST-segment elevation myocardial infarction after primary percutaneous coronary intervention. *Eur Heart J Cardiovasc Imaging* 2021;22:339–47. Doi:10.1093/ehjci/jeaa175.
- [34] Boe E, Russell K, Eek C, et al. Non-invasive myocardial work index identifies acute coronary occlusion in patients with non-ST segment elevation-acute coronary syndrome. *Eur Heart J Cardiovasc Imaging* 2015;16:1247–55. Doi:10.1093/ehjci/jev078.
- [35] Qin YY, Wu XP, Wang JT, et al. Value of territorial work efficiency estimation in non-ST-segment-elevation acute coronary syndrome: a study with non-invasive left ventricular pressure–strain loops. *Int J Cardiovasc Imaging* 2020. Doi:10.1007/s10554-020-02110-1.
- [36] Sun S, Chen N, Sun Q, et al. Association Between Segmental Noninvasive Myocardial Work and Microvascular Perfusion in ST-Segment Elevation Myocardial Infarction: Implications for Left Ventricular Functional Recovery and Clinical Outcomes. *J Am Soc Echocardiogr* 2023. Doi:10.1016/j.echo.2023.04.017.

- [37] Smiseth OA, Torp H, Opdahl A, et al. Myocardial strain imaging: How useful is it in clinical decision making? *Eur Heart J* 2016;37:1196–1207b. Doi:10.1093/eurheartj/ehv529.
- [38] Wood PW, Choy JB, Nanda NC, Becher H. Left ventricular ejection fraction and volumes: It depends on the imaging method. *Echocardiography* 2014;31:87–100. Doi:10.1111/echo.12331.
- [39] Mirea O, Pagourelas ED, Duchenne J, et al. Intervendor Differences in the Accuracy of Detecting Regional Functional Abnormalities A Report From the EACVI-ASE Strain Standardization Task Force. *JACC Cardiovasc Imaging* 2018;11:25–34. Doi: 10.1016/j.jcmg.2017.02.014
- [40] Van Everdingen WM, Paiman ML, Van Deursen CJM, et al. Comparison of septal strain patterns in dyssynchronous heart failure between speckle tracking echocardiography vendor systems. *J Electrocardiol* 2015;48:609–16. Doi:10.1016/j.jelectrocard.2014.12.021.
- [41] Barbier P, Mirea O, Cefalù C, et al. Reliability and feasibility of longitudinal AFI global and segmental strain compared with 2D left ventricular volumes and ejection fraction: Intra- and inter-operator, test-retest, and inter-cycle reproducibility. *Eur Heart J Cardiovasc Imaging* 2015;16:642–52. Doi:10.1093/ehjci/jeu274.
- [42] Barreiro-Pérez M, Curione D, Symons R, et al. Left ventricular global myocardial strain assessment comparing the reproducibility of four commercially available CMR-feature tracking algorithms. *Eur Radiol* 2018;28:5137–47. Doi:10.1007/s00330-018-5538-4.
- [43] Eghbali M, Weber KT. Collagen and the myocardium: fibrillar structure, biosynthesis and degradation in relation to hypertrophy and its regression. *Mol Cell Biochem* 1990;96:1–14. Doi:10.1007/BF00228448
- [44] De Jong S, Van Veen TAB, Van Rijen HVM, De Bakker JM. Fibrosis and Cardiac Arrhythmias. *J Cardiovasc Pharmacol* 2011;57:630–8. Doi:10.1097/FJC.0b013e318207a35f
- [45] McGavigan AD, Maxwell PR, Dunn FG. Serological evidence of altered collagen homeostasis reflects early ventricular remodeling following acute myocardial infarction. *Int J Cardiol* 2006;111:267–74. Doi:10.1016/j.ijcard.2005.08.045.
- [46] Cerisano G, Pucci PD, Sulla A, et al. Relation Between Plasma Brain Natriuretic Peptide, Serum Indexes of Collagen Type I Turnover, and Left Ventricular Remodeling After Reperfused Acute Myocardial Infarction. *Am J Cardiol* 2007;99:651–6. Doi:10.1016/j.amjcard.2006.09.114.
- [47] Ren HZ, Zhang XS, Wang LX. Effect of coronary revascularization on serum collagen biomarkers and left ventricular remodeling in patients with acute myocardial infarction. *Heart Lung* 2012;41:344–9. Doi:10.1016/j.hrtlng.2011.09.013.
- [48] Radovan J, Vaclav P, Petr W, et al. Changes of collagen metabolism predict the left ventricular remodeling after myocardial infarction. *Mol Cell Biochem* 2006;293:71–8. Doi:10.1007/s11010-006-2955-5.
- [49] Poulsen SH, Høst NB, Egstrup K, et al. Coronary Care Long-Term Changes in Collagen Formation Expressed by Serum Carboxyterminal Propeptide of Type-I Procollagen and Relation to Left Ventricular Function after Acute Myocardial Infarction. *Cardiology* 2001;96:45–50. Doi:10.1159/000047385

- [50] Manhenke C, Ørn S, Squire I, et al. The prognostic value of circulating markers of collagen turnover after acute myocardial infarction. *Int J Cardiol* 2011;150:277–82. Doi:10.1016/j.ijcard.2010.04.034.
- [51] Löfsjögård J, Kahan T, Díez J, et al. Usefulness of Collagen Carboxy-Terminal Propeptide and Telo peptide to Predict Disturbances of Long-Term Mortality in Patients ≥60 Years With Heart Failure and Reduced Ejection Fraction. *Am J Cardiol* 2017;119:2042–8. Doi:10.1016/j.amjcard.2017.03.036.
- [52] Murakami T, Kusachi S, Murakami M, et al. Time-dependent changes of serum carboxy-terminal peptide of type I procollagen and carboxy-terminal telo peptide of type I collagen concentrations in patients with acute myocardial infarction after successful reperfusion: correlation with left ventricular volume indices Enzymes and Protein Markers. *Clin Chem* 1998;44:2453–61. Doi not available.
- [53] Mathur A, Fernández-Avilés F, Bartunek H, et al. The effect of intracoronary infusion of bone marrow-derived mononuclear cells on all-cause mortality in acute myocardial infarction: the BAM1 trial. *Eur Heart J* 2020;41:3702–10. Doi:10.1093/eurheartj/ehaa802.
- [54] Møller JE, Hillis GS, Oh JK, et al. Wall motion score index and ejection fraction for risk stratification after acute myocardial infarction. *Am Heart J* 2006;151:419–25. Doi:10.1016/j.ahj.2005.03.042.
- [55] Pocock SJ, Wang D, Pfeffer MA, et al. Predictors of mortality and morbidity in patients with chronic heart failure. *Eur Heart J* 2006;27:65–75. Doi:10.1093/eurheartj/ehi555.
- [56] Solomon SD, Anavekar N, Skali H, et al. Influence of ejection fraction on cardiovascular outcomes in a broad spectrum of heart failure patients. *Circulation* 2005;112:3738–44. Doi:10.1161/CIRCULATIONAHA.105.561423.
- [57] Dorosz JL, Lezotte DC, Weitzenkamp DA, et al. Performance of 3-dimensional echocardiography in measuring left ventricular volumes and ejection fraction: A systematic review and meta-analysis. *J Am Coll Cardiol* 2012;59:1799–808. Doi:10.1016/j.jacc.2012.01.037.
- [58] O'Dell WG. Accuracy of Left Ventricular Cavity Volume and Ejection Fraction for Conventional Estimation Methods and 3D Surface Fitting. *J Am Heart Assoc* 2019;8:e009124. Doi:10.1161/JAHA.118.009124.
- [59] Afzal MR, Samanta A, Shah ZI, et al. Adult Bone Marrow Cell Therapy for Ischemic Heart Disease: Novelty and Significance. *Circ Res* 2015;117:558–75. Doi:10.1161/CIRCRESAHA.114.304792.
- [60] Van Slochteren FJ, Teske AJ, Van Der Spoel TIG, et al. Advanced measurement techniques of regional myocardial function to assess the effects of cardiac regenerative therapy in different models of ischaemic cardiomyopathy. *Eur Heart J Cardiovasc Imaging* 2012;13:808–18. Doi:10.1093/ehjci/jes119.
- [61] Lima MSM, Villarraga HR, Abduch MCD, et al. Global Longitudinal Strain or Left Ventricular Twist and Torsion? Which Correlates Best with Ejection Fraction? *Arq Bras Cardiol* 2017;23–9. Doi:10.5935/abc.20170085.
- [62] Potter E, Marwick TH. Assessment of Left Ventricular Function by Echocardiography: The Case for Routinely Adding Global Longitudinal Strain to Ejection Fraction. *JACC Cardiovasc Imaging* 2018;11:260–74. Doi:10.1016/j.jcmg.2017.11.017.

- [63] Cho GY, Marwick TH, Kim HS, et al. Global 2-Dimensional Strain as a New Prognosticator in Patients With Heart Failure. *J Am Coll Cardiol* 2009;54:618–24. Doi:10.1016/j.jacc.2009.04.061.
- [64] Stanton T, Leano R, Marwick TH. Prediction of all-cause mortality from global longitudinal speckle strain: Comparison with ejection fraction and wall motion scoring. *Circ Cardiovasc Imaging* 2009;2:356–64. Doi:10.1161/CIRCIMAGING.109.862334.
- [65] Sun QW, Zhen L, Wang Q, et al. Assessment of Retrograde Coronary Venous Infusion of Mesenchymal Stem Cells Combined with Basic Fibroblast Growth Factor in Canine Myocardial Infarction Using Strain Values Derived from Speckle-Tracking Echocardiography. *Ultrasound Med Biol* 2016;42:272–81. Doi:10.1016/j.ultrasmedbio.2015.09.010.
- [66] Miao Q, Shim W, Tee N, et al. iPSC-derived human mesenchymal stem cells improve myocardial strain of infarcted myocardium. *J Cell Mol Med* 2014;18:1644–54. Doi:10.1111/jcmm.12351.
- [67] Rickers C, Gallegos R, Seethamraju RT, et al. Catheter Interventions in Congenital Heart Disease—Part I Applications of Magnetic Resonance Imaging for Cardiac Stem Cell Therapy. *J Interv Cardiol* 2004;17:37–46. Doi:10.1111/j.1540-8183.2004.01712.x
- [68] Amado LC, Schuleri KH, Saliaris AP, et al. Multimodality Noninvasive Imaging Demonstrates In Vivo Cardiac Regeneration After Mesenchymal Stem Cell Therapy. *J Am Coll Cardiol* 2006;48:2116–24. Doi:10.1016/j.jacc.2006.06.073.
- [69] Bonios M, Chang CY, Pinheiro A, et al. Cardiac resynchronization by cardiosphere-derived stem cell transplantation in an experimental model of myocardial infarction. *J Am Soc Echocardiogr* 2011;24:808–14. Doi:10.1016/j.echo.2011.03.003.
- [70] Cai C, Guo Y, Teng L, et al. Preconditioning Human Cardiac Stem Cells with an HO-1 Inducer Exerts Beneficial Effects after Cell Transplantation in the Infarcted Murine Heart. *Stem Cells* 2015;33:3596–607. Doi:10.1002/stem.2198.
- [71] Chen Y, Ye L, Zhong J, et al. The Structural Basis of Functional Improvement in Response to Human Umbilical Cord Blood Stem Cell Transplantation in Hearts with Post-Infarct LV Remodelin. *Cell Transplant* 2015;24:971–83. Doi:10.3727/096368913X675746.
- [72] Duran JM, Makarewich CA, Sharp TE, et al. Bone-Derived stem cells repair the heart after myocardial infarction through transdifferentiation and paracrine signaling mechanisms. *Circ Res* 2013;113:539–52. Doi:10.1161/CIRCRESAHA.113.301202.
- [73] Jaussaud J, Biais M, Calderon J, et al. Hypoxia-preconditioned mesenchymal stromal cells improve cardiac function in a swine model of chronic myocardial ischaemia. *Eur J Cardiothorac Surg* 2013;43:1050–7. Doi:10.1093/ejcts/ezs549.
- [74] Karantalis V, Suncion-Loescher VY, Bagno L, et al. Synergistic effects of combined cell therapy for chronic ischemic cardiomyopathy. *J Am Coll Cardiol* 2015;66:1990–9. Doi:10.1016/j.jacc.2015.08.879.
- [75] Quevedo HC, Hatzistergos KE, Oskouei BN, et al. Allogeneic mesenchymal stem cells restore cardiac function in chronic ischemic cardiomyopathy via trilineage differentiating capacity. *Proc Natl Acad Sci U S A* 2009;106:14022–7. Doi:10.1073/pnas.0903201106.

- [76] Schneider C, Krause K, Jaquet K, et al. Intramyocardial Transplantation of Bone Marrow-Derived Stem Cells: Ultrasonic Strain Rate Imaging in a Model of Hibernating Myocardium. *J Card Fail* 2008;14:861–72. Doi:10.1016/j.cardfail.2008.08.005.
- [77] Schuleri KH, Amado LC, Boyle AJ, et al. Early improvement in cardiac tissue perfusion due to mesenchymal stem cells. *Am J Physiol Heart Circ Physiol* 2008;294:H2002-2011. Doi:10.1152/ajpheart.00762.2007.
- [78] Schuleri KH, Feigenbaum GS, Centola M, et al. Autologous mesenchymal stem cells produce reverse remodelling in chronic ischaemic cardiomyopathy. *Eur Heart J* 2009;30:2722–32. Doi:10.1093/eurheartj/ehp265.
- [79] Yamada S, Nelson TJ, Kane GC, et al. Induced pluripotent stem cell intervention rescues ventricular wall motion disparity, achieving biological cardiac resynchronization post-infarction. *Journal of Physiology* 2013;591:4335–49. Doi:10.1113/jphysiol.2013.252288.
- [80] Beitnes JO, Gjesdal O, Lunde K, et al. Left ventricular systolic and diastolic function improve after acute myocardial infarction treated with acute percutaneous coronary intervention, but are not influenced by intracoronary injection of autologous mononuclear bone marrow cells: A 3 year seria; echocardiographic sub-study of the randomized-controlled ASTAMI study. *Eur J Echocardiogr* 2011;12:98–106. Doi:10.1093/ejehocardiography/jeq116.
- [81] Bhatti S, Al-Khalidi H, Hor K, et al. Assessment of Myocardial Contractile Function Using Global and Segmental Circumferential Strain following Intracoronary Stem Cell Infusion after Myocardial Infarction: MRI Feature Tracking Feasibility Study. *ISRN Radiol* 2013;2013:371028. Doi:10.5402/2013/371028.
- [82] Lebrun F, Berchem G, Delagardelle C, et al. Improvement of exercise-induced cardiac deformation after cell therapy for severe chronic ischemic heart failure. *J Card Fail* 2006;12:108–13. Doi:10.1016/j.cardfail.2005.10.011.
- [83] Nasser BA, Kukucka M, Dandel M, et al. Two-Dimensional Speckle Tracking Strain Analysis for Efficacy Assessment of Myocardial Cell Therapy. *Cell Transplant* 2009;18:361–70.
- [84] Nasser BA, Ebelt W, Dandel M, et al. Autologous CD133+ bone marrow cells and bypass grafting for regeneration of ischaemic myocardium: The Cardio133 trial. *Eur Heart J* 2014;35:1263–74. Doi:10.1093/eurheartj/ehu007.
- [85] Heldman AW, DiFede DL, Fishman JE, et al. Transendocardial mesenchymal stem cells and mononuclear bone marrow cells for ischemic cardiomyopathy: The TAC-HFT randomized trial. *JAMA* 2014;311:62–73. Doi:10.1001/jama.2013.282909.
- [86] Herbots L, D'Hooge J, Eroglu E, et al. Improved regional function after autologous bone marrow-derived stem cell transfer in patients with acute myocardial infarction: A randomized, double-blind strain rate imaging study. *Eur Heart J* 2009;30:662–70. Doi:10.1093/eurheartj/ehn532.
- [87] Hopp E, Lunde K, Solheim S, et al. Regional myocardial function after intracoronary bone marrow cell injection in reperfused anterior wall infarction - A cardiovascular magnetic resonance tagging study. *J Cardiovasc Magn Reson* 2011;13:22. Doi:10.1186/1532-429X-13-22.
- [88] Karatasakis G, Leontiadis E, Peristeri I, et al. Intracoronary infusion of selected autologous bone marrow stem cells improves longitudinal myocardial strain and strain rate in patients

- with old anterior myocardial infarction without recent revascularization. *Eur J Echocardiogr* 2010;11:440–5. Doi:10.1093/ejehocard/jep235.
- [89] Malliaras K, Makkar RR, Smith RR, et al. Intracoronary cardiosphere-derived cells after myocardial infarction: Evidence of therapeutic regeneration in the final 1-year results of the CADUCEUS trial (Cardiosphere-derived autologous stem cells to reverse ventricular dysfunction). *J Am Coll Cardiol* 2014;63:110–22. Doi:10.1016/j.jacc.2013.08.724.
- [90] Williams AR, Trachtenberg B, Velazquez DL, et al. Intramyocardial stem cell injection in patients with ischemic cardiomyopathy: Functional recovery and reverse remodeling. *Circ Res* 2011;108:792–6. Doi:10.1161/CIRCRESAHA.111.242610.
- [91] Plewka M, Krzemińska-Pakuła M, Lipiec P, et al. Effect of Intracoronary Injection of Mononuclear Bone Marrow Stem Cells on Left Ventricular Function in Patients With Acute Myocardial Infarction. *Am J Cardiol* 2009;104:1336–42. Doi:10.1016/j.amjcard.2009.06.057.
- [92] Qi Z, Duan F, Liu S, et al. Effectiveness of bone marrow mononuclear cells delivered through a graft vessel for patients with previous myocardial infarction and chronic heart failure: An echocardiographic study of left ventricular remodeling. *Echocardiography* 2015;32:937–46. Doi:10.1111/echo.12787.
- [93] Van Ramshorst J, Atsma DE, Beeres SLMA, et al. Effect of intramyocardial bone marrow cell injection on left ventricular dyssynchrony and global strain. *Heart* 2009;95:119–24. Doi:10.1136/hrt.2007.129569.
- [94] Van Ramshorst J, Antoni ML, Beeres SLMA, et al. Intramyocardial bone marrow derived mononuclear cell injection for chronic myocardial ischemia: The effect on diastolic function. *Circ Cardiovasc Imaging* 2011;4:122–9. Doi:10.1161/CIRCIMAGING.110.957548.
- [95] Chamuleau SAJ, Van der Naald M, Climent AM, et al. Translational Research in Cardiovascular Repair: A Call for a Paradigm Shift. *Circ Res* 2018;122:310–18. Doi:10.1161/CIRCRESAHA.117.311565.
- [96] Van Der Naald M, Chamuleau SAJ, Menon JML, et al. Preregistration of animal research protocols: Development and 3-year overview of preclinicaltrials.eu. *BMJ Open Science* 2022;6:e100259. Doi:10.1136/bmjos-2021-100259.
- [97] Shen T, Xia L, Dong W, et al. A Systematic Review and Meta-Analysis: Safety and Efficacy of Mesenchymal Stem Cells Therapy for Heart Failure. *Curr Stem Cell Res Ther* 2021;16:354–65. Doi:10.2174/1574888X15999200820171432.
- [98] Van der Spoel TIG, Gathier WA, Koudstaal S, et al. Autologous Mesenchymal Stem Cells Show More Benefit on Systolic Function Compared to Bone Marrow Mononuclear Cells in a Porcine Model of Chronic Myocardial Infarction. *J Cardiovasc Transl Res* 2015;8:393–403. Doi:10.1007/s12265-015-9643-3.
- [99] Kastrup J, Haack-Sørensen M, Juhl M, et al. Cryopreserved Off-the-Shelf Allogeneic Adipose-Derived Stromal Cells for Therapy in Patients with Ischemic Heart Disease and Heart Failure—A Safety Study. *Stem Cells Transl Med* 2017;6:1963–71. Doi:10.1002/sctm.17-0040.

- [100] Heeger CH, Jaquet K, Thiele H, et al. Percutaneous, transendocardial injection of bone marrow-derived mononuclear cells in heart failure patients following acute ST-elevation myocardial infarction: ALSTER-Stem Cell trial. *EuroIntervention* 2012;8:732–42. Doi:10.4244/EIJV8I6A113.
- [101] Paitzoglou C, Bergmann MW, Vrtovc B, et al. Rationale and design of the European multicentre study on Stem Cell therapy in IschEmic Non-treatable Cardiac disease (SCIENCE). *Eur J Heart Fail* 2019;21:1032–41. Doi:10.1002/ehf.1412.
- [102] McManus DD, Shah SJ, Fabi MR, et al. Prognostic Value of Left Ventricular End-Systolic Volume Index as a Predictor of Heart Failure Hospitalization in Stable Coronary Artery Disease: Data from the Heart and Soul Study. *J Am Soc Echocardiogr* 2009;22:190–7. Doi:10.1016/j.echo.2008.11.005.
- [103] Kwon DH, Hachamovitch R, Popovic ZB, et al. Survival in patients with severe ischemic cardiomyopathy undergoing revascularization versus medical therapy: Association with end-systolic volume and viability. *Circulation* 2012;126:S3-8. Doi:10.1161/CIRCULATIONAHA.111.084434.
- [104] Mathiasen AB, Qayyum AA, Jørgensen E, et al. Bone marrow-derived mesenchymal stromal cell treatment in patients with severe ischaemic heart failure: A randomized placebo-controlled trial (MSC-HF trial). *Eur Heart J* 2015;36:1744–53. Doi:10.1093/eurheartj/ehv136.
- [105] Greupner J, Zimmermann E, Grohmann A, et al. Head-to-head comparison of left ventricular function assessment with 64-row computed tomography, biplane left cineventriculography, and both 2- and 3-dimensional transthoracic echocardiography: Comparison with magnetic resonance imaging as the reference standard. *J Am Coll Cardiol* 2012;59:1897–907. Doi:10.1016/j.jacc.2012.01.046.
- [106] Hoffmann R, Barletta G, Von Bardeleben S, et al. Analysis of left ventricular volumes and function: A multicenter comparison of cardiac magnetic resonance imaging, cine ventriculography, and unenhanced and contrast-enhanced two-dimensional and three-dimensional echocardiography. *J Am Soc Echocardiogr* 2014;27:292–301. Doi:10.1016/j.echo.2013.12.005.
- [107] Van Klarenbosch BR, Chamuleau SAJ, Teske AJ. Deformation imaging to assess global and regional effects of cardiac regenerative therapy in ischemic heart disease - a systematic review. *J Tissue Eng Regen Med* 2019;13:1872-82. Doi: 10.1002/term.2937
- [108] Gyöngyösi M, Dib N. Diagnostic and prognostic value of 3D NOGA mapping in ischemic heart disease. *Nat Rev Cardiol* 2011;8:393–404. Doi:10.1038/nrcardio.2011.64.
- [109] Kurzewski R, Barański K, Caluori G, et al. Correlation between electromechanical parameters (NOGA XP) and changes of myocardial ischemia in patients with refractory angina. *Postępy w Kardiologii Interwencyjnej* 2021;17:281–9. Doi:10.5114/aic.2021.109168.
- [110] Van Slochteren FJ, Van Es R, Koudstaal S, et al. Multimodality infarct identification for optimal image-guided intramyocardial cell injections. *Neth Heart J* 2014;22:493–500. Doi:10.1007/s12471-014-0604-2.
- [111] European Society of Radiology (ESR). The new EU General Data Protection Regulation: what the radiologist should know. *Insights Imaging* 2017;8:295–9. Doi:10.1007/s13244-017-0552-7.

- [112] Lang RM, Badano LP, Victor MA, et al. Recommendations for cardiac chamber quantification by echocardiography in adults: An update from the American Society of Echocardiography and the European Association of Cardiovascular Imaging. *J Am Soc Echocardiogr* 2015;28:1-39. e14. Doi:10.1016/j.echo.2014.10.003.
- [113] Voigt JU, Pedrizzetti G, Lysyansky P, et al. Definitions for a common standard for 2D speckle tracking echocardiography: consensus document of the EACVI/ASE/Industry Task Force to standardize deformation imaging. *Eur Heart J Cardiovasc Imaging* 2015;16:1-11. Doi:10.1093/ehjci/jeu184.
- [114] Mathiasen AB, Qayyum AA, Jørgensen E, et al. Bone marrow-derived mesenchymal stromal cell treatment in patients with ischaemic heart failure: final 4-year follow-up of the MSC-HF trial. *Eur J Heart Fail* 2020;22:884-92. Doi:10.1002/ehf.1700.
- [115] Qayyum AA, Mouridsen M, Nilsson B, et al. Danish phase II trial using adipose tissue derived mesenchymal stromal cells for patients with ischaemic heart failure. *ESC Heart Fail* 2023;10:1170-83. Doi:10.1002/ehf2.14281.
- [116] Murry CE, Soonpaa MH, Reinecke H, et al. Haematopoietic stem cells do not transdifferentiate into cardiac myocytes in myocardial infarcts. *Nature* 2004;428:664-8. Doi:10.1038/nature02446.
- [117] Van der Naald M. Enhancing quality in translational research - Learning from experiences in cardiac repair. 2022. ISBN:978-94-6423-950-8.
- [118] Braunwald E. Cell-Based Therapy in Cardiac Regeneration - An Overview. *Circ Res* 2018;132-9. Doi:10.1161/CIRCRESAHA.118.313484.
- [119] Nowbar AN, Mielewicz M, Karavassilis M, et al. Discrepancies in autologous bone marrow stem cell trials and enhancement of ejection fraction (DAMASCENE): Weighted regression and meta-analysis. *BMJ* 2014;348:g2688. Doi:10.1136/bmj.g2688.
- [120] Chien KR, Frisén J, Fritsche-Danielson R, et al. Regenerating the field of cardiovascular cell therapy. *Nat Biotechnol* 2019;37:232-7. Doi:10.1038/s41587-019-0042-1.
- [121] Nienke Zoetbrood. Die ene cel waardoor het hart zichzelf kan repareren... die bestaat niet. *Volkskrant* 2019.
- [122] Pezhouman A, Nguyen NB, Kay M, et al. Cardiac regeneration – Past advancements, current challenges, and future directions. *J Mol Cell Cardiol* 2023;182:75-85. Doi:10.1016/j.jmcc.2023.07.009.





# Appendix

Nederlandse samenvatting

List of publications

Acknowledgements / dankwoord

Curriculum vitae

## NEDERLANDSE SAMENVATTING

Dit proefschrift richt zich op nieuwe diagnostische strategieën en celtherapie-gebaseerde behandelingen voor patiënten met ischemisch hartlijden. Ischemische hartziekten vormen een belangrijk klinisch probleem, en zijn wereldwijd de belangrijkste oorzaak van ziekte en premature mortaliteit. De verwachting is dat de incidentie van acuut myocardiinfarct in de toekomst zal stijgen. Dit gegeven, gecombineerd met een verbeterende overleving na een acuut hartinfarct door alsmaar verbeterende behandeling, zal leiden tot een verdere toename van het aantal patiënten met ischemisch bepaald hartfalen. Kenmerk van het ischemisch beschadigde hart is dat het functionele myocard wordt vervangen door fibrose, en de mate van fibrose in het hart is een belangrijke prognostische factor ten aanzien van mortaliteit en het ontstaan van hartfalen. Vooralsnog is er geen curatie door middel van regeneratie van de hartspeer mogelijk.

### Deel 1 – geavanceerde diagnostiek bij patiënten met ischemische hartziekte

Het eerste deel van dit proefschrift richt zich op de diagnostiek bij patiënten die een acuut hartinfarct doorgemaakt hebben. Het identificeren van patiënten die baat zullen hebben bij uitgebreidere medicamenteuze antifibrotische therapie of agressieve reperfusetherapie is een klinische uitdaging. In de huidige praktijk worden zowel biochemie (creatine kinase en troponine) als beeldvorming ingezet om de mate van schade na een hartinfarct te bepalen. De meest gebruikte parameter is de linker ventrikel ejectiefractie (LVEF), en richtlijnen geven veelal aanbevelingen ten aanzien van behandeling aan de hand van deze parameter. Echter, LVEF is een mate van globale linker ventrikelfunctie, en daardoor mogelijk niet accuraat genoeg om de regionale schade in te schatten zoals dat bij een hartinfarct optreedt. Daar bovenop kan gezond myocard overcompenseren voor beschadigd myocard waardoor LVEF de mate van schade onderschat. Anderzijds kan myocard na een acuut hartinfarct tijdelijk disfunctioneren zonder dat er definitieve schade is opgetreden. Dit fenomeen wordt stunning genoemd, en kan ervoor zorgen dat LVEF de mate van schade juist overschat. Tot slot kent LVEF significante inter- en intra-operator variabiliteit. Cardiale magnetic resonance met late gadolinium aankleuring (LGE-CMR) is de gouden standaard voor het bepalen van fibrose en myocardiale littekenvorming. Echter, deze techniek kent beperkte beschikbaarheid, en in de directe post-acute fase kan reactieve inflammatie de mate van fibrose overschatten.

In **hoofdstuk 2** onderzoeken wij de waarde van tweedimensionale speckle-tracking echocardiografie (2D-STE) in de post-acute fase na een hartinfarct. Dit is een techniek waarmee myocardiale deformatie, ook wel strain genoemd, wordt gemeten. Hiermee kan de hartfunctie op gedetailleerde wijze worden gemeten, op zowel globaal, regionaal als laag-specifiek niveau. We vergeleken deze techniek met LVEF en een visuele inschatting van wandbewegingen en gebruikten LGE-CMR, verricht 4-6 maanden na het infarct, als referentiestandaard. We vonden dat segmentele strain  $< -13.3\%$  voorspelt voor niet

aangedaan segment, terwijl segmentele strain tussen -13.3% en -11.5% voorspelt voor een subendocardiaal litteken en een segmentele strain  $> -11.5\%$  voorspelt voor een transmuraal litteken. Echter, globale strain in de post-acute fase correleert niet beter met infarctgrootte dan parameters gebaseerd op conventionele echografie. Laag-specifieke strainanalyse is niet van toegevoegde waarde.

Hoewel strainanalyse een veelbelovende techniek is, kent deze ook nadelen. Eén daarvan is dat de resultaten afhankelijk zijn van de vullingsstatus van de patiënt. Dit is juist in de post-acute fase van een hartinfarct van belang, waarbij zowel het hartinfarct als de medicamenteuze behandeling daarvan veranderingen in zowel preload als afterload teweeg brengen. **Hoofdstuk 3** is een hypothese-genererend onderzoek naar myocardiale arbeid (Engels: myocardial work) bij patiënten met een hartinfarct. Dit is een nieuwe techniek waarbij met behulp van 2D-STE en de gemeten bloeddruk een druk-strain curve wordt gegenereerd, van waaruit vulling-onafhankelijke parameters van myocardiale functie kunnen worden afgeleid. We vonden dat de parameters 'global work index', 'global work efficiency' en 'global constructive work' verbeterden van de periode enkele dagen na het hartinfarct tot maanden na het hartinfarct. 'Global wasted work' toonde geen significante verandering over de tijd. In de periode direct na een hartinfarct lijken deze parameters segmenten zonder litteken te kunnen onderscheiden van transmuraal geïnfarceerde segmenten, maar ze presteren hierin niet beter dan reguliere strainanalyse. In geval van een chronisch litteken lijkt deze techniek niet van diagnostische waarde te zijn.

Naast beeldvormende technieken richt dit proefschrift zich in **hoofdstuk 4** op circulerende biomarkers. In de klinische praktijk worden creatine kinase en troponine toegepast om infarct en infarctgrootte in te schatten, beiden markers van cardiomyocytyerval. Echter, deze biomarkers zeggen niet direct iets over de mate van fibrose. Wij onderzochten de rol van biomarkers van collageen homeostase, C-terminale propeptide van procollagen type I (PICP) en C-terminale telopeptide van type I collagen (ICTP), in het proces van littekenformatie bij patiënten met een blanco cardiale voorgeschiedenis, waarbij de verwachting is dat er geen pre-existente myocardiale fibrose is. De concentratie van PICP, een maat van collageensynthese, neemt toe tussen enkele dagen en zes weken na een acuut hartinfarct, en normaliseert vijf maanden later weer tot vergelijkbare waardes ten opzichte van de baselinewaarde. De PICP-concentratie zes weken na een acuut hartinfarct correleert zwak met LGE-CMR gemeten infarctgrootte. Concentraties van ICTP, dat collageendegradatie reflecteert, nemen toe vanaf de baselinewaarde in de dagen na een acuut hartinfarct tot zes weken nadien, en blijven op een verlaagd niveau vijf maanden na het hartinfarct. ICTP concentraties op zowel zes weken als vijf maanden na een acuut hartinfarct correleren zwak met infarctgrootte. De zwakke correlaties hebben mogelijk te maken met het feit dat de collageenhuishouding zich niet zuiver tot het hart beperkt en door uitermate veel factoren wordt beïnvloed. PICP en ICTP hebben daardoor beperkte

klinische toepasbaarheid, zeker ten opzichte van de biomarkers die momenteel in de klinische praktijk worden toegepast.

### Deel 2 – toepassing van geavanceerde beeldvorming bij nieuwe behandelingen voor ischemisch hartfalen

Het regenereren van het ischemisch beschadigde hart wordt beschouwd als een heilige graal binnen het cardiologische onderzoeksveld. Sinds 2001 wordt de toepassing van stamcellen in de klinische setting onderzocht. Hoewel eerder onderzoek laat zien dat de bij patiënten ingebrachte cellen zich niet tot cardiomyocyten differentiëren, lijkt de toegepaste behandeling wel een mogelijke verbetering van de linkerventrikelfunctie te bewerkstelligen. Het effect van deze celtherapieën wordt doorgaans bepaald aan de hand van beeldvormingseindpunten, zoals de linkerkamerdimensie, linkerkamervolume of LVEF, als surrogaat voor harde eindpunten zoals overleving of hospitalisatie. Zoals eerder gesteld worden deze eindpunten beperkt door inter- en intra-operator variabiliteit en zijn ze mogelijk niet accuraat genoeg om de subtiele regionale effecten van celtherapie vast te stellen.

**Hoofdstuk 5** is een systematische review naar de toepassing van strainanalyse in het onderzoeksveld van cardiale regeneratieve therapie. In totaal vonden wij 15 preklinische en 15 klinische studies. Twaalf van de 15 preklinische studies vonden een positief effect van celtherapie op zowel LVEF als strainparameters; één studie vond geen effect van celtherapie op zowel LVEF als strainparameters; en twee studies vonden geen veranderingen in LVEF, maar wel in strainparameters. Voor wat klinische studies betreft, zeven studies vonden geen positief effect van celtherapie. Vier studies vonden een effect op zowel LVEF als strainparameters, en nog eens vier studies vonden geen effect op LVEF maar wel op strainparameters. Deze bevindingen onderschrijven dat strainparameters mogelijk superieur zijn ten opzichte van conventionele beeldvormingseindpunten.

**Hoofdstuk 6** beschrijft de achtergrond en studie-opzet van de Stem Cell therapy in IschEmic Non-treatable Cardiac disease (SCIENCE) trial. Hierin worden de veiligheid en het effect van intramyocardiaal ingebrachte CSCC\_ASC, een allogene mesenchymale stromale cel afkomstig uit vetweefsel van gezonde donoren, onderzocht. In totaal werden 133 patiënten met symptomatisch hartfalen met een LVEF <45% twee-op-één gerandomiseerd naar de behandeling-arm of de placebo-arm. Het primaire eindpunt was eind-systolische diameter, zes maanden na toediening van het studieproduct. Secundaire eindpunten waren LVEF en eind-diastolische diameter, alsook NT-proBNP concentraties en de 6-minuten looptest, op zowel zes als twaalf maanden na behandeling. Vanwege de aan echocardiografie inherente beperkingen in beeldkwaliteit werden ook CT-scans en MRI-scans vervaardigd, maar omdat de resultaten hiervan niet samen te voegen zijn met echoparameters werden alleen de eindpunten gemeten op echocardiografie gebruikt. De volumina en LVEF gemeten op CT en MRI, alsook strainparameters, zullen onderdeel zijn van een toekomstige substudie die geen onderdeel uitmaakt van dit proefschrift.

**Hoofdstuk 7** geeft de resultaten van de SCIENCE trial weer. In zowel de behandel-arm als de placebo-arm verbeterde de LVEF, met respectievelijk 1.2% en 2.8%. Het verschil tussen beide groepen was niet significant. Er waren ook geen significante verschillen in eind-systolisch volume, LVEF en 6 minuten looptest. Enkel de NT-proBNP waarde na twaalf maanden was significant lager bij patiënten behandeld met CSCC-ASC. De resultaten van de SCIENCE trial komen niet overeen met eerder onderzoek naar het effect van celtherapie bij ischemisch bepaald hartfalen, maar zijn wel in lijn met een parallelle nationale fase II studie die in Denemarken is uitgevoerd. De hypothese dat CSCC-ASC sterkere endocriene en paracriene effecten heeft dan eerder toegepaste cellijnen wordt door deze resultaten weerlegd. Hierbij is de vraag of het gekozen primaire eindpunt (eind-systolisch volume) het juiste is, maar als er al een effect op hartfunctie is, rijst direct de vraag of het ongetwijfeld kleine effect van celtherapie op het ischemisch beschadigde hart klinisch relevant is. Daarbij is er de laatste jaren steeds meer controverse ten aanzien van het onderzoeksveld van cardiale regeneratieve therapie ontstaan, onder andere door een gebrek aan wetenschappelijke integriteit. Het concept van klinische celtherapie lijkt geen toekomst te hebben. Het regenereren van het ischemisch beschadigde hart blijft vooralsnog een utopie, en aandacht zal moeten verschuiven naar alternatieve manieren van het elektromechanisch integreren van functioneel myocard.

Concluderend hebben we in dit proefschrift geavanceerde beeldvormingstechnieken, alternatieve biomarkers en het effect van celtherapie bij het ischemisch beschadigde hart onderzocht. Strainanalyse lijkt van waarde te zijn in de diagnostiek naar infarctgrootte en geeft een meer gedetailleerd beeld van hartfunctie dan conventionele echocardiografie. Het is tijd voor het incorporeren van deze techniek in de klinische praktijk. De waarde van circulerende biomarkers van collageenhomeostase is beperkt, en niet van klinische toegevoegde waarde. Strainanalyse is veelbelovend in het veld van cardiale klinische celtherapie, maar het veld zelf is dat allerminst. Hoewel toekomstige studies naar cardiale celtherapie gebruik zouden moeten maken van strain-afgeleide eindpunten, zou vooral de aandacht van het onderzoeksveld uit moeten gaan naar alternatieve manieren voor het bewerkstelligen van klinisch relevante verbetering van het ischemisch beschadigde hart.

## LIST OF PUBLICATIONS

Koopsen T, Van Osta N, Van Loon T, Meiburg R, Huberts W, Beela AS, Kirkels FP, **Van Klarenbosch BR**, Teske AJ, Cramer MJ, Bijvoet GP, Van Stipdonk A, Vernooy K, Delhaas T, Lumens J. Parameter subset reduction for imaging-based digital twin generation of patients with left ventricular mechanical discoordination. *Biomed Eng Online*. 2024 May 13;23(1):46. Doi:10.1186/s12938-024-01232-0

Qayyum AA, **Van Klarenbosch BR**, Frljak S, Cerar A, Poglajen G, Traxler-Weidenauer D, Nadrowski P, Paitazoglou C, Vrtovec B, Bergmann MW, Chamuleau SAJ, Wojakowski W, Gyöngyösi M, Kraaijeveld A, Hansen KS, Vrangbaek K, Jorgensen E, Helqvist S, Joshi FR, Johansen EM, Follin B, Juhl M, Hojgaard LD, Mathiasen AB, Ekblond A, Haack-Sorensen M, Kastrup J; SCIENCE Investigators. Effect of allogeneic adipose tissue-derived mesenchymal stromal cell treatment in chronic ischaemic heart failure with reduced ejection fraction – the SCIENCE trial. *Eur J Heart Fail*. 2023 Apr;25(4):576-587. Doi:10.1002/ehf.2772

Koopsen T, Van Osta N, Van Loon T, Van Nieuwenhoven FA, Prinzen FW, **Van Klarenbosch BR**, Kirkels FP, Teske AJ, Vernooy K, Delhaas T, Lumens J. A Lumped Two-Compartment Model for Simulation of Ventricular Pump and tissue Mechanics in Ischemic Heart Disease. *Front Physiol*. 2022 May 11;13:782592. Doi: 10.3389/fphys.2022/782592

Groen MHA, Van Es R, **Van Klarenbosch BR**, Stehouwer M, Loh KP, Doevendans PAFM, Wittkampf FH, Neven K. In vivo analysis of the origin and characteristics of gaseous microemboli during catheter-mediated irreversible electroporation. *Europace* 2021;23(1):139-146. DOI:10.1093/europace/eaab243

Uiterwijk M, Smits AIPM, Van Geemen D, **Van Klarenbosch BR**, Dekker S, Cramer MJ, Van Rijswijk JW, Lurier EB, Di Luca A, Brugmans MCP, Mes T, Bosman AW, Aikawa E, Gründeman PF, Bouten CVC, Kluin J. In Situ Remodeling Overrides Bioinspired Scaffold Architecture of Supramolecular Elastomeric Tissue-Engineered Heart Valves. *JACC Basic Transl Sci*. 2020 Nov 25;5(12):1187-1206. Doi:10.1016/j.jacbs.2020.09.011

**Van Klarenbosch BR**, Chamuleau SAJ, Teske AJ. Deformation imaging to assess global and regional effects of cardiac regenerative therapy in ischaemic heart disease: A systematic review. *J Tissue Eng Regen Med*. 2019 Oct;13(10):1872-1882. Doi:10.1002/term.2937

Paitazoglou C, Bergmann MW, Vrtovec B, Chamuleau SAJ, **Van Klarenbosch BR**, Wojakowski W, Michalewska-Wludarczyk A, Gyöngyösi M, Ekblond A, Haack-Sorensen M, Jaquet K, Vrangbaek K, Kastrup J; SCIENCE investigators. Rationale and design of the

European multicentre study on Stem Cell therapy in IschEmic Non-treatable Cardiac disease (SCIENCE). *Eur J Heart Fail.* 2019 Aug;21(8):1032-1041. Doi:10.1002/ehhf/1412

Gathier WA, Van der Naald M, **Van Klarenbosch BR**, Tuinenburg AE, Bemelmans JL, Neef K, Sluijter JP, Van Slochteren FJ, Doevendans PA, Chamuleau SAJ. Lower retention after retrograde coronary sinus infusion compared with intracoronary infusion of mesenchymal stromal cells in the infarcted porcine myocardium. *BMJ Open Sci.* 2019 Jan 7;3(1)e:000006. Doi:10.1136/bmjos-2018-000006

Jansen R\*, **Van Klarenbosch BR\***, Cramer MJ, Meijer RCA, Westendorp PHM, Meijburg HWJ, Bucx JJJ, Chamuleau SAJ, Kluin J. Longitudinal echocardiographic and clinical follow-up of patients undergoing mitral valve surgery without concomitant tricuspid valve repair. *Neth Heart J.* 2018 Nov;26(11):552-561. Doi: 10.1007/s12471-018-1159-4

Ellenbroek GHJM, De Haan JJ, **Van Klarenbosch BR**, Brans MAD, Van de Weg SM, Smeets MB, De Jong S, Arslan F, Timmers L, Goumans MTH, Hoefer IE, Doevendans PA, Pasterkamp G, Meyaard L, De Jager SCA. Leukocyte-Associated Immunoglobulin-like Receptor-1 is regulated in human myocardial infarction but its absence does not affect infarct size in mice. *Sci Rep.* 2017 Dec 21;7(10):18039. Doi: 10.1038/s41598-017-13678-5

\*Shared first authorship

### **Manuscripts in preparation / submitted manuscripts**

**Van Klarenbosch BR**, Driessen HE, Kirkels FP, Cramer MJ, Velthuis BK, Vos MA, Chamuleau SAJ, Ter Meulen - De Jong S, Teske AJ. Global, segmental, and layer-specific two-dimensional speckle tracking echocardiography immediately after acute myocardial infarction as a predictive tool to assess myocardial viability and scar size. Submitted to *Journal of Echocardiography*.

**Van Klarenbosch BR**, Driessen HE, Kirkels FP, Cramer MJ, Velthuis BK, Vos MA, Chamuleau SAJ, Ter Meulen - De Jong S, Teske AJ. Predicting scar transmural extent after acute myocardial infarction; myocardial function assessment by echocardiographic derived global and segmental myocardial work. Submitted to *International Journal of Cardiovascular Imaging*.

**Van Klarenbosch BR**, Driessen HE, Kok GJM, Vos MA, Cramer MJ, Teske AJ, Van Veen TAB, Velthuis BK, Ter Meulen - De Jong S. Correlation between circulating biomarkers of collagen homeostasis and scar size using magnetic resonance imaging in patients after acute myocardial infarction. In preparation.



## DANKWOORD

Ik wil graag iedereen bedanken die – direct of indirect – betrokken is geweest bij de totstandkoming van dit proefschrift of op een andere manier belangrijk is geweest voor mij. Een aantal mensen wil ik daarbij in het bijzonder noemen.

**Prof. dr. S.A.J. Chamuleau**, beste Steven. Ontzettend bedankt voor de kans die je mij hebt gegeven en de begeleiding tijdens dit promotietraject. Tijdens ons kennismakingsgesprek heb je mij weten te enthousiasmeren voor de klinische celtherapie en zijn we dit traject met focus op beeldvorming aangegaan. Helaas is mijn van mijn enthousiasme voor de celtherapie de afgelopen jaren weinig overgebleven. Je hebt mij in het diepe gegooid en daardoor heb ik ontzettend veel geleerd. Soms liep het niet zoals wij zouden willen, het was bij vlagen een moeizaam traject. Ik ben je ongelooflijk dankbaar voor hoe je mij begeleidt hebt en de tijd die je eigenlijk helemaal niet had vrij maakte. Zo heb je me er toch doorheen gesleept. Ik bewonder je niets aflatende enthousiasme voor alles en iedereen. Ook naast de werkvloer hebben we mooie momenten beleefd - borrels, tennissen, maar bovenal dat de kwartfinale van de Europa League, Schalke – Ajax (Viergever!) in Gelsenkirchen. Dankzij jou ben ik in opleiding tot cardioloog gekomen en ik had geweldig gevonden als onze samenwerking als opleider-AIOS zich in Utrecht had voortgezet. Je hebt, helaas voor ons maar geweldig voor jou, voor je droombaan in Amsterdam gekozen.

**Dr. A.J. Teske**, beste Arco. Ik herinner het me nog goed (en jij ook, dat weet ik) – ik was net bij Steven geweest en enthousiast geworden over celtherapie. Kom ik vervolgens bij mijn co-promotor, en het eerste wat diegene zegt is 'die stamcellen werken niet'. Een internationale placebo-gecontroleerde randomized trial verder moet ik je gelijk geven. Dank voor al je begeleiding in dit traject. Voor het regelen van mijn echostage in Amersfoort waardoor ik het kunstje heb kunnen leren, voor je kritische feedback op zowel vorm, inhoud als efficiëntie van het echoën en tot slot voor je ijzersterke analyse van en feedback op alles wat de inhoud van dit proefschrift heeft gevormd. Door jouw begeleiding heb ik een tweede hobby ontwikkeld, de cardiale beeldvorming, en ik hoop dat ik ooit ook maar een beetje in de buurt kom van jouw kennis en kunde. Ik kijk uit naar alles wat je mij daarin nog te leren hebt en hoop dat onze samenwerking zich nog lang mag voortzetten.

**Dr S. Ter Meulen - De Jong**, beste Sanne. Dank dat je mij jouw troetelkindje, de DEFI-MI studie, hebt toevertrouwd. Het is wat improviseren geweest maar uiteindelijk komen er een aantal mooie studies uit. Dank voor de leuke koffiemomentjes in het stratenum om de voortgang te bespreken, waarbij zeker niet alleen de DEFI-MI ter sprake kwam. Ook ontzettend bedankt voor je grote steun tijdens de snel naderende deadline voor de main paper afgelopen jaar, mede door jou is dat allemaal goedkomen. En Siem is groot fan geworden van de Gruffalo.

**Dr. A.O. Kraaijeveld**, beste Adriaan. Dank voor je samenwerking en uiteindelijk begeleiding en supervisie. Na het vertrek van Steven werd jij verantwoordelijk voor de

SCIENCE studie, en dankzij jou zijn de analyses tot een goed einde gebracht. En nog steeds zie je mij aanmodderen, maar nu als mijn polisupervisor. Dingen zijn niet veranderd, als ik weer eens ten onrechte een echo aanvraag hoor ik dat luid en duidelijk. Ik waardeer je directheid. Dank voor alles en ik hoop dat we de samenwerking in de kliniek kunnen voortzetten.

**Prof dr. J. Kastrup**, dear Jens. Thank you for your leading the SCIENCE consortium. Your enthusiasm within the management of the consortium was inspiring and motivating. Also thank you for your patience at times of setback. It's a shame that the results of the SCIENCE trial are not how we had hoped in the beginning, but I hope that you and your research group continue your quest of helping patients with ischemic heart failure. Also, thank you to the other participants of the SCIENCE trial, especially **Anne Lavigne, Sabina Frljak** and **Christina Paitazoglou**, for your support with the imaging core lab.

**Prof. dr. P.A.F.M. Doevendans**, beste Pieter. Hoewel geen onderdeel van het promotieteam ben je toch erg betrokken geweest bij mij en mede door jou ben ik waar ik nu sta. Bedankt daarvoor. Ik vind het ook ontzettend mooi dat je in de leescommissie van mijn proefschrift plaats hebt genomen. Onze gedeelde passie van wielrennen heeft tot mooie tochten geleid, en het is een eer dat ik daarbij mocht zijn. Ik kon ook wel genieten van de '1 MINUUT!' als we na een paar lange klimmen in de zinderende hitte net even op een bankje zaten – maar ik was daarin één van de weinigen geloof ik. Dank ook aan alle andere fietsers **Yolande, Geert, Annemieke, Nienke**. Volgend jaar naar Madrid?

**Dr. M.J. Cramer**, beste Maarten Jan, hoewel ik niet één van 'jouw' promovendi ben (gelukkig heb je er daar al genoeg van), heb je mij toch vanaf dat ik student was onder je vleugels genomen en mede door jou ben ik in dit promotietraject terecht gekomen. Dank voor je aanstekelijke enthousiasme, je kennis van de dierencardiologie en samenwerking bij de beeldvorming en sportcardiologie. Ik hoop dit komende jaren voort te zetten en te intensiveren!

Graag bedank ik de leden van de leescommissie, **prof. dr. M.H. Emmelot – Vonk, prof. dr. J.J. Bax, prof. dr. Doevendans, prof. dr. J. Kluin** en **prof. dr. J. Sluijter**.

Bedankt aan **alle patiënten** die bereid zijn geweest om onderdeel te zijn van de onderzoeken binnen dit proefschrift. Tevens bedankt en alle **co-auteurs** die hebben bijgedragen aan de totstandkoming van de artikelen in dit proefschrift.

Dank aan alle ondersteuners binnen de research. **Ingrid**, bedankt voor al je hulp binnen de ChamPhD groep en met name al je hulp in de verwerking van de beeldvorming van de SCIENCE – hoewel dat soms tot hoofdpijn geleid zal moeten hebben bleef je altijd positief en kon ik altijd op je rekenen. Zonder jou was het misschien allemaal niet gelukt, dank daarvoor. **Karen**, ik heb ik het je in het begin niet makkelijk gemaakt als ik weer eens te laat voor een echo aankwam, maar volgens mij is het uiteindelijk allemaal goed gekomen tussen ons. Dank voor al je hulp! Verder ook veel dank aan **Jeannette, Joni, Han** en **Manon**. Dank aan alle leden van de ChamPhD groep die elders in dit dankwoord niet aan bod komen. Dank aan de afdeling radiologie, in het bijzonder **prof. dr. Leiner, prof. dr. Velthuis, Daniel Araya Roos** en **Niels Blanken**.

Dank aan alle **echolaboranten van het UMC Utrecht**, en in het bijzonder **Jeannette**, voor de ondersteuning. Ook dank aan **Dr. De Vrey** en de **echolaboranten van het Meander MC**, dat ik welkom was om de kunst der echocardiografie te leren. Dank aan **alle medewerkers van de verschillende secretariaten** voor de ondersteuning. Dank aan de **verpleegkundigen van B4west en de CCU** voor de gezelligheid en ondersteuning bij het includeren van patiënten in de studies, en de gezellige samenwerking in de kliniek. En, hoewel geen onderdeel van dit proefschrift, dank aan de onderzoeksgroep van **prof. dr. J. Kluin, Marcelle** en **alle medewerkers van het GDL** – ik heb veel geleerd van de iValve- en OneValve studies.

Voordeel van (te) lang doen over je promotie is dat je ontzettend veel leuke arts-onderzoekers leert kennen. Allereerst dank aan **Freek** en **Roos**, voor het introduceren van de onderzoekswereld. Mede dankzij jullie ben ik dit promotietraject terecht gekomen. En Roos, als we nog eens samen gaan fietsen zal ik niet meer zo hard wegrijden aan het einde. Kan ik tegenwoordig ook niet meer. Dan natuurlijk dank aan alle collega-onderzoekers in de Villa. **René**, op je rots in de villa waar je altijd je ongezouten mening ventileerde, dank voor de mooie momenten in het dierenlab, de schaak- en whiskyavonden en nog veel meer mooie momenten. Ook dank aan al je studenten. **Mira**, partner in crime van de stamcelstudies. Tevens partner in crime in boybands, Mainstreet blijft de favoriet. Geweldig dat je na al je omzwervingen gewoon in het UMC terecht bent gekomen! **Thijs**, stille kracht van de appendix, je kwam op PhDrinking uitjes altijd volledig tot wasdom. **Steven**, oftewel Swenker90, Swenker91 en Swenker92. Ben je inmiddels al Swenker129? Dank voor de samenwerking, schaakpotjes en de trip naar Portoroz. Succes in Zwolle. **Odette** (van de Salden), we blijven elkaar tegenkomen – van de Villa naar Diak naar nu collega AIOS. Knap hoe je de onzin die in de Villa ter sprake kwam zo lang hebt kunnen tolereren. **Marijn**, eerst student en later volwaardig Villabewoner, dank voor de leuke tijd. Mede dankzij jou heb ik een nu een mooi dakterras. **Sanne** en **Rutger**, latere aanwinsten. **Sanne**, jammer dat je die fiets niet van mij wilde kopen. **Rutger**, we moeten nog een keer wat uitgebreider over kamperen op IJsland praten. **Cheyenne** en **Dirk**, grappig dat jullie van kamergenoten naar inmiddels supervisors in de kliniek zijn gegaan. Dank voor de fijne samenwerking, ik leer veel van jullie! **Remco**, medisch ramptoerist en geweldige skiër, maar je hebt het nooit onder de knie gekregen om een wakker schaap te echoën. **Thomas**, straint alles wat los en vast zit, en viert het liefst elke dag een vrijdagmiddagborrel. Ik genoot van je relativerende (zo zal ik het maar noemen) kijk op de cardiologie. **Karim** echo-god, dank voor de dartpotjes. **Feddo**, dank voor je hulp bij de DEFI-MI-gerelateerde strainstukken. Blij dat, terug uit Leuven, de auto van de opleider gewoon heel is gebleven – ondanks de escalatiemix.

Dan alle onderzoekers die elders in de krochten van het UMC waren ondergebracht, waarvan de meesten later boven water kwamen in de kliniek. **Peter Paul**, eigenlijk gewoon Villabewoner natuurlijk, jij kwam ons altijd met je pasje zwaaiend om je vinger halen voor de lunch. Ik begrijp niet waar jij je energie vandaan haalt. Dank voor al je hulp! **Lena**,

we go way back als onderzoeker maar inmiddels ben je onze zorgzame puppet master. We moeten vaker een boybandje opzetten op vrijdagmiddag. **Arjan**, wat is er meneer! Dank voor het medeorganiseren van de PhDrinking in Warschau en het ouwehoeren over auto's. **Jelte** (je weet hoe je dit uit moet spreken), de meest stijlvolle skiër die ik ooit heb gezien. Onze wetenschappelijke samenwerking is er niet helemaal gekomen, maar in de kliniek wel. Dank voor je luisterend oor. **Marloes**, mede-chaoot, dank voor de mooie tijd samen en succes/sterkte met de vrouwencardiologie. **Cas**, dank voor de gezellige tijd op de kamer en het beoordelen van de ECG's met een Duits accent. En, Tonnie! Mag je hier roken? **Professor Fiolet**, er ontstaan vaak levendige discussies als jij de kamer inloopt. Bizar dat ik er pas na jaren achter kwam dat je een Volvo Amazon hebt. We houden marktplaats in de gaten voor oude Espace's. **Mirthe**, koningin van Q, dank voor je gezelligheid op de fiets. Ik kijk uit naar onze verdere samenwerking bij de sportcardiologie. **Wouter**, de Tor, dank voor je werkelijk ein-de-loze geouwehoer onderweg. Prachtige druiven! **Helen**, dank voor de samenwerking bij de DEFI-MI. Verder dank aan alle andere onderzoekers: **Timion, Janine, Phillippe, Evangeline, Marijke, Mark, Rob, Rik, Laurens, Loek, Mimount, Nynke, Odilia, Martine, Iris en Max** en iedereen die ik per ongeluk vergeten ben. **Lennart**, ongelofelijk dat je er niet meer bent, rust in vrede.

Dank aan alle **stafleden van de afdeling cardiologie** voor jullie begeleiding en prettige samenwerking in de kliniek tijdens mijn opleiding. In het bijzonder veel dank aan het opleidingsteam **drs. N. Clappers** en **dr. G.Tj. Sieswerda** en de voormalig opleider **dr. J.H. Kirkels**, jullie maakten en maken de opleiding tot een groot succes. Gertjan, dank voor de ruimte die je bood toen ik het bij een naderende deadline voor mijn proefschrift allemaal even niet meer zag zitten, ik waardeer dat enorm. Dank ook aan de **internisten, cardiologen en arts-assistenten van het Diakonessenhuis** voor de fijne tijd die ik daar heb gehad. Dank ook aan **alle (voormalige) arts-assistenten cardiologie** van het UMC waar ik mee heb samengewerkt. **Danny**, goeroe in de sportcardiologie, altijd prachtige verhalen. Fijn voor je dat je weer thuis onder de rivieren bent. **Nanette**, dank voor je gezelligheid en sorry dat ik moet afhaken voor de skireis... **Willem**, de jovialiteit zelf, ga vooral door met grapjes maken en pas later bedenken of ze wel handig waren. **Merel**, vraagt elke patiënt naar hun huisdieren. Dank voor de mooie tijd in het Diak en super dat we die nu in het UMC voortzetten! **David**, heb jij Merel wel eens verteld dat jij onderzoek deed bij Beagles met een AV-block? Zit me nog altijd niet lekker dat jij sneller was op de Ventoux. **Bram**, dank voor je hulp bij het analyseren van CT-scans toen ik er niet uit kwam met de software.

Dank aan al mijn vrienden voor de uitlaatklep die ik tijdens het afgelopen jaren bij vlagen goed kon gebruiken. In het bijzonder dank aan de **Burgers** voor etentjes. **Rob**, 31 december weer vuurwerk. **Daan**, euuuuh! **Zondagmeisjes**, dank voor de gezelligheid tijdens het fietsen. Mannen van **Het Vlaggenschip**, dank voor het voetballen, derdehelften en de oprechte interesse voor mijn onderzoeksgestuntel. En sorry voor mijn zwakke knie. Dank aan families **Van Klarenbosch** en **Van der Velde** voor jullie interesse. **Cal en Jacq**, ik hoop

dat Siem nog vaak wil komen peje! Dank ook aan mijn schoonfamilie. **Sam en Kirsten**, veel succes met jullie kleintje, gelukkig hoeven jullie geen proefschrift af te maken. En Sam, altijd welkom voor medisch advies. **Stephan**, dank dat Siem altijd welkom is bij jullie, en voor je hulp bij het maken van de kaft. **Inge**, ik ben ontzettend dankbaar voor je lieve zorgen voor Siem (en voor ons) en dat je elke week weer voor ons klaarstaat.

**Thom**, ik ben vereerd dat je mijn paranimf wilt zijn. Ik leerde je eerst kennen als wielrenner en kon met m'n tong op mijn stuur een rondje Werkhoven in je wiel volmaken. De andere paranimf lag er toen al wel af. Later leerde ik je kennen als ontzettend goede dokter. Maak je geen zorgen, die opleidingsplek komt er wel. Succes met jouw promotietraject, gelukkig hebben mijn ervaringen je niet afgeschrikt. Ook heb ik enorm genoten van Project Thom, ongeloofelijk hoe je in een Spartaans trainingsschema geen blokje overgeslagen hebt. Als Joyce het goed vindt gaan we er volgend jaar weer voor!

**Einar**, wij leerden elkaar als jonge honden kennen in de Villa. Door gedeelde passies cardiologie en wielrennen (en ok, ik vind tennis en schaken ook wel leuk) is er een mooie vriendschap uit gekomen. Dank dat je ook mijn paranimf wilt zijn. Je beticht iedereen van het hebben van een bizar gevoel voor humor, maar dat eigenlijk een pot/ketel kwestie. Ik heb ontzettend gelachen om al jouw 'Einarretjes', maar Arcometeencee is wel mijn favoriet. Dank voor de fietstochten en dat je mij als kamergenoot tolereerde, volgende keer neem ik een MRA mee. Je bent een geweldige dokter en collega, Breda mag zich in z'n handjes wrijven. Succes met de interventiecardiologie.

**Tim en Luc**, broers en vrienden. **Tim**, gelukkig hebben we het ruziën in onze puberteit achtergelaten. Je bent gesetteld met een prachtig gezin en ik bewonder hoe je dat allemaal doet. Dank voor het slap ouwehoeren over auto's. **Luc**, ik heb veel respect voor hoe jij bent geworden en hoe je in het leven staat. Je eigen huis is je ontzettend gegund!

**Papa en mama**, ontzettend bedankt voor alles wat jullie voor mij gedaan hebben en nog steeds doen en voor jullie onvoorwaardelijke steun. Pa, ik ben je soort van achterna gegaan in de medische wereld, en dat maakt dat we nu leuke discussies kunnen hebben over onze vakken. Het is heel mooi om te horen hoe men in het ziekenhuis over jou spreekt, je wordt enorm gewaardeerd. Mam, zonder jou was dit proefschrift er niet gekomen. Dank voor de zorgen over Siem, hij geniet ontzettend van bij jullie zijn. Daardoor kon ik me lekker kon opsluiten op de studeerkamer. Dank voor de heerlijke lunch die ik dan achter de laptop naar binnen kon schuiven. Dank voor dat je altijd voor mij/ons klaarstaat.

Lieve Edje (**Siem** eigenlijk!), ondanks dat jij er bent is dit proefschrift er toch gekomen. Je bent het mooiste wat mij ooit is overkomen. Dit promotietraject heeft mij dingen geleerd waar jij misschien ook wat aan zal hebben, maar daar hebben we het later wel over. Kleine **Fluppel**, tot snel! Als jij er bent heb ik gelukkig weer echt een papadag in plaats van een verkapte onderzoeksdag.

Lieve **Kelly**, al de helft van ons leven samen en nog steeds is het een feestje. Het maken van dit proefschrift heeft wat van mij gevergd, en daardoor ook van jou, en ik ben je ontzettend dankbaar voor je luisterend oor, je steun als het moeilijk was en het vieren bij het bereiken van elk mijlpaaltje. Zonder jou had ik het niet gekund. Ik hou van jou.

## CURRICULUM VITAE

Bas Rémond van Klarenbosch was born on November 4th 1990 in Utrecht, to Jan van Klarenbosch and Erna van der Velde. He grew up in Utrecht and Hilversum, together with older brother Tim and younger brother Luc. In 2008, he graduated from the International School Hilversum 'Alberdingk Thijm' following the International Baccalaureate program. Upon completion, Bas decided to pursue a medical career at Universiteit Utrecht, and moved to the city in 2009. During medical school, he worked as a clinical assistant at the Velthuis Clinic and as a research assistant for Hemologic B.V., and during this period his interest in cardiology and circulation was growing. During medical training, Bas did research rotations at the department of cardiology of the University Medical Center Utrecht under supervision of Freek Nijhoff and Rosemarijn Jansen, and completed the 'Dedicated Schakeljaar Vitale Functies'. In 2016, Bas commenced a PhD program under supervision of prof. dr. S.A.J. Chamuleau and dr. A.J. Teske, focusing on advanced imaging in ischemic heart disease and cell based therapy for patients with ischemic heart failure. He got trained in echocardiography in the Meander Medisch Centrum and subsequently performed imaging analysis for the SCIENCE-trial under principal investigator prof. dr. J. Kastrup and gathered imaging- and biomarker data for the DEFI-MI trial, which ultimately culminated into this clinical trial. In 2018, Bas interrupted his PhD program to obtain clinical experience as a medical doctor, working in the cardiology department of the University Medical Center Utrecht. Subsequently, in July 2019 he started his cardiology training under supervision of dr. G.Tj. Sieswerda and drs. N. Clappers. Until June 2021, he received his training in internal medicine at the Diaconessenhuis under supervision of dr. A.F. Muller and dr. G.A.J. van Boekel. From June 2021 until July 2022 he worked at the department of cardiology at the Diaconessenhuis, supervised by dr. C.E.E. van Ofwegen-Hanekamp. Since July 2022, he receives his training at the University Medical Center Utrecht. Bas lives in Utrecht with Kelly van Reisen, having met in high school. They have a son, Siem, and at time of publication, Kelly is pregnant with their second child.

